THE FLOTATION OF ULTRA-FINE PARTICLES

A Thesis submitted for the degree of Ph.D.

in

The University of London

by

Howard Lewis Shergold

Department of Mining
and Mineral Technology,
Royal School of Mines,
Imperial College,
London, S.W.7.

September 1968

ABSTRACT

The problems associated with the flotation of fine mineral particles are discussed. Particular reference is made to slime coatings and the small flotation rates of very fine particles.

An investigation has been made of the concentration of fine hematite and quartz particles at the non-polar oil/water interface of an oil in water emulsion. The collectors and non-polar oil employed were sodium dodecyl sulphate, dodecylamine and dodecanoic acid, and iso-octane (i.e. 2.2.4. trimethylpentane) respectively. Potentiometric and analytical methods revealed that for dodecylamine and dodecanoic acid, neutral amine and fatty acid molecules were distributed between the organic phases. The effect of this distribution on the concentration of quartz and hematite at the oil/water interface was evaluated. Distribution coefficients were determined.

Contact angle, zeta potential, and adsorption density results showed that the concentration of the minerals at the oil/water interface in the presence of sodium dodecyl sulphate and dodecylamine is dependent on the sign and magnitude of the charge on the mineral particles, and the concentration of collector ions in the aqueous phase. These results also indicated that the primary mechanism of adsorption of dodecylamine and sodium dodecyl sulphate at the solid/water interface is one of coulombic attraction of the collector ions for the oppositely charged surface. Two steps were involved in the adsorption processes. The reasons for this are discussed.

The concentration of hematite at the oil/water interface using dodecanoic acid as a collector appeared not to be dependent on the charge of the hematite particles.

Interfacial tensions, determined using the drop volume method, were used, in the Young's expression to evaluate the work of adhesion of the oil drop to the hematite and quartz surfaces. A good correlation was obtained between the works of adhesion, percent extraction (i.e. the percent of the total solid, added, concentrated at the oil/water interface), and the adsorption density.

ACKNOWLEDGEMENTS

I should like to express my sincere gratitude to Dr. O. Mellgren for his guidance and encouragement over the past three years.

I am grateful to Drs. J.A. Kitchener and A.P. Prosser for their helpful suggestions and criticisms during this work. Finally I should like to thank my friends and colleagues in the Royal School of Mines for their frequent assistance and useful discussions.

I am indebted to the Science Research Council for financial support during the course of this work.

CONTENTS

1.00. INTRODUCTION

1.10. Problems Associated with the Flotation of Fine Mineral Particles

In flotation processes the presence of fine mineral particles of below 20 microns in diameter can give rise to three basic problems. Firstly because of their large surface area, fine particles consume large quantities of collector and modifying reagents. Secondly fine particles (slimes) can coat the coarser particles to be floated and inhibit flotation, and finally the flotation response of small particles differs from that of coarser particles.

The formation of slime coatings on a mineral to be floated has been attributed to electrostatic forces of attraction (1) (2) and also to a chemical interaction process (3) (4) (5). Recently Fuerstenau, Gaudin and Miaw (6) related the slime coating density with the flotation recovery and properties of the electrical double layer. They found that slime coatings were heaviest when the slime was uncharged or charged oppositely to the mineral being floated. Thus quartz was only floated with amine in the presence of hematite slimes when both the hematite and quartz had negative surface charges. Iwasaki, Cooke, Harraway and Choi (7) substantiated the results of Fuerstenau and coworkers by showing that negatively charged kaolinite and bentonite had no effect on the flotation of quartz with amine at pH 6.0, whereas neutral or positively charged goethite slimes depressed flotation almost completely. On the other hand, at pH 3.0 with sodium dodecyl

sulphate as a collector positively charged goethite slimes had no effect on the flotation of goethite, whereas negatively or neutrally charged quartz, bentonite and kaolinite all depressed the flotation of goethite. These authors also investigated the effect of slimes of different sizes and showed that in the flotation of quartz with amine, a decrease in the size of the goethite slime particles produced a marked decrease in the quartz recovery.

The mechanism of floating fine particles is basically the same as floating any size particle, in so far as the particle must come into contact with the bubble surface. The intervening film of aqueous surface active agent must then be ruptured so that a finite contact angle between bubble and particle can be established. Many authors (8) (9) (10) (11) have shown that the optimum particle size for flotation is approximately 50 microns and that below this value the rate of flotation and recovery decreases. Gaudin, Schuhmann and Schlecten (12) showed that for galena with sufficient potassium ethyl xanthate as collector, the flotation rate was proportional to the particle size down to a size of 5 microns and below this size remained constant. A detailed investigation by Tomlinson and Fleming (13) revealed that for apatite, hematite and galena, under conditions of 'free' flotation, the flotation rate was first order with respects to the concentration of the size fraction being floated and dependant on the square of the particle diameter. Under conditions of 'inhibited' flotation the flotation rate was zero order with respect to the concentration and not so dependant on the particle diameter.

Flotation was classified as 'free' or 'inhibited' depending on whether the flotation rate was controlled by the particle or bubble concentration.

A number of theories have been postulated to explain the decrease in flotation rate with decrease in particle size. The first detailed attempt to develop a relationship between the flotation rate and collision hydrodynamics was made by Sutherland (14). He derived a relationship between the flotation rate (k) and particle size (r), which was of the form

$$k = \frac{K_1 r}{K_2 + r} \qquad (1)$$

where K_1 and K_2 are constants. Although Sutherland (14) showed that the data obtained by Gaudin and co-workers (12), on galena, fitted an approximate form of eq^n (1) the agreement is probably fortuitous, because in Sutherland's theoretical analysis the intertial effects of the particle were assumed to be negligible. Philippoff (15) considered that the small flotation rate obtained with small particle sizes was attributable to the particles having insufficient time, during a bubble-particle collision, to rupture the film and form a finite contact angle. It was considered that when a particle collided with a bubble, it had sufficient inertia to deform the bubble surface and when the bubble regained its normal shape, both particle and water were ejected from the bubble surface. Calculations of the time in which a fine particle was in contact with the bubble showed that it was unlikely that during this time the disjoining film (16) would

thin sufficiently for the film to rupture, and for a finite contact angle to be formed. Tomlinson and Fleming (13) from considerations of the classical hydrodynamics of Langmuir and Herne showed that the probability of a collision between a particle and bubble was a function of the square of the particle diameter. Their experimental results verified this.

In most of the theoretical analysis on bubble - particle contact the emphasis has been based on the probability of bubble-particle collisions. It must however be realized that although a bubble and particle may collide with each other, adherence of the particle to the bubble does not necessarily follow.

Recently Derjaguin and Dukin (17) have made a theoretical analysis of bubble-particle collisions in terms of a dynamic double layer. Meloy (18) has summarised these analyses qualitatively. When a bubble rises water streams past its surface sweeping the adsorbed surface active ions rearwards and forming a new surface at the forward pole of the bubble. As the old surface is swept rearwards the surface concentration of adsorbed surface active species decreases as the surface approaches the equator and then increases as the surface contracts. At a certain critical latitude the surface will become supersaturated with respect to the surface active ions and as a result ions will diffuse off of the back of the bubble. Thus the surface concentration goes all the way from near zero at the front of the bubble to supersaturation at its tail.

At the front of the bubble, surface active ions will diffuse

toward the bubble, to counteract the difficiency of ions at the bubble surface. The movement of these ions will create a 'zone of depletion' in the liquid just outside the bubble surface. Furthermore since the surface active ions are charged, the bubble surface will be charged and counter ions will diffuse toward the surface. In the 'zone of depletion', therefore, there will be a deficiency of both counter ions and surface active ions. The diffusion of counter ions to the 'zone of depletion' will be greater than that of the surface active ions. As a result, the zone of depletion will acquire a charge opposite to that on the bubble surface, which will build up until the rate of diffusion for the two types of ions is the same. Dukin (19) considers that the electric field from the charge will extend as far as 10 microns from the bubble surface and that it can have an intensity as high as 3000 volt/cm. (20). At the rear of the bubble the charge will be opposite to that at the front part of the bubble because of the diffusion of ions from the bubble surface. It follows, therefore, that a particle will only be attracted to the front part of the bubble if the charge on its surface is of the same sign as that actually on the bubble surface. Alternatively if the particle has an opposite sign to that of the bubble charge, it may be collected at the tail of the bubble.

Derjaguin and Dukin (17) showed that in the absence of all forces except hydrodynamic ones, particles smaller than a critical size would never come into contact with the bubble because they would be carried around the bubble in the streamlines. In the presence of a

diffused layer, however, and when the particle diameter was smaller than the diffused layer thickness, a diffusio-phoretic force would be present. This would either enhance or inhibit the passage of the particle to the bubble surface. As a result of this force the critical particle size for cessation of bubble-particle contact would be modified. Furthermore, it was shown that even if particles were attracted into the diffused layer, contact with the bubble surface did not necessarily follow. A too high charge on the particle surface would result in the repulsive forces between the bubble and particle being greater than the attractive forces. As a result, the particle would be repelled from the bubble surface. Such a particle could be collected at the rear of the bubble where the surface charge was opposite in sign to that at the front of the bubble.

Derjaguin and Dukin (17) also showed that for particles of diameter between the thickness of the diffused layer and that required for the onset of inertial effects, the particles could no longer be treated as pin points embedded in the diffusion zone, as they would themselves alter both the streamlines and the electric field of the diffusion boundary layer. It was shown that for such particles to become attached to the bubble, the disjoining film would have to be thinned at a far greater rate than that predicted from gravitational forces. On the basis of further calculations it was proposed that between the bubble and particle, very strong diffusio-phoretic forces could be formed. The particle as well as bubble, would carry an equilibrium adsorption layer and on approaching each other, surface

active ions could diffuse from the solid to the depleted bubble surface. As a result of this diffusion process a diffusion gradient amounting to thousands of volts cm^{-1} could be established in the small gap between the bubble and particle. Since the surface active ion would generally be the slower moving one, the field would pull the particle toward the bubble surface.

The dynamic nature of the double layer arising from bubble-particle collisions suggests that 'fruitful' collisions are dependant on the bubble and particle size and charge, the diffusion rates of the ions, the collector concentration and the partition of collector adsorbed on the bubble and particle surfaces. In view of the complex nature of these variables it is impossible to predict the flotation behaviour of fine particles.

1.20. Methods of Floating Fine Particles

In many processes the fines are not floated directly, but they are either flocculated, agglomerated or picked up by coarser minerals and then floated. Gaudin and Malozemoff (21) found that by selectively flocculating sulphide minerals with heteropolar sulphur bearing substances, the flotation of fine sulphide minerals could be successfully accomplished. The process whereby fine particles are floated by attachment to larger carrier minerals has found considerable application in the beneficiation of kaolin (22). In essence the process consists of using a finely divided auxillary mineral as carrier for

the fine particles to be floated. The carrier mineral is then floated and the fines are 'piggybacked' into the froth.

At the Minerals and Chemicals Philipp Corporation (23) (24) plant, crude clay is slurried with water, degritted through a 325 mesh screen and then dispersed with 3.5 lb. per ton of sodium silicate. The reagent addition per ton of ore treated is as follows. The clay is conditioned with 6 lb. ammonium sulphate and 600 lb. of coarse marble particles and sufficient water added to give a pulp density of 22% solids. An emulsion of 4 lb. of crude tall oil, 4 lb. of neutral calcium petronate and 3 lb. of aqueous ammonia is then added and conditioning continued. Eight pounds of light hydrocarbon oil is then added and after further conditioning the marble particles coated with an impurity of anastase are floated in conventional flotation cells. The size of the particles floated in this process are 9 microns and the size of the carrier mineral about 325 mesh.

Neutral hydrocarbon oils, of the alkane type, are generally used in the flotation of minerals whose crystal structure is such that they are not readily wetted by water (25). Such minerals as graphite, sulphur, coal, diamonds and molybdenite fall into this category. Neutral oils are also used in conjunction with fatty acids in the flotation of manganese (26) (27) and ilmenite (28) (29) ores. Flotation processes utilizing oil have been termed 'agglomeration' or 'emulsion' flotation processes. This terminology has been adopted more as a matter of convenience rather than as an accurate discription of the principles involved. In principle there is very

little difference between a process using a neutral oil and one that uses no oil. In both processes single, or clusters of, hydrophobic particles are floated by attachment to air bubbles. The addition of oil to the flotation circuit merely increases the hydrophobicity of particles which would otherwise find it difficult to adsorb sufficient collector to become hydrophobic enough for bubble-particle contact. The oil is added to the mineral pulp as an oil in water emulsion containing suitable collectors and sometimes emulsifiers. After conditioning, the mineral pulp is treated in conventional flotation cells.

The metallurgical results obtained from a flotation process in which oil is utilized are very dependant on the nature of the conditioning process. A thorough study of the conditioning and flotation of an ilmenite ore using fatty acid collectors and fuel oil has been made by Lapidot and Mellgren (30). By measuring the power consumption as a function of conditioning time, the distribution of reagents on the products and by determining the flotation characteristics, these authors showed that the conditioning process could be divided into five periods. These periods have been termed the 'induction period', 'flocculation period', 'flocculation peak', 'deflocculation period' and the 'dispersion period'. During the 'induction period' the recovery of ilmenite was low and the reagents were adsorbed on both the ilmenite and gangue minerals as a result of random collisions with the oil drops. As the particles adsorbed more reagents agglomeration of both the gangue and ilmenite particles occurred ('flocculation period') until at the 'flocculation peak' all of the minerals were in

an agglomerated form. A further increase in the conditioning time resulted in the agglomerates breaking ('deflocculation period') and the redistribution of reagents so that only the ilmenite particles were coated. During the 'dispersion period' the reagent was slowly removed from the ilmenite particles by attrition. Flotation tests showed that although good flotation was obtained at the 'flocculation peak' the selectivity was very low. A high selectivity and recovery of ilmenite was best obtained at the end of the 'deflocculation period'.

Some authors (31) (29) maintain that in processes utilizing oil, the fine particles can be treated with the coarse particles. The only effect of the fine particles, being to increase the reagent consumption. The work of Lapidot and Mellgren (30), however, clearly showed that slimes could be treated, if the conditioner pulp density was increased to above 70%. Furthermore they showed that the slimes should be separated and added to the conditioner after the 'deflocculation peak'. In this way the reagent made redundant, as a result of the deflocculation process, was adsorbed onto the slime particles.

Exactly how the hydrocarbon oil effects the flotation of a given mineral is not clearly understood. Gates (26) and others (29) consider that good flotation is obtained as a result of the agglomeration of the mineral particles. The oil being a necessary prerequisite for agglomeration. Mellgren and Lapidot (30), however, showed that a 'flocculation period' and a 'deflocculation period', were obtained whether the neutral oil was present or not. In view of these results

it would appear that both flotation and flocculation (or agglomeration) are manifestations of the mineral hydrophobicity and that the function of the oil is to increase the hydrophobicity of the particles and to reduce the collector consumption, rather than to cause agglomeration.

In certain processes the use of oil to form spherical mineral agglomerates has found considerable application. Once again, however, it is difficult to elucidate the exact function of the oil. Bisse and Mc. Morris (32) showed that by injecting oil into a vigorously agitated coal slurry, preferential oil wetting of the coal particles resulted and flocculation occurred. After more gentle agitation, spherical agglomerates (or pellets) were formed which were removable from the gangue minerals by vibratory screening and centrifugation. In recent years Farnand and co-workers (33) have shown that, by using suitable fatty acid collectors such a technique might be applicable to the beneficiation of tin ores. A continuous agglomeration process for upgrading tin ores has been investigated by Meadus and co-workers (34).

The quantity of oil added to a flotation or spherical agglomeration process (35) (36) (37) (38) is generally such that a separate oil phase is not obtained at the end of the conditioning process. Thus in flotation plants the consumption of oil per ton of ore ranges from one pound to two hundred pounds (27). Little research has been conducted on processes which utilize considerable quantities of oil so that a separate oil phase is obtained. It is the purpose of this work to investigate such a system.

1.30. The Concentration of Minerals at the Oil/Water Interface

If a mixture of two immiscible or partially immiscible liquids is shaken, a dispersion of one in the other results; but in order to attain any degree of stability, a third component is necessary. This third substance need not necessarily be a surface active agent, but can be a finely divided solid. If the two immiscible liquids are a neutral oil and water then depending on the relative phase volumes of the oil and water, and the type of solid, either an oil in water (O/W) or water in oil (W/O) dispersion will result.

Young's expression (40) of wetting of solids by liquids, is

$$\gamma_{SO} - \gamma_{SW} = \gamma_{WO} \cos\theta$$

where θ is the contact angle in the aqueous phase and γ_{SW}, γ_{WO} and γ_{SO} are the interfacial tensions of the solid-water, water-oil and solid-oil interfaces respectively. According to Von Reinders (41) three situations may occur:

1) If $\gamma_{SO} > \gamma_{WO} + \gamma_{SW}$, the solid will remain dispersed in the aqueous phase.

2) If $\gamma_{SW} > \gamma_{WO} + \gamma_{SO}$, the solid will be dispersed in the organic phase.

3) If $\gamma_{WO} > \gamma_{SW} + \gamma_{SO}$, or if none of the three interfacial tensions is greater than the sum of the other two, the solid particles will concentrate at the water-oil boundary. When the solid collects at the liquid-liquid interface Young's expression can be utilized to give the following results.

1) If $\gamma_{SW} < \gamma_{SO}$, then Cos θ is positive and $\theta < 90^{\circ}$; this will result in the major portion of the solid being in the aqueous phase.

2) If $\gamma_{SO} < \gamma_{SW}$, cos θ is negative, $\theta > 90^{\circ}$, and the major portion of the particle will be in the organic phase.

3) In the (unlikely) case when the contact angle is exactly 90°, the particle will be equally wetted by both the organic and aqueous phase.

The above theory suggests that it should be possible to modify the contact angle by the use of suitable surface-active reagents so that the mineral particles concentrate either at the liquid-liquid interface or in the organic phase. Schulman and Leja (42) have shown the validity of this reasoning by elaborate investigations of emulsions stabilized by barium sulphate particles. They found that by increasing the concentration of such collectors as sodium laurate and sodium dodecyl sulphate, the three phase contact angle, barium sulphate, benzene and water, could be increased from zero to a maximum of 135° for the sodium dodecyl sulphate and 115° for sodium laurate. When the contact angle was above 90°, water in oil emulsions were formed and when below 90°, oil in water emulsions were stabilized. This latter finding was consistent with the postulate of Hildebrand (43) which states that the phase preferentially wetting the solid will be the continuous phase. At high concentrations of sodium oleate the contact angle approached 180° and there was a tendency for the barium sulphate particles to be

dispersed in the organic phase. (von Reinders case 2).

Takakuwa and Takamori (44) have used the fact that emulsions stabilized by particles invert when the contact angle exceeds 90°, to determine the optimum conditions of collector concentration and pH necessary for the flotation of sulphide minerals. Although this work clearly shows the importance of collector concentration on the type of emulsion, it does not take into account the fact that 90° contact angles are not required for good flotation and also that some collectors depending on the pH will be distributed between the aqueous and organic phases.

Recently Coleman, Sutherland and Capper (45) have shown that calcite can be successfully extracted from an aqueous suspension of shale into an organic phase. The technique used involved making the particles oleophilic by ball milling the shale in aqueous suspension in the presence of (a collector of) sodium oleate. The calcite particles were then selectively extracted into a viscous petroleum oil which was brought into contact with the suspension. Calcite removal from the shale was improved by increasing the sodium oleate concentration, the time of grinding and the oil/suspension contact time.

1.40. Aim of the Present Work

The aim of this work is to study the interfacial phenomena of collector in water solutions in the presence of iso-octane, and the behaviour of minerals such as quartz and hematite in such

systems. The iso-octane phase takes the place of the air used in conventional flotation systems.

The techniques utilized in these studies involves contact angle, interfacial tension, adsorption, electrokinetic and extraction measurements. An attempt is made to correlate the experimental data and to elucidate the mechanism of collector adsorption at the mineral/water interface.

2.00. SOLUTION EQUILIBRIUM STUDIES

2.10. General

Collectors are chemical reagents which have the ability to impart a degree of hydrophobicity to a mineral surface. Collector molecules consist of an anionic or cationic group attached to a non polar group, such as an alkyl or aryl radical. Anionic collectors are generally organic derivatives of an inorganic acid and they can be categorized into either oxhydryl or sulphydryl collectors, depending on whether the hydrocarbon chain is linked to the acidic hydrogen (or equivalent metal atom) by an oxygen or sulphur atom. Oxhydryl collectors include such compounds as organo sulphates, sulphonates, phosphates and carboxylates, whereas sulphydryl collectors are thio compounds of similar radicals.

Cationic collectors are represented by the amines of which the most commonly used, in flotation studies, is the alkyl primary amine, dodecylamine.

In this research work three collectors, each with a twelve carbon hydrocarbon chain, have been used. The collectors are

a) dodecylamine

$$C_{12}H_{25} - N\begin{matrix}H\\H\end{matrix} \quad \text{or } RNH_2$$

b) sodium dodecyl sulphate

$$C_{12}H_{25} - O - \overset{\overset{O}{\|}}{\underset{\underset{O}{\|}}{S}} - O\,N_a \quad \text{or} \quad R\,SO_4\,N_a$$

and c) dodecanoic acid

$$C_{11}H_{23} - \underset{\underset{O}{\|}}{C} - O\,H \quad \text{or} \quad RCOOH.$$

Of these three collectors a) is cationic and b) and c) are anionic.

In aqueous solutions dodecylamine and dodecanoic acid ionize. The degree of ionization depends on their dissociation constant and the pH of the solution. Sodium dodecyl sulphate being a strong electrolyte, remains completely ionized (46) over a wide pH range. The ionization of dodecylamine is represented by the equation

$$RNH_3^{+} \rightleftharpoons RNH_2 + H^{+} \; ; \; pK = 10.6 \; (47) \; (48) \text{ at } 25^{\circ}C.$$

and the dissociation of dodecanoic acid is represented by the reaction

$$RCOOH \rightleftharpoons RCOO^{-} + H^{+} \; ; \; pK = 5 \; (49) \text{ at } 25^{\circ}C.$$

Neutral dodecylamine and dodecanoic acid molecules are quite soluble in a neutral oil, such as iso-octane, but only slightly soluble in water (50) (51). If iso-octane is added to an aqueous amine or fatty acid solution, a distribution of neutral molecules takes place between the aqueous and organic phases. The collectors in ionic form do not enter into a neutral oil phase because of their hydrophilic nature. The magnitude and nature of the neutral molecule distribution in water and oil was investigated by potentiometric titrations, followed by a direct analytical proce-

dure to check the results.

2.20. Theoretical

Assume that the dodecylamine is dissolved in an excess of hydrochloric acid and that sodium hydroxide is added to increase the pH. As the pH is increased the reaction

$$RNH_3^+ \rightleftharpoons RNH_2 + H^+, \text{ for which}$$

$$K = \frac{[RNH_2]_A [H^+]}{[RNH_3^+]} \qquad (1)$$

proceeds to the right. The RNH_2 produced will become distributed between the aqueous and iso-octane phase. The partition coefficient D will be $[RNH_2]_O / [RNH_2]_A$

or rearranged $D [RNH_2]_A = [RNH_2]_O$ (2)

where,

$[RNH_2]_O$ = concentration of neutral amine in the organic phase in moles litre^{-1}.

and $[RNH_2]_A$ = concentration of neutral amine in the aqueous phase in moles litre^{-1}.

A distribution coefficient (K_D) involving, both neutral and ionic species may be defined as

$$K_D = \frac{\text{Total amine in aqueous phase}}{\text{Total amine in organic phase}}$$

$$= \frac{[RNH_3^+] + [RNH_2]_A}{[RNH_2]_O}$$

assuming that the ionic species is absent in the organic phase. Simplification of eq^n (3) by substitution from (1) and (2) gives

$$K_D = \frac{[H^+]}{DK} + \frac{1}{D}. \qquad (4)$$

The total amine balance at any particular pH is given by the expression

$$V_A [RNH_2]_T = V_A [RNH_3^+] + V_A [RNH_2]_A + V_O [RNH_2]_O \qquad (5)$$

where V_A = volume of the aqueous phase (ml)

V_O = volume of the organic phase (ml)

and $[RNH_2]_T$ = total dodecylamine concentration expressed in moles litre^{-1} of aqueous phase.

The total amount of neutral amine in the system is given by the relationship

$$V_A \; A = V_O [RNH_2]_O + V_A [RNH_2]_A \qquad (6)$$

Where A is the concentration, in moles per litre, of sodium hydroxide available after the neutralisation of excess hydrochloric acid, for reaction with cationic amine according to the equation

$$RNH_3^+ + Cl^- + NaOH = RNH_2 + NaCl + H_2O.$$

Combination of eq^{n} (1) and (2) gives

$$\left[RNH_3^+\right] = \frac{\left[RNH_2\right]_0\left[H^+\right]}{DK} \qquad (7)$$

and from eq^{n} (6) $\qquad \left[RNH_2\right]_0 = \frac{V_A\ A}{V_0 + V_A/D}$

Substituting in (5) for $\left[RNH_3^+\right]$ and $\left[RNH_2\right]_A$ leads to

$$V_A\left[RNH_2\right]_T = \frac{V_A\left[RNH_2\right]_0\left[H^+\right]}{K\ D} + \frac{V_A\left[RNH_2\right]_0}{D} + V_0\left[RNH_2\right]_0 \qquad (7a)$$

and substituting in (7a) for $\left[RNH_2\right]_0$, from eq^{n} (6), gives after rearranging

$$\frac{1}{A} = \frac{V_A\left[H^+\right]}{K\left[RNH_2\right]_T\left[V_0D + V_A\right]} + \frac{1}{\left[RNH_2\right]_T} \qquad (8)$$

Equation (8) indicates that if V_A, K, $\left[RNH_2\right]_T$, V_0 and D are constant a linear relationship exists between $^{1}/_{A}$ and $\left[H^+\right]$. A determination of the slope of this line will enable an evaluation of D to be made. Alternatively the slope can be set equal to Y so that

$$Y = \frac{V_A}{K\left[RNH_2\right]_T\left[V_0D + V_A\right]}$$

$$\text{or } \frac{1}{Y} = \frac{V_0\ DK}{V_A}\left[RNH_2\right]_T + K\left[RNH_2\right]_T \qquad (9)$$

This equation indicates that if the reciprocal of the slope of eq^{n} (8) is measured for different volumes of the organic phase, a linear relationship should exist between $^{1}/_{Y}$ and V_0 provided that V_A, D,

K, and $[RNH_2]_T$ are kept constant. The slope of this line incorporates an average value of D.

A similar theoretical treatment is valid for dodecanoic acid. If the acid is initially dissolved in excess sodium hydroxide the equations obtained analogous to (4) and (8) are

$$K_D = \frac{K}{[H^+]\,D} + \frac{1}{D} \qquad (10)$$

$$\text{and } \frac{1}{A} = \frac{K\ V_A}{[H^+][V_A + V_0 D][RCOOH]_T} + \frac{1}{[RCOOH]_T} \qquad (11)$$

$$\text{where } K_D = \frac{[RCOO^-]_A + [RCOOH]_A}{[RCOOH]_0} \text{ and } K = \frac{[RCOO^-][H^+]}{[RCOOH]_A}$$

and A is the amount of acid available, after neutralisation of excess sodium hydroxide, for reaction with dodecanoate ions.

2.30. Experimental

2.31. Apparatus and Materials

The titration vessel consisted of a 50 ml. 'Quickfit' reaction vessel, fitted with a multi-socket, flanged lid. Through the lid sockets were inserted a calomel and glass electrode, nitrogen inlet and outlet pipes, and a 2 or 5 ml. burette. A magnetic stirrer was applied and the pH was measured with a Pye 'Dynacap' pH meter.

The dodecylamine and dodecanoic acid used were both better than 99% pure and were supplied by B. Newton Maine Limited and B.D.H. respectively. The iso-octane was supplied by B.D.H. as a

'general purpose reagent' and was further purified by passage through a column of activated alumina. All other reagents, unless otherwise stated, were of 'analar' grade.

2.32. Method

A solution containing 1.34×10^{-3} moles/litre of cationic dodecylamine ions and 1.63×10^{-3} moles/litre of hydrogen ions was prepared. A 20 ml aliquot of this amine solution was pipetted into the titration vessel with a known volume of iso-octane. The resulting mixture was then titrated potentiometrically against 0.1M sodium hydroxide under an atmosphere of 'white spot' nitrogen. Similar titrations were conducted with different volumes of iso-octane.

The procedure employed with dodecanoic acid was slightly different, as 0.5 ml of 0.1M dodecanoic aoid solution in iso-octane was added to a known volume of iso-octane and 20 mls of 6×10^{-3}M sodium hydroxide in the titration vessel. The mixture was then agitated for 30 minutes under an atmosphere of 'white spot' nitrogen. It was assumed that at the end of this period most of the dodecanoic acid had left the organic phase and formed dodecanoate ions according to the reaction $RCOOH + NaOH \rightarrow RCOO^- Na^+ + H_2O$. The resulting mixture of carboxylic ions and excess sodium hydroxide was then potentiometrically titrated against 0.1M hydrochloric acid. This procedure was repeated for different volumes of the organic phase.

2.41. Results of the iso-octane - dodecylamine solution titrations

The titration results obtained with dodecylamine are shown in fig. (1). Curve (1) shows the titration of 0.1M NaOH with the total amount of hydrochloric acid added in the dissolution of the RNH_2. (i.e. the excess HCl + the stoichiometric amount required to convert the RNH_2 to RNH_3^+) and curve (2) shows the titration of 0.1M NaOH with the solution containing both the cationic amine and the excess hydrogen ions. Since the pK value of dodecylamine is high the difference in end points of these two titrations should be equivalent to the total concentration of cationic amine in the original solution. The end points of titrations (1) and (2) correspond to 3.00×10^{-3}M HCl and 1.62×10^{-3}M HCl respectively, giving a difference of 1.38×10^{-3}M. This difference reveals that there was a complete conversion of RNH_2 to RNH_3^+ when the dodecylamine was dissolved in excess hydrochloric acid. Curves (3) to (10) refer to the titrations conducted in the presence of different volumes of iso-octane.

The values of A in eq^n (6) were determined by measuring the difference between curves (3) to (10) and curve (2) at different pH values. The volumetric values of A so obtained, were converted into concentrations after corrections were made for the increase in volume of the aqueous phase, due to additions of NaOH. Plots of 1/A against hydrogen ion concentration are shown in fig. 2 for different values of V_0. According to eq^n (8) the intercept of the straight lines obtained in fig. (2) should be equal to the reciprocal of the total amine concentration. Table I summarises the slopes and intercepts

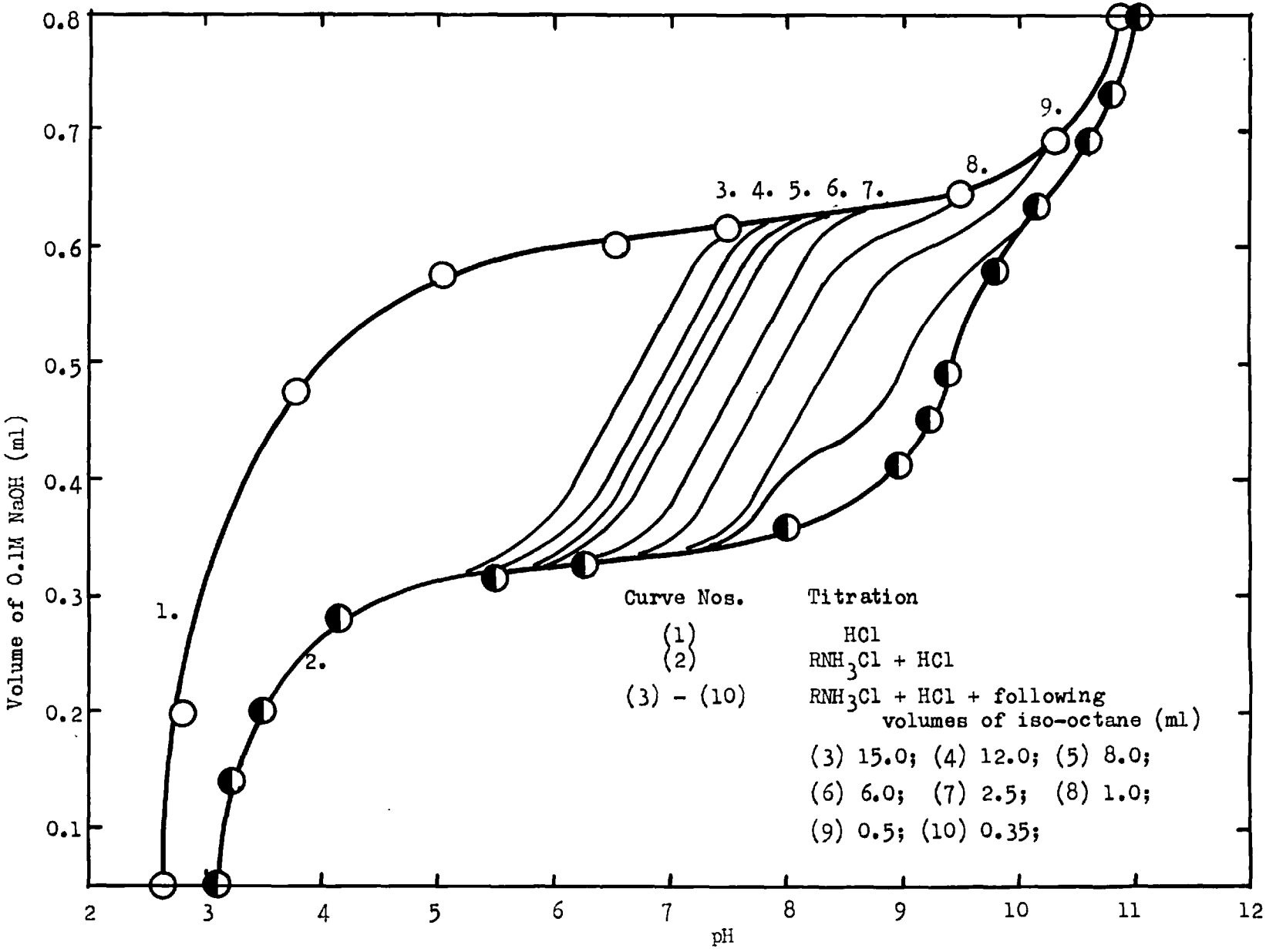

Fig. 1. Titration of dodecylamine hydrochloride with NaOH in the presence of iso-octane.

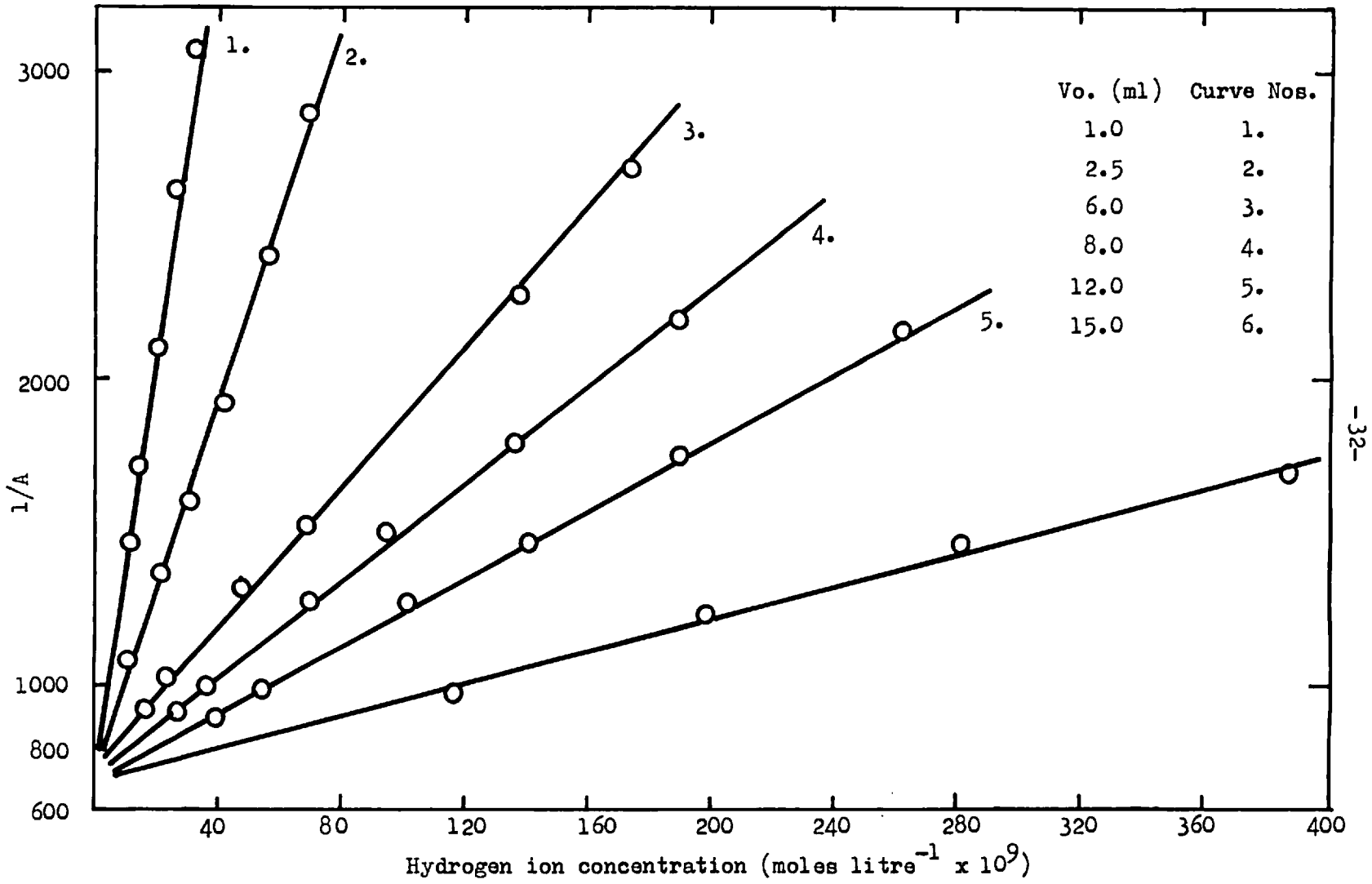

Fig. 2. Plots of 1/A vs hydrogen ion concentration for different volumes of the organic phase.

of these lines for different volumes of the organic phases.

TABLE I

Volume of Organic phase. (ml).	Slope (Y) x 10^{-9}	$\frac{1}{Y}$ x 10^{9}	Intercept
1.0	67.8	0.015	710
2.5	28.6	0.035	740
6.0	11.4	0.088	740
8.0	8.2	0.122	710
12.0	5.4	0.185	710
15.0	2.6	0.385	720

The average value of the intercept was 719 $\pm$ 29 which corresponds to a total dodecylamine concentration of (1.38 $\pm$ 0.04) x 10^{-3}M compared to the prepared solution of 1.34 x 10^{-3}M.

The linear relationship between $^{1}/_{Y}$ and V_0 (eq^{n} 9) has been verified in fig. 3. According to eq^{n} (9) the intercept of this line should be K $[RNH_2]_T$ and the slope DK $[RNH_2]_T$ /V_A. The smallness of the intercept, however, prevented an accurate determination of K $[RNH_2]_T$ from being made. From the slope of this straight line and the literature value of K equal to 2.4 x 10^{-11} (47), the value of the partition coefficient D was determined to be 9.8 x 10^{+3}. This potentiometric method of determining D was checked by deducing the value of the partition coefficient from direct determinations of K_D at different pH values. The experimental procedure for this determination is given in section 4.24 but the theoretical considera-

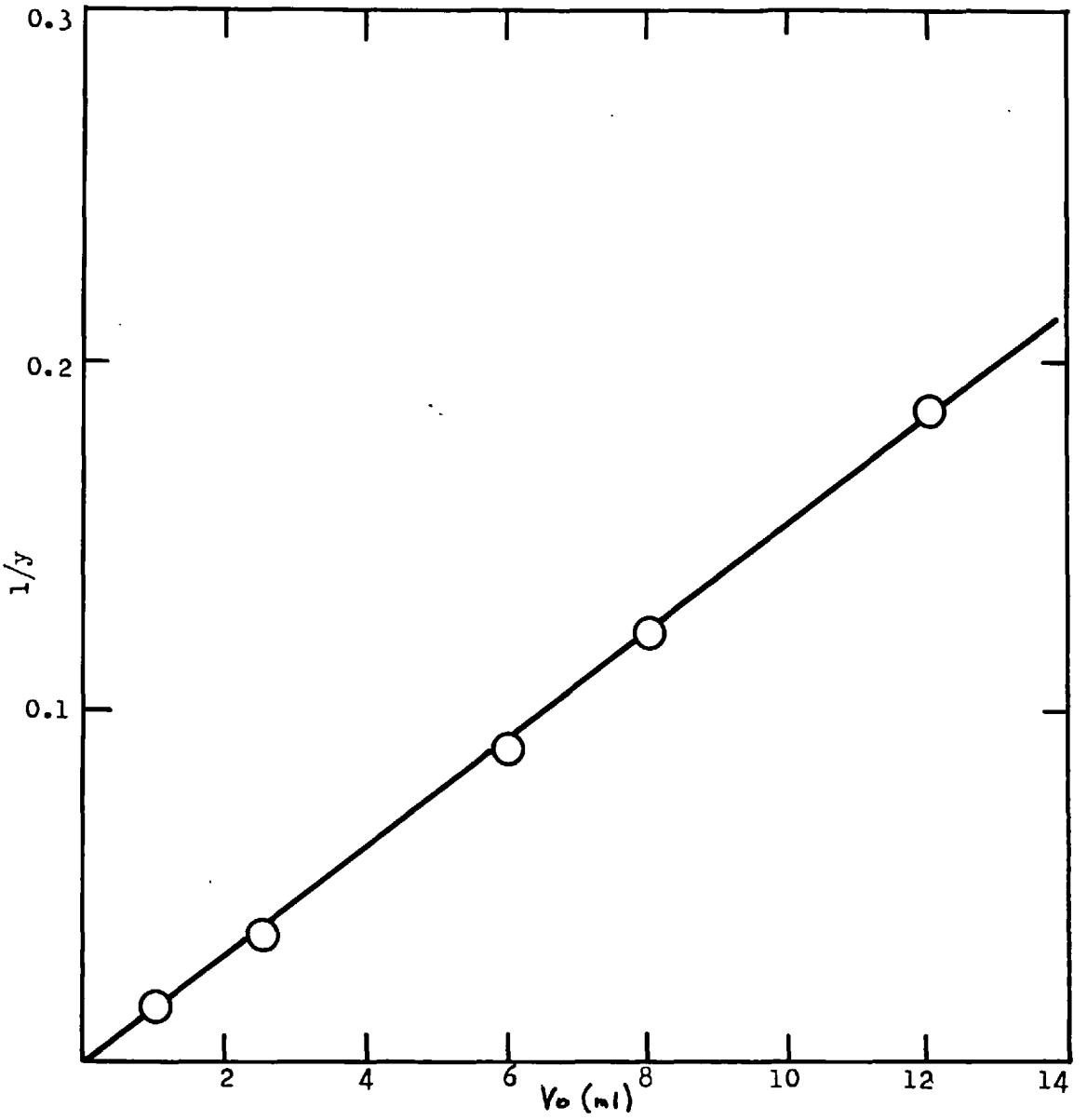

Fig. 3. Plot of 1/y as a function of the volume of the organic phase for dodecylamine.

tions are given here.

The equation relating K_D to $[H^+]$, K and D i.e. eq^n (4) can be simplified and rewritten in the logarithmic form

$$\log K_D = -pH - (\log K + \log D) \qquad (12)$$

if $H^+ \gg K$ i.e. if $pH \ll 10.6$. If K_D is evaluated by direct determination of the concentration of amine in the aqueous and organic phases, and the logarithm of K_D presented as a function of pH, a straight line should result with slope -1 and intercept -(log K + log D). Fig. 4 shows the experimental plot of log K_D against pH. The slope obtained was -1.05 and the value of D calculated from the intercept was $(1.0 \pm 0.2) \times 10^4$. This value of D is in excellent agreement with that found potentiometrically. A value of 1.0×10^4 has been used for D, in all subsequent calculations of the concentration of the various amine species in the system.

Figure 5 illustrates how the concentration of the various amine species varies with change in pH at a total amine concentration of 1.25×10^{-3}M. The volumes of the organic and aqueous phase were 6 ml and 20 ml respectively. Equations (3) and (5) were used to deduce the values of $[RNH_2]_O$ concentrations and equations (2) and (1) were used to evaluate the values of $[RNH_3^+]$ and $[RNH_2]_A$. The calculations showed that the predominant amine species in the system at pH values below 6.5 was the cationic form and above pH 6.5 the neutral form in the organic phase. Deductions of the concentration of neutral amine in the aqueous phase revealed that over most of the pH range

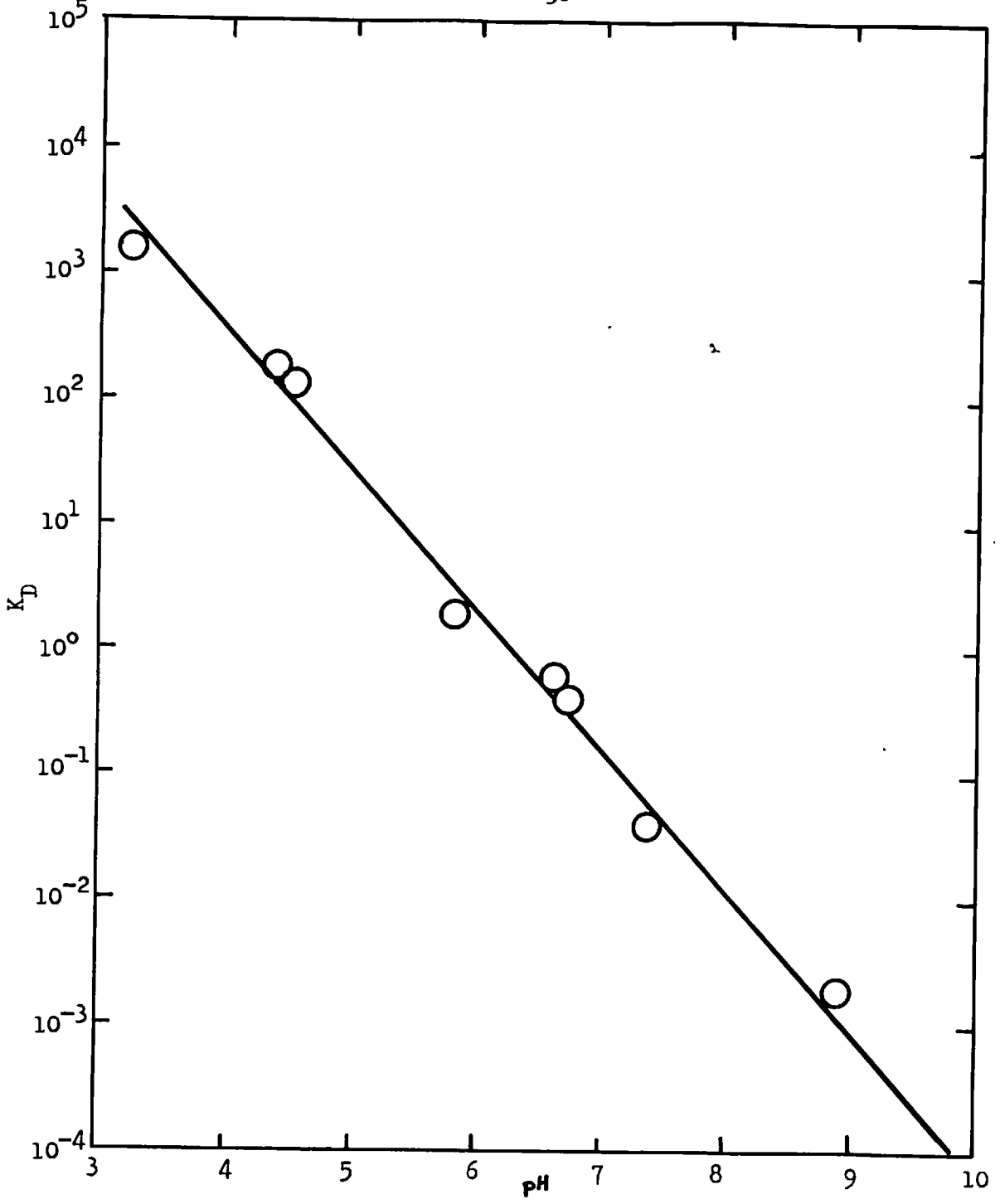

Fig. 4. Variation of K_D (for dodecylamine) with pH.

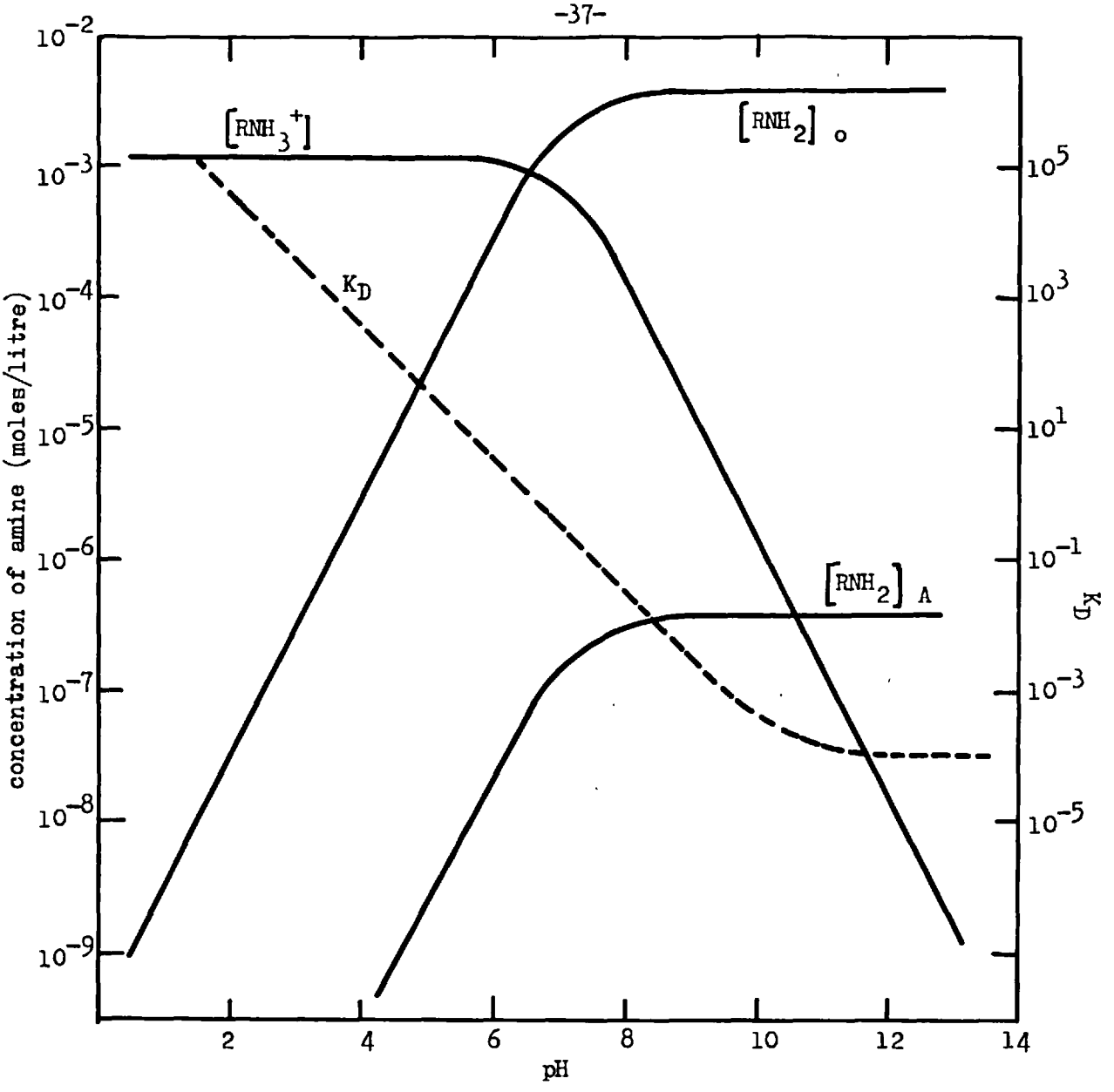

Fig. 5. Concentration of amine species and K_D as functions of pH.

(V_A = 20 ml, $[RNH_2]_T = 1.25 \times 10^{-3}$M; V_o = 6 ml)

the concentration of this species was much lower than any other species. However, at pH 10.6, i.e. the P^K value, and above the concentration of neutral amine in the aqueous phase exceeded that of the cationic amine.

2.42. The results of the iso-octane - dodecanoic acid titrations

The titration results obtained with dodecanoic acid are illustrated in fig. (6). Curves (1) and (2) show the titration of 0.1M hydrochloric acid with 6×10^{-3}M sodium hydroxide and 6×10^{-3}M. NaOH + 2.9×10^{-3}M. RCOOH, respectively. Curves (3) to (9) refer to the titrations conducted in the presence of different volumes of iso-octane. These results were treated in a similar way to those obtained with dodecylamine.

Values of $^1/A$ were determined and plotted as a function of the hydrogen ion concentration. The slopes and intercepts of the linear curves obtained are summarised in Table II for different volumes of the organic phase.

TABLE II

Volume Organic Phase V_O (ml).	Slope (Y) $\times 10^7$	$\frac{1}{Y} \times 10^{-4}$	Intercept
1.0	72.3	13.8	328
2.0	49.6	20.2	340
3.0	33.8	29.6	330
6.0	18.1	52.0	328
10.0	11.8	84.8	330
15.0	10.2	97.6	335

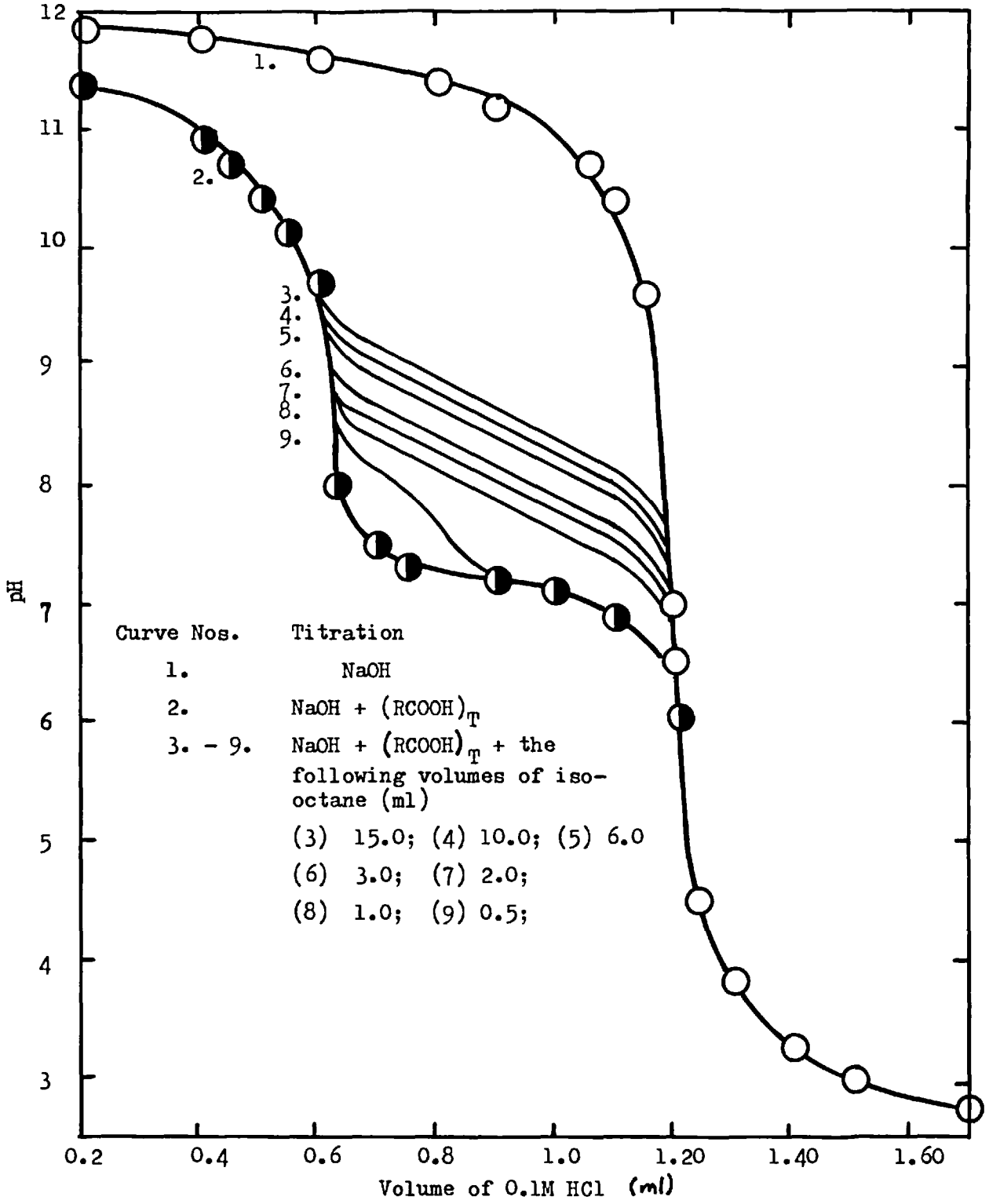

Fig. 6. Titration of dodecanoic acid with HCl in the presence of iso-octane.

The average value of the intercept was (332 ± 9) and this corresponded to a dodecanoic acid concentration of $3.0 \pm 0.1 \times 10^{-3}$M. This value was in excellent agreement with the original strength of the solution. From the slope of the linear relationship obtained when $^1/_Y$ was plotted as a function of V_O the value of D was determined to be $5.6 \times 10^{+3}$. A value of K equal to 10^{-5} was used in this determination.

Values of the distribution coefficient K_D at different pH values were determined by using eq^n (10). Further calculations were made to evaluate the concentration of the various fatty acid species at different pH values. The results of these caloulations for $V_A = 20$, $V_O = 6$ and $[RCOOH]_T = 3.0 \times 10^{-3}$M. are summarised in fig. 7. At pH values below 8.8 the predominant fatty acid species, in the system, was the neutral acid molecule in the organic phase. Above pH 8.8. the anionic species in the aqueous phase predominated. When the pH of the aqueous phase was below 5 i.e. the pH corresponding to the pK value for the reaction $RCOOH \rightleftharpoons RCOO^- + H^+$, the concentration of the neutral acid in the aqueous phase was greater than that of the anion concentration. Above pH 5, the converse was true.

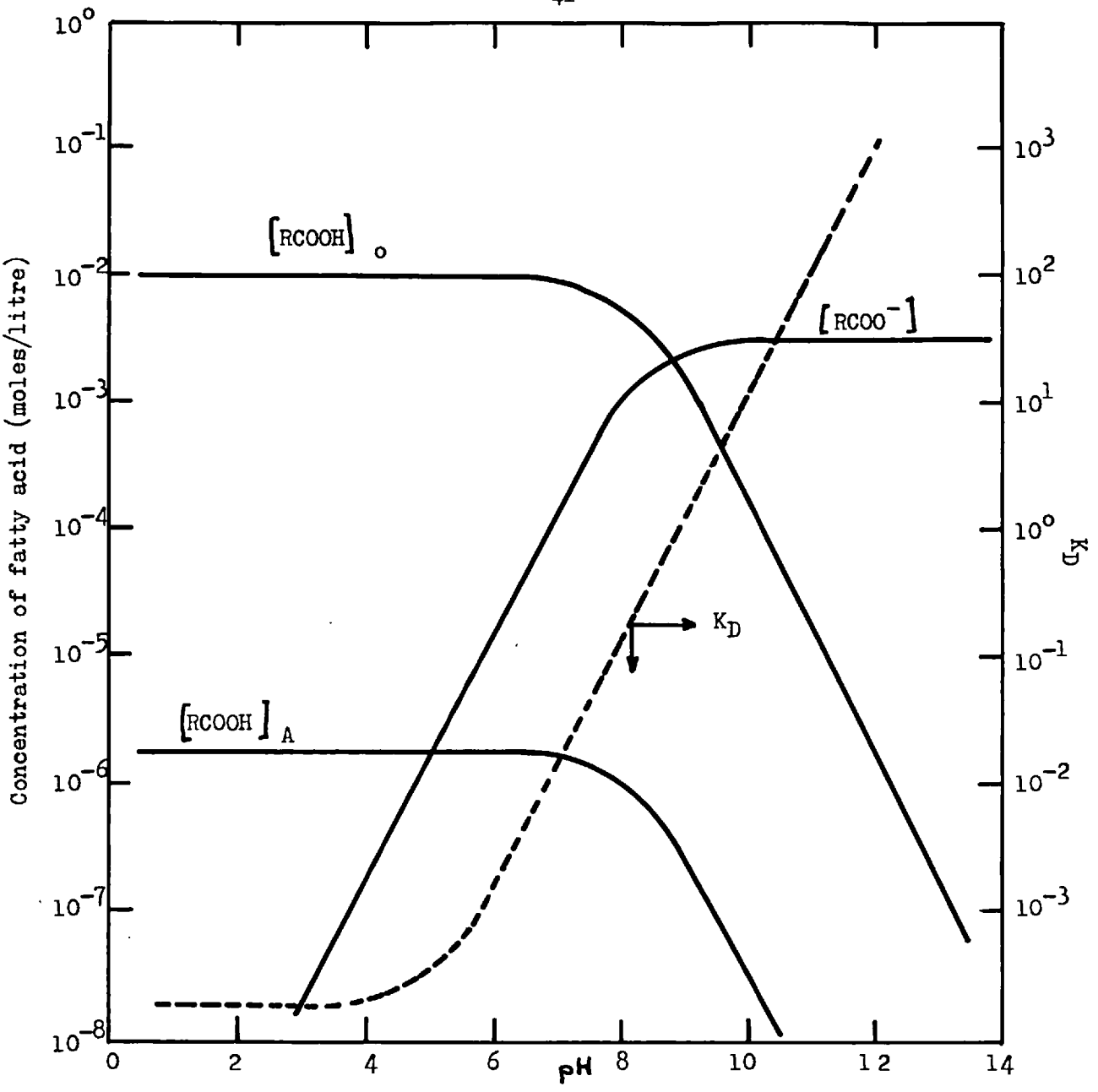

Fig. 7. Concentration of fatty acid species and K_D as functions of pH.

(V_A = 20 ml; $[RCOOH]_T$ = 3.0×10^{-3}M; V_o = 6 ml)

3.00. INTERFACIAL TENSION STUDIES

3.10. General

Molecules in the interior of a liquid are surrounded by the uniform field of force of neighbouring molecules (or ions). A molecule at the liquid interface or surface is however, subjected on one side to the cohesive force of like molecules and on the other side to forces from the molecular constituents of the other phase. If the two phases are immiscible, the net force acting on the surface molecule is directed towards the bulk of the phase from which it originated. To extend the area of the interface separating the two phases, work must be done against the cohesive forces between like molecules, so that molecules can be brought from the bulk phase to the interface. The work done by the surface in increasing the surface area by an amount dA is given by

$$dW = - \gamma \, dA. \qquad (1)$$

Where γ, the interfacial tension, is a force measured in dynes cm^{-1}. Numerically γ is equal to the increase in interfacial energy, expressed in ergs cm^{-2}, when the surface or interfacial area is extended by 1 cm^2.

Consider a two phase system, denoted by phase I and II and illustrated diagrammatically in fig. 8a.

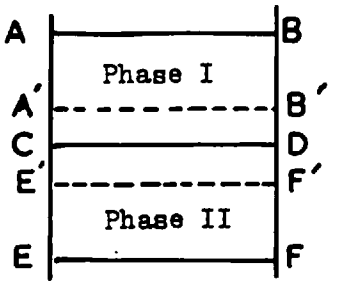

Fig. 8a.

If it is assumed that the number of moles of the i components is, N_1, N_2 ..... N_i, that the pressure is constant and that the two phases are incompressible, the internal energy (dU) of the system is given by the expression

$$dU = \gamma\, dA + TdS + \sum_i \mu_i\, dN_i \qquad (2)$$

in which T = absolute temperature.

S = entropy of the system.

and μ_i = chemical potential of the i^{th} component.

Equation (2) is a homogenous function of the first degree in the extensive properties A, S and N_i. Therefore in accordance with Eulers theorem

$$U = \gamma A + TS + \sum_i \mu_i N_i \qquad (3)$$

Differenciation of eq^n (3) and subtraction of eq^n (2) gives

$$Ad\gamma + SdT + \sum N_i d\mu_i = 0 \qquad (4)$$

which is valid for any part of the system. However, the Gibbs-Duhem relation is valid for every part of phase I and II so that

$$S^{I}.\ dT + \Sigma N_i{}^{I} d\mu_i = 0; \quad S^{II}.dT + \Sigma N_i{}^{II}\ d\mu_i = 0; \qquad (5)$$

Combination of eq^{n} (5) and (4) gives

$$A d\gamma + (S-S^{I}-S^{II})\ dT + \sum_{i}(N_i-N_i{}^{I}-N_i{}^{II}) d\mu_i = 0 \qquad (6)$$

Since eq^{n}(4) and (6) are invariant with respects to volume the quantity $SdT + \sum_i N_i d\mu_i$ will not change if the dimensions of the vessel (fig. 8a)are reduced from ABEF to A'B'E'F'. It is now possible to introduce a mathematical plane near the interface between the two phases. As the transistion from one phase to another is never really discontinuous the location of this plane cannot be accurately indicated. If AB and EF are made to approach CD, a system is obtained which mainly displays the properties of the interfacial zone.

Gibbs (52) assumed that AB and EF were coincident with CD so that the system was comprised of two three-dimensional homogeneous phases and a two-dimensional boundary. In this case the extensive parameters of eq^{n} (6) represent the difference between those of two phases which are homogeneous up to the interface and those of the real system. This difference is caused by the fact that in real systems the extensive parameters do not remain constant up to a mathematical interface, but show gradual changes. For example changes occur in the concentration of the components of the phase near the interface and a number of components are adsorbed at the interface. If N_i is the number of moles of component i in the system and $N_i{}^{I}$ and $N_i{}^{II}$ those of the homogenous systems ABDC and EFDC, the following

is generally true

$$N_i - N_i^{I} - N_i^{II} = N_i^{s}.$$

Similarly $S - S^{I} - S^{II} = S^{s}$.

The quantity N_i^{S} is known as the 'superficial' number of moles in the system ABEF and its value will depend upon the choice of the mathematical delineation between the two phases. Substituting for N_i^{s} and S^{s} in eq^{n} (6) gives

$$A d\gamma + S^{s} dT + \sum_i N_i^{s} d\mu_i = 0. \qquad (7)$$

and dividing this expression by the area A at constant temperature leads to the equation

$$d\gamma = -\sum_i \Gamma_i d\mu_i \qquad (8)$$

Where Γ_i the adsorption or surface excess, in moles cm^{-2} is equal to N_i^{s}/A. Equation (8) is known as the Gibbs equation for adsorption at an interface.

Guggenheim (53) has derived a similar expression to eq^{n} (8) but in his treatment Γ_i may be defined as the amount of component i in a volume element of unit cross-sectional area (parallel to the physical interface) and of sufficient thickness τ to include the whole of the non-uniform region. The results obtained from both these treatments are of course the same, but the Guggenheim method has the advantage that the thermodynamic functions can be applied directly to the three dimensional interface.

For a two component system, such as a solute in a solvent eq^{n} (8) becomes

$$d\gamma = -\Gamma_1 d\mu_1 - \Gamma_2 d\mu_2 \qquad (9)$$

Where 1 denotes the solute and 2. the solvent. If the mathematical delineation is situated in such a position that the excess or deficit of the solvent is zero, then

$$d\gamma = -\Gamma_1 d\mu_1 \qquad (10)$$

In this equation μ_1, the chemical potential can be converted to a more usable parameter by using the thermodynamic relations

$$\mu = \mu^{o} + RT \text{ Ln } C + RT \text{ Ln } f$$

where μ^{o} is the standard chemioal potential and f is the activity coefficient of the solute in the bulk solution. In dilute solutions f is close to unity, and its change with concentration will be zero to a first approximation, so that eq^{n} (10) becomes

$$d\gamma = -RT.\Gamma_i \; d \text{ Ln } C$$

$$\text{or} \quad \Gamma_i = -\frac{1}{RT} \frac{d\gamma}{d \text{ Ln } C} \qquad (11)$$

Equation (11) forms the basis of adsorption measurements at the air-water interface in the presence of a surface-active agent. i.e. an agent that lowers the interfacial tension. The surface tension is measured as a function of the surface-active agent concentration at

constant temperature, and from the curve of γ *vs* log C obtained, the surface excess (Γ) is deduced.

For a three component system containing say an organic phase, an aqueous phase and a surface-active solute eq^{n} (10) becomes

$$d\gamma = -\Gamma_{1\,sol.}\, d\mu_{sol.} - \Gamma_{org.}\, d\mu_{org} - \Gamma_{H_2O}\, d\mu_{H_2O} \quad (12)$$

Equation (10) will only become similar to equation (11) if the assumption is made that the mathematical plane is so positioned that both the surface excess of the water and organic phases are zero. If this assumption is physically reasonable i.e. if adsorption of a solute is confined to a monolayer, then eq^{n} (11) can be used to interpret the interfacial tension results. This treatment makes the further assumption that the solute is only soluble in one of the phases.

In this work the interfacial tensions between iso-octane and aqueous collector solutions have been determined for the purpose of a) substitution in the Young's expression to determine works of adhesion (cf. sect. 1 and 4.13.) and b) obtaining an indication of the adsorption at the oil-water interface. The determinations were made using the drop-volume method used by Gaddum (54). In essence the method consisted of measuring the volume of a drop of one phase which had been formed in the other phase. This was done by delivering drops from a syringe that was operated by a micrometer. In this way the volume of the drop was measured accurately to 0.0001 ml. The interfacial tension was then deduced from the formula

$$\gamma = \frac{F.\ V.\ (\rho_1 - \rho_2)\ g}{R.} \qquad (13)$$

where R = radius of the tip.

g = accelleration due to gravity.

$(\rho_1 - \rho_2)$ = difference in density of the two phases.

V = volume of drop.

and F = factor.

The factor F is dependant on the ratio V/R^3 and values of F were readily obtained by reference to the empirical tables constructed by Harkins and Brown (55).

3.20. Experimental

3.21. Apparatus and Materials

The apparatus was similar to that used by Adam (56) and consisted of a U tube with one arm connected to a water manometer and the other housing a glass capillary (fig. 8b). The U tube was partially immersed in a thermostated water bath controlling at $25 \pm 0.2^{\circ}C$. An 'Agla' micrometer syringe was attached to one end of the glass capillary by a small piece of 'Teflon' tubing. The free end of the capillary had been polished by successively finer grades of silicon carbicle 'paper' so that, its cross-section was at right angles to its length and, there were no edge imperfections when viewed at a magnification of x 20. Measurements of the diameter of

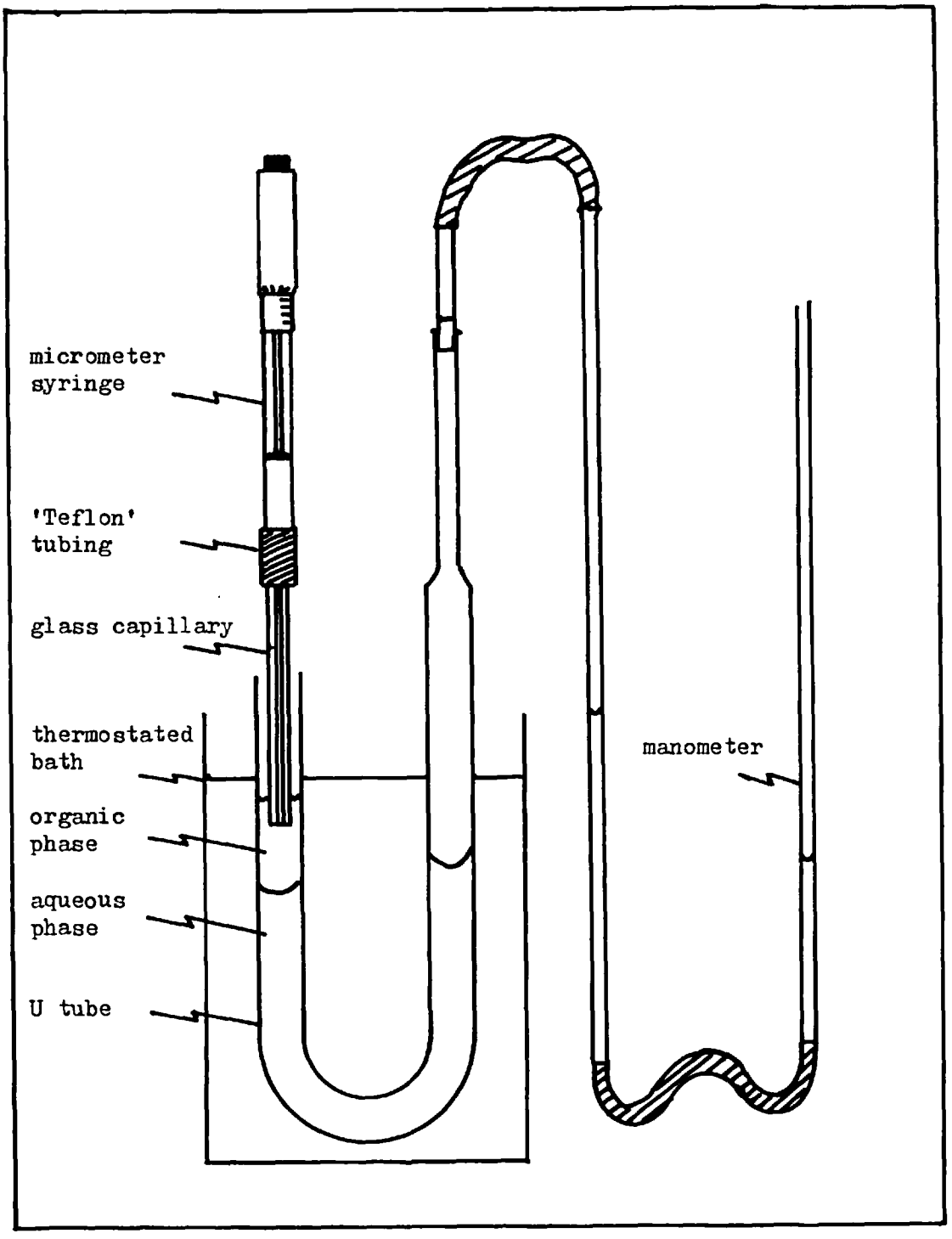

Fig. 8.b. Diagram of Apparatus used for interfacial tension measurements.

the capillary were made by travelling microscope and the mean diameter was 0.553 ± 0.001 cm.

All glassware was cleaned by conc. nitric acid and ethyl alcohol until the surfaces were hydrophilic. The pH was measured using a glass and calomel electrode assembly connected to a Pye 'Dynacap' meter.

The dodecylamine, dodecanoic acid and iso-octane used were the same as those used in section 2. and the sodium dodecyl sulphate was a 'chemically pure' sample supplied by B. Newton Maine Ltd. Conductivity studies on aqueous solutions of the sodium dodecyl sulphate revealed that the C.M.C. of the sample was at 7.80×10^{-3}M and this value was in good agreement with literature values (57) (58). This suggested that the purity of the sample was high.

3.22. Method

Samples of dodecylamine (D.D.A.) and sodium dodecyl sulphate (S.D.S.) were dissolved in hydrochloric acid of sufficient concentration to give a total ionic strength of 6×10^{-3}. Aliquots of 40 ml were taken from these solutions and shaken, in 100 ml conical flasks for 45 minutes under an atmosphere of 'white spot' nitrogen, with 12 ml of iso-octane and sufficient 0.1M sodium hydroxide to give a required pH. The resulting emulsions were centrifuged and after separation of the two phases the pH of the aqueous phase was measured.

With dodecanoic acid (D.A.) the procedure was slightly different.

A solution of D.A. in iso-octane was prepared and 12 ml aliquots of this solution shaken, under an atmosphere of 'white spot' nitrogen with 40 ml of hydrochloric acid and sufficient 0.1M NaOH to give a required pH. The concentration of HCl was chosen so that when all the dodecanoic acid was in the aqueous phase an ionic strength of 6×10^{-3} was obtained. After shaking for 45 minutes the resulting emulsion was treated in a similar way to the D.D.A. and S.D.S. solutions.

A 20 ml sample of the aqueous phase was pipetted into the U tube and 6 ml of the organic phase added to the arm containing the capillary tube. The micrometer syringe was filled with the aqueous phase and placed in position so that the capillary tip was about 0.3 cm below the iso-octane surface. After a thermal equilibration time of 15 minutes a drop of the aqueous phase was formed at the tip of the capillary. The volume of this drop was increased until it began to 'neck' and was then left for an ageing period of 5 minutes, after which the volume was slowly increased until the drop became detached. At the point of the detachment the micrometer reading was recorded and then the procedure repeated. After the detachment of the second drop the difference in micrometer readings between the detachment of the first drop and the second drop was determined. This value corresponded to the volume of a drop. Subsequent drops were formed in such way that 90% of their volume was formed within the first 30 seconds of the drop formation time. The last 10% of their volume was added slowly after the 'ageing' period of five

minutes. In all, ten drop volumes were measured for each determination of the interfacial tension.

The syringe was refilled by moving one of the arms of the water manometer relative to the other so that the phase levels in the U tube rose until the capillary tip was in the aqueous phase. A sample from the aqueous phase was sucked into the syringe by winding back the micrometer. After returning the phase levels to their original positions the drop formation procedure was repeated. During the formation of the drops the end of the capillary was viewed through a cathetometer to ensure that the capillary was completely wetted by the drop.

Preliminary tests were carried out on the different collector solutions to establish the length of the ageing period. In all cases it was found that after five minutes, the determined interfacial tension remained constant. An 'ageing' period or drop formation time of 5 minutes was therefore used for all subsequent determinations. Drop formation times (or ageing periods) of 3 to 5 minutes have been found adequate by other authors (59) (60) (61) for similar systems. The values of the constants substituted into equation (13) were as follows.

g = 980.4

ρ_1 = density of water at 25°C = 0.99708

and ρ_o = density of iso-octane at 25°C = 0.6896.

(This value was determined experimentally).

3.30. Results

The drop volumes obtained with two different samples of water are shown in Table III as a function of drop formation time.

TABLE III

Drop form. time (min.)	Drop Volumes (ml)	
	Sample I.	Sample II.
1.	0.17566	
3.	0.17492	0.18630
5.	0.17470	0.18624
7.	0.17458	0.18626

Sample I was a 'singly' distilled water and sample II was a 'surface-active free' (S.A.F.) water produced from the process of Musslewhite (62) and Read (63). The mean error for the drop volumes of sample I was $\pm$ 0.34% and for the S.A.F. water 0.04%. The drop volumes of the singly distilled water showed a tendency to decrease in size with increase in drop formation time, whereas the volumes of the S.A.F. drops remained constant regardless of the time of formation. Interfacial tensions deduced from these volumes gave 46.4 for sample I after an 'ageing' period of 5 minutes and 49.69 $\pm$ 0.02 dynes cm^{-1} for the S.A.F. water. This latter value was in excellent agreement with that obtained by Aveyard and Haydon (64). The low value found for sample I was attributed to the presence of small amounts of surface-active compounds in the water which gradually adsorbed at the oil-water interface. In the presence of added

surface-active agents i.e. collectors, the water from sample I gave constant drop-volumes after formation times of four minutes. Because of this and the fact that the S.A.F. water was only produced in small quantities, water from sample I was used in all subsequent determinations. Variation of the pH of both samples I and II between pH 3 and 9 did not produce a variation in the interfacial tension.

The interfacial tensions obtained between iso-octane and water at four different constant concentrations of D.D.A., and at varying pH values, are illustrated in fig. 9. The results show that, for a given total concentration of D.D.A. the interfacial tension decreased with increasing pH until a minimum was reached at pH 5.2. Above this pH value the interfacial tension increased to a value slightly lower than that observed at low pH values. An increase in the total D.D.A. concentration produced a shift in the curve correlating the interfacial tension with the pH to lower interfacial tension values. Studies on the equilibrium chemistry of dodecylamine (section 2) showed that the predominant amine species, at low pH values was the cationic amine in the aqueous phase and at high pH values the neutral amine in the organic phase. On using the assumption that only RNH_3^+ was adsorbed at the oil/water interface at pH 2.3 and only RNH_2 from the organic phase at pH 10.0, the interfacial tensions were plotted in fig. 11 (curves (1) and (2)) as functions of the logarithm of the amine concentration in the organic and aqueous phases.

The interfacial tension results illustrated in fig. 10 were those obtained for the iso-octane/water interface in the presence

of three different total concentrations of D.A. As the pH of the system was increased the interfacial tension decreased to a minimum at about a pH of 7.5. A further increase in the pH resulted in a slight increase in the interfacial tension before it finally levelled off at values substantially lower than those obtained at low pH values. In section 2. it was shown that the predominant fatty acid species at low pH values, was the neutral form in the organic phase and at high pH values the anionic form in the aqueous phase. Assuming that only the $(RCOOH)_o$ was adsorbed at pH 2.3 and only the $RCOO^-$ at pH 10.0. the relationships between the interfacial tension and the logarithm of both the concentration of fatty acid in the organic phase and the concentration of carboxylic ions in the aqueous phase, were established as shown in fig. 11 (curves (3) and (4)).

Investigations into the influence of pH on the interfacial tension between iso-octane and water in the presence of sodium dodecyl sulphate are summarised in Table IV.

TABLE IV

(Total concentration of $R.SO_4$ Na. = 1.0×10^{-4}M
Ionic strength 6×10^{-3})

pH	Interfacial tension dynes/cm.
2.20	33.66
3.00	33.66
4.10	34.47
4.80	35.10
5.85	35.28
6.90	35.67
10.30	35.40

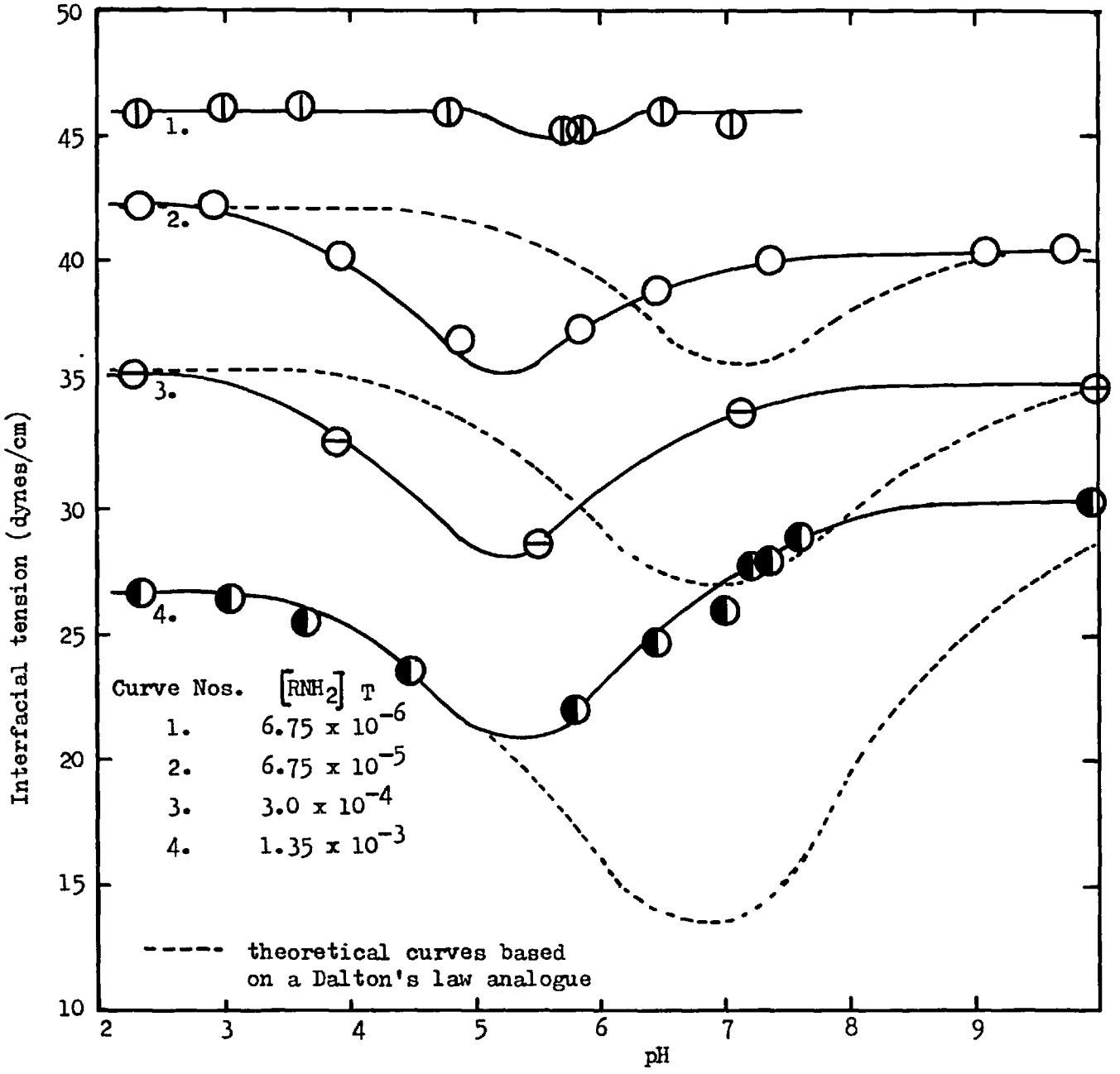

Fig. 9 Interfacial tension as a function of pH at various total amine concentrations (moles litre^{-1}) (ionic strength 6 x 10^{-3})

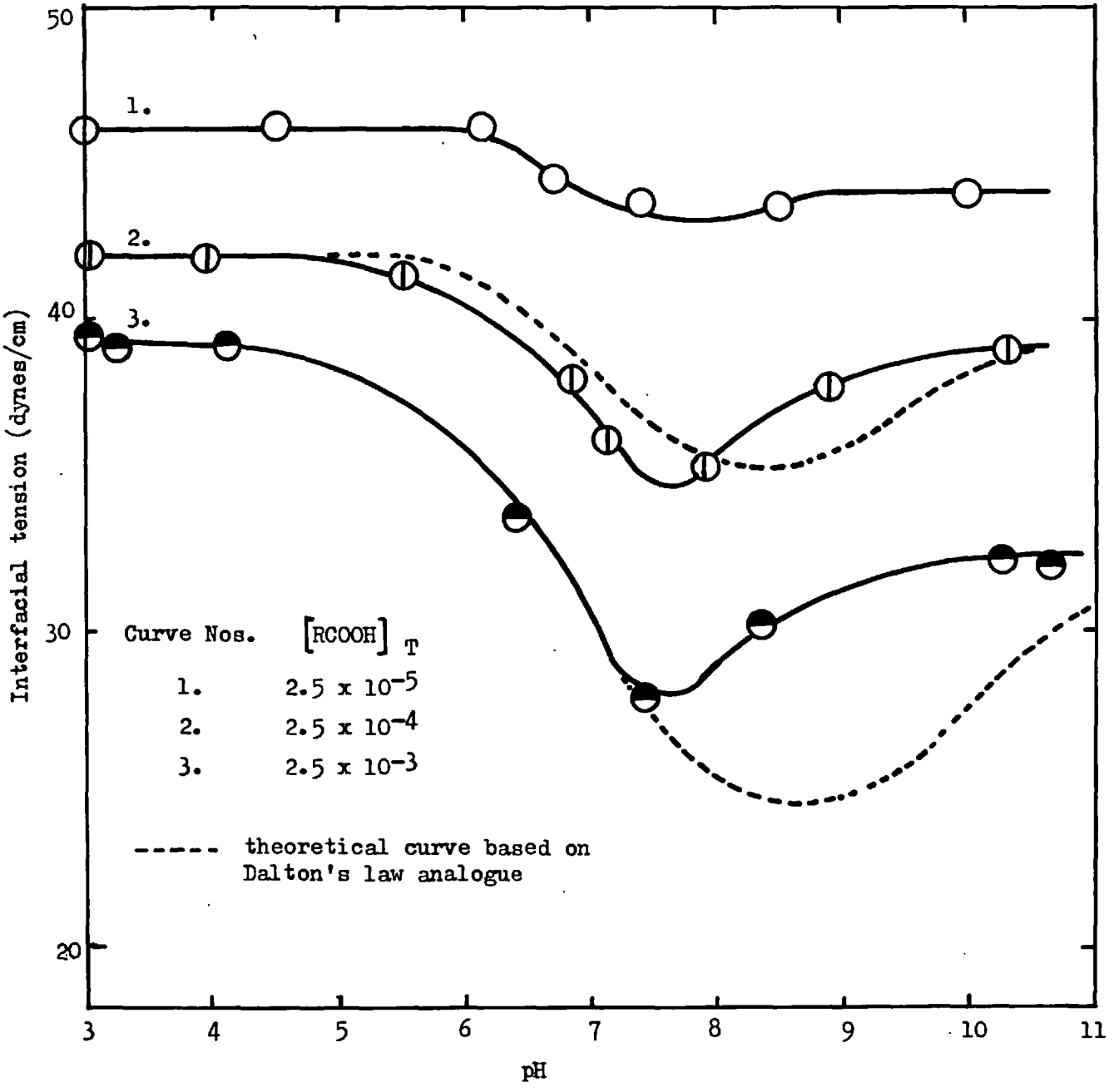

Fig. 10 The effect of pH on the interfacial tension at various total concentrations of dodecanoic acid

(ionic strength 6×10^{-3})

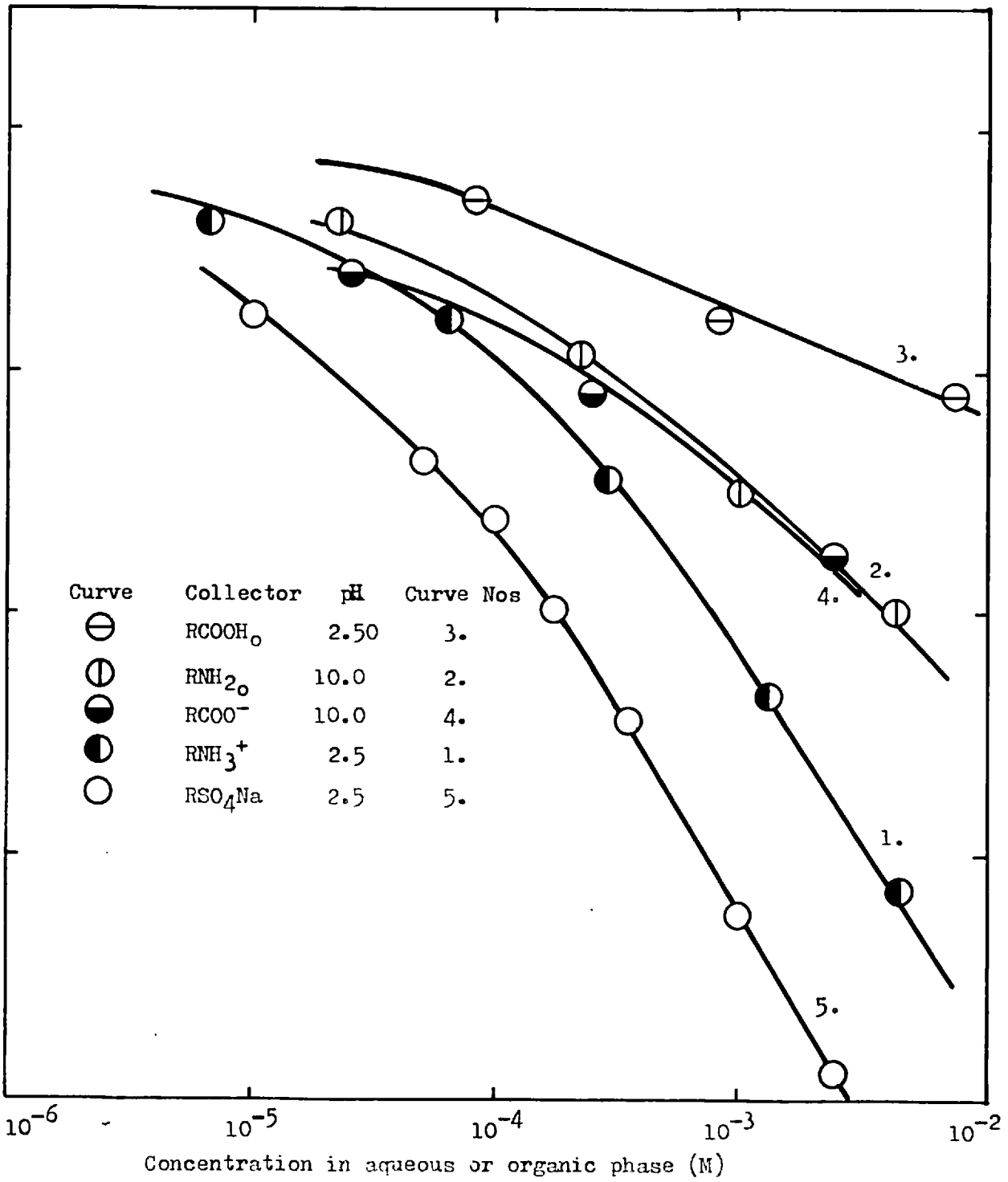

Fig. 11 Interfacial tensions as a function of collector concentration

(ionic strength 6 x 10^{-3})

The results show that as the pH was increased the interfacial tension increased very slightly between approximately pH 4 and 6.5. Cockbain (65) has attributed the slightly lower interfacial tension below pH 5.0 to hydrogen ion adsorption. Analogous to these interfacial tension results are the surface tension results found by Cook and Talbot (66). These authors found that the surface tension increased between pH 5 and 8 and they attributed this to the presence of fatty acid impurities or to a surface hydrolysis reaction.

As the interfacial tension did not change appreciably with variation in pH the interfacial tension was determined as a function of concentration at pH 2.4. The results of these determinations are shown in fig. 11 (curve (5)). Figure 11 shows that the surface active agents in order of decreasing ability to lower the interfacial tension were RSO_4^-, RNH_3^+, $RCOO^-$, $(RNH_2)_o$ and finally $(RCOOH)_o$, the last two species being in the organic phase.

3.40. Theoretical considerations

3.41. Water - sodium dodecyl sulphate - iso-octane system

Although the interfacial tension between iso-octane and water was not studied over a wide range of S.D.S. concentrations, an indication of the surface excess at the oil-water interface can be readily obtained. From electrostatic and kinetic considerations Davies (67) showed that the Gibbs equation in the approximate form

$$- d\gamma = RT\Gamma' d \operatorname{Ln} C \qquad (14)$$

should apply to the adsorption of uni-univalent surface active electrolytes at the oil/water interface, in the presence of excess inorganic salt. In this equation Γ' is the surface excess of the long chain electrolyte and C its molar concentration. The same equation has been derived thermodynamically by Pethica (46), the main assumptions made, in both the derivations, being that the products $\Gamma' d\mu$ for the inorganic salt were negligible compared with $\Gamma' d\mu$ for the surface active species and that the activity of the surface active species was directly proportional to the molar concentration. In agreement with these theoretical conclusions Davies (67) has shown that eq^n (14) holds well for dilute solutions of cetyltrimethylammonium bromide at the oil-water interface in the presence of excess cloride ion.

In the absence of excess inorganic electrolyte an allowance must be made for the counter ions which accompany the long-chain surface active ions. Cockbain (65) has shown by interfacial tension and direct adsorption measurements that the adsorption of S.D.S. at the n-decane/water interface, in the absence of excess electrolyte, can be represented by

$$-d\gamma = 2RT\,\Gamma'\,d\,\mathrm{Ln}\,C. \qquad (15)$$

This equation has also been verified by Haydon and Phillips (58) for the petroleum ether/water interface in the presence of sodium dodecyl sulphate and trimethyl ammonium bromide.

The conditions under which the measurements were made in this

investigation were such that the hydrogen (or sodium) and chloride ions were in excess, although not greatly at high concentrations of S.D.S. Surface excesses of S.D.S. were therefore calculated using eq^{n} (14). The results obtained are summarised in Table V.

TABLE V

Adsorption of S.D.S. at the iso-octane/water interface

Concentration of S.D.S.	Adsorption density
moles/litre	x 10^{10} moles/cm^2
1.0×10^{-5}	1.30
2.0×10^{-5}	1.52
5.0×10^{-5}	1.93
1.0×10^{-4}	2.46
2.0×10^{-4}	2.62
5.0×10^{-4}	3.03
1.0×10^{-3}	3.03
2.0×10^{-3}	3.03

The adsorption of S.D.S. at the oil/water interface increased with increasing S.D.S. concentration until the adsorption density became constant and independent of the concentration at above 5×10^{-4} moles/litre.

A number of authors (68) (69) (70) have shown that, for a given surface-active reagent, a linear relationship exists between the interfacial tension and the logarithm of the concentration for the concentration range from the C.M.C. to a quarter of this value.

This implies that there was an approximately constant adsorption in this concentration range. Van Voorst Vader (71) (72) has termed this constant adsorption the 'saturation adsorption' and found that for S.D.S. adsorbed at the heptane/water interface, the area of the adsorbed ion corresponding to saturation adsorption was 54 $\AA^2$. Klinge and Lange (57) found that the area per ion for a similar system at 50°C was 56 $\AA^2$. Rehfield (59) determined the influence of S.D.S. on the interfacial tension between different n-alkanes and water, in the absence of constant ionic strength and excess electrolyte, and found slightly lower areas per ion at the C.M.C. The value obtained in this work, calculated from a constant adsorption density of 3.03×10^{-10} moles/cm^2, was 55 $\AA^2$. It would thus appear that when the adsorption density becomes constant the area per dodecyl sulphate ion adsorbed at the iso-octane/water interface does not differ from that obtained for the n-alkane/water interface.

An area per sulphate group of 54 - 55 $\AA^2$ is large compared to that found from measurements made from atomic molecules. The ionic surface active species adsorbed at the oil/water interface will be orientated so that the hydrocarbon group points into the organic phase and the polar group into the aqueous phase. As a result of the charge on the polar group the ionic part of the surface active ion will be hydrated. Van Voorst Vader (71) considers that, when two such hydrated groups are brought close together, short range repulsive forces may arise from the closely bounded water. If the charge on the ionic group is such that the bound water is strongly

held then the repulsive forces may give rise to a limit to the number of ions that can be adsorbed at the interface. When this limit is reached no more ions will be adsorbed regardless of an increase in the concentration.

3.42. Water - dodecylamine - iso-octane system

The adsorption of surface-active species at the oil/water interface in the presence of dodecylamine is more complex than the adsorption of S.D.S. at such an interface. It was shown in section 2.00 that at any particular pH, there were two forms of dodecylamine present in the iso-octane/water system: the cationic amine in the aqueous phase and the neutral amine which was distributed between the two phases. Both of these species are likely to be adsorbed at the oil/water interface and the relative amounts of each species at the interface will depend on the pH of the aqueous phase.

Consider the iso-octane/water system with a constant total amount of dodecylamine, and excess chloride ions, in the system. The Gibbs equation for this system can be represented as

$$\partial\gamma = -\sum_i \Gamma_i \partial\mu_i{}_{Aq} - \sum_i \Gamma_i \partial\mu_i{}_{Org} \qquad (16)$$

If the pH of the aqueous phase is increased by small additions of 0.1M NaOH and if it is assumed that the activity coefficients can be approximated to unity and that the interface is such that Γ_{H_2O} and $\Gamma_{\text{iso-octane}}$ are equal to zero, eq^{n} (16) can be expanded to

include all the species in the system.

$$-\partial\gamma = -RT\left\{\Gamma_{R^+}\,\partial(\mathrm{Ln}\,C_{R^+}) + \Gamma_{RA}\,\partial(\mathrm{Ln}C_{RA}) + \Gamma_{RO}\,\partial(\mathrm{Ln}\,C_{RO}) + \Gamma_{H^+}\partial(\mathrm{Ln}\,C_{H^+}) + \Gamma_{Cl^-}\,\partial(\mathrm{Ln}\,C_{Cl^-}) + \Gamma_{Na^+}\partial(\mathrm{Ln}\,C_{Na^+}) + \Gamma_{OH^-}\,\partial(\mathrm{Ln}\,C_{OH^-})\right\} \quad (17)$$

where C denotes concentration in moles litre^{-1} and

$R^+ = RNH_3^+$.

RA = (RNH_2) in aqueous phase.

RO = (RNH_2) in organic phase.

In section 2. it was shown that

$$C_{RA} = \frac{C_{R^+}\,K.}{C_{H^+}} \quad \text{and} \quad C_{RO} = \frac{C_{R^+}\,D.K.}{C_{H^+}}$$

Furthermore if the original concentration of HCl = C_O.

$$C_O - C_{H^+} = C_{Na^+} \quad \text{if } C_O \gg C_{R^+}.$$

$$\therefore \quad -\partial C_{H^+} = \partial C_{Na^+}.$$

$C_{OH^-} = K_W/C_{H^+}$. where K_W = ionic product of water

$$\therefore \partial(\mathrm{Ln}\,C_{OH^-}) = -\partial(\mathrm{Ln}\,C_{H^+}).$$

Substituting in eq^n (17)

$$-\partial\gamma = RT\left\{\Gamma_{R^+}\frac{\partial c_{R^+}}{c_{R^+}} + \Gamma_{RA}\frac{c_{H^+}}{c_{R^+}}\partial\left(\frac{c_{R^+}}{c_{H^+}}\right) + \Gamma_{RO}\frac{c_{H^+}}{c_{R^+}}\partial\left(\frac{c_{R^+}}{c_{H^+}}\right)\right.$$

$$\left. + \Gamma_{H^+}\frac{\partial c_{H^+}}{c_{H^+}} + \Gamma_{Na^+}\frac{\partial c_{Na^+}}{c_{Na^+}} + \Gamma_{Cl^-}\frac{\partial c_{Cl^-}}{c_{Cl^-}} - \Gamma_{OH^-}\frac{\partial c_{H^+}}{c_{H^+}}\right\} \quad (18)$$

Simplification of (18) by expanding the differentials leads to

$$-\partial\gamma = +RT\left\{\left[\Gamma_{R^+} + \Gamma_{RO} + \Gamma_{RA}\right]\frac{\partial c_{R^+}}{c_{R^+}} + \partial(pH)\left[\Gamma_{RA} + \Gamma_{RO} + \Gamma_{OH^-} - \Gamma_{H^+}\right]\right.$$

$$\left. - \Gamma_{Na^+}\frac{\partial c_{H^+}}{c_{H^+}} + \Gamma_{Cl^-}\frac{\partial c_{Cl^-}}{c_{Cl^-}}\right\} \quad (19)$$

Equation (19) indicates how the adsorption and $\partial\gamma$ varies with change in pH at constant temperature. This equation is very difficult to solve because the variables are dependent on each other. If however the pH is kept constant and the total concentration of D.D.A. is varied eq^n (19) will become

$$\partial\gamma = -RT\left\{\left[\Gamma_{R^+} + \Gamma_{RA} + \Gamma_{RO}\right]\frac{\partial c_{R^+}}{c_{R^+}} + \Gamma_{Cl^-}\frac{\partial c_{Cl^-}}{c_{Cl^-}}\right\} \quad (20)$$

If the ionic strength is constant and the concentration of the chloride ions is much larger than that of the cationic amine ions equation (20) will become

$$\partial\gamma = -RT\left[\Gamma_{R^+} + \Gamma_{RO} + \Gamma_{RA}\right]\frac{\partial c_{R^+}}{c_{R^+}} \quad (21)$$

In section 2.00 it was shown that at low pH values most of the D.D.A. was in the aqueous phase in the cationic form, so that to a first approximation the equation

$$\partial \gamma = -RT.\left[\Gamma_{R^+}\right] \frac{\partial C_{R^+}}{C_{R^+}} \qquad (22)$$

is valid at these pH values. This is the equation for the adsorption of ionic surface active species at the oil-water interface in the presence of excess inorganic salt. Similarly it was shown that at high pH values most of the D.D.A. was in the organic phase so that

$$\partial \gamma = -RT\ \Gamma_{RO}\ \frac{\partial C_{RO}}{C_{RO}} \qquad (23)$$

Equation (23) represents the adsorption of a neutral surface-active species at the oil/water interface.

Although eq^n (19) describes the relationship between $\partial\gamma$, adsorption density, pH, and cationic amine concentration, it does not readily explain the shape of the experimental curves obtained in fig. 9. An alternative approach is to assume that there are no interactions between the two adsorbed species so that an interfacial analogue of Dalton's law of partial pressures can be applied. If it is assumed that the adsorption of neutral amine from the aqueous phase is negligible, then

$$\Delta \gamma_T = \Delta \gamma_{RNH_3^+} + \Delta\gamma_{RNH_2O} \qquad (24)$$

Where $\Delta\gamma_T$ is the total interfacial tension lowering due to both the cationic amine $\Delta\gamma_{RNH_3^+}$ and the neutral amine in the organic phase $\Delta\gamma_{RNH_{20}}$.

Calculations were made of the concentrations of (RNH_3^+) and $(RNH_2)_O$ at different pH values and the interfacial tension lowering for each of these components was deduced from the γ vs log C_{R^+} and γ vs log C_{RO} curves (fig. 11). A theoretical curve of interfacial tensions against pH was then obtained by subtracting $\Delta\gamma_T$ from the interfacial tension between pure water and iso-octane. The theoretical curves obtained are plotted with the experimental results in fig. 9.

The significant difference between the theoretical and experimental results was that the theoretical curve was displaced to more alkaline pH values, and that at the highest concentrations of dodecylamine, the theoretical minimum interfacial tension was much lower, than the experimental value. The pH value corresponding to the theoretical minimum appeared at the pH where the RNH_3^+ concentration in the system was equal to the RNH_2 concentration in the organic phase. Differences between experimental interfacial tension results and those predicted from ionization considerations are not uncommon (73) (74). Danielli (74) has suggested that the interfacial tension curves of some surface active mixtures can be displaced from that predicted from ionization data because the pH at the interface is different from that in the bulk. A number of

authors (73) (75) (76) have shown that theoretically the surface pH, $(pH)_S$, should be equal to

$$(pH)_{bulk} + \frac{\epsilon \psi}{2.3.kT.}$$ where ψ is the surface potential,

ϵ the electronic charge, k the Boltzman's constant and T the absolute temperature. Only when $\psi = 0$ will the surface and bulk pH values be the same, and, if ψ is negative, $pH_s < pH_b$ because the charge will attract hydrogen ions into the vicinity of the surface.

At high pH values, in the presence of dodecylamine, the surface pH is expected to be approximately equal to the bulk pH, because the adsorption of charged amine will be negligible. Only the neutral amine will be adsorbed and as a result the net charge will be very small. Similarly at low pH values the surface pH will be approximately equal to the bulk pH because although the surface will be highly charged, due to the adsorption of cationic amine, there will be far more chloride counter ions present than hydroxyl ions. This means that the theoretical curves were conducted on the assumption that $pH_s = pH_b$. throughout the pH range. The surface potential of the iso-octane/water interface will be positive due to the adsorption of cationic amine and hence pH_s will be greater than pH_b. It is therefore suggested that if the experimental results had been based on $(pH)_S$ instead of $(pH)_b$ a better correlation between the experimental results and theoretical results would have been obtained.

At high concentrations of D.D.A. the interfacial tension corresponding to the minimum value (fig. 9) was lower for the theoretical curve than for the experimental curve. This indicated that to a certain extent there were interactions between the adsorbed amine species. It was not possible to deduce the nature of these interactions. Cockbain and Mc.Mullen (60) used the Daltons law analogue to determine whether there were molecular interactions at the water/decane and water/benzene interfaces in the presence of soap in the aqueous phase and alcohol in the organic phase. It was found that whereas Dalton's law was applicable to the benzene/water interface, it was not for the decane/water interface. The deduction was therefore made that the molecular interactions at the decane/water interface were considerable compared to those at the benzene/water interface.

At concentrations of cationic amine above 4×10^{-4}M an approximately linear relationship between γ and log C_{R^+} existed (fig. 11). The slope of this linear function corresponded to an adsorption density of 2.7×10^{-10} moles cm^{-2} and an area per adsorbed ion of 62 Å^2. Although it was not possible to ascertain whether the adsorption of neutral amine from the organic phase reached a constant value it was possible to deduce that over the concentration range studied the cationic amine was more strongly adsorbed than the neutral amine.

When the interfacial tension was plotted as a function of log. C_{R^+} at pH 5.2. i.e. the pH corresponding to the experimental minimum

interfacial tension, a linear relationship was obtained at concentrations greater than 2×10^{-5}M. The slope of this line corresponded to an adsorption density of 2.0×10^{-10} moles cm^{-2} and an area per adsorbed species of 83 $\AA^2$. It would therefore appear that when constant adsorption is reached for the mixed film the area per ion is considerably larger than that for the ionic species in a ionic film.

3.43. Water - dodecanoic acid - iso-octane system

A number of authors have determined the effect of different concentrations of fatty acids on the interfacial tension between an organic and a aqueous phase (77) (78) (79). Unfortunately most of these investigations were carried out under the pH conditions where the fatty acid was either completely unionised or completely ionised. Only a few authors (79) (73) (80) have studied the interfacial tension throughout the pH range and in these investigations it is not certain whether the phases were equilibrated in the presence of the fatty acid.

The interfacial tension results obtained between iso-octane and water in the presence of dodecanoic acid were treated in the same way as the dodecylamine results. A relationship, similar to eq^n (19) was obtained between $\partial \gamma$ and the adsorption of the various fatty acid species. At low pH values the Gibbs expression became:

$$\partial \gamma = -RT \; \Gamma_{RCOOH_0} \; \partial \left(Ln \, C_{RCOOH_0} \right) \qquad (25)$$

and at high pH values

$$\partial\gamma = -RT.\ \Gamma_{RCOO^-}\ \partial\,(Ln\ C_{RCOO^-}) \qquad (26)$$

Where $RCOOH_o$ denotes the fatty acid in the organic phase and $RCOO^-$ the carboxylic ion in the aqueous phase.

Using the Dalton's law analogy, the theoretical curves shown in fig. 10 were constructed and these curves show that at low concentrations of dodecanoic acid there was a fairly good agreement between the calculated and experimental results. At high concentrations of dodecanoic acid there was a disagreement between the deduced and experimental curves in the pH range 7.5 to 10.0. In the presence of carboxylic ions the surface potential (Ψ) will be negative and, if the equation $(pH)_s = (pH)_b + \epsilon\Psi/2.3KT.$ is valid, the surface pH will be lower than the bulk pH. At low and high pH values $(pH)_s$ is expected to be approximately equal to $(pH)_b$ and this means that both the theoretical and experimental curves were based on the assumption that $(pH)_s = (pH)_b$ throughout the pH range. In the case of the iso-octane/water system in the presence of cationic amine ions it was shown that the $(pH)_s$ was likely to be larger than $(pH)_b$ and it was suggested that if the experimental results had been based on $(pH)_s$, a better agreement between the experimental and theoretical curves would have been obtained. In the presence of dodecanoic acid, however, such a suggestion does not appear to be valid. If the experimental data were based on $(pH)_s$ instead of $(pH)_b$ the experimental curve would be displaced to more acid pH values, i.e. away

from the theoretical curve.

Too much emphasis cannot be placed on the apparent discrepancy between the experimental and theoretical curves because it must be realised that at pH 10.0 eq^{n} (26) is not strictly valid. Both eq^{n} (26) and the plot of log. ($RCOO^{-}$) vs γ were based on the assumption that the concentration of neutral acid in the organic phase was negligible. Reference to fig. 7 (section 2) shows that this is not so. For example consider a concentration of $RCOO^{-}$ at pH 10.0 of 2.5×10^{-3}M. The concentration of fatty acid in the organic phase in equilibrium with the $RCOO^{-}$ is 1.60×10^{-4}M. Reference to fig. 11 shows that $(RCOOH)_{0}$ of 1.60×10^{-4}M lowers the interfacial tension by approximately 5 dyne cm^{-1}. If this correction were taken into consideration, it would decrease the discrepancy between the experimental curve and the deduced curve. Before an accurate assessment of these results could be made the interfacial tension would have to be determined over a wider range of dodecanoic acid concentrations.

4.00. MINERAL - COLLECTOR SOLUTION - ISO-OCTANE SYSTEM

4.10. INTRODUCTION

4.11. Extraction Studies

In this investigation mineral particles were concentrated at the oil/water interface of an oil in water emulsion. In principle emulsions are of two types, oil in water (O/W) or water in oil (W/O) depending on which phase is the continuous one. The continuous phase for a W/O emulsion is the oil phase and for an O/W emulsion the aqueous phase. The major parameters which control the type of emulsion obtained when two immiscible liquids are shaken together are, the relative volumes of the two phases, the concentration and nature of the emulsifying agent, the nature of the organic phase, the electrolyte constituents of the aqueous phase and the mechanism of agitation.

Emulsifying agents may be placed in three main classes; the highly surface active compounds of soaps and detergents, the macromolecular compounds such as gums and starches, and finely divided insoluble solids. In this research finely divided solids modified by ionic surface-active agents have been used to stabilize O/W emulsions.

a) The influence of the phase volume ratio

Ostwald (81), using the fact that uniform spheres of equal diameter are in the position of closest packing when they occupy

74.02% of the total assembly volume, supposed that inversion or breaking of an emulsion resulted when the internal phase volume exceeded 74% of the total volume. Consequently, it was considered that, at internal phase volumes between 26% and 74% both O/W and W/O emulsions were possible and that below 26% and above 74% only one form could exist. Although there seems to be some justification (82) for this theory both Pickering (83) and Becher (84) have produced O/W emulsions with the internal phase volume greater than 95% of the total volume.

If the spheres are not of equal diameter, small spheres concentrate in the interstices of larger spheres so that the maximum internal volume becomes greater than 74%. Still larger volumes can be filled if the spheres are deformable. Manegold (85) has taken into account the extreme cases where the emulsions appear like polyhedral foams and has constructed a diagram relating the type of emulsion to the phase volume ratio. The basis of this diagram is however the original theory of Ostwald.

b) Stabilization of emulsions by ionic emulsifiers

The nature and concentration of an ionic emulsifier greatly affects the type of emulsion obtained. Clowes (86) found that the alkali metal soaps gave O/W emulsions whereas generally speaking the divalent and trivalent soaps gave W/O emulsions. Wellman and Tartar (87) found that with polyvalent metal soaps O/W and W/O emulsions were obtained depending on the conoentration and

temperature. The effect of concentration on the type of emulsion formed was shown by King (88) for the system benzene/water in the presence of sodium oleate. At low concentrations of sodium oleate a W/O emulsion was obtained and at higher concentrations an O/W emulsion resulted.

The early theories of emulsion stability, which were either based on the geometry of the adsorbed emulsifier ion (89) or the accompanying interfacial tension lowering at the oil/water interface (90), are reviewed by Becher (84) and Clayton (91). Perhaps the most useful empirical law to come from this early work was that of Bancroft (92) who suggested that the phase in which the emulsifier was more soluble would be the continuous phase. In recent years more importance has been placed on the properties of the interfacial film, with reference to its thickness, viscosity, composition, and electrical characteristics.

Consider an oil drop of an O/W emulsion stabilized by sodium dodecyl sulphate. An anionic charge will reside on the oil drop surface because of the adsorption and orientation of the dodecyl sulphate ion so that the hydrocarbon chain penetrates the organic phase and the anionic sulphate group points into the aqueous phase. Similarly if a cationic emulsifier was used the droplet surface would acquire a net positive charge. The presence of a layer of adsorbed anions or cations at the oil/water interface will give rise to an electrical double layer.

Both Verwey (93) and van den Tempel (94) have considered the

two double layers existing at the oil/water interface. One double layer being in the aqueous phase and the other in the organic phase. Verwey (93) indicated that in the absence of emulsifiers the double layer in the aqueous phase was so small that when two drops were brought together coalescence resulted. In the presence of ionic emulsifiers, however, the double layer on the aqueous side of the interface becomes considerable and according to van den Tempel (94) it may become so large that the capacity of the double layer in the organic phase can be neglected. If this is the case it is possible to apply the 'Theory of Stability of Lyophobic Colloids' as developed by Derjaguin (95) and Landau (95) and by Verwey and Overbeek (96) to the stabilisation of emulsions against flocculation and coagulation. Although an emulsion might flocculate or coagulate this does not mean that the drops will coalesce. Coalescence will depend on the nature of the interfacial film and the ease with which it can be ruptured.

Although a number of theories have been postulated to explain the various characteristics of emulsions, no one theory has satisfactorily explained all the characteristics. Gilbert (97) has indicated that four postulates can be stated for the stabilisation of emulsions by ionic surface active agents and these can be summarised as

a) an interfacial film must be formed between the aqueous and organic phase, which acts either as a mechanical or electrical barrier to the coalescence of drops.

b) molecular interaction between the molecules at the interface gives rise to a complex interfacial film (98).

c) the interfacial film is formed by adsorption from one or both phases and must be in equilibrium with each, and

d) the physico-chemical structure of the interface will depend on the distribution of these surface active molecules between the two phases.

This distribution will depend on the length and structure of the hydrocarbon chain in the molecule, the nature of the polar groups and their interaction at the interface, the type of organic phase, the composition of the aqueous phase, the temperature and the phase volume ratio.

c) Stabilisation by Solid Emulsifiers

The first extensive investigation of emulsions stabilized by solids was conducted by Pickering (99) who found that the basic sulphates of iron, copper, nickel and zinc in moist conditions acted as emulsifying agents for the formation of petroleum oil in water emulsions. Pickering also observed that materials such as dried calcium carbonate, lead arsenate and fine clays could stabilize emulsions. Briggs (100) noted that ferric hydroxide, arsenic sulphide and silica produced O/W emulsions and that carbon black, rosin and lanolin stabilized W/O emulsions. Cheesman and King (101) were able to demonstrate that with a given solid they could obtain both types of emulsion merely by varying the technique of shaking.

A survey conducted by King, Berminster and Thomas (102) showed that the necessary requirement for the stabilisation of an emulsion was a gelatinous structure and a basic nature. In recent years considerable work has been done by Muckerjee and Srivastava (103) (104) on the stabilisation of emulsions by solids. The solids used were the hydroxides and oxides of thirty five different metals. All the emulsions obtained were of the O/W type and the greatest stability was obtained when using moist, highly gelatinous, fine precipitates and when the metal was polyvalent. Although the emulsions were coarse they were still fairly stable and unaffected by electrolytes and acids.

Srivastava (105) deduced that the thickness of the interfacial film for emulsions of kerosene in water stabilized by metal hydroxides and carbonates was of colloidal rather than molecular dimensions. He concluded that although a special thickness of film was a prerequisite of emulsion stability there was no direct relationship between film thickness and stability and that the criteria which had a direct bearing on the stability, was the surface of the solid and the nature of the ions adsorbed there.

In section 1.00. it was shown that the particles must exhibit a substantial contact angle at the three phase (oil/solid/water) boundary for the stabilisation of an emulsion. In this research collectors were used to modify the contact angle so that the minerals did in fact concentrate at the oil/water interface. However it must be realized that the collectors which modify the mineral surface

will also be adsorbed at the oil/water interface (section 3.00) and will act as emulsifiers.

d) Creaming of emulsions

All dilute emulsion whether stabilized by solids or any other emulsifier will cream, if the continuous phase is truly fluid. Creaming is the rise of the dispersed droplets under the action of gravity, the droplets remaining in close proximity to each other but not coalescing. According to Stokes the sedimentation rate of spherical particles in a viscous liquid is given by

$$U = \frac{2gr^2 (d_1 - d_2)}{9 \eta} \qquad (1)$$

Where U is the rate of sedimentation, g the accelleration due to gravity, r the particle radius, $(d_1 - d_2)$ the difference in density of the two phases and η the viscosity of the continuous phase. Although eq^n (1) does not give the true (106) creaming or sedimentation rate of an emulsion, unless all the drops are of uniform size, it does show that the creaming rate will be high when the droplets are large. The large difference between d_1 and d_2 in the present work, where water and iso-octane was used, lead to rapid creaming of the O/W emulsions.

For the system iso-octane/quartz/water it can be readily shown that an oil drop of radius r_1 will pick up quartz of effective radius $0.55\ r_1$ before sedimentation occurs. The percentage by weight of

its own weight which a drop will pick up under these conditions is given by $(0.55)^3 d_3\ 100/d_1 = 63\%$. Where d_3 = density of quartz and d_1 the density of iso-octane. In other words an iso-octane drop will cream if the amount of quartz on the surface is less than 63% of the weight of the drop.

In this research an iso-octane in water emulsion stabilized by mineral particles and collector reagents was obtained and allowed to cream. After a short period the emulsion creamed into two distinct layers, one consisting of oil droplets coated with mineral particles and the other consisting of an aqueous phase containing free mineral particles. By separating these two layers it was possible to ascertain the percentage of solid concentrated at the oil/water interface. The ratio of the organic phase volume to the aqueous phase volume was kept constant at 3:10 i.e. the organic phase was less than 25% of the total volume. It was thought that by keeping the organic phase volume low an O/W emulsion would be obtained under most of the conditions encountered.

4.12. Electrokinetic Studies

a) The electrical double layer

When a particle is immersed in a liquid its surface acquires an electrical charge which is caused mainly by the dissociation of ionogenic groups in the surface or the preferential adsorption of ions. As the system as a whole is electrically neutral an equal charge of opposite sign to that on the surface must be present

in the surrounding liquid. In consequence of the attraction between unlike charges, counter ions remain in the neighbourhood of the solid/liquid interface, forming an electrical double layer.

The double layer was originally thought by Helmholtz (107) to consist of two planes of equal and opposite charge separated by a constant distance of molecular dimensions. One plane being at the solid surface and the other a small distance away in the liquid. Gouy and Chapman (108) independently modified the Helmholtz concept of the double layer by assuming that one layer of charge was smeared over the solid surface and that an equal and opposite charge of ions (counterions) was unequally distributed throughout the aqueous phase as point like charges. According to this theory the relation between surface charge σ coulombs per cm^2, total double layer potential Ψ_o, total concentration of symmetrical electrolyte, n ions per cm^{-3}, and the valency of the ions v is given by

$$\sigma = \sqrt{\frac{2n \epsilon kT.}{\pi}} \quad \text{Sinh} \quad \frac{ve \Psi_o}{2kT.} \qquad (2)$$

Where ϵ = dielectric constant of the liquid.

k = Boltzmann constant.

e = electronic charge.

and T = absolute temperature.

When the potential is small ($\ll$ 25 mv) the exponentials can be expanded and eq^n (2) becomes

$$\sigma = \sqrt{\frac{2 \epsilon nk}{\pi}} \quad \frac{ve \psi_o}{2 kT.} = \frac{\epsilon \psi_o}{4 \pi} \sqrt{\frac{8 \pi nv^2 e^2}{\epsilon kT.}} \qquad (3)$$

The term $(8 \pi nv^2 e^2 / \epsilon kT)^{\frac{1}{2}}$ is known as the Debye-Huckel function χ. which is associated with the size of the ionic atmosphere round an ion. The reciprocal of χ is generally called the ionic radius and is taken as a measure of the double layer thickness. Substitution of χ into eq^n (3) gives

$$\sigma = \frac{\epsilon \chi}{4 \pi} \psi_o \qquad (4)$$

which shows that the surface charge (when $\psi_o \ll 25$ mV) is proportional to the surface potential and that the double layer behaves as a parallel plate condenser with distance $1/\chi$ between the plates. This equation is analogous to the original theory of Helmholtz.

Other useful relationships obtained from the Gouy-Chapman treatment are that for small values of ψ_o the potential (ψ) at a distance x from the surface, is given by

$$\psi = \psi_o e^{-\chi x.} \qquad (5)$$

and for ve $\psi_o / kT \gg 1$ and ve $\psi / kT \ll 1$

$$\psi = \frac{4 kT.}{ve} \theta \; e^{-\chi x.} \qquad (6)$$

Where $\theta = \frac{\exp.\ (ve\ \psi_o/2kT) - 1}{\exp.\ (ve\ \psi_o/2kT) + 1}$

Equation (5) shows that, for small surface potentials, the potential falls off exponentially with increase in distance from the solid surface.

The Gouy-Chapman treatment of the double layer is essentially, based on the Boltzmann distribution law. This treatment, however, breaks down at small values of κx when ψ_o is large. For example if ψ_o is 200 mV in a 0.1M uni-univalent electrolyte the surface concentration according to the Boltzmann law should amount to

$$n = n_o \exp.\ \frac{(ve\ \psi_o)}{(kT)} \approx 300M \qquad (7)$$

Where n_o is the concentration of electrolyte in moles per litre. Clearly this is an unrealistic value.

Stern(109) was the first to realize that the inadequacy of the Gouy-Chapman treatment was due to the rôle played by the dimensions of the ions in the layers nearest the surface. Stern suggested that the hydrated counter ions could only approach to within a few angstroms from the solid surface and as a result they formed an immobile layer at a distance δ from the surface. Beyond this layer which is generally known as the Stern layer, the Gouy-Chapman theory is applicable. Sternalso considered the possibility of the specific adsorption of ions and assumed that these would

be located close to the surface and within the Stern layer.

Grahame (110) supplies evidence that the Stern layer can be divided into two regions which he designates the 'inner' and 'outer' Helmholtz planes. The outer Helmholtz plane is considered to be the locus of nearest approach of the centres of the hydrated counter ions and the inner Helmholtz plane the locus of nearest approach of the centres of specifically adsorbed ions. In the absence of specific adsorption, no centres of ions occur between the outer Helmholtz plane and the surface charge.

According to the Stern model of the double layer the total potential drop ψ_o is divided into a potential ψ_ζ over the diffuse part and $\psi_o - \psi_\zeta$ over the molecular condenser i.e. that part of the double enclosed between the edge of the Stern layer and the surface charge. The total capacity of the double layer C_t will be equivalent to the capacity of the diffuse layer (C_d) and the capacity of the molecular condenser (C_m) placed in series.

$$\text{Therefore } C_t = \frac{C_m \; C_d}{C_m + C_d} \qquad (8)$$

In dilute solutions where the double layer thickness is large, the capacity of the double layer is determined mainly by the value of C_d and is therefore a function of the total electrolyte concentration at constant double layer potential (ψ_o). With increasing electrolyte concentration the double layer is compressed until

eventually $C_d = 0$. The double layer then reaches a constant capacity C_m independant of the concentration.

The specific adsorption of ions into the Stern layer can be represented by the expression

$$n = 2r\ n_o\ \exp.\ (-W/kT) \qquad (9)$$

Where r is the radius of the unhydrated ion, n the number of ions per cm^2 in the layer and n_o the number of ions per cm^3 in the bulk. The term W represents the work done in bringing an ion to the inner Helmholtz plane. It can be split into an electrical and non-electrical term so that

$$W = ve\psi_\delta - \phi \qquad (10)$$

The introduction by Sternand Grahame, of ϕ into the Boltzmann equation allows for the forces (such as van der Waals and chemical forces) which may exist between the adsorbed species and the solid surface.

The total potential drop ψ_o across the double layer is generally a function of the concentration of ions known as potential determining ions. These ions are usually the same as those which oonstitute the crystal lattice of the solid. Thus for barium sulphate they are Ba^{2+} and SO_4^{2-} and for the oxide minerals H^+ and OH^- ions. The term potential determining ion implies that a change in their concentration will bring about a change in the total potential difference $\Delta\phi$ between the two bulk phases in contact

with each other. The total potential difference between two phases is given by the equation

$$\Delta\phi = \psi_o + \chi \qquad (11)$$

Where χ represents that part of the total potential difference determined by the orientation of dipoles and polarisations at the surface. Only on the assumption that this χ potential is not affected by changes in electrolyte concentration will d ψ be equal to d $\Delta\phi$. If this assumption is fulfilled the potential difference across the double layer will be determined by the ooncentration of potential determining ions.

If the potential determining ion concentration is changed, then the corresponding changes in the thermodynamic potential ($\Delta\mu$) and the surface potential are given by

$$\Delta\mu = kT \text{ Ln } a/a_1 \qquad (12)$$

$$\text{and } \Delta\psi_o = \psi_o - (\psi_o)_1 = \frac{\Delta\mu}{ve} = \frac{kT}{ve} \text{ Ln } a/a_1 \qquad (13)$$

Where a denotes the activity of the potential determining ion. If a_o is the activity at the zero point of charge (z.p.c.) of the solid where $\psi_o = 0$ then equation (13) becomes

$$\psi_o = \frac{kT}{ve} \text{ Ln } \left(\frac{a_1}{a_o}\right) \qquad (14)$$

and ψ_o can be calculated for any concentration of the potential determining ions provided that the concentration corresponding to the z.p.c. is known. Equation (14) is analogous to the Nerst expression used in electrode systems.

In addition to the potential determining ions which change ψ_o there are some ions known as indifferent ions which change ψ_δ without changing ψ_o. Ions which reverse the sign of ψ_δ without changing the double layer potential are known as surface active indifferent electrolytes. This reversal of sign shows that the ions are adsorbed by some force other than that of coulombic attraction. Figure 12 shows the double layer diagrammatically for two sets of conditions a) in the absence of surface active indifferent electrolytes and b) in the presence of specifically adsorbed ions.

In fig. (12) a new potential, the zeta potential (ξ) has been included. When the liquid moves relative to the charged solid only part of the ionic atmosphere surrounding the particle will move with it because some of the innermost layers of ions near the surface will be fixed by strong electrical or chemical forces. The potential difference located in the mobile part of the double layer is called the zeta potential. This potential, between the zone of shear and the bulk of the liquid, is the only potential that can be measured by electrokinetics. The zeta potential will of course be dependant on the position of the zone of shear but generally it is assumed to be so close to ψ_δ that substitution of ξ instead of ψ_δ into the double layer equations does not incur any great inaccuracies.

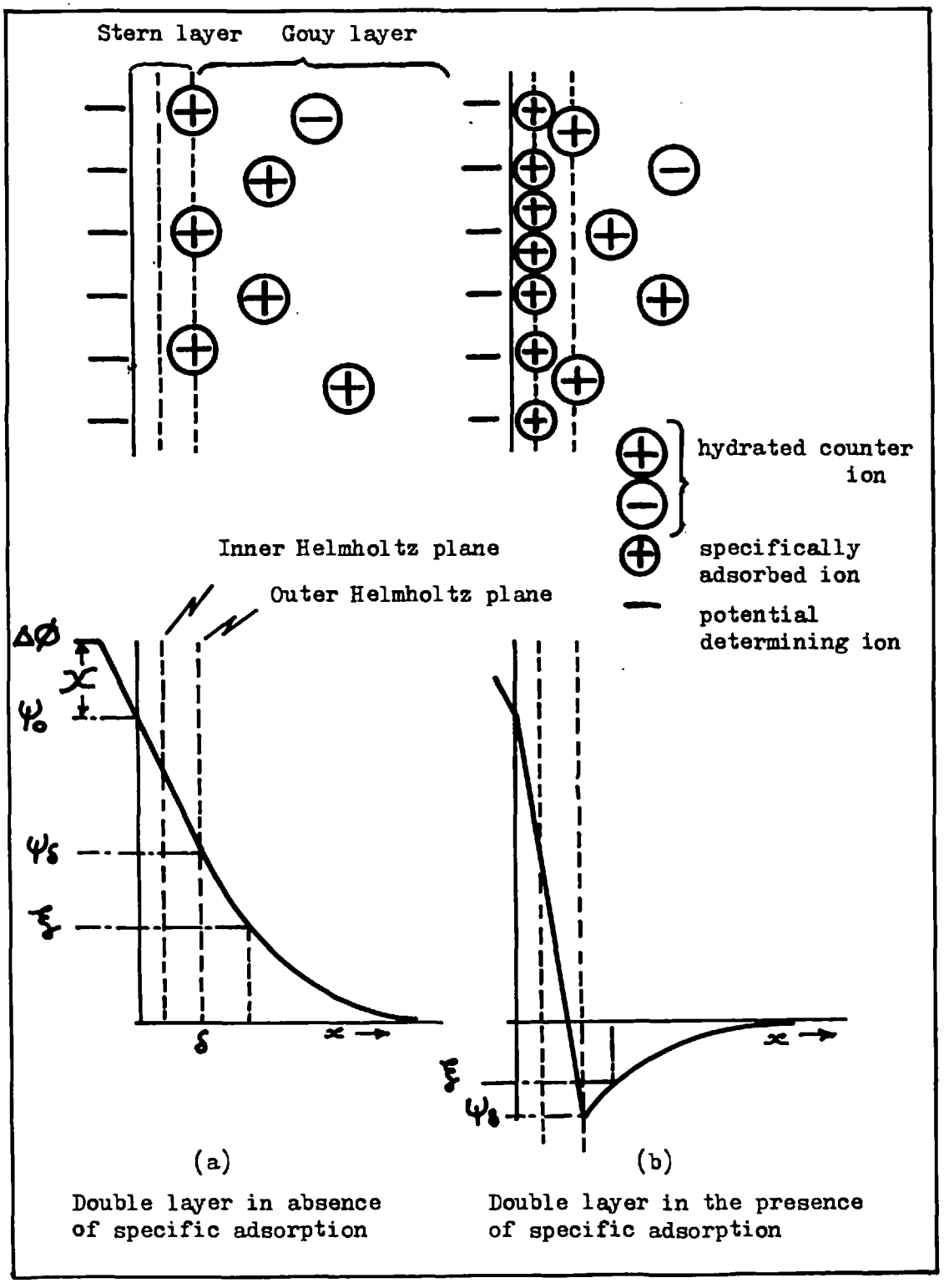

Double layer in absence of specific adsorption

Double layer in the presence of specific adsorption

Fig. 12

The adsorption of collector ions onto a mineral surface may change the zeta potential of the mineral by specific adsorption of the ions. It is therefore of importance to establish the relationship between the zeta potential and the potential determining ion concentration and also the collector ion concentration. When a mineral is charged it is reasonable to expect that the primary mechanism of adsorption of a collector ion will be that of coulombic attraction between the charged surface and the oppositely charged ion in solution. The determination of the zeta potential will not only indicate the surface characteristics of the mineral, but will also show whether the ions are specifically adsorbed or not.

Zeta potentials are determined from four different electrokinetic effects: streaming potentials, electro-osmosis, sedimentation potentials and electrophoresis. The method of electrophoresis has been used in this work because of its suitability to fine mineral particles.

b) Electrophoresis

When an electrical field is applied to a suspension of charged particles they migrate towards one of the electrodes. The direction of migration will depend on the net sign of the charge at the shear plane and the polarity of the electrodes. If the particles are negatively charged, they will migrate to the positive electrode and if positive they will move toward the negative electrode. Such movement of particles under the influence of an applied electric field is called electrophoresis.

The relationship between the electrophoretic mobility, defined as the velocity of migration of the particle under unit potential gradient, and the zeta potential is dependant on the ionic strength, viscosity, dielectric constant of the liquid phase and the particle size and shape. When the particle is a non-conducting sphere of radius much smaller than the thickness of the double layer (i.e. $1/\chi$) the relationship between the zeta potential and the electrophoretic mobility is given by the Debye-Huckel equation (111)

$$u = \frac{D\zeta}{6\pi\eta} \qquad (15)$$

Where u = electrophoretic mobility.

D = dielectric constant.

and η = viscosity.

The derivation of this equation includes Stokes law for flow in a viscous medium and the classical definition of the capacity of a spherical condenser. Both of these assumptions are only valid if the particle is spherical. However, it can be shown that in general

$$u = \frac{\zeta D C}{\eta} \qquad (16)$$

Where C a constant, depends on the shape and orientation of the particles. In the special case of rod shaped particles for migration in directions parallel and perpendicular to the orientation direction, equation (16) becomes

$$u = \frac{\xi D}{4\pi\eta} \quad \text{and} \quad u = \frac{\xi D}{8\pi\eta} \tag{17}$$

respectively.

When the radius of curvature at any point of the particle is large compared to the thickness of the double layer, the particle plus double layer can be treated as a condenser with distance $1/\chi$ between the plates. The equation derived from this treatment is generally referred to as the Helmholtz - Smoluchowski (112) equation

$$u = \frac{D\xi}{4\pi\eta} \tag{18}$$

In the derivation of equation (18) a number of assumptions are made and these are listed below,

a) The usual hydrodynamical equations for the motion of viscous fluid may be assumed to hold both in the bulk of the liquid and within the double layer.

b) The liquid at the particle surface has the velocity of the particle and the velocity gradient begins at the surface.

c) The applied field may be taken as simply superimposed on the field due to the electrical double layer

and d) The thickness of the double layer is small compared to the radius of curvature at any point on the surface.

Henry (113) has discussed the validity of these assumptions and using assumptions (a), (b) and (c) with the further assumption that the eleotrical distribution in the ionio atmosphere is of the

Debye-Huckel type, he has shown that the general equation

$$u = \frac{D\zeta}{6\pi\eta} \quad f_1 (\chi a) \qquad (19)$$

should apply for all non-conducting particles. The values of $f_1 (\chi a)$ which depend on the shape, size and orientation of the particles are tabulated in 'Electrophoresis of proteins' (114). Determinations of $f_1 (\chi a)$, commonly known as Henry's factor, can be readily obtained from Henry's equation

$$u = \frac{D\zeta}{6\pi\eta} \left[1 + \frac{(\chi a)^2}{16} - 5\frac{(\chi a)^3}{48} - \frac{(\chi a)^4}{96} + \frac{(\chi a)^5}{96} \right] \qquad (20)$$

For $\chi a \gg 1$ $\quad f_1 (\chi a) = 1.5$ and eq^n (20) reduces to that of Smoluchowski.

For $\chi a \ll 1$ $\quad f_1 (\chi a) = 1.$ and eq^n (20) approximates to the Debye-Huckel equation.

Overbeek (115) and Booth (116) independently corrected the Henry's equation for the influence of the relaxation effect on the particle velocity. The relaxation effect arises from the fact that when a particle suspension is subjected to an electric field, the outer part of the double layer moves in a direction opposite to that of the particle, thus deforming the original symmetry of the double layer. By electrio conduction and diffusion the double layer tends to restore its symmetry but a short time known as the 'relaxation time' is necessary before this can happen. As a result the double layer tends to lag behind the particle, giving rise to an electrio

field oppositely directed to the applied field, which tends to slow down the particle. Overbeek's simplified electrophoretic equation for a particle in a symmetrical electrolyte is

$$u = \frac{D\xi}{6\pi\eta}\left[f_1(\kappa a) - v^2\left(\frac{e\xi}{kT}\right)^2 f_3(\kappa a) - \frac{(P_+ + P_-)}{2e}\,\frac{DkT}{6\pi\eta e}\left(\frac{e\xi}{kT}\right)^2 f_4(\kappa a)\right] \tag{21}$$

Where $f_1(\kappa a)$ is Henry's function, the values of $f_3(\kappa a)$ and $f_4(\kappa a)$ were tabulated by Overbeek, and P_+ and P_- are the frictional constants for the cation and anion respectively.

The following conclusions can be derived from this equation

1) When $\xi < 25$ mV. the relaxation effect is not important over the whole range of (κa).

2) For small values and large values of (κa) the relaxation affect may be neglected.

3) For intermediate values of (κa) the relaxation effect is an important correction factor, especially when ξ is not small. Recently Wiersema, Loeb and Overbeek (117) have established a computer programme to determine the relaxation correction factor in the range $0.2 < \kappa a < 50$. This range covers part of the range outlined in conclusion (3) above.

Booth (118) and Henry (119) independently extended Henry's equation by including a correction factor to take into account the surface conductivity effect. The surface conductivity is due to the fact that the electrical double layer contains a higher concentration of ions than the bulk of the solution. However, both

Booth (116) and Overbeek (115) allowed for the diffuse double layer conductivity in their corrections for the relaxation effect, and so a separate correction is not required.

c) The Microscope Electrophoresis Method

The microscope method of electrophoresis involves the direct observation of microscopically visible particles as they migrate in an electric field. The particles are suspended in a solution and placed in a small flat or cylindrical transparent cell over which a potential is applied. The time for a particle to cover a given distance, as measured with a graticule in the eyepiece of a microscope, is determined by the operator for each individual particle. From this the particle velocity is determined, and from the current, conductivity of the solution, and cross sectional area of the cell the electric field strength is evaluated.

Microscope electrophoresis apparatuses have in common a cell into which a microscope can be focussed, an electrode system, and a system by which the cell is filled, emptied and closed. In the work described in section 4.2.3. a flat rectangular cell was used and the following theoretical considerations are related to the movement of particles in a rectangular cell.

If an electric field is applied to a liquid in a closed glass cell, the liquid nearest the cell wall will move towards one of the electrodes because of the charge and hence the double layer residing at the cell wall. This electroosmotic streaming of the liquid past

the cell walls cannot be eliminated by any known method and so it is imperative that it be taken into account. The electro-osmotic effect is shown in fig. 13.

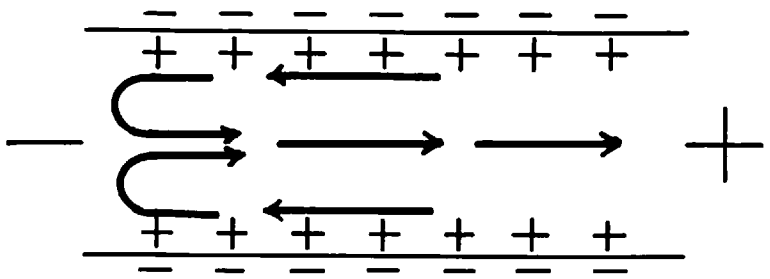

Fig. 13 Electro-osmosis in closed tube

Since the net flow of liquid in the cell must be zero the flow of liquid moving along the sides of the cell must be balanced by a flow of liquid in the opposite direction at the centre of the cell. At some particular depth in the cell, therefore, there should be a position where the liquid velocity is zero, i.e. the electro-osmotic flow equals the return flow. Clearly, if the microscope is focussed on these levels where the liquid velocity is zero (stationary levels) the true mobilities of the particles can be determined.

If it is assumed that the ratio of cell width to thickness is large then the following hydrodynamics can be applied to show the variation of liquid velocity as a function of cell depth. Consider a point at distance x from the centre of the cell having a liquid velocity Vw and a velocity gradient of $\frac{dVw}{dx}$. From the definition

of viscosity the viscous force (F_1) at this point will be

$$F_1 = \eta \frac{dVw}{dx} \quad \text{Area.} \tag{22}$$

where η is the viscosity and the area is equal to the width of the cell (y) times its length (l). Equation (22) therefore becomes

$$F_1 = \eta \, l \, y \quad \frac{dVw}{dx} \tag{23}$$

If one considers a layer of cell length l, cell width y and thickness dx, the viscous force on this layer will be

$$F_2 = \eta \, l \, y \quad \frac{d}{dx} \left(\frac{dVw}{dx} \right) \quad dx \tag{24}$$

The effect of the osmotic streaming in the closed cell will be to produce a pressure difference P between the ends of the cell. Therefore the electro-osmotic force on the liquid element of length l, width y and thickness dx will be given by Py.dx. This force must be equal and opposite to F_2. Equilibrating these two forces the expression

$$\frac{P}{l} = \left(\frac{d^2Vw}{dx^2} \right) \tag{25}$$

is obtained. If it is assumed that the total thickness of the cell is 2a and that x varies from -a to +a integration of equation (25) gives

$$Vw = \frac{P}{2\eta l} \, x^2 + cx + b \tag{26}$$

where c and b are constants of integration. This is an equation of a parabola and since x is measured from the centre of the cell, symmetry requires that C = 0. At the points where $x = \pm a$ the liquid velocity (Vw) will be equal to the osmotic velocity (V_o). Applying these conditions to eq^n (26) gives

$$b = V_o - \frac{P}{2\eta l} a^2$$

and
$$V_w = \frac{P}{2\eta l} (x^2 - a^2) + V_o \qquad (27)$$

The total flow of liquid in the cell must be zero so that

$$\int_{-a}^{+a} V_w \, dx = 0 \qquad (28)$$

Substituting (27) in (28) and integrating

$$\int_{-a}^{+a} V_w dx = \left[\frac{P}{6\eta l} x^3 - \frac{a^2 x P}{2\eta l} + V_o x \right]_{-a}^{a}$$

$$= 0$$

Solving this expression for P

$$P = \frac{3\eta \, l \, V_o}{a^2} \qquad (29)$$

Substitution of eq^n (29) into (27) gives

$$V_w = \frac{V_o}{2}\left[\frac{3x^2}{a^2} - 1\right] \qquad (30)$$

The observed velocity of the particles within the electrophoretic cell will be equal to the sum of the liquid velooity (V_w) and the velocity of the particles relative to the liquid (V). Thus

$$V_{ob} = V + V_w \qquad (31)$$

From eq^n (30) the value of x is 0.578a when $V_w = 0$. This means that if the microscope is focussed on levels corresponding to 0.21 and 0.79 of the whole depth of the cell the effect of V_w will be eliminated and $V_{obs} = V$.

In the cell used in this work the ratio of cell width to depth was not large, and although for a thin cell a parobolic velocity profile is obtained (114), it was necessary to use Komagata's theory (120). Acoording to this if a_o is the position of the stationary levels ($V_w = 0$) in terms of practical depth from the top of the cell, and B is the ratio of cell width to cell thickness, then

$$a_o = \frac{1}{2} + \sqrt{\frac{1}{12} + \frac{32}{\pi^5 B}} \qquad (32)$$

Thus for the particular cell used in this work where B = 10, a_o = 0.194 the stationary levels occurred at 0.194 and 0.806 of the total cell depth.

The electrophoresis method was used to determine the zeta potential of fine hematite and quartz as a function of pH and collector concentration.

4.13. Contact Angle and Adsorption Studies

a) Contact Angles

In section 1.00. the Young's equation was used to show the interfacial tension and contact angle conditions necessary for mineral particles to concentrate at the oil/water interface. According to the Young's equation

$$\gamma_{so} - \gamma_{sw} = \gamma_{ow} \cos\theta \qquad (33)$$

the cosine of the contact angle at the three phase point of contact water/solid/oil, should have one well defined value equal to $(\gamma_{so} - \gamma_{sw}) / \gamma_{ow}$; where γ_{so}, γ_{sw} and γ_{ow} are the interfacial tensions solid/oil, solid/water and oil/water respectively. Actually it is found in many experiments that the value of the contact angle depends on whether one phase, say the oil phase, is receding or advancing over the solid surface.

This hysteresis effect has been of considerable interest for a number of years especially for contact angles measured at the air/solid/water, line of contact. Originally it was thought by Edser (121) and Sulman (122) that the extent of the hysteresis determined whether the mineral was floatable or not. It now seems likely that these workers were in error in thinking this. There may be an indirect correlation between floatability and hysteresis, but many other factors are involved.

Two basic explanations have been offered for the hysteresis effect. According to some authors (123) (124) roughness of the

surface causes apparent contact angles that are different from the receding and advancing angles although the local contact angle may be completely determined by equation (1). Wenzel (125) has pointed out that solids have rough surfaces on the sub-microscopic scale. Quantitatively the average roughness of the surface is measured by r the ratio of the real to the apparent surface area. Wenzel's relationship

$$\text{Cos}\ \bar{\theta} = r\ \text{Cos}\ \theta_e \qquad (34)$$

where $\bar{\theta}$ is the apparent contact angle, connects the observed and equilibrium contact angles.

The other explanation of hysteresis, which was promoted by Cassie (126) suggests that the solid/air interface after the liquid has just receded is different from the same interface when no liquid has previously covered it. De Bruyn, Overbeek and Schuhmann (127) consider that for each pair of phases there is an equilibrium composition belonging to the corresponding interface. Gaudin (128) has suggested that at the contact line between the three phases there is a join between the three adsorbed layers. Accordingly for an air bubble in contact with a polished mineral surface the composition of the solid-gas layer will be different from that of the solid-liquid layer. Gaudin indicates that if the bubble is laterally displaced, there should be a rearrangement of the adsor bed species but as this is not a spontaneous process the leading and trailing contact angles will be different. Gaudin and coworkers (129) (130)

have suggested a similar reason for the hysteresis at solid/water/oil lines of contact.

It should be said that although a number of attractive models have been constructed to account qualitatively for hysteresis effects no really quantitative results have been obtained. Many theories of contact angle hysteresis appear to be speculative.

b) The Relation between Contact Angle and Adsorption

The contact angle at the air/water/solid interface is a measure of the hydrophobicity of the solid surface. When the contact angle is zero (as measured through the aqueous phase) the surface is said to be hydrophilic and when greater than zero the surface is said to have obtained a degree of hydrophobicity. A completely hydrophobic surface is obtained when the contact angle is 180°. These three cases are shown in Fig. 14

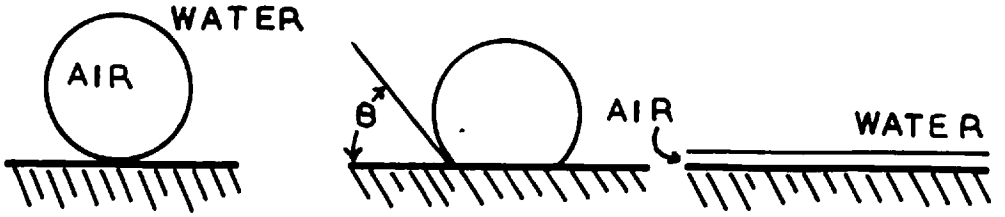

Fig. 14.

It must be realized that just because a surface is hydrophobic, it need not necessarily be oleophilic (131). Although in Fig. 14 (b) the surface is shown to have a degree of hydrophobicity substitution of an oil drop instead of an air bubble might result in no contact (or even greater contact).

In conventional flotation systems the surface of a solid is given a degree of hydrophobicity by the adsorption or reaction of collectors at the mineral/water interface. It would therefore seem likely that a simple relationship should exist between the degree of hydrophobicity (or the contact angle) and the amount of collector on the mineral surface.

A number of authors (132) have shown that although the value of the contact angle and adsorption results plotted as a function of the logarithm collector concentration are similar, no direct simple relation exists between the contact angle and the adsorption density. Some authors (133) (134), however, have indicated a linear relationship between either the contact angle and the adsorption density or the cosine of the angle and the adsorption density.

It has been the tradition in the past to assume that the adsorbed species is uniformly distributed over the surface of the solid. Figures have then been quoted of the adsorption density that corresponds to the formation of a monolayer. In recent years however the validity of this practice has been questioned. Autoradiography (135) studies have revealed that the collector is adsorbed in 'patches' and that there is the possibility of multilayer adsorption

even before the completion of a monolayer.

Although large amounts of collector can be adsorbed the resulting surface need not necessarily be hydrophobic. Contact angles will reveal whether this is so or not and they will also indicate the orientation of the adsorbed species at the interface. Recently Billet and Ottewill (136) have shown that although adsorption, of dodecylpyridinium bromide on silver iodide, did not change appreciably over a wide range of concentration, the contact angle did. The authors attributed this change in contact angle to a change in the orientation of the adsorbed species. Other workers (137) (138) have found similar results for different systems and they have interpreted them in a similar way.

4.20. EXPERIMENTAL

4.21. Materials

a) Hematite

Large lumps of a polycrystalline Swedish hematite were divided into two fractions, one fraction being for extraction, electrokinetic and adsorption studies, and the other for contact angle determinations. The fraction for extraction studies etc. was crushed in a laboratory jaw crusher and pulveriser, and the size fraction - 52 + 72 mesh, retained and cleaned by magnetic separation and wet tabling. After drying at 120°C, the hematite was stored in a bottle with a ground glass stopper. A microscopic examination of this sample revealed that the main impurity present was quartz at less than 0.05%.

When required a 25g sample of the - 52 + 72 mesh hematite was ground in a vibratory agate mill for a period of 35 minutes. The ground sample obtained was 100% - 44μm and 50% - 10μm as determined by the Andreasen pipette. The specific surface areas, as determined by the B.E.T. method, of the hematite samples used for the evaluation of the dodecylamine and sodium dodecyl sulphate adsorption densities, were 2.92 metre^2 and 3.48 metre^2 respectively. Calculation of the mean particle diameter from the surface areas gave approximately 0.35 μm. An agate mill was used for the grinding because of the ease with which grease and other impurities could be removed from the grinding 'surface' by the use of chromic-sulphuric acid. The

- 44μm hematite was stored under vacuum in the presence of silica gel crystals.

The lumps of hematite to be used for contact angle studies were ground by a fine diamond wheel into blocks about 15 mm long, 15 mm wide and 5 mm thick. After a microscopic examination of the surfaces the purest and most homogeneous surface was polished by successively finer grades of silicon carbide 'paper'. The final polishing was conducted on a well worn 625 grade paper followed by a light polish with alumina on a 'hyprocel' paper. After the measurement of each contact angle the hematite sample was cleaned with nitric acid and alcohol, soaked in 0.1M sodium hydroxide for five minutes, washed with distilled water until the pH remained constant and finally repolished with a 625 grade silicon carbide paper and the alumina treatment. This treatment was repeated until the surface became hydrophilic. The polished samples were stored under distilled water.

b) Quartz

Two samples of quartz were selected, one a synthetic optical quartz of high purity and the other a mineral quartz from the Isle of Man. The optical quartz was used for comparative purposes in the electrokinetic and contact angle studies.

Selected pieces of mineral quartz were crushed in a laboratory jaw crusher and pulveriser. The - 52 + 72 mesh size fraction was retained and leached with successive washes of hot concentrated

hydrochloric acid to remove iron impurities. This treatment was repeated until no iron, was detected by ammonium thiocyanate, in the solution. The quartz sample was then washed thoroughly with distilled water until the conductivity of the wash water assumed that of distilled water.

Samples of 25g of the - 52 + 72 mesh quartz were ground for 5.25 minutes in a agate vibratory mill. The product obtained was 100% - 44μm and 57% - 10μm. A specific surface area determination of the sample used for the adsorption studies gave a value of 0.94 metre^2 g^{-1}, which corresponded to a mean particle diameter of 2.4μm. The - 44μm quartz was stored under vacuum in the presence of silica gel crystals.

To avoid iron contamination, from the laboratory crushing apparatus, the optical quartz was wrapped in a cloth and crushed with a hammer. The - $\frac{1}{4}$" pieces were ground in a agate vibratory mill to 100% finer than 44μm. No attempt was made to measure the speoific surface area of this sample.

The optical quartz sample obtained for oontact angle studies had already been 'optically' polished and this sample was cleaned by washing with nitric acid in alcohol. The mineral quartz was prepared for contact angle studies by a method similar to that used for the preparation of the hematite samples. After each contact angle determination the surface was cleaned with the alcohol in nitrio acid treatment until the surface became hydrophilic. The sample was then stored under distilled water until required.

c) Other Materials

All the other materials used in this work were similar to those used in section 2.00 and 3.00. The collector solutions, with the exception of dodecanoic acid, were prepared in hydrochloric acid so that the total ionic strength was 6×10^{-3}. Values of pH between approximately 2.3 and 11 were obtained by addition of 0.1M NaOH, thus keeping the ionic strength constant. Dodecanoic acid solutions were usually prepared by dissolving dodecanoic acid in the iso-octane phase and allowing equilibrium to establish itself in contact with aqueous sodium hydroxide and/or hydrochloric acid at a constant ionic strength of 6×10^{-3}.

4.22. Extraction Studies

a) Apparatus

The apparatus designed to investigate the concentration of minerals at the oil/water interface is shown in Fig. 15. It consisted of a pH modifying cell (1), a conditioning cell (2) containing a set of 'Perspex' baffles, and a separating column (3). Iso-octane was injected into the conditioning cell from a drawn out capillary, situated at the level of a rotating, polythene-coated impellor. This method of oil addition facilitated close control of the oil injection rate. It also gave a fairly even distribution of oil droplets (139) and resulted in a faster attainment of equilibrium. The rate of rotation of the impellor, in the range 0 - 5000 r.p.m., was measured by a Smith tachometer

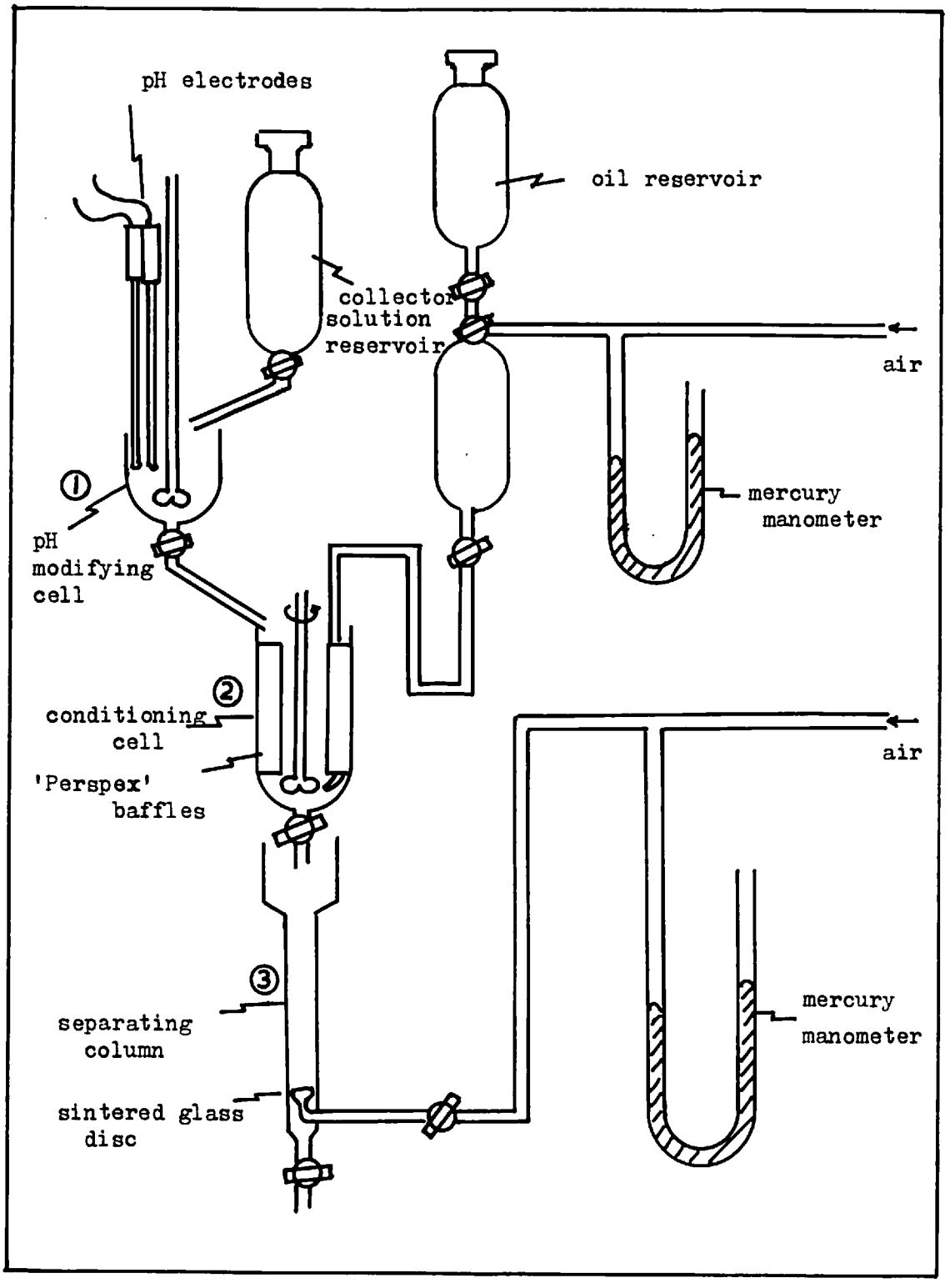

Fig. 15. Diagram of extraction apparatus.

The essential feature of the separating column was a sintered glass disc situated near the base of the column, through which air was introduced. The diameter of this disc was almost the same as that of the column. When liquid was added to the column, it rested on the disc and trapped a layer of air below it. Air entering through the disc then passed through all of the liquid before escaping to the atmosphere. Carbon dioxide and water were removed from the compressed air by passing the air through gas bubblers containing concentrated caustic soda and sulphuric acid.

The capacities of the pH modifying cell, conditioning cell and separating column were about 30 ml. Measurements of the pH, before and after the tests, were made using a glass electrode assembly and a Pye 'Dynacap' meter.

b) Method

Aliquots of 20 ml of collector solution were added to the pH modifying cell and the pH adjusted with 0.1M sodium hydroxide. The collector solution was then passed into the conditioning cell, where the impellor was rotating at the required speed, and approximately 0.5g of - 44 μm mineral added. After a conditioning period of 10 minutes, 6 ml of iso-octane was injected into the pulp and conditioned for a further 15 minutes. At the end of this period the pulp was drained into the separating column where the fine dispersion of air bubbles passing through the column increased the rate at which the hydrophobic particles attached to the oil droplets rose to the surface.

When the two phases had separated out the aqueous phase was drained into a weighed centrifuge tube, centrifuged and the pH of the aqueous phase measured. This pH was regarded as the equilibrium pH of the system. The organic phase was then recovered. Any particles adhereing to the walls of the separating column were washed, out with alcohol, into the centrifuge tube containing the organic phase. After centrifuging and discarding the liquid both products were dried at 100°C and then weighed.

c) The results of preliminary tests

Preliminary tests were conducted on quartz with a collector of dodecylamine to ascertain the optimum values of such variables as agitation rate, iso-octane injection pressure, phase volume, solid weight and conditioning time. It was assumed during these tests that the variables were independent of each other. The results illustrated in fig. 16 show the influence of various variables on the percent quartz extracted with an agitation rate of 2000 r.p.m. and a pH between 5.0 and 6.0.

Curve (1) shows the influence of the weight of quartz on the extraction efficiency when the organic phase volume was 23% of the total volume, the iso-octane injection pressure 25 cm Hg, the dodecylamine concentration 6.75×10^{-5}M and the conditioning time in the presence of iso-octane 15 minutes. It can be seen that as the solid weight was increased the percent extracted decreased in a way analogous to an exponential decay.

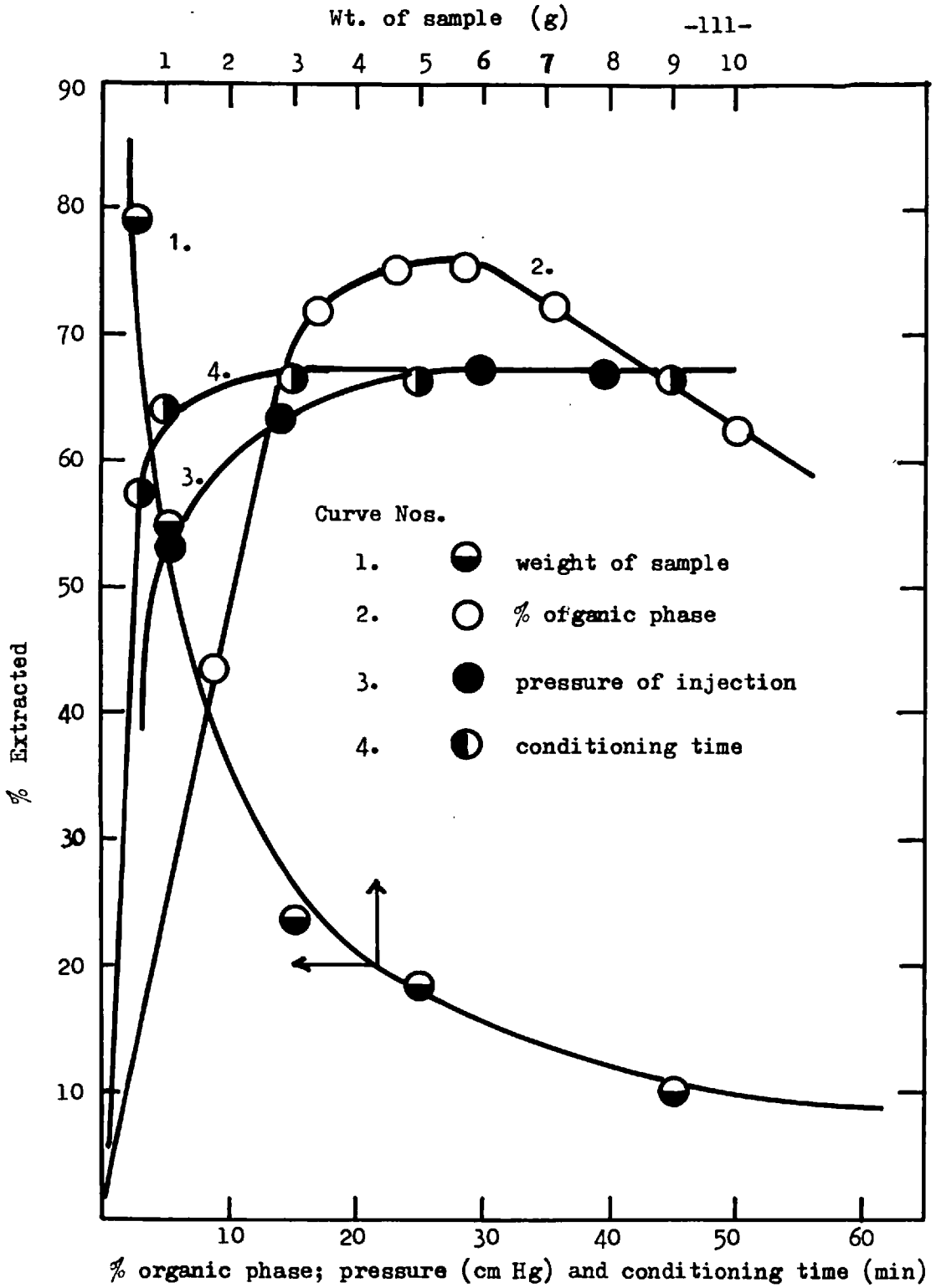

Fig. 16. Percent extraction as a function of the different variables.

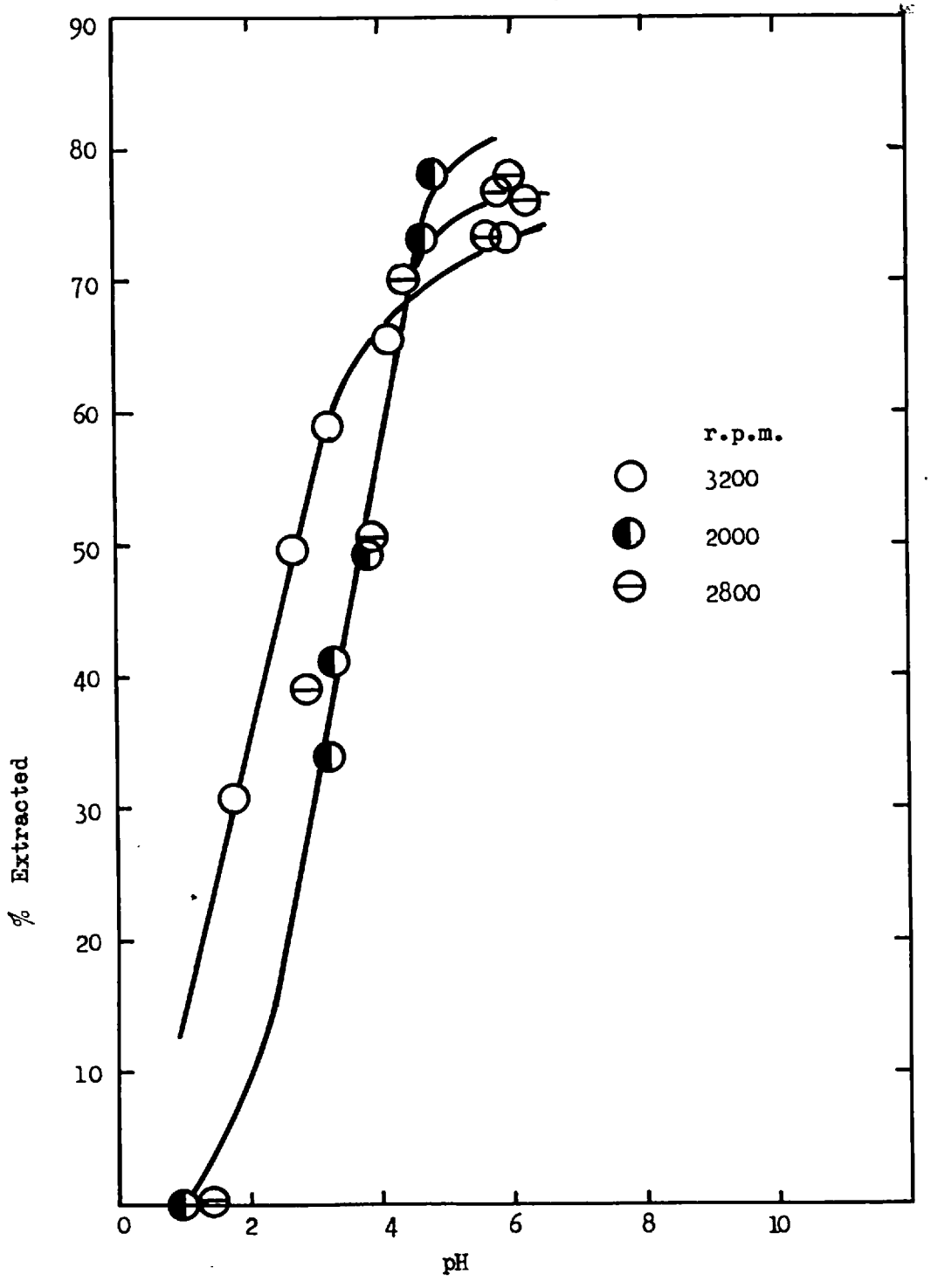

Fig. 16a. The influence of agitation rate on the extraction efficiency.

Curve (2) shows the influence of the organic phase volume on the quartz extraction efficiency, with a solid weight of 0.5g and all the other variables fixed at the values used for curve (1). As the organic phase volume was increased, the efficiency increased to a maximum at an organic phase volume of between 20 and 30 percent of the total volume and then decreased. The total volume in these tests was kept constant by decreasing the collector solution volume by an amount equal to the increase in volume of the organic phase.

Curves (3) and (4) show the influence of injection pressure of iso-octane and conditioning time on the extraction efficiency. The concentration of dodecylamine in these tests was 5.75×10^{-5}M and all the other variables were at the values indicated for curves (1) and (2). The percent extraction increased with increase in injection pressure and conditioning time and reached a constant value at 20 cms Hg and 10 min. respectively.

Figure 16 illustrates the effect of agitation rate on the extraction efficiency over a pH range. The concentration of dodecylamine was 6.75×10^{-5}M, the organic phase 23% of the total, the conditioning time 15 minutes, the sample weight 0.5g and the injection pressure 25 om Hg. The difference between the extraction efficiency at 2000 and 2800 r.p.m. was very small, however at 3200 r.p.m. the extraction was a little higher at low pH values. At agitation rates lower than 1800 r.p.m. the extraction effioiency decreased because of the sedimentation of particles to the base of the conditioning cell.

Tests were conducted to determine the influence of air addition to the separating column. It was found that, for a wide range of air flow rates, the precent extraction was only 4% higher than the percent extraction obtained in the absence of air. In the presence of air however the two layers separated more rapidly and the reproducibility was improved. As a result air, at a constant rate, was introduced in all subsequent extraction tests.

It was concluded from these tests that the following values (Table VI) should be given to the variables when investigating the influence of concentration of collector and pH on the percent extraction. The assumption was made that the values designated to the variables would be the same for the different mineral/collector soln/iso-octane systems.

TABLE VI

Variable	Value
Agitation rate	2000 r.p.m.
Injection pressure	25 cm Hg
Conditioning time	15 min
Volume of organic phase	6 ml
Volume of aqueous phase	20 ml
Weight of sample	0.5 g

4.23. Electrophoresis Studies

a) Apparatus

The electrophoresis cell developed from that of Marshall (140),

consisted of two similar electrode compartments and a demountable glass cell. The glass cell was supplied by Tintometer Sales Ltd. and was a 1 mm standard spectrophotometer cell 90 mm long and 10 mm wide constructed without ends. The electrode compartments were machined out of solid rectangular blocks of 'Perspex' and were cylindrical in shape (fig. 17). The glass cell fitted into the two electrode compartments by slots cut into one face of each rectangular box. One end of each cylindrical electrode compartment was composed of a 'Perspex' plug held in position by two brass bolts and a rubber 'O' ring. On the interior surfaces of the plugs were situated platinum foil electrodes which were connected to outside terminals by platinum wires passing through the plugs. Solution was passed in and out of the cell through holes cut through the 'Perspex' and, during filling, air was allowed to escape from the electrode compartments by a screw type valve system situated at the top of the electrode compartments. When the cell was in use the glass cell was sealed into the slots by silicone moulding paste and the whole assembly was clamped to the microscope stage.

The optical system of the microscope consisted of a dark field sub-stage condenser (Cooke, low-power D.G. numerical aperture 0.70 - 0.80), a x 40 long-working distance objective (Vickers - A.E.I. numerical aperture 0.57) capable of fooussing on any level within the cell, and a x 8 eyepiece. A micro-adjuster on the microscope enabled the objective to be focussed to within 0.005 mm on a particular level within the cell. Ten revolutions of the micro-

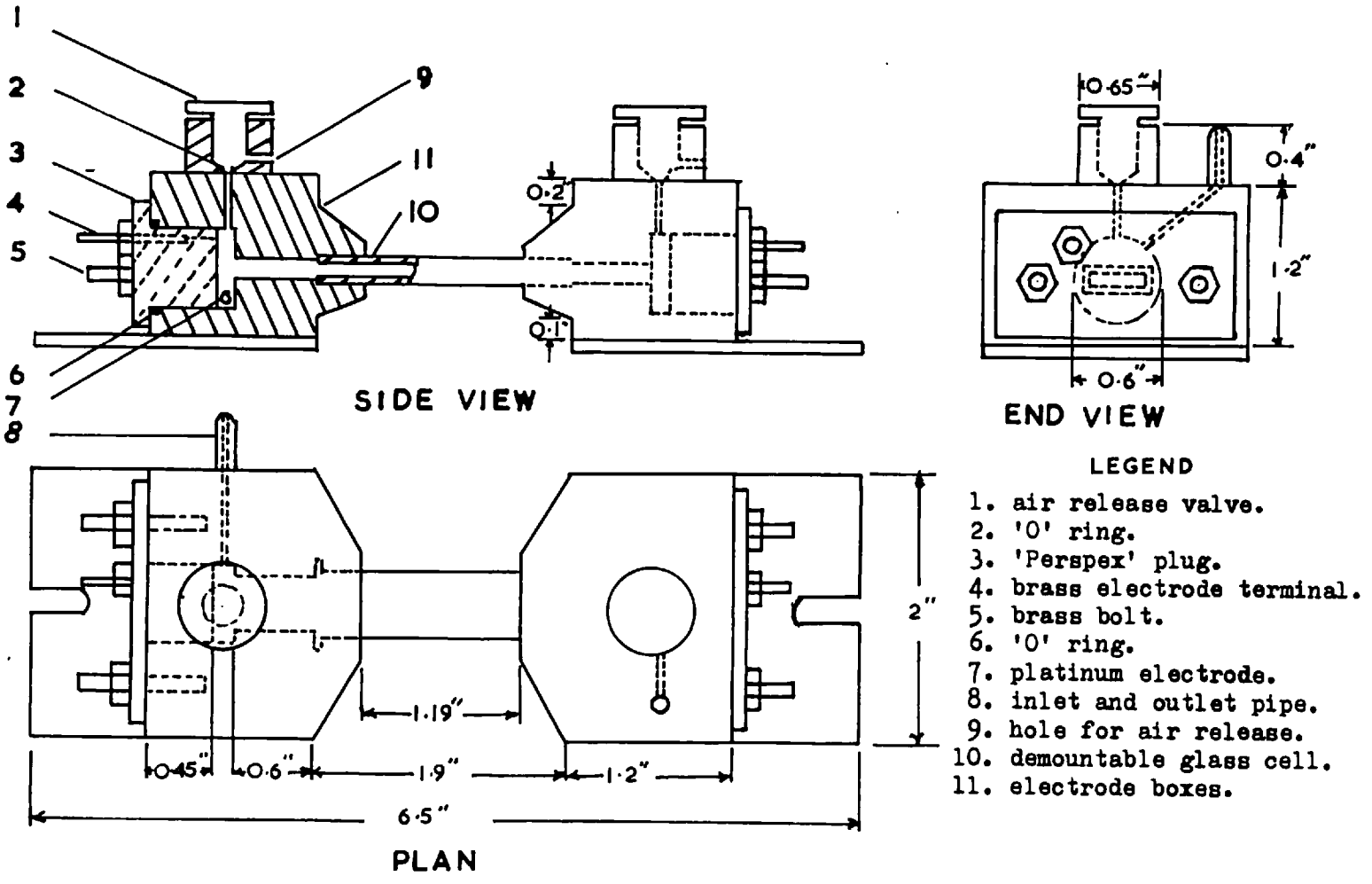

Fig. 17 Cell design

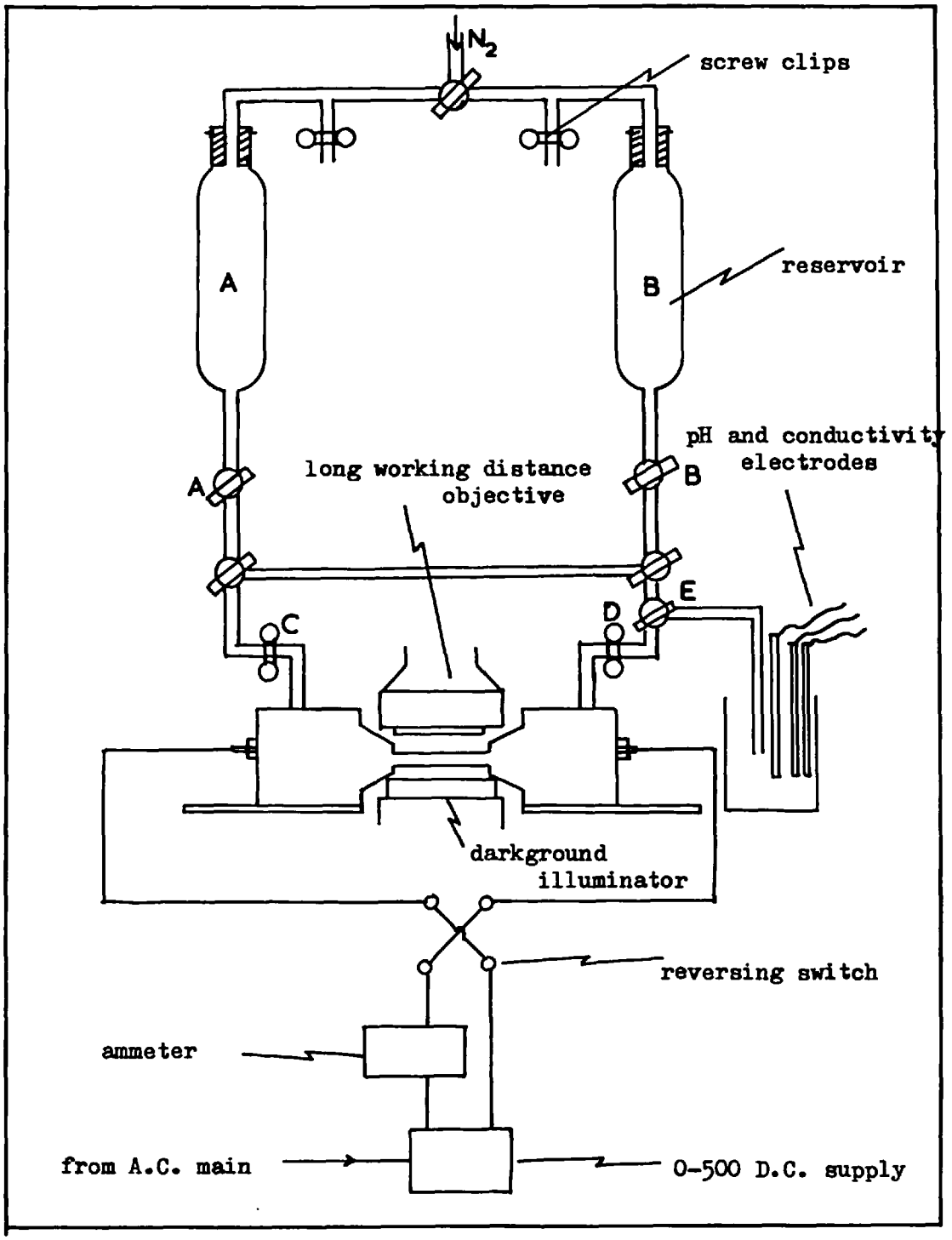

Fig. 18 Cell assembly

adjuster corresponded to 1 mm the thickness of the cell. Heat from the light source was removed by a copper sulphate solution filter.

The voltage applied across the electrodes was supplied by a 0 - 500 V stabilized power supply unit and the current passing through the cell was measured by a multimeter capable of reading 0.1 mA full scale deflection. A system of reservoirs (fig. 18) enabled the suspension of particles to be passed backward and forward through the cell until the system was at equilibrium. The pH and conductivity of the suspension were measured by a Pye 'Dynacap' pH meter and a Pye conductance bridge, respectively.

The advantages of the type of cell employed in this work were i) it was easy to assemble and could be clamped to the miscoscope stage, ii) cleaning of the cell was carried out even when the cell was clamped in position, iii) air bubbles were readily removed from the electrode compartments; and iv) the cell was robust, inexpensive and easily cleaned.

b) Determination of velocity profile

A dilute suspension of 'Fransil', a finely divided vitreous silica powder, in distilled water was passed into the electrophoresis cell and a potential of 40 V was applied across the electrodes. The microscope was then focussed on different levels within the cell and the time for the particles to move through a set distance noted. At each level ten particles were measured travelling in one direction and then the voltage was reversed and

ten particles were measured travelling in the reverse direction.

The distance over which the particles were timed, was measured by inserting a grid type graticule in the eyepiece of the microscope. This grid was calibrated by placing a standard 100 μm linear scale on the upper surface of the cell and then taking an average of the dimensions of several squares within the grid.

Moyer and Abramson (141) have shown that in general the parabola

$$Vobs = d\ (Z - Z^2) + e \qquad (35)$$

can be used to describe the Vobs-depth curve, where Z is the fraction of the cell depth at which the observed velocity Vobs. is obtained and d and e are constants. From eq^n (35) it follows that if Vobs is plotted against $(Z - Z^2)$ a straight line should result with gradient d and intercept e. Figure (19) shows the experimental velocity profile obtained compared to a theoretical velocity profile. The theoretical profile was obtained by plotting experimental values of Vobs against $(Z - Z^2)$ and drawing a statistical straight line through the points. From the straight line values of Vobs and Z were taken and plotted in fig. (19).

These results show that a parabolic profile, symmetrical about the centre of the cell, was obtained and that the cell was behaving as would be expected from theoretical considerations (c.f. section 4.12c).

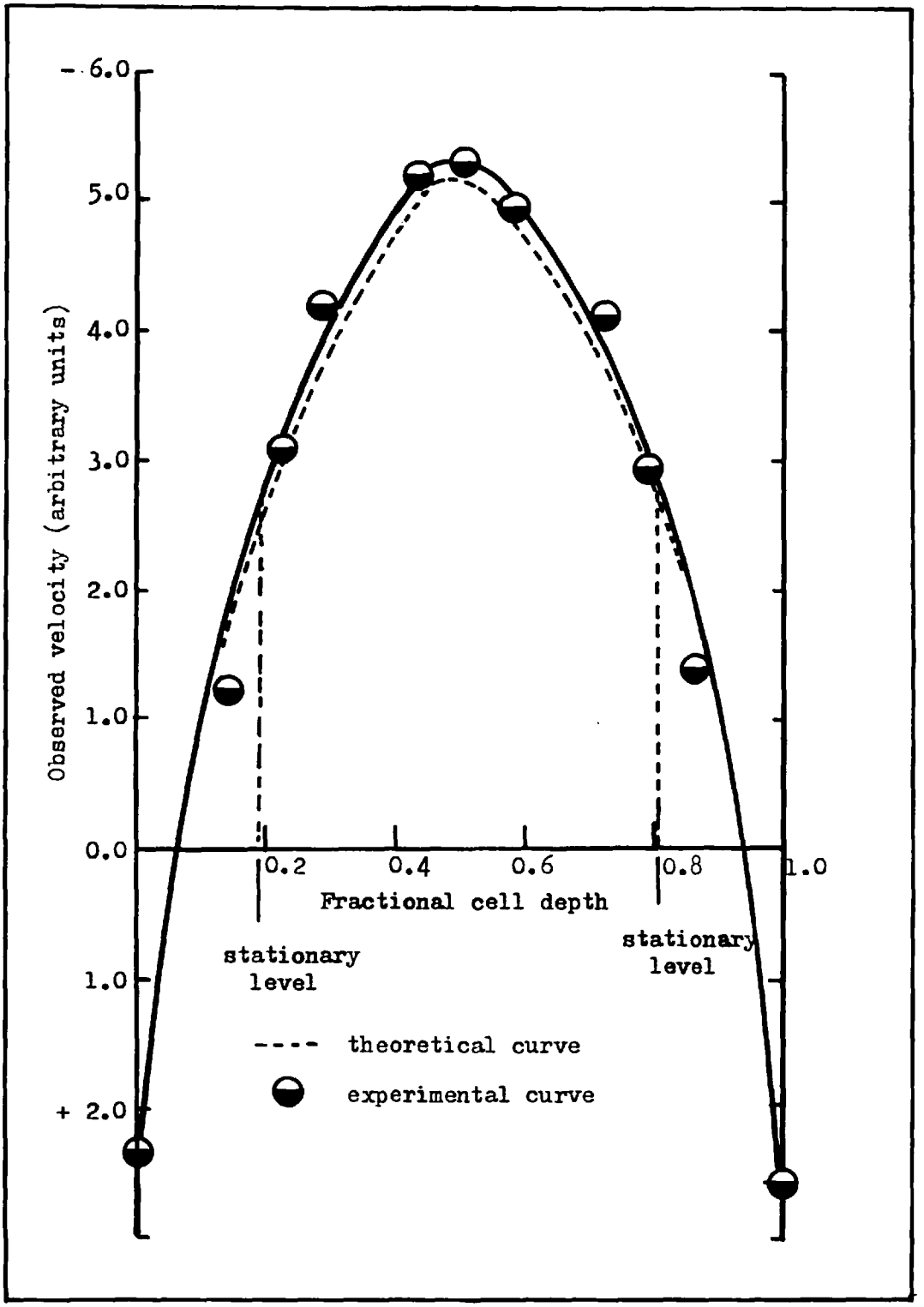

Fig. 19. Velocity profile.

c) Determination of the electrophoretic mobility of mineral particles

Electrophoresis studies have been carried out on hematite and quartz in the presence of various electrolyte solutions. The hematite for these tests was obtained by lightly grinding 1g of - 44μm hematite, with a little distilled water, in a mechanical agate mortar for ten minutes. The resulting pulp was then diluted with one litre of water and left until required.

Two samples of quartz were used, one the mineral quartz similar to that used in the extraction studies and the other the optical quartz. These samples were dry or wet ground in the mechanical mortar and were stored in a variety of ways, for different lengths of time, so that the aging properties of quartz could be examined.

Aliquots of two ml of the mineral suspension or a small amount of the dry solid were added to 40 ml of the acid or acidified collector solution and the resulting suspension agitated for fifteen minutes. The suspension was then allowed to stand for ten minutes, to allow any coarse particles to settle out, and then added to the electrophoresis cell via the reservoir system (fig. 18). After the suspension had been passed through the cell several times Tap A was closed so that most of the suspension was trapped in the electrophoresis cell and reservoir B. Air was then excluded from the electrode compartments by opening the valves, one at a time, and using the pressure generated by the head of liquid between the cell and the reservoir B to force the air out. Tap B was then

closed and screw clips C and D were tightened to eliminate particle drift in the cell due to leaking taps. The microscope objective was then focussed on the upper stationary level and the particles viewed to see if there were any leaks in the cell. After applying a voltage ten particle velocities were measured in one direction and then in the other direction by reversing the voltage. The current was measured in both directions and the average of these two values was determined.

The suspension was then drained, into a beaker containing pH electrodes and a conductivity cell, by opening clips C and D and taps A and E. The last drops of the suspension were forced out of the cell by blowing through 'white spot' nitrogen and the suspension in reservoir B was also allowed to drain into the beaker by opening tap B and reversing tap E. After measuring the pH and conductivity of the suspension the pH was increased by the addition of 0.1M sodium hydroxide. The suspension was then added to the reservoirs and the procedure repeated for different pH values.

The electrophoretic mobility (u) was evaluated from the particle velocity (V) and the conductivity of the suspension (K_s) by the following equation

$$u = \frac{V K_s S}{I} \qquad (36)$$

where S is the area of cross-section of the cell and $I/K_s S$ the field strength.

Values of the zeta potential were obtained from the electrophoretic mobility by the use of eq^{n} (2 1) (Section 4.12b). It was assumed in these calculations that a, the radius of the particle was not smaller than 0.4 μm. Under these conditions, with an ionic strength of 6 x 10^{-3}, the value of (κa) was greater than 100 and f(κa) approximated to 3/2 so that

$$u = \frac{D \zeta}{4\pi\eta} \qquad (37)$$

which is the Helmholtz-Smoluchowski form of the electrophoresis equation. At a temperature of 22^{o}C eq^{n} (37) becomes

$$\zeta = 13.6\ u \qquad (38)$$

4.24. Adsorption Studies

a) Determination of dodecylamine

The concentration of dodecylamine in solution was determined by complexing the amine with an acidified alcoholic solution containing sulphnapthelein indicator (142) (143), e.g. bromo-cresol green, as complexing agent, and then extracting the complex into chloroform. The indicator solution was prepared by dissolving 0.1g bromo-cresol green in 60 ml of ethyl alcohol, acidifying with 0.5 ml concentrated sulphuric acid and diluting with water to 100 ml. In each determination, 1 ml of indicator solution was added to 5 ml of the sample solution and diluted to 10 ml ; 5 ml of chloroform was then added and the mixture inverted rapidly about 100 times. The

chloroform phase was then separated and examined in a 1 cm cell in a Unicam S.P.500 spectrophotometer.

A % transmission *vs* wavelength plot (fig. 20) revealed that there were two wavelengths at which maximum absorption of light occurred, one at 416 mμ and the other at 290 mμ . Beer's law, however, was only obeyed at 416 mμ . Further tests indicated that an impurity in the dye was extracted into the chloroform, even in the absence of dodecylamine, and that this impurity absorbed light at 290 mμ . Figure 21 shows the plot of optical density *vs* concentration of dodecylamine at a wavelength of 416 mμ . This plot, shows that the Beer law was obeyed and so it was used as a calibration curve.

The dodecylamine in the iso-octane phase was extracted into an aqueous phase by shaking with 0.1M hydrochloric acid for forty-five minutes. The amine in the aqueous phase was then determined by the method elucidated above.

b) Determination of sodium dodecyl sulphate

The method used for the determination of sodium dodecyl sulphate was similar to that suggested by Gregory (144) for the determination of anionic surface active agents. The sodium dodecyl sulphate solutions were reacted with a copper triethylenetetramine complex in an alkaline medium of monoethanolamine and then the resulting complex extracted into a isobutanol-cyclohexane mixture. Addition of diethylammonium diethyldithiocarbamate to the extracted complex

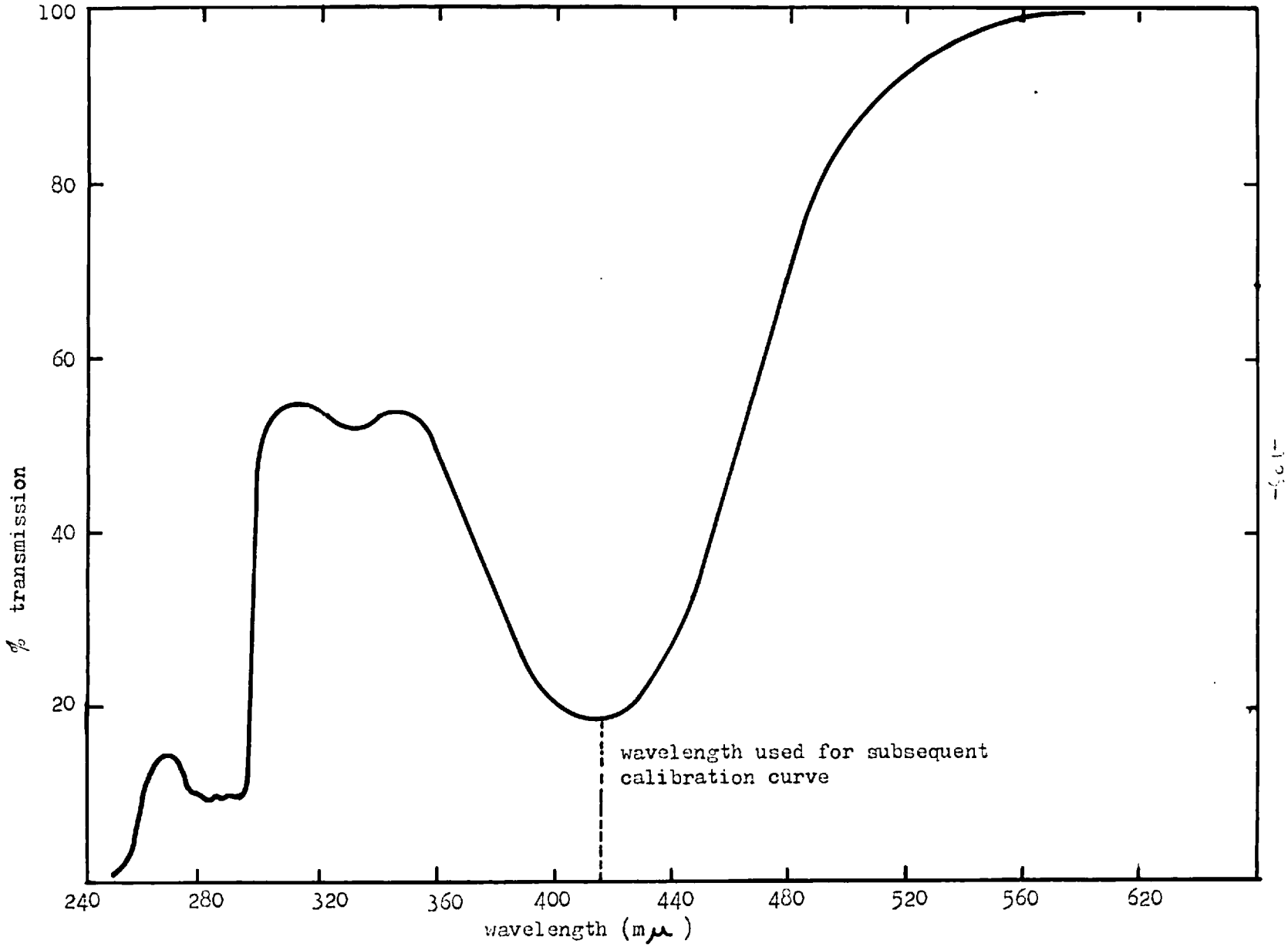

Fig. 20. Transmission as a function of wavelength for dodecylamine.

produced a colour whioh was determined spectrophotometrically in a Unicam S.P.500.

The reagents were prepared in the way indicated below:-

Copper - triethylenetetramine: 25g of Copper (II) nitrate trihydrate was dissolved in 125 ml of water and a solution containing 16.25g of triethylenetetramine in 125 ml water slowly added. A solution containing 250 ml of monoethanolamine in 250 ml of water was then added and the whole made up to 1 litre with distilled water.

Isobutanol-cylcohexane extractant: 200 ml of isobutanol was mixed with 800 ml of cyclohexane.

Diethylammonium diethyldithiocarbamate solution: 2g of diethylammonium diethyldithiocarbamate was dissolved in 100 ml of isobutanol. This solution was prepared fresh every two days.

In a determination 5 ml of the copper complex and 10 ml of the extractant was added to 25 ml of the sample and the mixture inverted rapidly 100 times. The organic phase was then separated from the aqueous phase and mixed with two drops of carbamate solution. After the sample had been left to stand in the dark for fifteen minutes, the optical density at a wavelength of 435 mμ was determined. Figure 21 shows the plot of optical density against concentration of sodium dodecyl sulphate, compared to the reference ourve of dodecylamine. Blank determinations were made for each fresh batch of reagents.

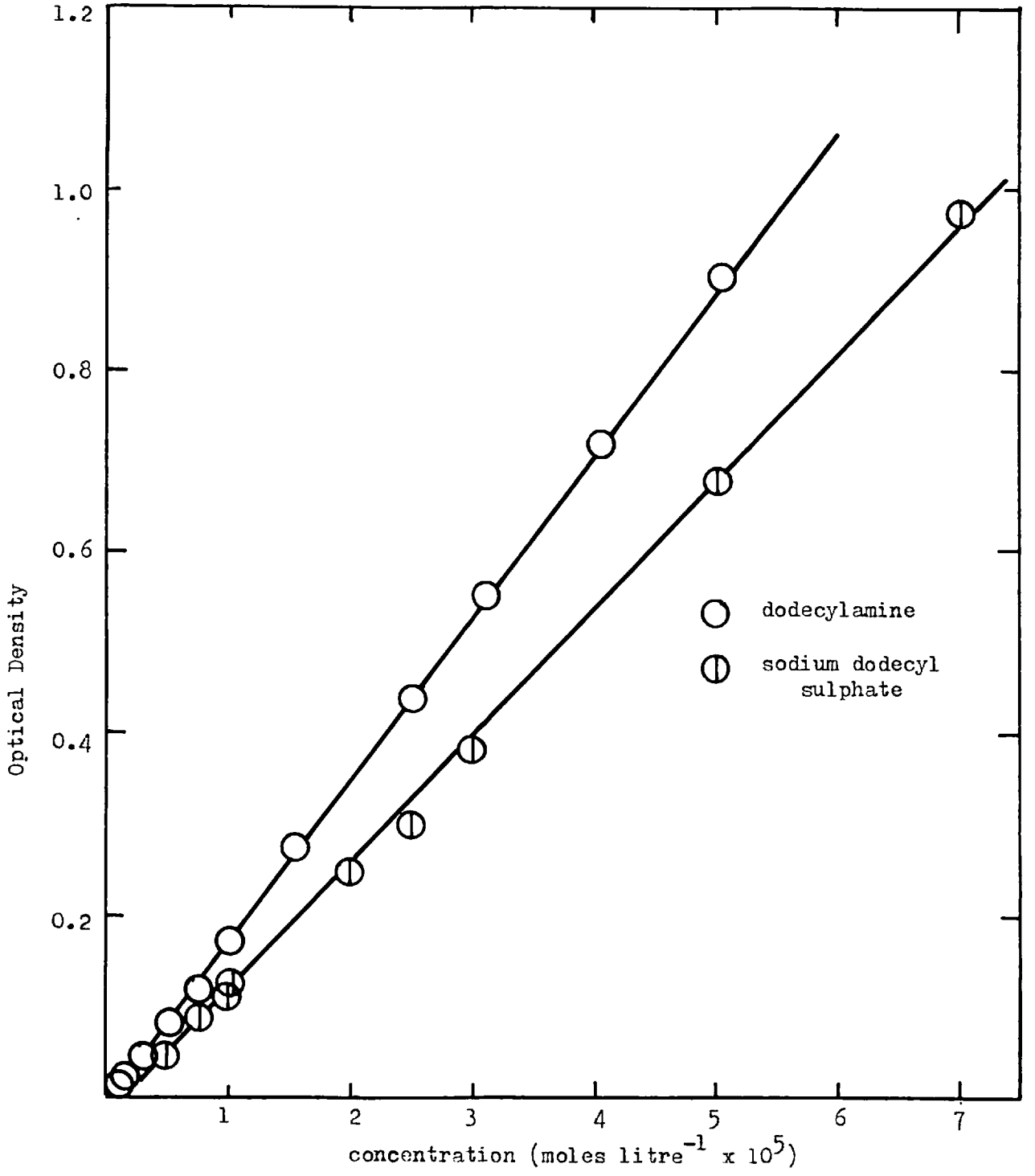

Fig. 21. Calibration curves for the determination of dodecylamine and sodium dodecyl sulphate.

c) Adsorption tests

The adsorption tests were conducted in 100 ml conical flasks fitted with B.19 stoppers. Before use each flask was cleaned with nitric acid in alcohol until the internal surface was completely hydrophilic. Samples of 1g of the -44 μm mineral were added with small amounts of 0.1M sodium hydroxide to a mixture containing 40 ml of acidified collector solution and 12 ml iso-octane. The resulting mixture was shaken for 45 minutes under an atmosphere of 'white spot' nitrogen, and then the oil in water emulsion obtained was centrifuged and the aqueous phase separated from the organic phase. After measuring the pH of the aqueous phase the dodecylamine content of the aqueous and organic phases, or the sodium dodecyl sulphate content of the aqueous phase was determined. The adsorption density was deduced from the difference between the total collector content before and after the adsorption had taken place.

The adsorption density, as deduced from solution analyses will be composed of adsorption at the oil/water, solid/water and sold/oil interfaces. In this work, however, the area of the oil/water, and solid/oil interface was considerably reduced by the centrifugation of the emulsion. Some oil was carried down with the sedimentated mineral particles but the amount was small, as evidenced by the fact that at the end of the centrifugation period the amount of clear organic phase was approximately the same as that added. It was therefore assumed, that the measured reduction in the amine concentration in the aqueous and organic phases (or the reduction in

the sodium dodecylsulphate concentration in the aqueous phase) was mainly attributable to the adsorption of collector at the solid/water interface and not at the other two interfaces.

The studies of the distribution of amine between iso-octane and water (fig. 5) showed that over much of the pH range, the cationic amine content was much higher than that of the neutral amine in the aqueous phase. The assumption was therefore made that the measured adsorption density was largely that of the cationic amine at the solid/water interface. At high pH values this assumption may not be strictly correct because the particles, after centrifugation from the oil/water interface, might have retained some neutral amine adsorbed from the organic phase. In the event of this happening the total measured adsorption density would have been composed of cationic amine and some neutral amine.

Preliminary tests were conducted in the absence of any mineral to (i) determine the variation of the concentration of dodecylamine in the organic and aqueous phase with pH (The results from these tests are shown in fig. 4 and they are discussed in section 2.4); and (ii) determine the adsorption of amine on the walls of the conical flasks in which the adsorption experiments were conducted.

The adsorption of amine by the flask walls was shown to be negligibly small by the fact that when 50.05×10^{-6} moles of dodecylamine was added to the dodecylamine solution/iso-octane system the determined average total over the pH range 2 to 10 was 50.67×10^{-6} with a standard deviation of $\pm 1.16 \times 10^{-6}$ moles.

The variation of the determined number, at each pH value (Table VII), from the average value was random and no correlation was found between the magnitude of the variation and the pH.

TABLE VII

pH	Total nos.of moles x 10^6	deviation from mean.
3.20	52.50	+ 1.83
4.32	50.05	- 0.62
4.46	50.00	- 0.67
5.80	50.20	- 0.47
6.58	52.60	+ 1.93
6.60	51.10	+ 0.43
7.35	49.00	- 1.67
8.88	49.70	- 0.97
9.48	50.90	+ 0.27
Mean.	50.67	Standard Dev. ± 1.16

In addition to measuring the adsorption of sodium dodecyl sulphate on hematite in the presence of iso-octane some tests were conducted in the absence of iso-octane. The procedure for these determinations was similar to that outlined above with the difference that the iso-octane was not present. During the series of tests conducted in the presence of iso-octane it was found necessary to investigate the separation of the equilibrated mixtures by filtration as well as centrifugation.

No attempts were made to determine the adsorption of sodium

dodecyl sulphate onto the walls of the glass flasks or onto the samples of quartz because the extraction tests revealed that sodium dodecyl sulphate was not a collector for quartz. Furthermore, Fuerstenau (145) has shown that anionic collectors merely act as indifferent electrolytes at the quartz/water interface. No specific adsorption takes place unless a polyvalent metal ion is added as an activator (146).

4.25. Contact Angle Studies

a) Apparatus

The apparatus consisted of a 3 cm absorptiometer cell fixed to the stage of a microscope which had been rotated through ninety degrees. Polished specimens were placed in the cell with collector solutions, and light was passed through the cell at a small angle of incidence to the polished surface. The reflected light and some of the incident light was directed through the microscope and brought to focus on a ground glass screen. A small angle of incidence was used so that the image of a drop as formed on the polished surface could be seen projected on the ground glass screen. This enabled the line of contact between the oil drop and the solid surface to be clearly distinquished. The microscope was fitted with a long working distance objective and the eyepiece was removed. Heat from the light source was kept to a minimum by a copper sulphate solution filter (fig. 22).

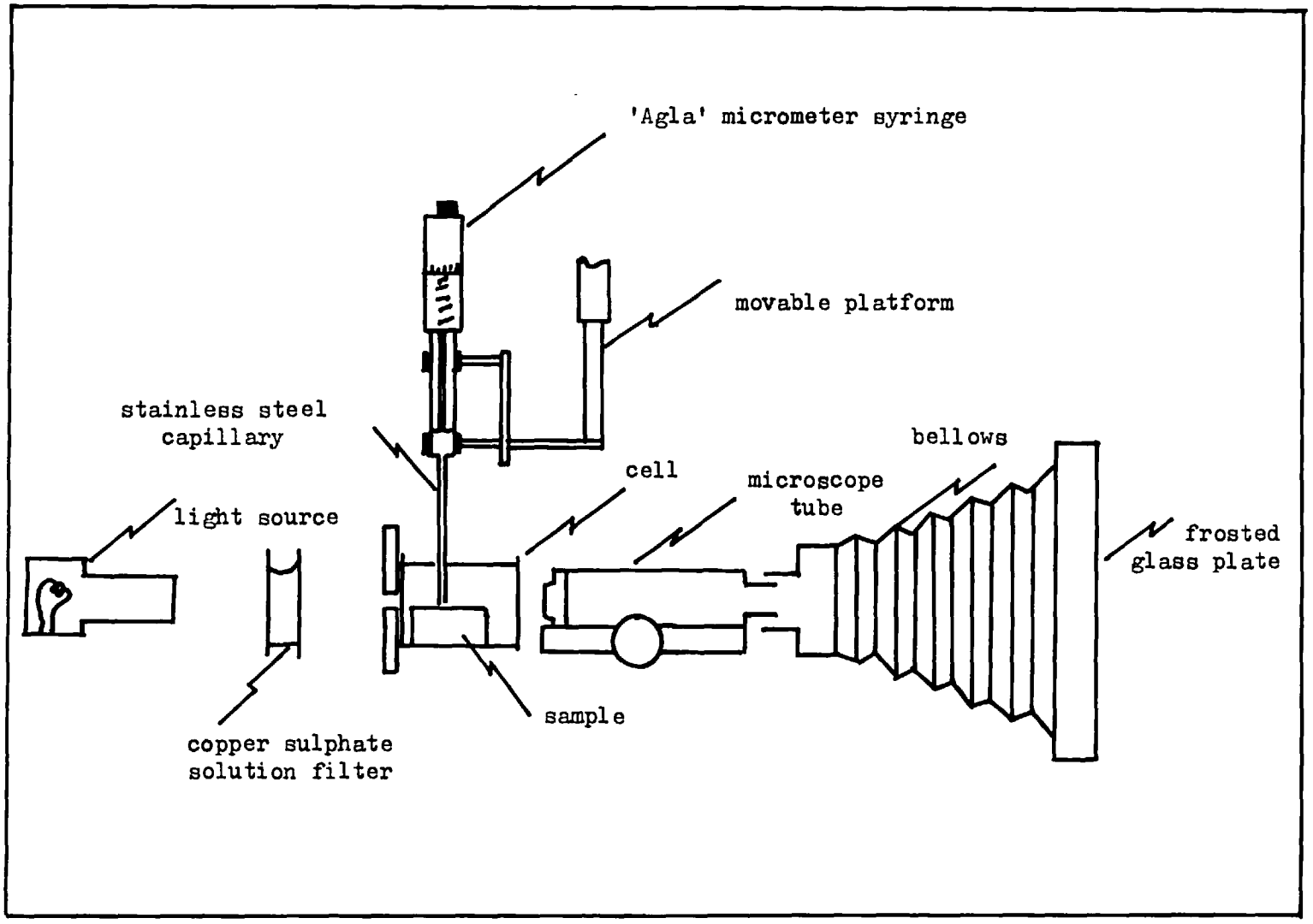

Fig. 22. Contact Angle apparatus.

Oil drops were formed at the tip of a stainless steel capillary by the use of a 'Agla' micrometer syringe. The micrometer syringe was fixed to a platform which was capable of movement in a horizontal and vertical plane. This device enabled the oil drop to be brought into contact with the polished specimen at any desired area on the surface of the sample. Contact angles were measured at the iso-octane/water/mineral line of contact by tracing the image of the angles obtained on the ground glass screen.

Before use the absorptiometer cell, stainless steel capillary and all glassware was cleaned with alcohol in nitric acid.

b) Method

Mixtures of 40 ml of acidified collector solution, and 12 ml iso-octane with small amounts of 0.1M sodium hydroxide were equilibrated by shaking under an atmosphere of 'white spot' nitrogen for 45 minutes. The resulting emulsions were centrifuged and the phases separated. After measuring the pH of the aqueous phase a 10 ml volume of the aqueous phase was added to the cell containing the polished specimen. After 10 minutes this solution was decanted and 20 ml of fresh solution added. This procedure was used to eliminate the possible error due to the dilution of the collector solution by adsorption on the cell and sample surfaces. Care was taken to ensure that, in all cases where the sample was transferred from one solution to another, the surface did not become dry.

The sample was equilibrated in the fresh solution for fifteen

minutes and then a drop of the organic phase, formed from the 'Agla' syringe, was brought just into contact with the sample surface. After the drop had advanced over the surface and had reached an equilibrium position, the contact angle (measured through the aqueous phase) was determined. This angle was termed the advancing contact angle.

The volume of the drop in contact with the mineral was then increased by a known amount and the system left to equilibrate. After this equilibration period the drop volume was decreased to its original volume and then after a further equilibration period the contact angle was determined. This contact angle was termed the receding contact angle. In all cases the contact angle on both the left and right sides of the projected image were measured and then an average of the two values taken.

A preliminary series of tests revealed that, if the mineral was initially conditioned in the collector solution for fifteen minutes, equilibration periods in excess of four minutes gave constant advancing and receding angles. For this reason equilibration periods of 5 minutes were used throughout the contact angle determinations.

4.30. Results

4.31. The system quartz/iso-octane/water in the presence of dodecylamine

a) Zeta potential results

i) The effect of ageing of quartz on its zeta potential

Suspensions of natural and optical quartz were aged for various lengths of time in distilled water. The suspensions were stored in 'Pyrex' containers. The results presented in fig. 23, show the dependence of the zeta potential of natural quartz on the pH, after different ageing times. At a given pH, the zeta potential first of all increased with an increase in time of ageing and then decreased to an equilibrium value. Optical quartz aged for 7 days gave similar results to those obtained for the natural quartz under the same conditions.

Several authors (147) (148) (149) have reached the conclusion that pulverized quartz particles are coated by a layer of amorphous or non-quartz like silica. When such particles are placed in water the surface layer will begin to dissolve to form monomeric silicic acid (150). The surface concentration of soluble silica, under these conditions, may become supersaturated so that silica is reprecipitated onto the surface as a gel. (151). It is probable that, during the ageing period, such a reaction will proceed until a dynamic equilibrium is reached between the dissolution and deposition of silica.

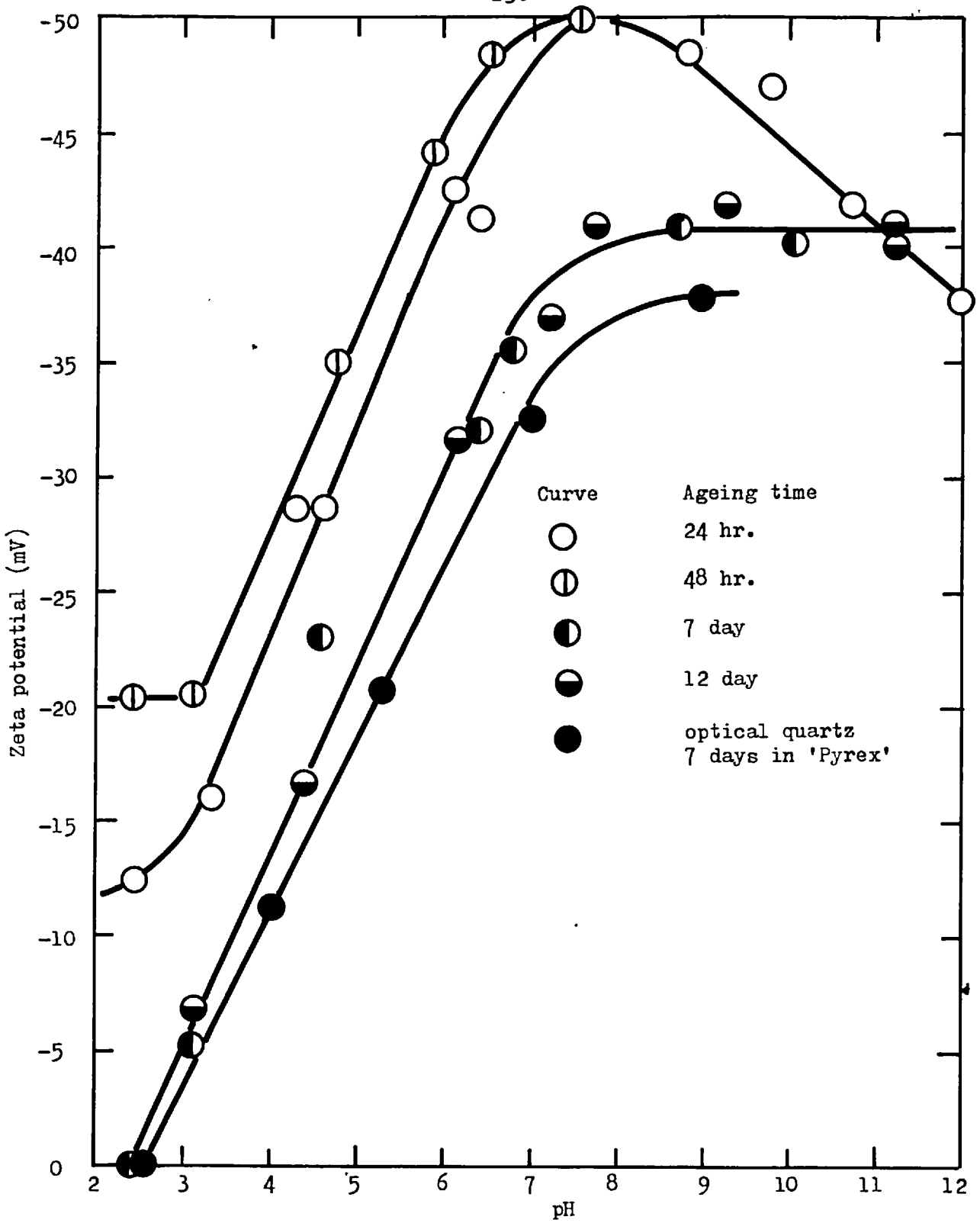

Fig. 23. The zeta potential of quartz as a function of pH after different times of ageing in a 'Pyrex' container.

The similarity between the results obtained with the natural and optical quartz samples indicates that the two samples were of the same purity. The results obtained for a natural quartz sample aged in a silica container were slightly more negative than those obtained for the samples aged in 'Pyrex'. This suggests that cations from the 'Pyrex' containers entered the solution and affected the zeta potential. All of the glass apparatus used in this work was constructed of 'Pyrex'. For this reason subsequent electrophoresis determinations were conducted on samples of natural quartz which had been aged in 'Pyrex'.

ii) The effect of pH on the zeta potential of quartz

Figure 23, shows that as the pH of the natural quartz, which had been aged for 7 and 12 days, was increased, the zeta potential increased and reached a maximum value at pH 8.5. For pH values below neutral the relationship between the pH and the zeta potential was linear. Extrapolation of the linear curves for both the natural and optical quartz samples gave zero points of charge (z.p.c.) at between pH values 2.50 and 2.60. The values of the zeta potentials at pH values below 7 were comparable to those found from streaming potential studies conducted under similar ionic conditions by Fuerstenau (152) and Li and de Bruyn (153). At pH values above 7, however, the zeta potentials obtained in this work were lower than those found by these other authors. Since no marked change in the zeta potential took place on quartz aged for more than 7 days, the quartz used in all subsequent electrophoresis tests was aged for

7 days in 'Pyrex', prior to use.

iii) The effect of dodecylamine concentration on the zeta potential of quartz

The dependence of the zeta potential of natural quartz on the pH, in the presence of five different total concentrations of dodecylamine, is demonstrated in fig. 24. For concentrations of dodecylamine below 4×10^{-5}M and at pH values below 6 the zeta potential was independent of changes in the amine concentration. At higher concentrations of amine and at all pH values, an increase in the amine concentration produced a decrease in the negative zeta potential until it eventually changed sign and became positive. The positive zeta potentials obtained at high concentrations of dodecylamine and at low pH values indicated that although the surface charge approached zero, substantial amounts of cationic amine were adsorbed.

In fig. 25 the zeta potential of natural quartz as a function of the logarithm of the amine concentration is presented at pH 3.0, 4.0, 6.5 and 9.0. A characteristic of this set of curves is that each curve can be divided into (i) a region where a variation in the logarithm of the amine concentration produced only a small variation in the zeta potential, and (ii) a region where a small change in the logarithm of the amine concentration produced a substantial change in the zeta potential. In the region of large zeta potential variation the negative zeta potential decreased to zero and then became positive. For example at pH 6.5, the negative

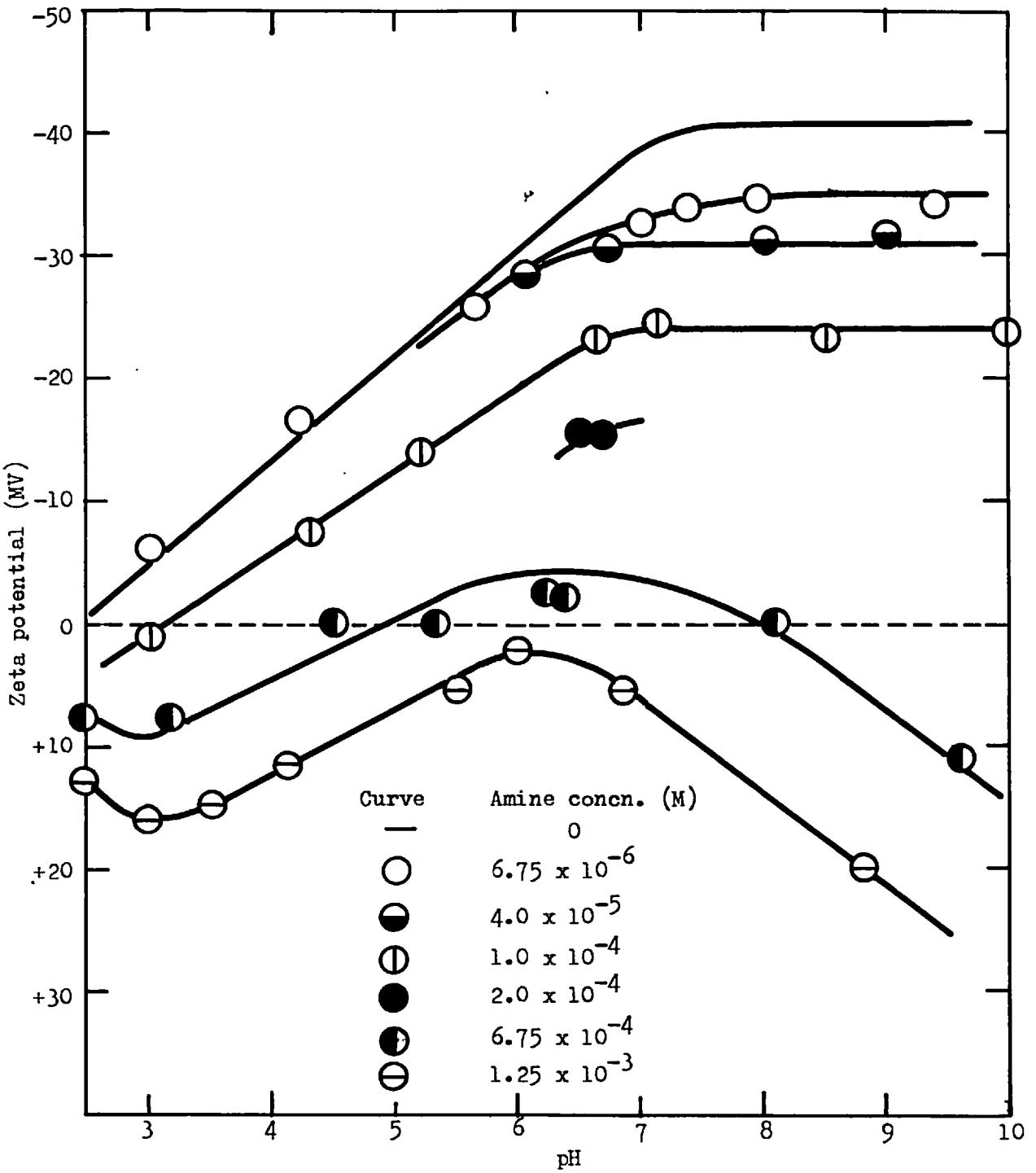

Fig. 24. Variation of the zeta potential of aged quartz with dodecylamine conc. and pH (ionic strength 6×10^{-3})

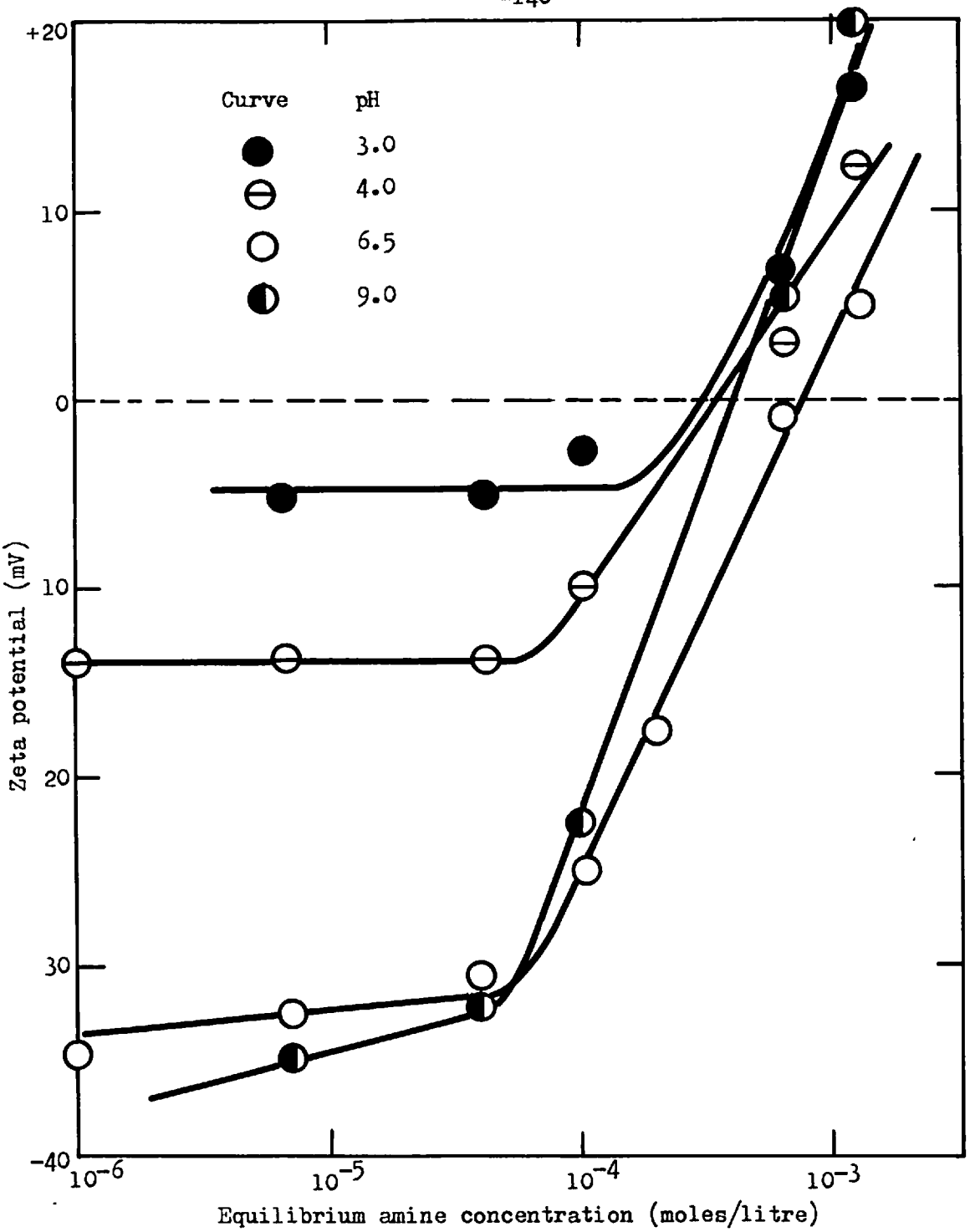

Fig. 25. Variation of the zeta potential of quartz with concentration of amine at various constant pH values.

(ionic strength = 6×10^{-3})

zeta potential decreased slowly with concentration up to a concentration of 10^{-4}M and then decreased rapidly and reached zero at an amine concentration of 6.9×10^{-4}M. The amine concentration corresponding to the transition from one region to the other was approximately independent of the value of the constant pH. A small random shift in the amine concentration was observed at zero zeta potential for the different pH values. These results were consistent with those obtained by Li and de Bruyn (153).

b) The adsorption of dodecylamine by quartz in the presence of iso-octane

The adsorption of dodecylamine at the quartz/water interface in the presence of iso-octane, was determined at different pH values and at four different "total concentrations" of dodecylamine. (The "total concentration" of amine means the concentration if all the amine species in the system, including the adsorbed ones, were in the aqueous phase). The results obtained are shown in fig. 26. For each 'total concentration' of amine, the logarithm of the adsorption density increased with increasing pH and reached a maximum at neutral pH, and then decreased as the pH was further increased. The increase in the logarithm of the adsorption density with increase in pH in acid solutions was small and approximately the same for each total concentration of amine. Considerable adsorption was observed, at high 'total concentrations' of amine, at pH values approaching the z.p.c. of quartz.

Plotted also in fig. 26, is the logarithm of the cationic amine

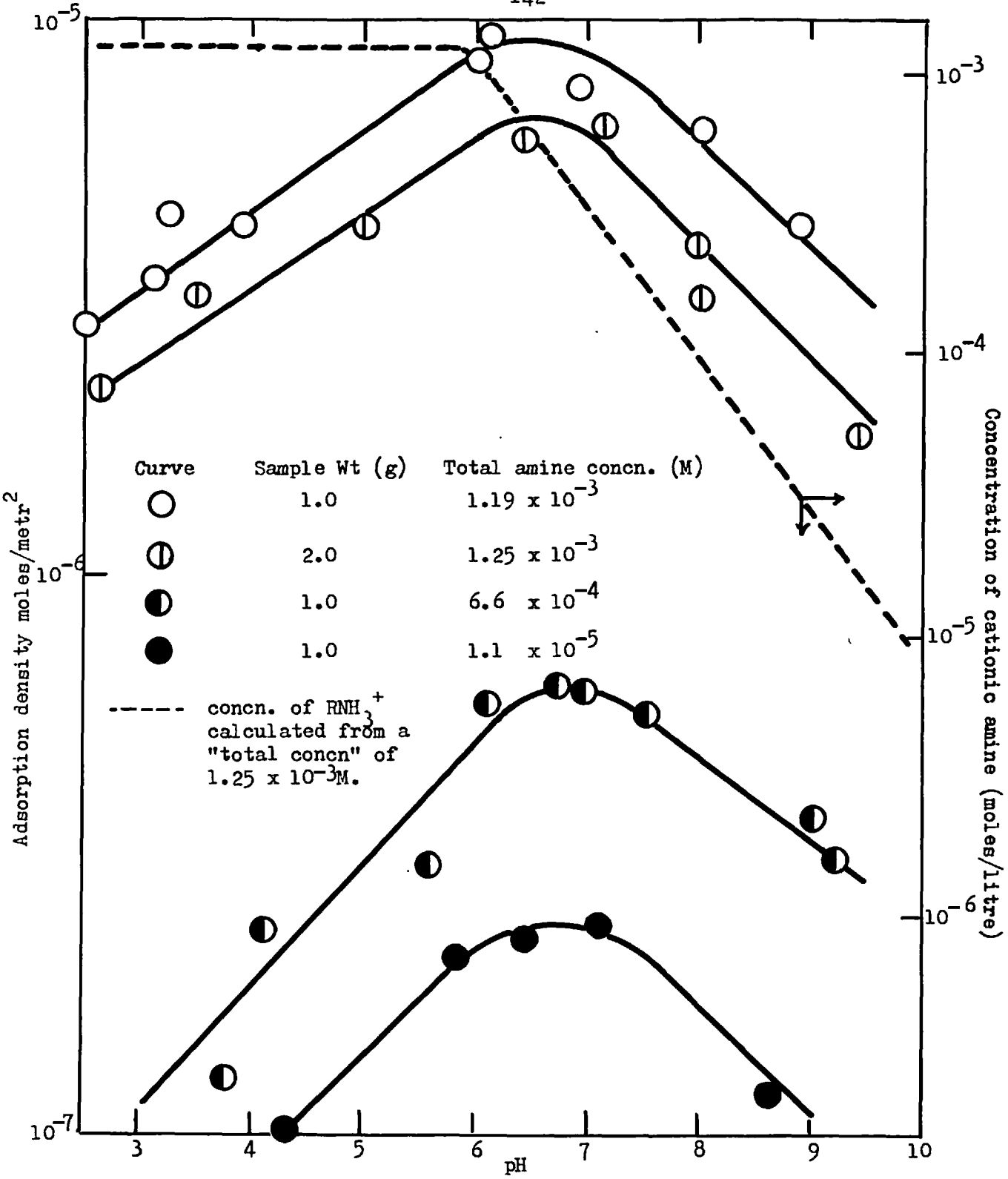

Fig. 26. Adsorption density of dodecylamine on quartz as a function of pH.
(ionic strength 6 x 10^{-3})

concentration in the aqueous phase as a function of pH for a 'total amine concentration' of 1.25×10^{-3}M. This curve was obtained for a system composed of only iso-octane and water in the presence of dodecylamine, using the equilibrium equations derived from section 2.00. It follows from these equations that similar curves would be obtained at different 'total concentrations'. Comparison of the adsorption density curves with the concentration curve shows that the decrease in adsorption density at pH values above neutral corresponded to a decrease in the cationic amine concentration of the aqueous phase.

In fig. 27 (a) the adsorption densities of dodecylamine on quartz, at three different constant pH values, are presented on a logarithmic basis as a function of the amine concentration in the aqueous phase. The points on these isotherms were obtained either from direct experimental determinations or from the following method. For each series of adsorption tests at constant 'total amine concentration', the determined amine concentrations in the organic and aqueous phases were plotted as a function of pH. From these curves the equilibrium concentration of amine in the aqueous phase was determined. The adsorption density at this pH was then read from the adsorption density curves (fig. 26).

The adsorption isotherm at pH 6.5 (fig. 27a) has been represented as two straight lines with slopes 0.70 and 1.50. These slopes are similar to the values of 0.5 and 1.20 obtained by de Bruyn (154) for the adsorption of amine at the quartz/water interface in the absence

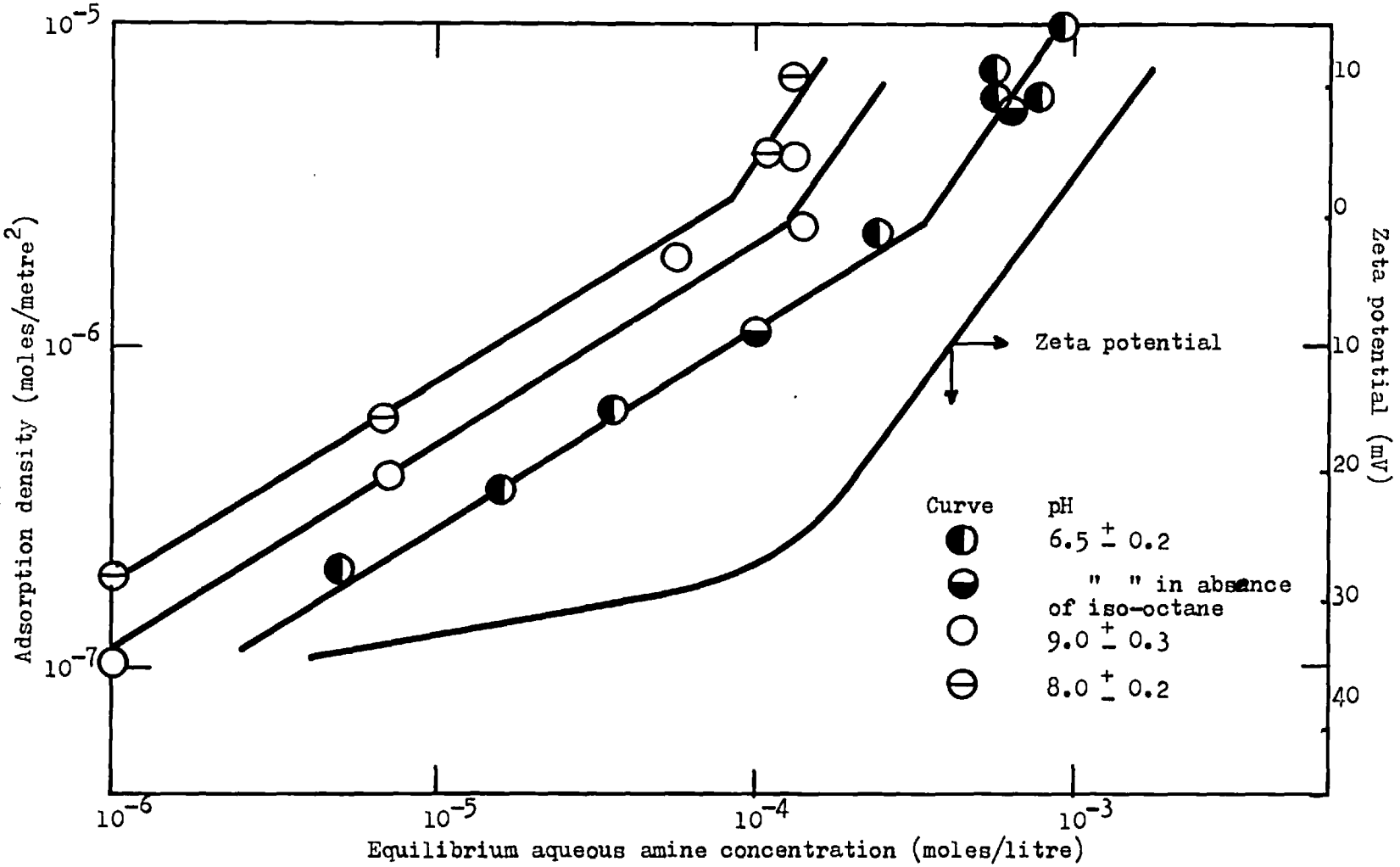

Fig. 27a. The logarithmic adsorption isotherm of dodecylamine on quartz.
(ionic strength 6×10^{-3})

-144-

of iso-octane and a constant ionic strength. The adsorption density and equilibrium concentration corresponding to the intersection of the two straight lines were 1.7×10^{-6} moles/metre^2 and 2.4×10^{-4} moles/litre respectively. These values were also essentially the same as those obtained by de Bruyn (154). Assuming the cross sectional area of the hydrocarbon chain of the amine ion to be 20Å^2, and greater than the cross sectional area of the polar group (155), the calculated adsorption density for a close packed vertically orientated monolayer is 8.4×10^{-6} moles metre^{-2}. This adsorption density was obtained at an amine concentration in the aqueous phase slightly higher than that required to reduce the quartz zeta potential to zero.

The two experimental points obtained in the absence of iso-octane, at pH 6.5, fell on the isotherm. This suggests that at this pH the adsorption of amine at the quartz/water interface was not affected by the presence of iso-octane.

Included also in fig. 27 (a) is the curve from fig. 25 relating the zeta potential of quartz, at pH 6.5, with the logarithm of the amine concentration. Comparison of this curve with the adsorption isotherm shows that both curves are similar in that they can be divided into two regions. Furthermore the concentration of aqueous amine at the intersection of the two linear curves of the adsorption isotherm corresponds closely to the range of amine concentration where the zeta potential became more dependent on the logarithm of the amine concentration.

The adsorption isotherms at pH 8.0 and 9.0 have been drawn as two straight lines in a similar way to the isotherm at pH 6.5. These isotherms are not presented with an adequate number of points to consider them completed, but since the data obtained were in good agreement with those of de Bruyn (154) it was thought unnecessary to include more points. In fig. 27 (b) the adsorption isotherm at pH 6.5 has been plotted on a linear basis. The shape of this isotherm indicates that the adsorption followed the type L_4 isotherm which Giles et al. (156) considers to be due to the adsorption of ionic substances with very strong intermolecular attraction, possibly with the association of ions into clusters before adsorption. The isotherm, as presented in fig. 27b shows that the adsorption density at the point of intersection of the logarithmic adsorption isotherm (fig. 27a) corresponds to a monolayer of amine if the area per adsorbed ion were 76Å^2. According to Klassen and Mokrousov (157) the length of a 12 hydrocarbon chain would be approximately 14Å. If it is assumed that the diameter of the chain is 4Å and that the area of the polar group is 20Å^2, then an area per adsorbed ion of 76Å^2 would correspond to a close-packed horizontally orientated monolayer. The adsorption density increased only by a small amount between an equilibrium aqueous amine concentration of 2.5×10^{-4}M and 5.5×10^{-4}M. Above this latter concentration the adsorption density increased rapidly and reached a maximum at an adsorption density corresponding to a close-packed vertically orientated monolayer.

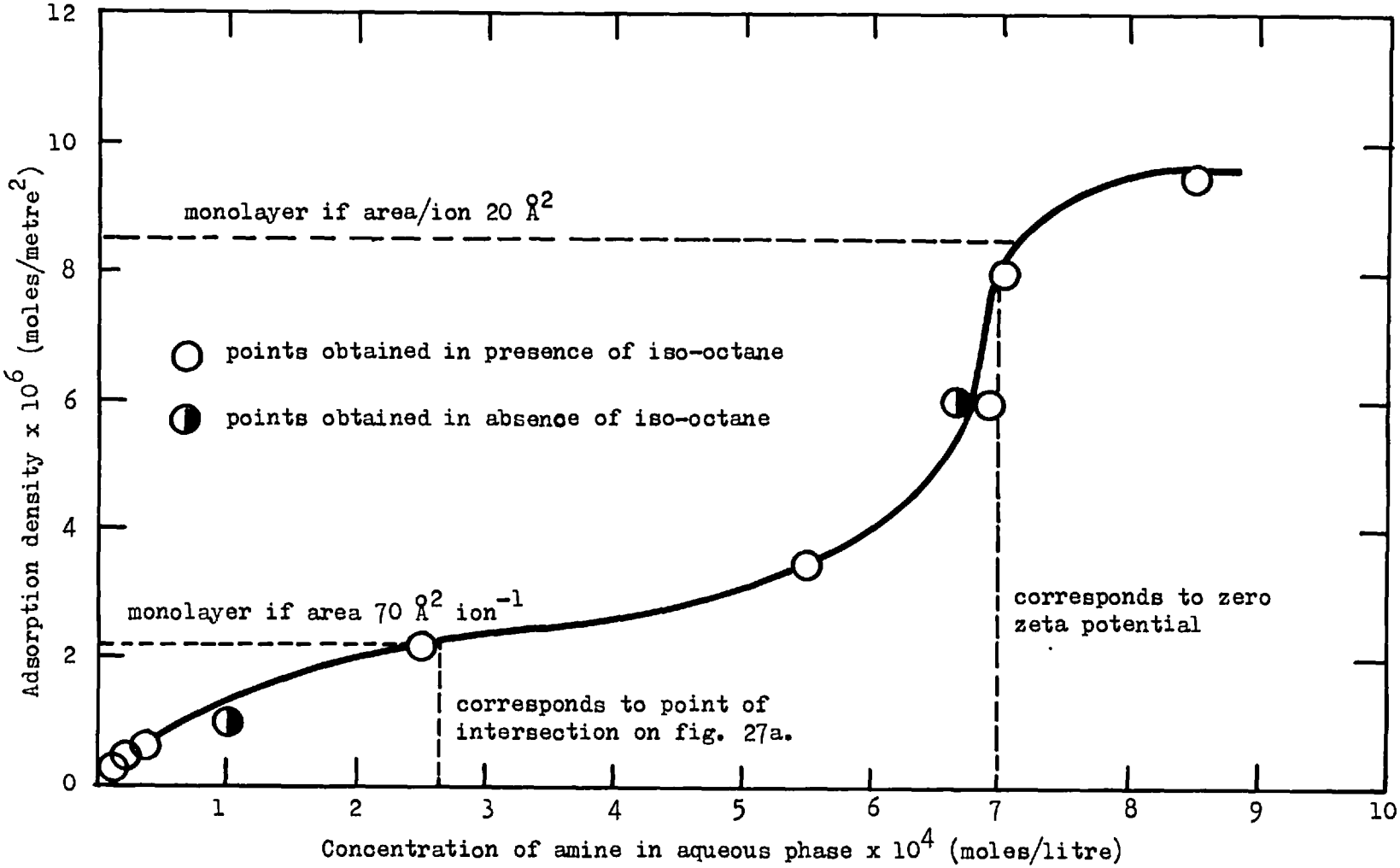

Fig. 27b. Adsorption density of dodecylamine on quartz as a function of the aqueous amine concentration.

(pH 6.5 $\pm$ 0.2; ionic strength 6 x 10^{-3})

c) The effect of dodecylamine concentration on the contact angles

The receding contact angles of iso-octane on natural and optical quartz, in the presence of six different 'total concentrations' of dodecylamine, as a function of pH are shown in figs. 28 and 29. In the absence of amine the contact angles on both the quartz samples were zero at pH values above 5. Below pH 5, however, although the receding angles were too small to measure ($\ll 10$) there was a tendency for the oil drop to show a small degree of 'stickiness', when receded completely from the quartz surface. In distilled water the contact angle was zero. This was in accordance with the findings of Gaudin and co-workers (129).

For each 'total concentration' of amine the receding contact angles increased from 0 at pH values below 3 to a maximum at between pH values 7 and 8 and then decreased as the pH was further increased. Comparison of the curves correlating the receding contact angles and the adsorption density with the pH (figs. 28, 29 and 26) shows that the decrease in contact angle in alkaline media corresponded to a decrease in both the adsorption density and the cationic amine concentration of the aqueous phase. This comparison also shows that the contact angles approaching the z.p.c. of quartz, were small and nearly independent of the total amine concentration, although considerable amounts of amine were adsorbed.

The advancing angles for the iso-octane drops on the quartz samples have not been included in figs. 28 and 29 because, in general, the relationship between the advancing angles was of the

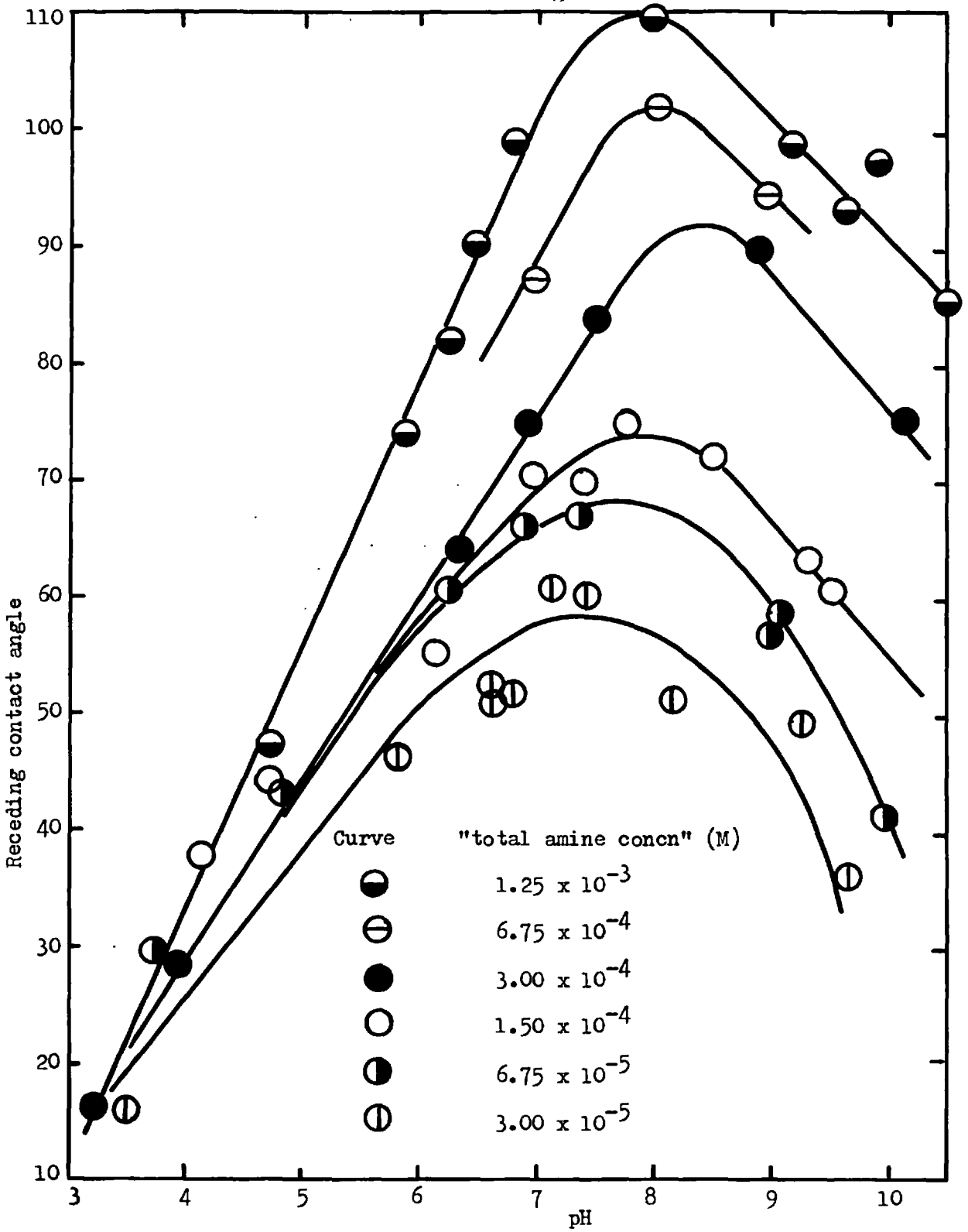

Fig. 28. Receding contact angles on optical quartz in the presence of dodecylamine as a function of pH. (ionic strength 6×10^{-3})

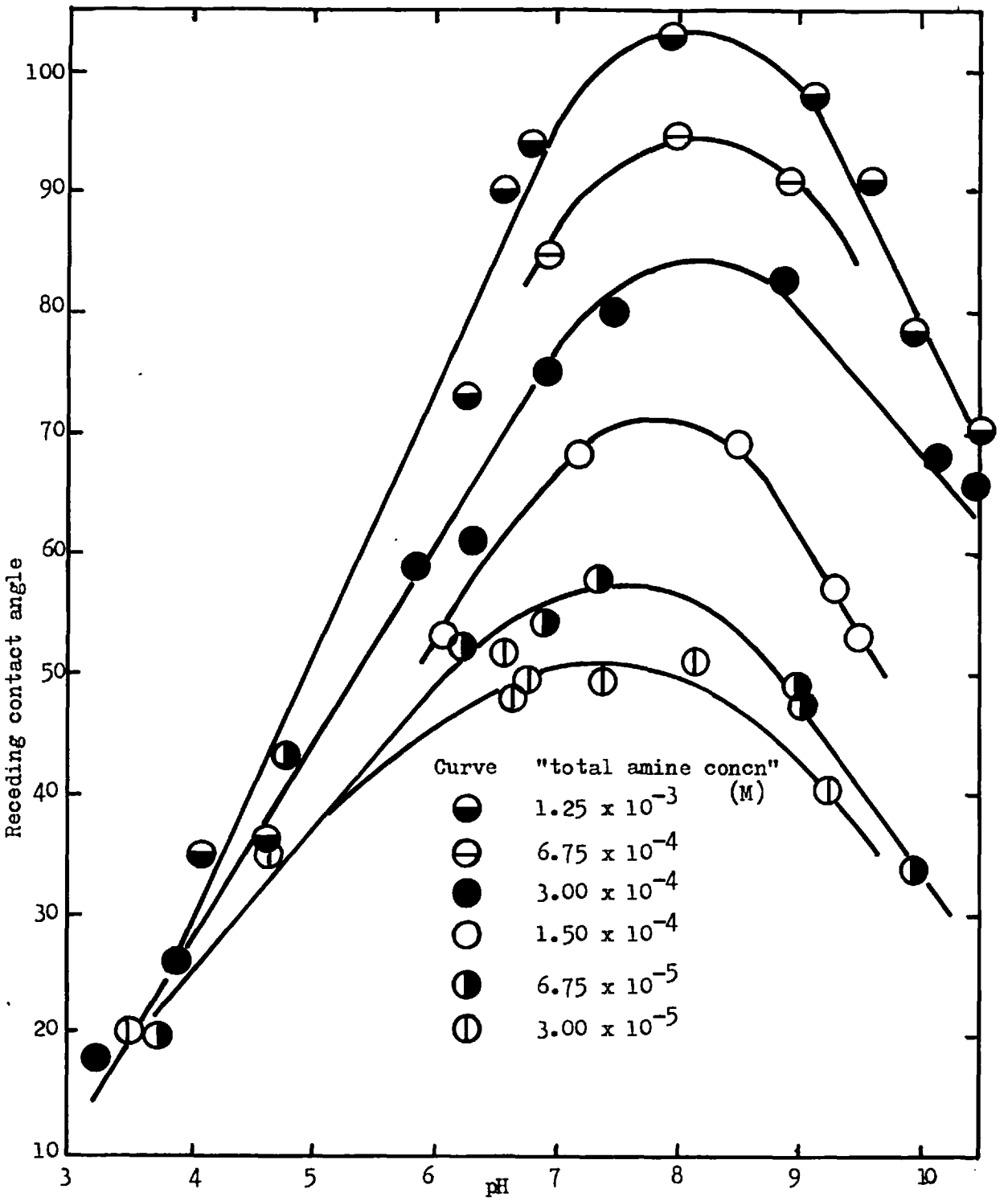

Fig. 29. Receding contact angles on natural quartz, in the presence of dodecylamine, as a function of pH.
(ionic strength 6×10^{-3})

same form as the relationship between the receding angles and the pH. For the optical quartz the receding angles were approximately 20° greater than the advancing angles, and for the natural quartz the difference was $30-35^{\circ}$ at high 'total amine concentrations' and about 20° at low concentrations.

The receding and advancing contact angles on the natural and optical quartz have been presented in fig. 30, as functions of the logarithm of the equilibrium dodecylamine concentration in the aqueous phase at pH values 6.5 and 8.0. The concentrations of amine in the aqueous phase were deduced from the total amine concentrations by using the equilibrium equations derived in section 2.00. The amine adsorbed on the sample surface of only a few square centimetres was negligible compared to the total amount of amine in the system. Figure 30 shows that the relationship between both the receding and advancing angles and the logarithm of the aqueous amine concentration can also be divided into two linear regions. In the first region the contact angles increased slowly with an increase in the logarithm of the amine concentration and in the second region the contact angle increased more rapidly. The slopes of the two linear parts of the curves were approximately 15 and 35 degrees per tenfold increase in concentration, respectively. The receding and advancing angles corresponding to the transition from one region to the other were 60° and 50° respectively. For the natural quartz sample, at pH 6.5, the aqueous amine concentrations at the transition contact angles were 1.0×10^{-4}M for the receding angles and 2.5×10^{-4}M for

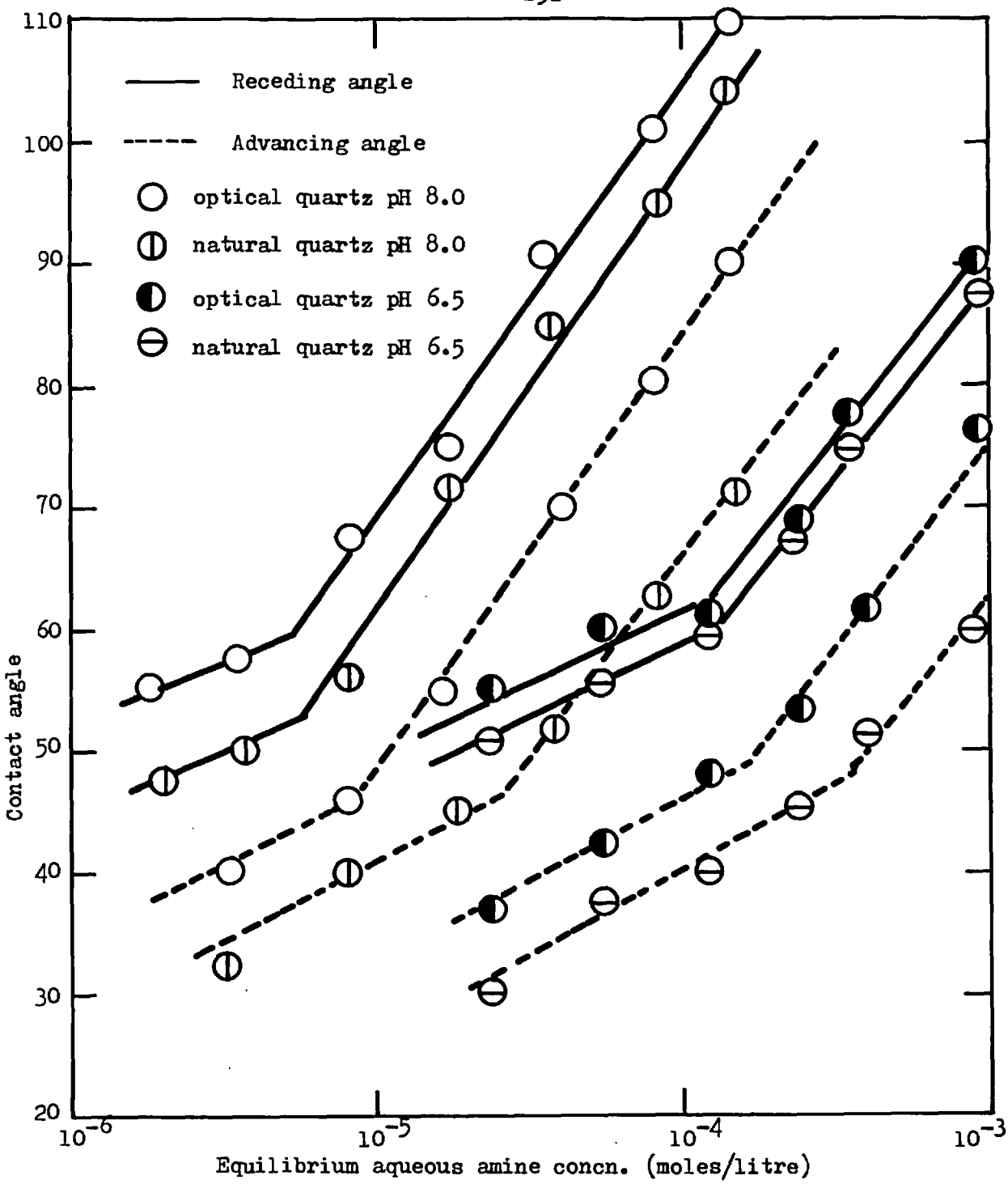

Fig. 30. Receding and advancing angles on optical and natural quartz as a function of amine concentration.
(ionic strength 6×10^{-3})

the advancing angles. Both of these concentrations are in good agreement with the equilibrium aqueous amine concentration at the intersection of the two linear parts of the adsorption isotherm (fig. 27a). However, although the shape of the curves correlating the contact angles with the logarithm of the aqueous amine concentration were similar to the adsorption isotherm, no such agreement was found at pH 8.0.

d) Extraction results

The results obtained from the tests designed to determine the percentage of quartz extracted or concentrated at the iso-octane/water interface, in the presence of five different "total concentrations" of amine are presented in fig. 31 as a function of pH. At each 'total concentration of amine' an increase in the pH produced an increase in the percent extraction from zero, at low pH values, to a maximum at approximately neutral pH values and then a decrease to zero at high pH values. The pH range over which maximum extraction was obtained at each 'total amine concentration' was dependent on the magnitude of the 'total concentration'. Thus, maximum extraction occurred between pH values 5 and 6.5 for a 'total amine concentration' of 3.2×10^{-5}M and between 3.5 and 8.5 for a concentration of 1.35×10^{-3}M.

In fig. 32 the percent extraction, adsorption density, receding contact angles and concentration of cationic amine in the aqueous phase (calculated from equations in section 2) are plotted as a function of pH. These curves show that, in general, there was a

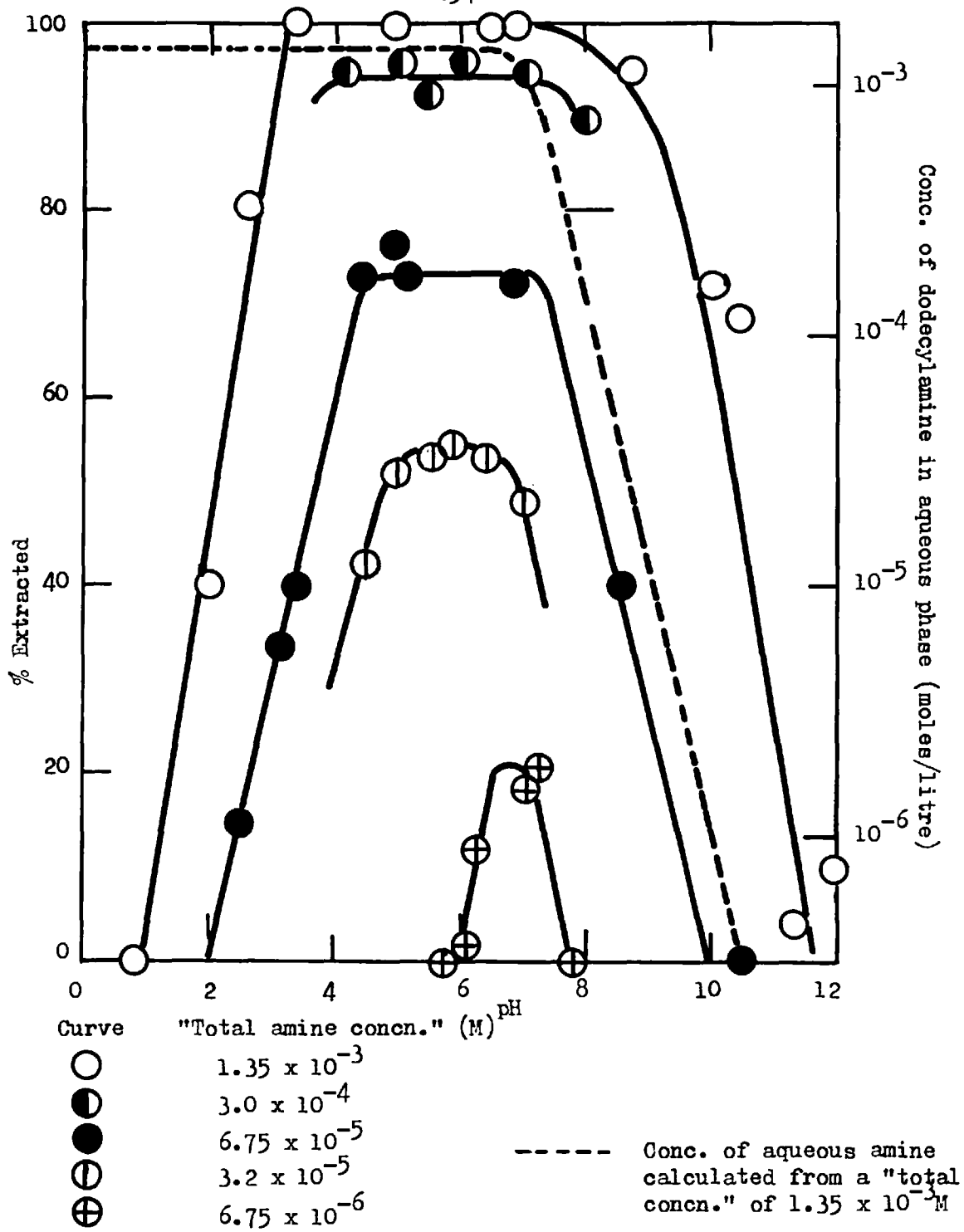

"Fig. 31. Percent extraction of quartz as a function of pH with dodecylamine as collector.

(ionic strength 6 x 10^{-3})

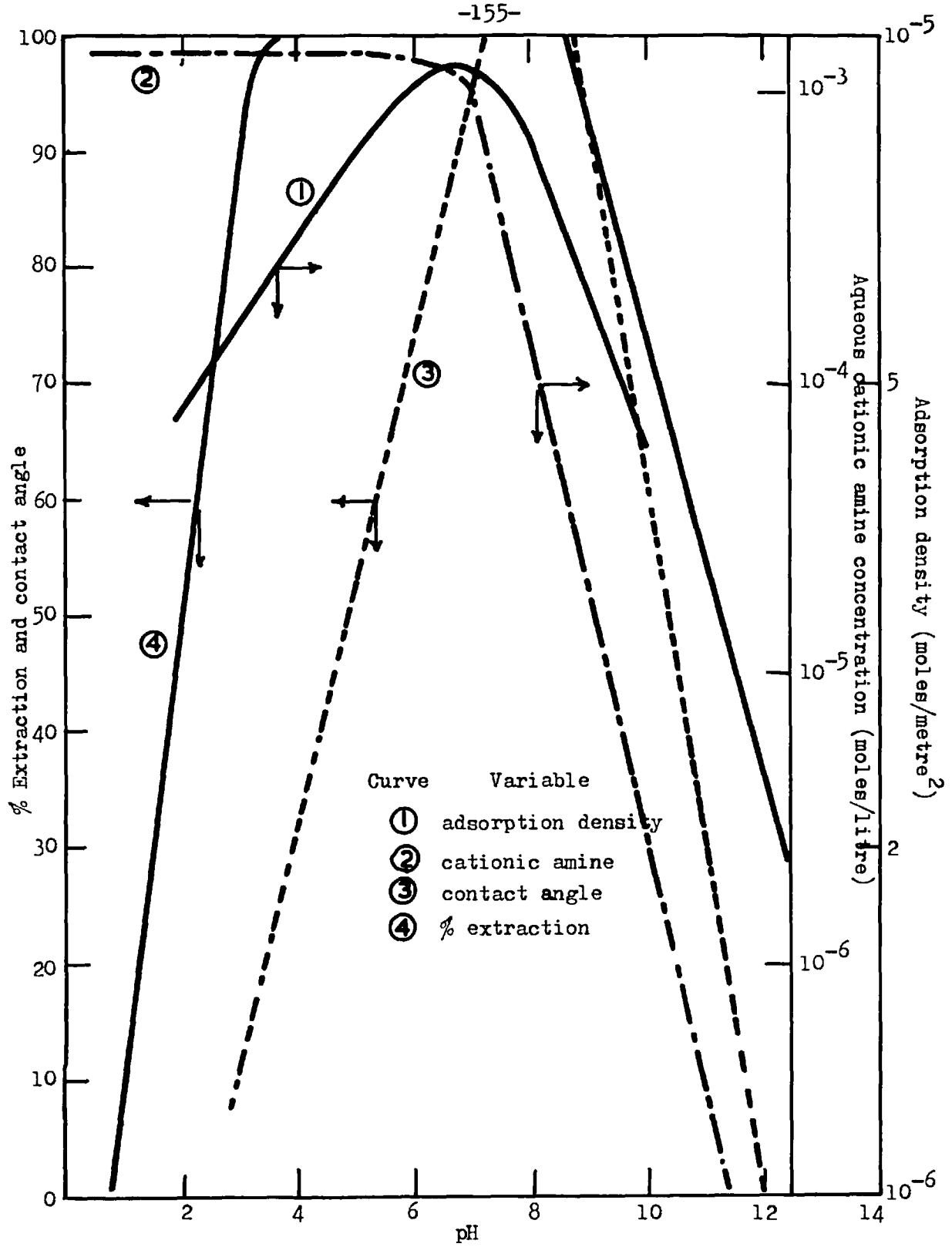

Fig. 32. Percent Extraction, contact angle, adsorption density and aqueous cationic amine concn. as functions of pH.

(ionic strength 6×10^{-3}; $(RNH_2)_T = 1{\cdot}25 \times 10^{-3}$M)

good correlation between the four variables describing the conditions in the oil/water/quartz system. As the pH was increased the adsorption density, contact angles and percent extraction increased to a maximum and then decreased as the pH became more alkaline. The decrease in the magnitude of these variables in alkaline media corresponded to a decrease in the cationic amine concentration of the aqueous phase. The zeta potential results have not been included in fig. 32 because they were obtained in the absence of iso-octane and therefore under conditions where amine was not removed from the aqueous phase with an increase in pH. The appearance of the oil drops in the upper layer of the separating column is shown in Plates I and II. The samples for these photographs were obtained by diluting a small volume of the upper layer with amine solution at the relevant pH and concentration. It can be seen that each drop was covered by small quartz particles and that in some cases the particles were so tightly packed that the oil drop was distorted from a spherical shape.

Figure 33 presents the percent extraction at pH 6.5 as a function of the receding contact angles and the logarithms of the 'total amine concentration', the equilibrium aqueous amine concentration and the adsorption density. The equilibrium aqueous amine concentration for a given extraction test was deduced from knowledge of the 'total amine concentration' and the adsorption isotherm. (figs. 26 and 27a). Using the equilibrium concentrations, so obtained, the receding contact angles were obtained from fig. 30. These curves show that

Plate I

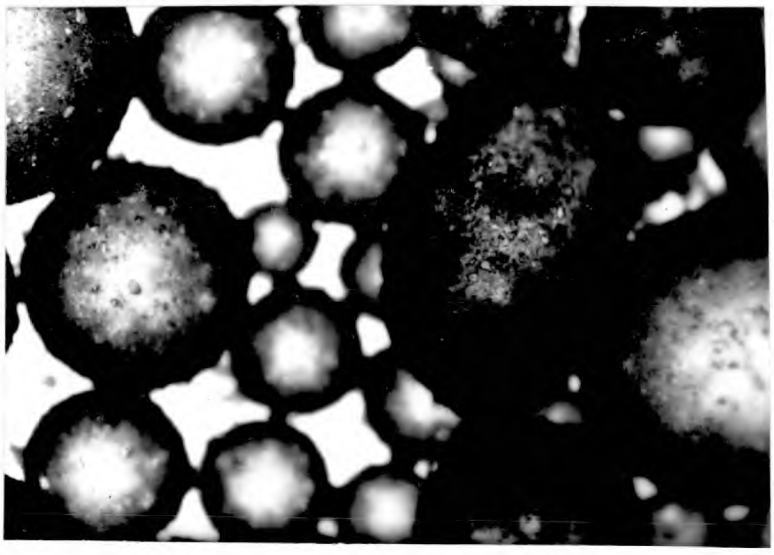

Plate II

Quartz particles concentrated at the oil/water interface in the presence of a "total amine concentration" of 10^{-3}M.

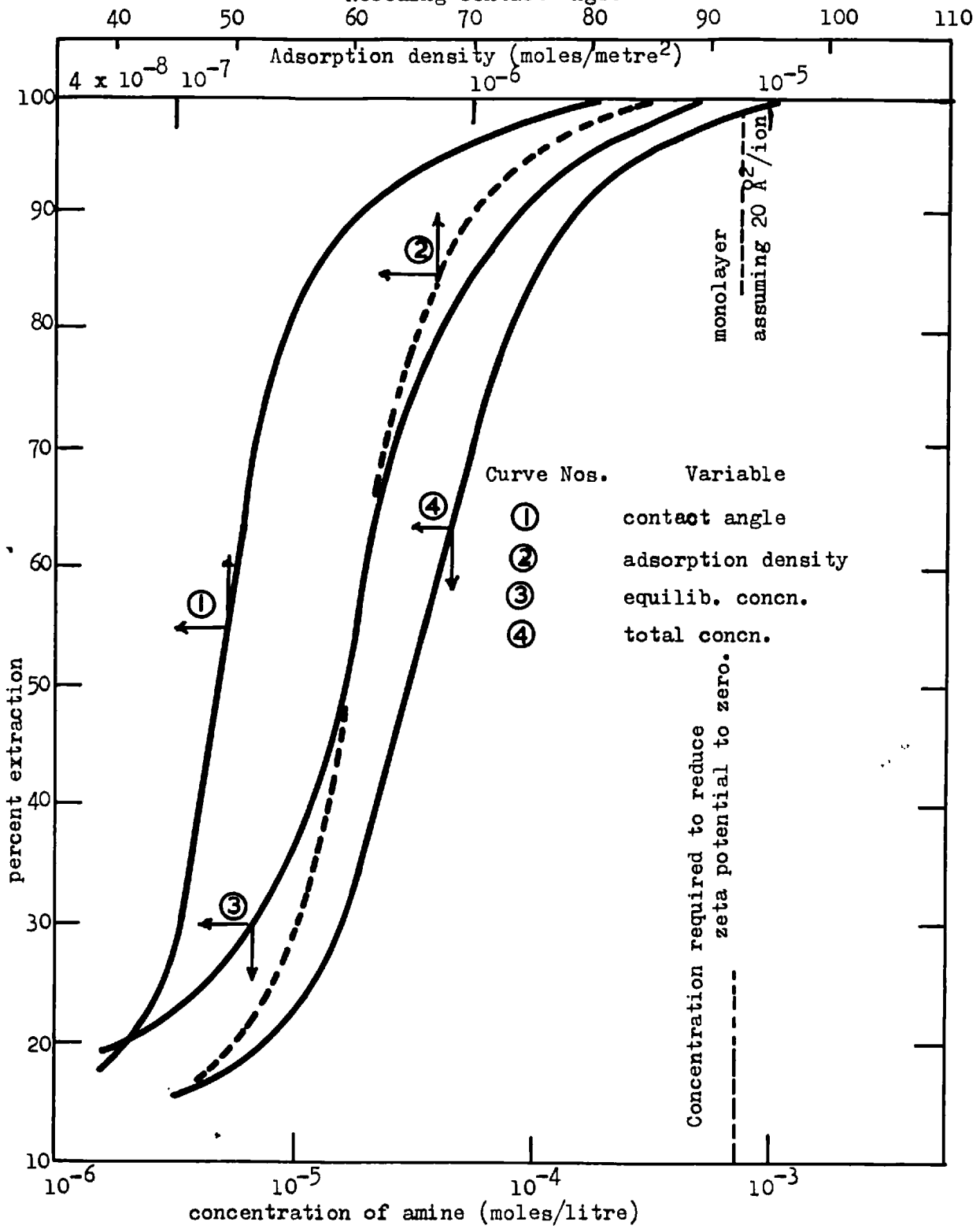

Fig. 33. % Extraction as a function of amine concentration, adsorption density and contact angle.

(ionic strength 6×10^{-3}; pH 6.5)

100% extraction was obtained when the following conditions were satisfied: a) the equilibrium concentration and adsorption density were such that the zeta potential was zero. This adsorption density also corresponded approximately to a close packed vertically orientated monolayer. b) the receding contact angle was 90 degrees.

Comparison of curves (1), (2) and (3) with figs. 27a and 30 shows that 90% extraction corresponded to the contact angle at the transition from one linear region to the other in the curve correlating the receding contact angle with the logarithm of the equilibrium aqueous amine concentration, and also corresponded to the adsorption density and equilibrium concentration at the point of intersection of the linear parts of the adsorption isotherm. Below an extraction of 90 percent a small decrease in the receding contact angle, or the logarithms of the aqueous amine concentration and the adsorption density, produced a large decrease in the percent extraction.

4.32. The hematite/iso-octane/sodium dodecyl sulphate system

a) Electrokinetic results

i) The effect of the pH and different anions on the zeta potential

Tests were conducted to ascertain whether the ageing of hematite in distilled water influenced the zeta potential or not. It was found that provided the sample was stored in distilled water for 24 hours before use, the zeta potential became independent of time.

The dependence of the zeta potential on the pH in the presence of the four anions ClO_4^-, NO_3^-, Cl^- and SO_4^{2-} is shown in fig. 34. In the presence of the anions ClO_4^-, NO_3^- and Cl^- an increase in the pH produced a decrease in the positive zeta potential to zero at pH 4.75 (zero point of charge). As the pH was increased above 4.75 the zeta potential changed sign and became increasingly more negative. At pH values below the zero point of charge (z.p.c.) the positive zeta potential was independent of the anions, but above the z.p.c. the negative zeta potential was increased by changing the anions in the order ClO_4^-, NO_3^-, Cl^-.

In the presence of sulphate ions, the curve correlating the zeta potential with the pH was displaced to more negative zeta potentials, and as a result the pH corresponding to the z.p.c. was decreased from 4.75 to 3.5.

ii) The effect of sodium dodecylsulphate on the zeta potential

The variation of the hematite zeta potential with pH in the presence of eight different concentrations of sodium dodecyl sulphate (S.D.S.) is shown in fig. 35. All of the S.D.S. solutions were prepared in hydrochloric acid and so the curve at zero S.D.S. concentration represents the HCl- NaOH curve from fig. 34. The curve correlating the zeta potential with the pH, at each concentration of S.D.S., was similar to that obtained in the absence of S.D.S., except that it was displaced to more acid pH values. The pH corresponding to zero zeta potential decreased as the S.D.S. concentration increased. An increase in the S.D.S. concentration produced a

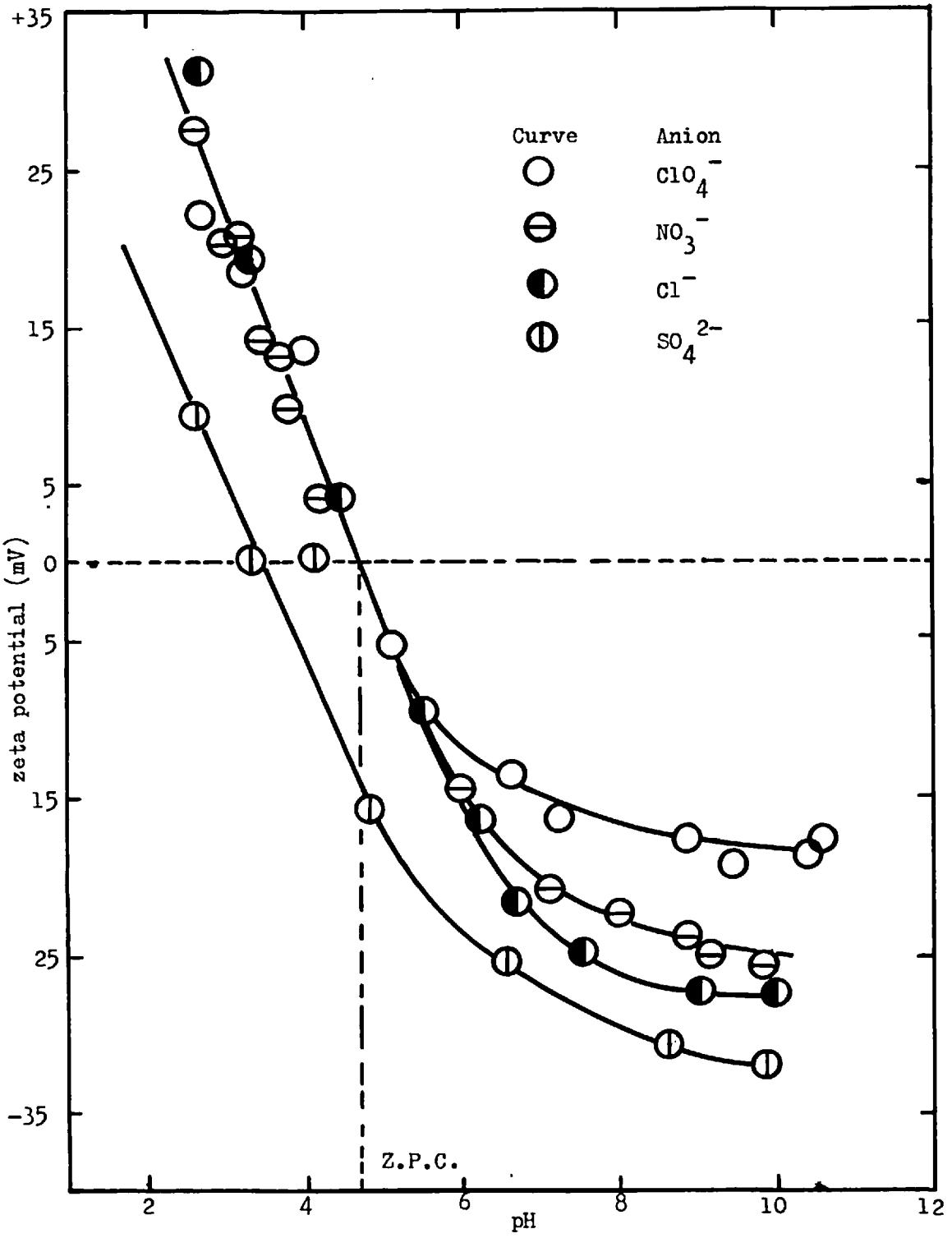

Fig. 34. Zeta potential of hematite as a function of pH in the presence of various anions.
(ionic strength 6×10^{-3})

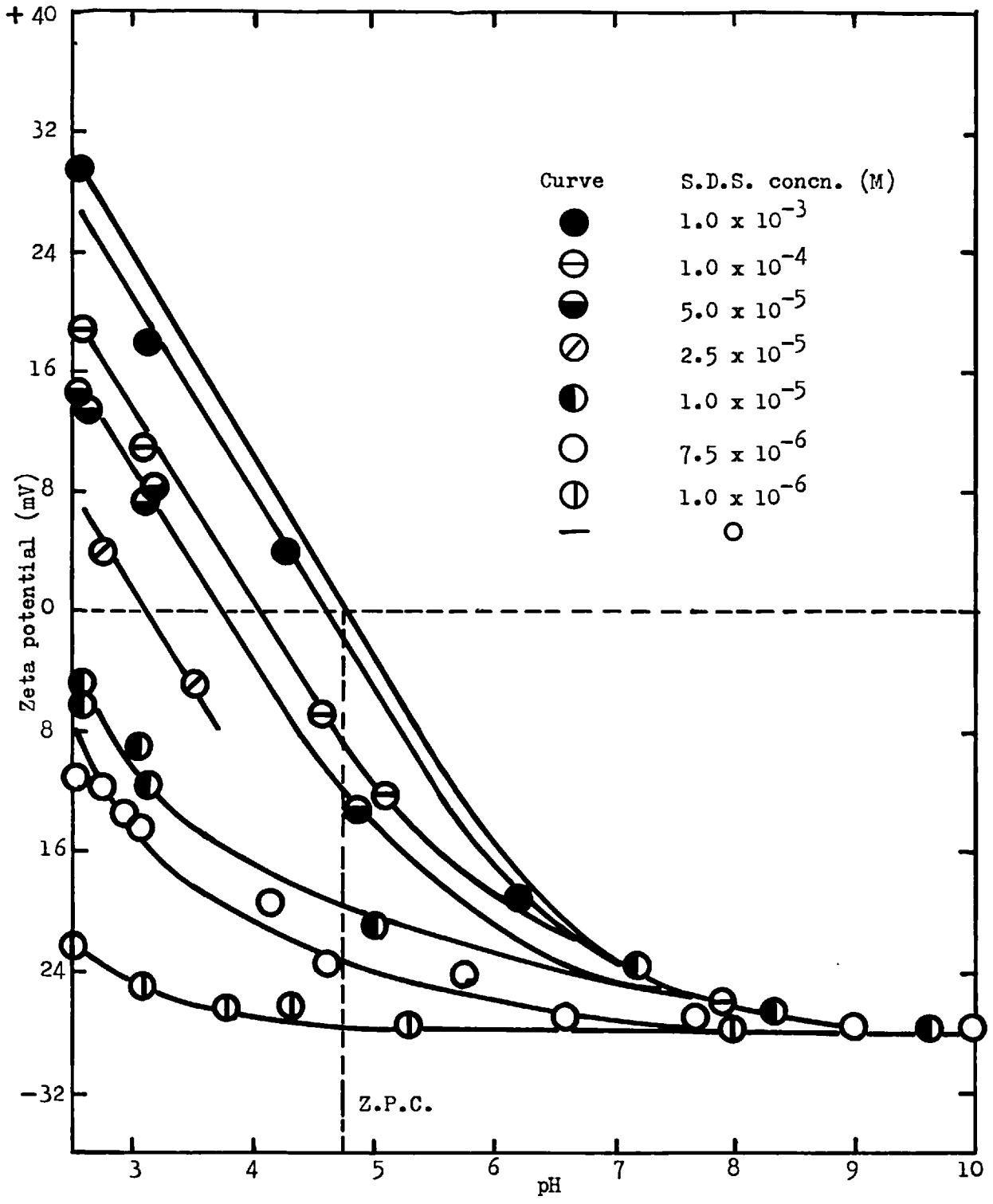

Fig. 35. Zeta potential of hematite as a function of pH in the presence of various S.D.S. concentrations.

(ionic strength 6 x 10^{-3})

decrease in the positive zeta potential, at pH values below the z.p.c., until it eventually changed sign and became negative, and an increase in the negative zeta potential at pH values above the z.p.c.

The difference ($\Delta\xi$) between the zeta potential at a given pH in a given concentration of sodium dodecyl sulphate and the zeta potential at the same pH in the absence of S.D.S., decreased as the pH was increased. However, at pH values slightly above the z.p.c. $\Delta\xi$ was still large and this indicated that although the hematite surface was negative considerable quantities of S.D.S. were adsorbed. At high pH values, and at all concentrations, $\Delta\xi$ became zero.

The zeta potential data from fig. 35, has been used in fig. 36 to show the dependence of the hematite zeta potential on the logarithm of the S.D.S. concentration at pH 2.5, 3.0, 5.0 and 6.0. At pH values 2.5 and 3.0 and at S.D.S. concentrations between 5×10^{-6}M and 10^{-4}M the relationship between the zeta potential and the logarithm of the S.D.S. concentration was essentially linear with a slope of -25 millivolts per tenfold increase in concentration. In this linear region the positive zeta potential decreased to zero and then became negative. A zero zeta potential was obtained at a concentration of 4×10^{-5}M at pH 2.5. At high ($> 10^{-4}$M) and low ($< 5 \times 10^{-6}$M) concentrations the curve correlating the zeta potential with the logarithm of the concentration deviated from a straight line and the zeta potential became less dependent on the logarithm of the S.D.S. concentration.

At pH values 5.0 and 6.0 the negative zeta potential gradually

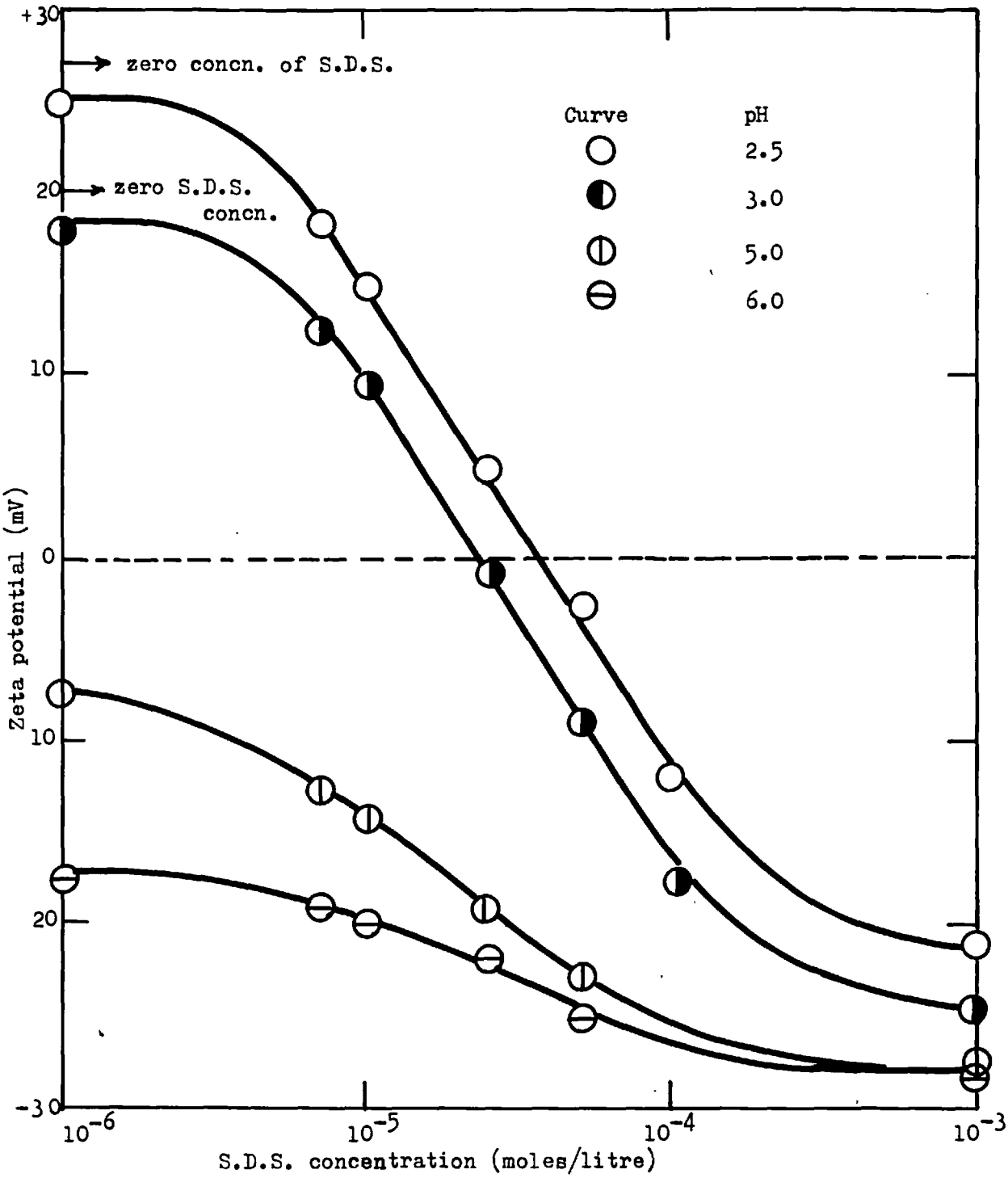

Fig. 36. Zeta potential of hematite as a function of S.D.S. concentration at different pH values.

(ionic strength 6×10^{-3})

increased with an increase in the logarithm of the S.D.S. concentration. The dependenoe of the zeta potential on the S.D.S. concentration decreased as the pH was increased.

b) The adsorption of sodium dodecyl sulphate by hematite

The results of the tests conducted to determine the adsorption density of S.D.S. on hematite at various pH values, in the presence of four different initial concentrations are shown in fig. 37. The 'initial' concentration refers to the concentration of S.D.S. in the aqueous phase prior to the addition of the hematite. For any given concentration of S.D.S. and at pH values below 4, a change in the pH produced only a small variation in the logarithm of the adsorption density. As the pH approached the z.p.c. of hematite i.e. pH 4.75, the logarithm of the adsorption density decreased rapidly. An inorease in the initial concentration of S.D.S. produced a shift in the curve correlating the logarithm of the adsorption density with the pH, to higher adsorption densities.

Plotted also in fig. 37 as a function of pH is the logarithm of the zeta potential difference ($\Delta\zeta$) between the zeta potential in 10^{-3}M S.D.S. and that in the absence of S.D.S. Comparison of this curve with the logarithm of the adsorption density curves shows that the decrease in adsorption density with increase in pH corresponded quite well to a decrease in $\Delta\zeta$.

The results of the adsorption tests conducted in the presence of iso-octane at three different initial conoentrations of S.D.S. are shown in fig. 38. Comparison of this figure with fig. 37 shows

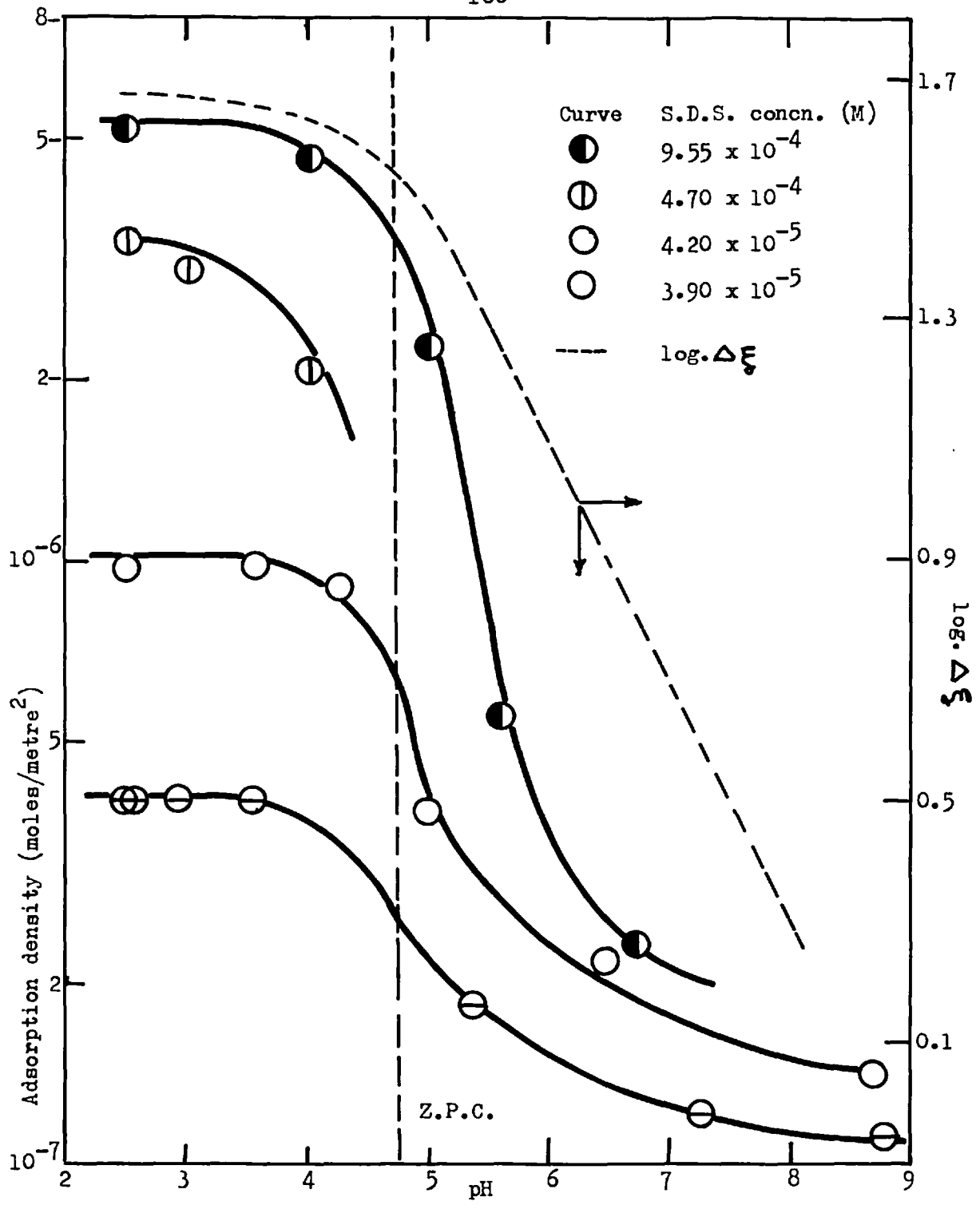

Fig. 37. Adsorption density of S.D.S. on hematite as a function of pH.

(ionic strength 6×10^{-3})

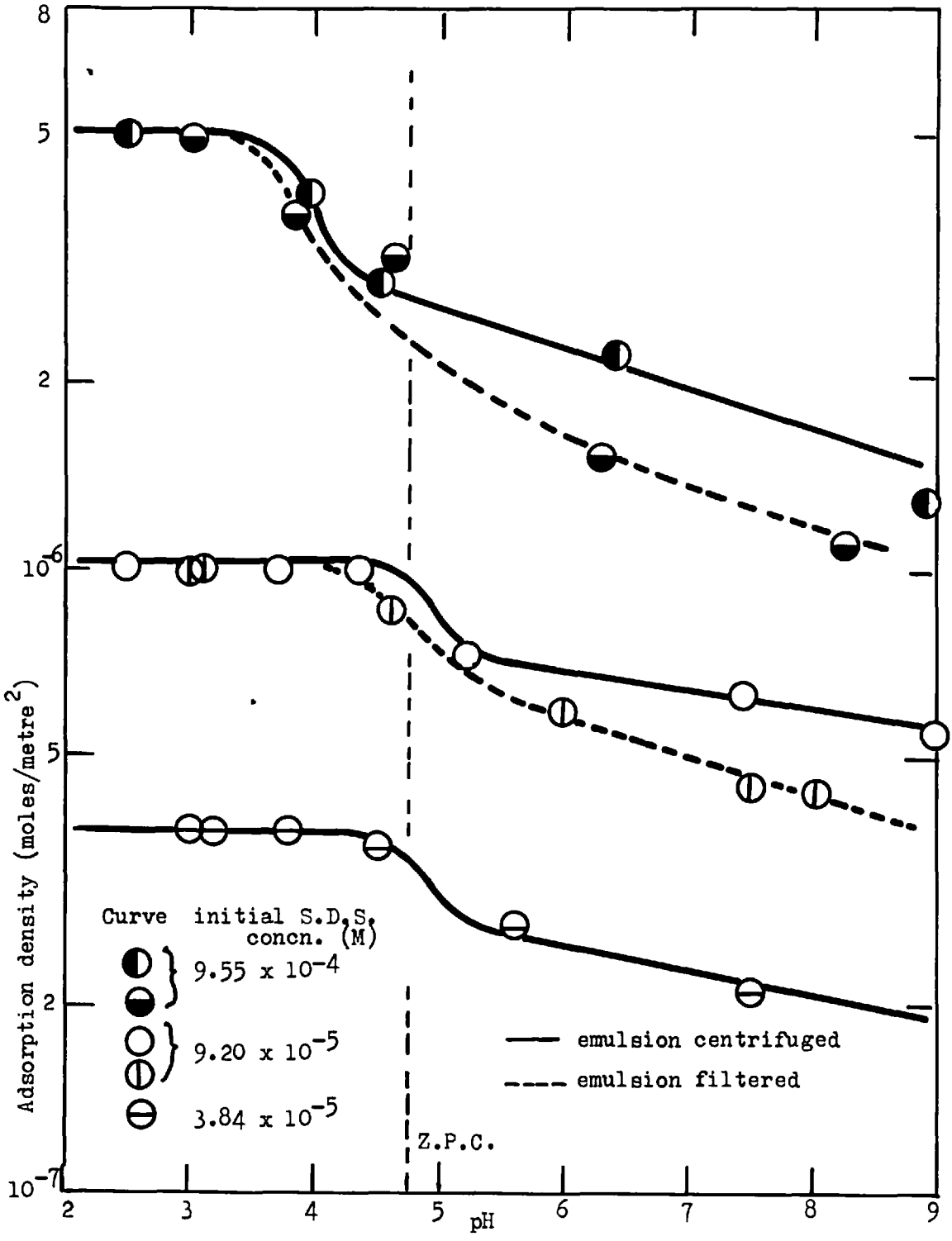

Fig. 38. Adsorption of S.D.S. on hematite, in the presence of iso-octane, as a function of pH.
(ionic strength 6 x 10^{-3})

that at pH values below the z.p.c. of hematite the adsorption density was independent of the presence of iso-octane. At pH values above the z.p.c. the presence of iso-octane apparently increased the magnitude of the adsorption density. This increase was, however, dependent on the method used, to break the O/W emulsion and to separate the hematite from the two liquid phases. The most efficient way of breaking the emulsion was filtration which produced lower adsorption densities than centrifugation. A complete breaking of the emulsion was not, however, obtained even with filtration and as a result some heavily hematite coated, iso-octane drops were filtered out with the free hematite.

The curve correlating the adsorption density with the equilibrium concentration of S.D.S. at pH 2.6 $\pm$ 0.1, is presented in fig. 39 on a logarithmic basis. This isotherm was obtained in the absence of iso-octane which was considered unnecessary in view of the independence of the adsorption density on the presence of iso-octane at pH values below the z.p.c. (figs. 37 and 38). The isotherm is divided into three regions. Region I extends over the concentration range below that required to reduce the zeta potential to zero. In this region the logarithm of the adsorption density increased rapidly with anincrease in the logarithm of the equilibrium concentration until a concentration of 4×10^{-5}M (the onset of region II) was reached. The adsorption density at this concentration corresponded to a close packed monolayer if the area per adsorbed ion was 70Å^2. This area is slightly less than the area which a dodecyl sulphate ion would

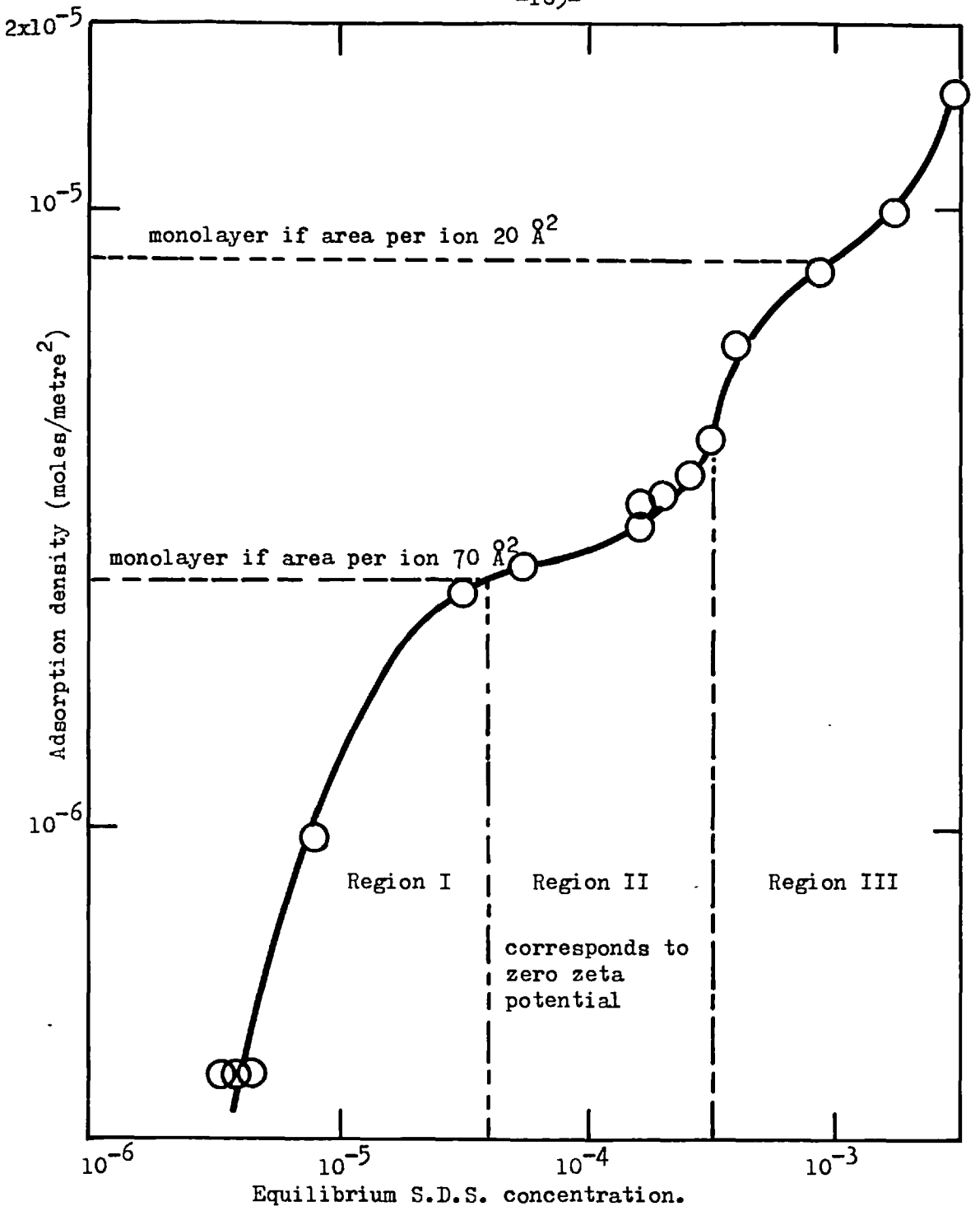

Fig. 39. Adsorption density of S.D.S. on hematite as a function of equilibrium concentration.
(ionic strength 6×10^{-3}: pH 2.6 ± 0.1)

occupy in a close packed horizontally orientated monolayer. In region II the logarithm of the adsorption density increased slowly at first, with an increase in the logarithm of the equilibrium concentration, and then more rapidly as the concentration approached 3.2×10^{-4}M. Above this concentration (region III) the adsorption density increased rapidly, levelled off at an adsorption density of 8.6×10^{-6} moles/metre^2, and then increased again. An adsorption density of 8.6×10^{-6} moles/metre^2 corresponds to a monolayer if the area per adsorbed ion is 20Å^2; an area similar to the 25Å^2 (155) which a dodecyl sulphate ion occupies in a close packed vertically orientated monolayer.

o) <u>The effect of sodium dodecyl sulphate concentration on the contact angles</u>

The receding contact angles of iso-octane on hematite in the presence of sodium dodecyl sulphate at eight different concentrations are shown in fig. 40 as a function of pH. In the absence of S.D.S. both the receding and advancing angles were zero. The curves correlating the contact angle with the pH show that as the pH was increased the receding contact angles decreased, slowly at first, and then more rapidly as the pH approached 4. An increase in the initial concentration produced larger receding angles. Comparison of fig. 40 with fig. 37 shows that the decrease in contact angle with inorease in pH corresponded to a decrease in the logarithms of the adsorption density and $\Delta\zeta$.

The receding contact angles, from fig. 40 have been used in

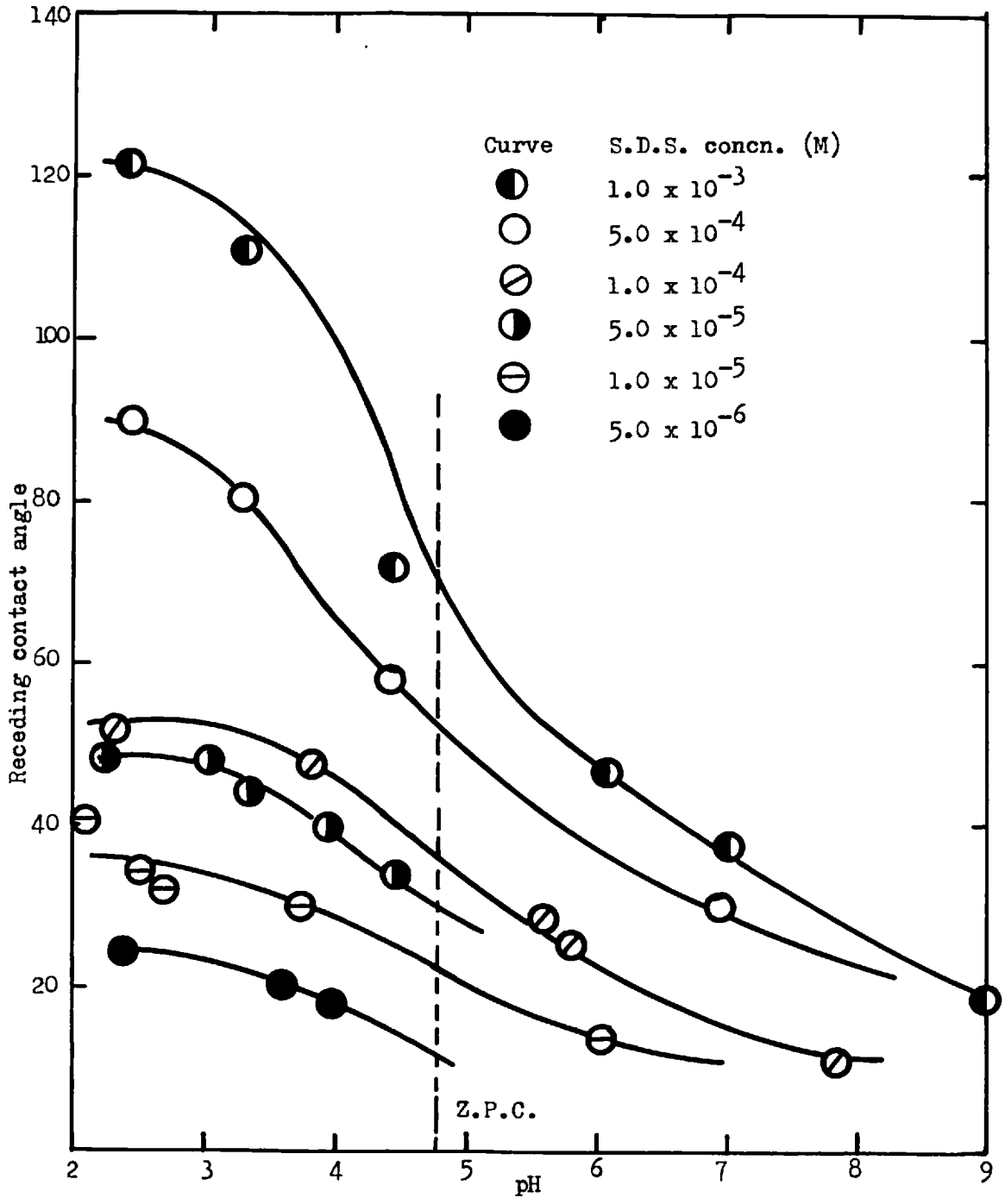

Fig. 40. Receding contact angle on hematite, in the presence of various concentrations of S.D.S., as a function of pH.

(ionic strength 6×10^{-3})

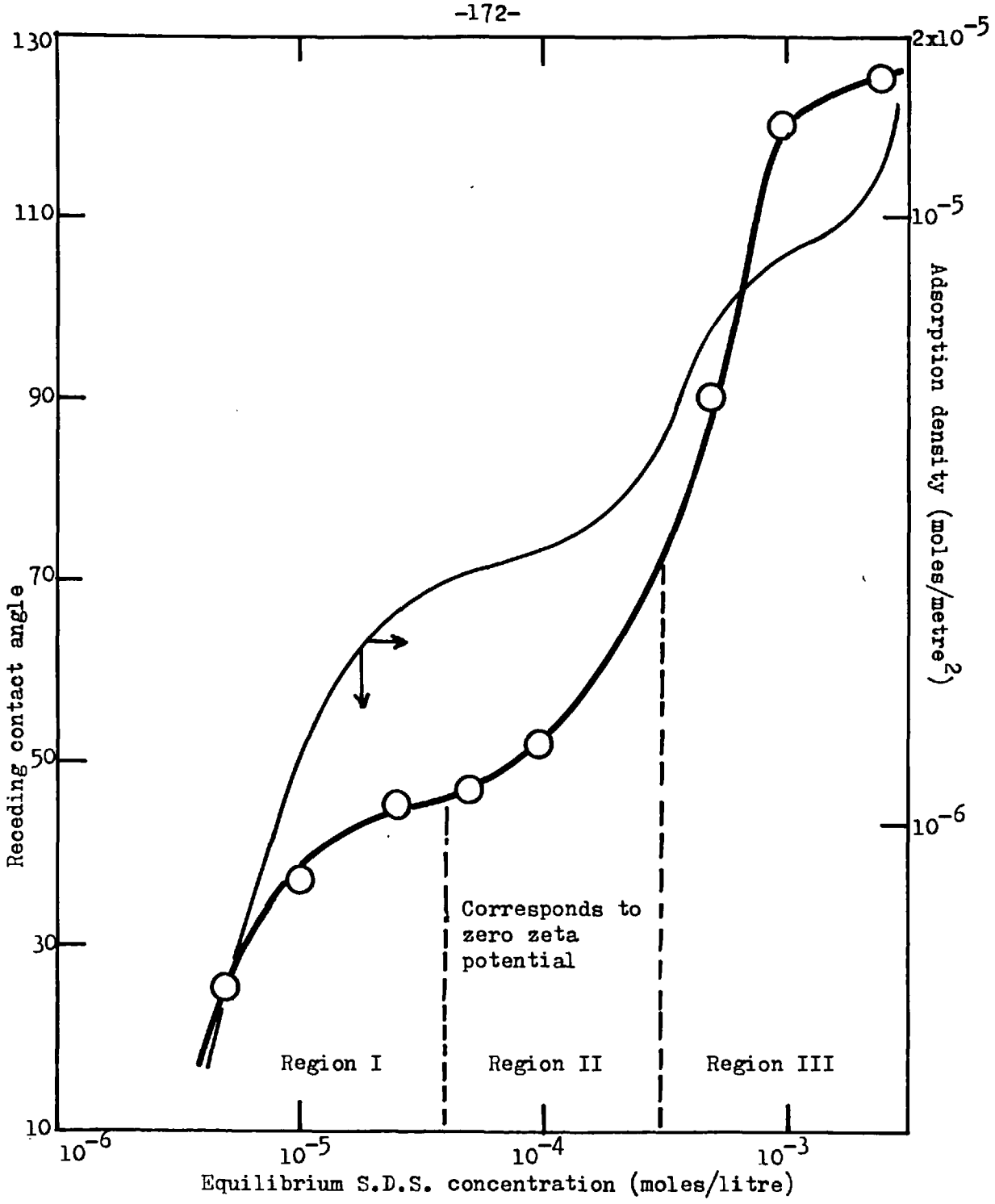

Fig. 41. Receding contact angles on hematite as a function of S.D.S. equilibrium concentration.
(ionic strength 6 x 10^{-3}; pH 2.6)

fig. 41 to correlate the contact angles with the logarithm of the concentration of S.D.S. at pH 2.6. Also plotted in fig. 41 is the adsorption isotherm from fig. 40. Because of the similarity in shape of these two curves the contact angle curve is also divided into three regions. Each region extends over the same concentration range as that used for the adsorption isotherm. In region I the contact angle increased rapidly with an increase in the logarithm of the S.D.S. concentration and then levelled off at a concentration corresponding to zero zeta potential. In region II the contact angle increased slowly at first and then more rapidly as the logarithm of the concentration increased. This increase in contact angle continued into region III where a maximum contact angle of 124° was reached. Comparison of the contact angle curve with the adsorption isotherm shows that, in general, an increase in the adsorption density corresponded to an increase in the contact angle.

The advancing contact angles of iso-octane on hematite have not been included because they were much smaller than the receding angles. In some cases the hysteresis amounted to as much as 60°.

d) Extraction results

The extraction results at four different initial concentrations of S.D.S. are shown in fig. 42 as a function of pH. The S.D.S. solutions were made in both hydrochloric and perchloric acid, and sodium hydroxide was used to control the pH. The results show that for each initial concentration of S.D.S. an increase in the pH produced a slight increase in the percent extraction to a maximum

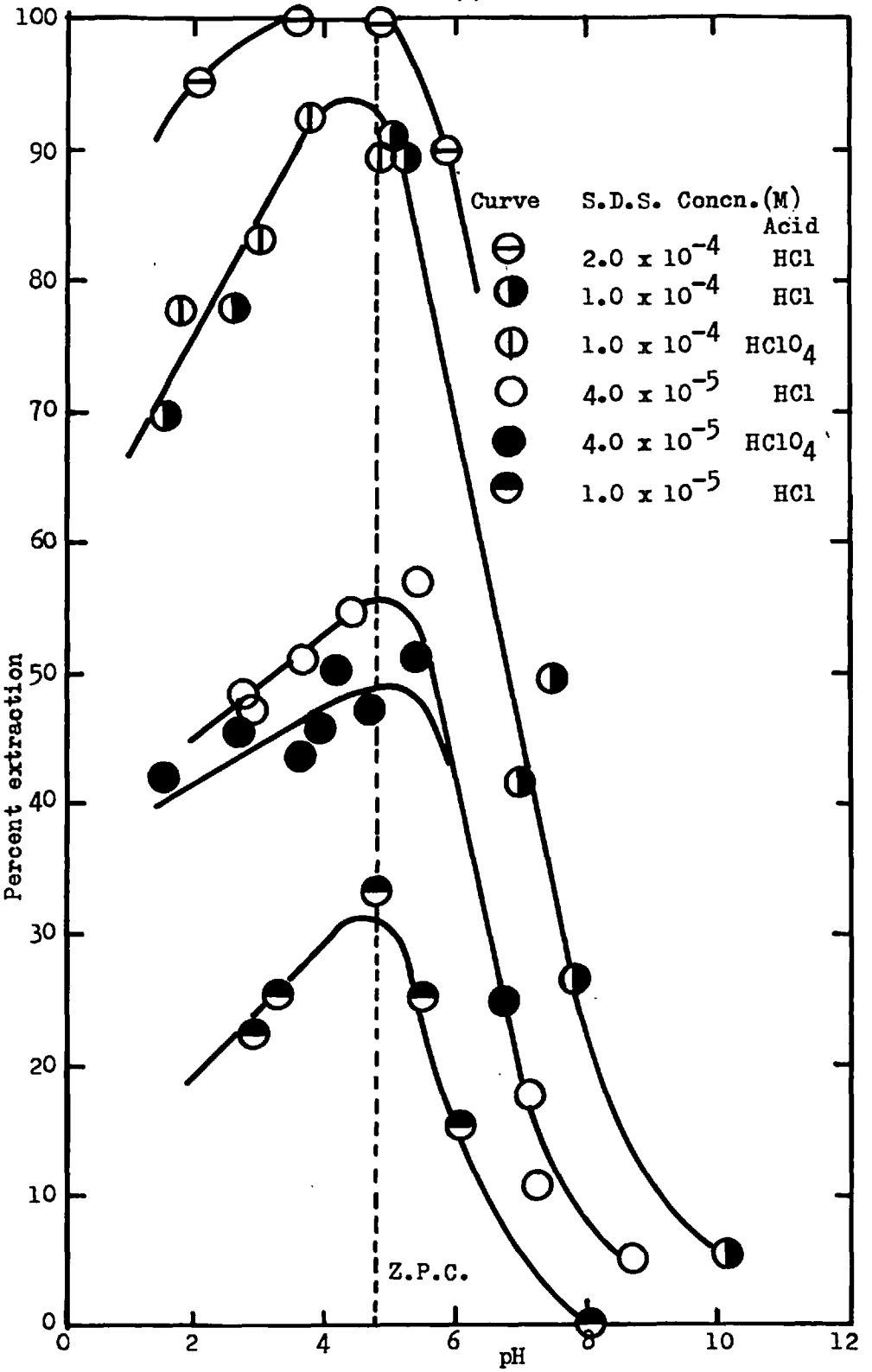

Fig. 42. Percent extraction of hematite, in the presence of various concentrations of S.D.S., as a function of pH.

at the z.p.c. of hematite. Above the z.p.c. the extraction decreased rapidly. An increase in the initial concentration produced higher percent extractions. The use of perchloric acid as a pH modifier did not produce significantly different results from those obtained using hydrochloric acid.

In fig. 43 the percent extraction, contact angle and logarithms of the adsorption density and $\Delta\zeta$ have been plotted as functions of pH for an initial S.D.S. concentration of 1×10^{-4}M. The data for these curves was obtained from figs. 40, 41 and 42. At a given pH and initial concentration of S.D.S. the magnitudes of the zeta potentials, contact angles, percent extraction and adsorption density are not directly comparable because of the different sample areas used in the different series of tests. In the electrokinetic and contact angle tests the sample areas were negligible and the equilibrium concentrations were equal to the initial concentrations. However, in the extraction and adsorption tests this was not the case because large sample areas were used. The curves, in fig. 43, show that in general as the pH was increased up to the hematite z.p.c. the percent extraction, adsorption density, contact angle and $\Delta\zeta$ decreased.

Figure 44 shows the percent extraction at a pH of 2.6 ± 0.1 as a function of the logarithms of the adsorption density and the equilibrium concentration of S.D.S. The curve correlating the percent extraction with the logarithm of the equilibrium concentration shows that as the concentration was increased, the percent extraction increased rapidly and reached 100% at a concentration

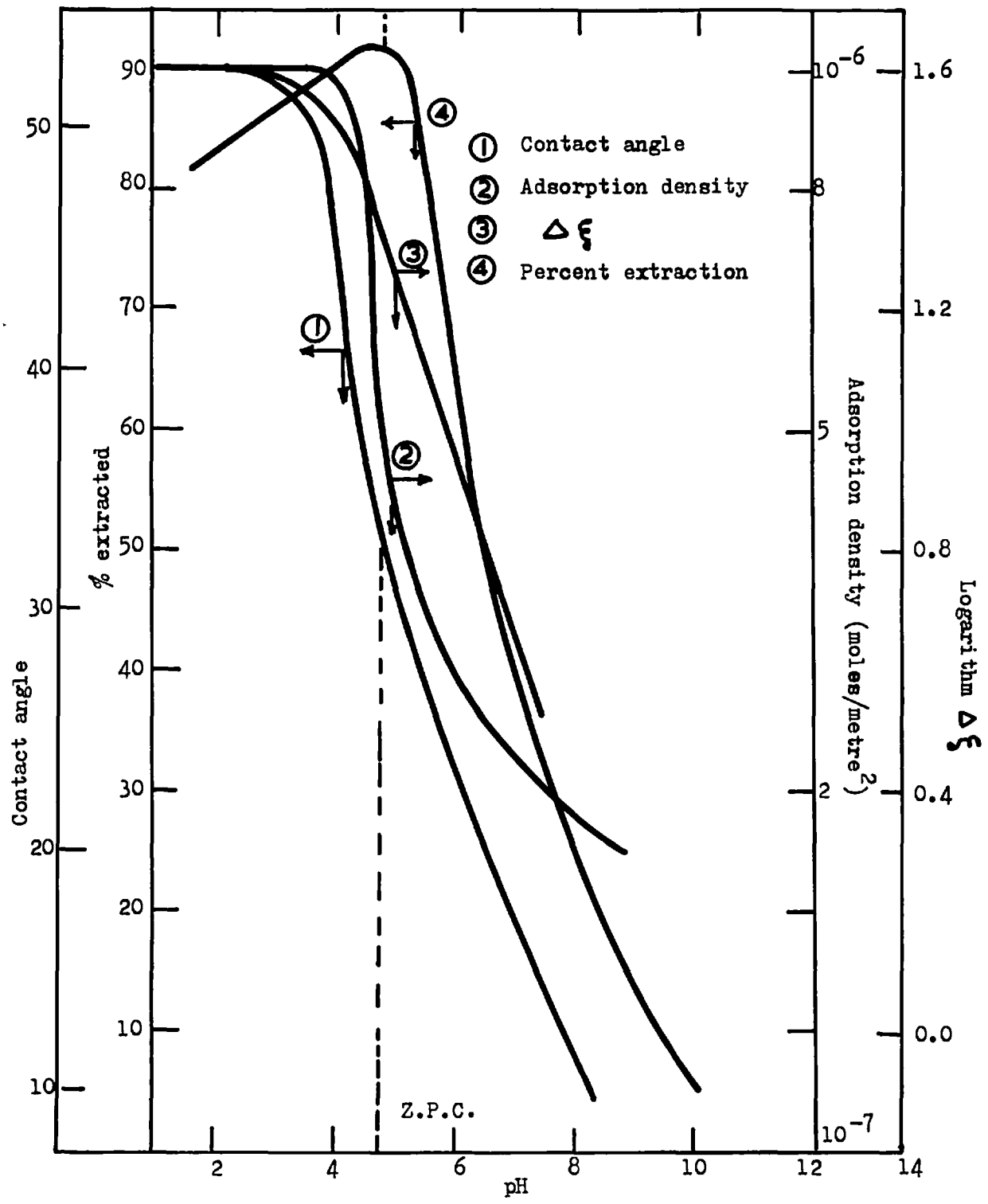

Fig. 43. Comparison of curves correlating percent extraction, adsorption density, contact angles and $\Delta\xi$ with pH.
(ionic strength 6×10^{-3}; initial concn. S.D.S. 1×10^{-4}M)

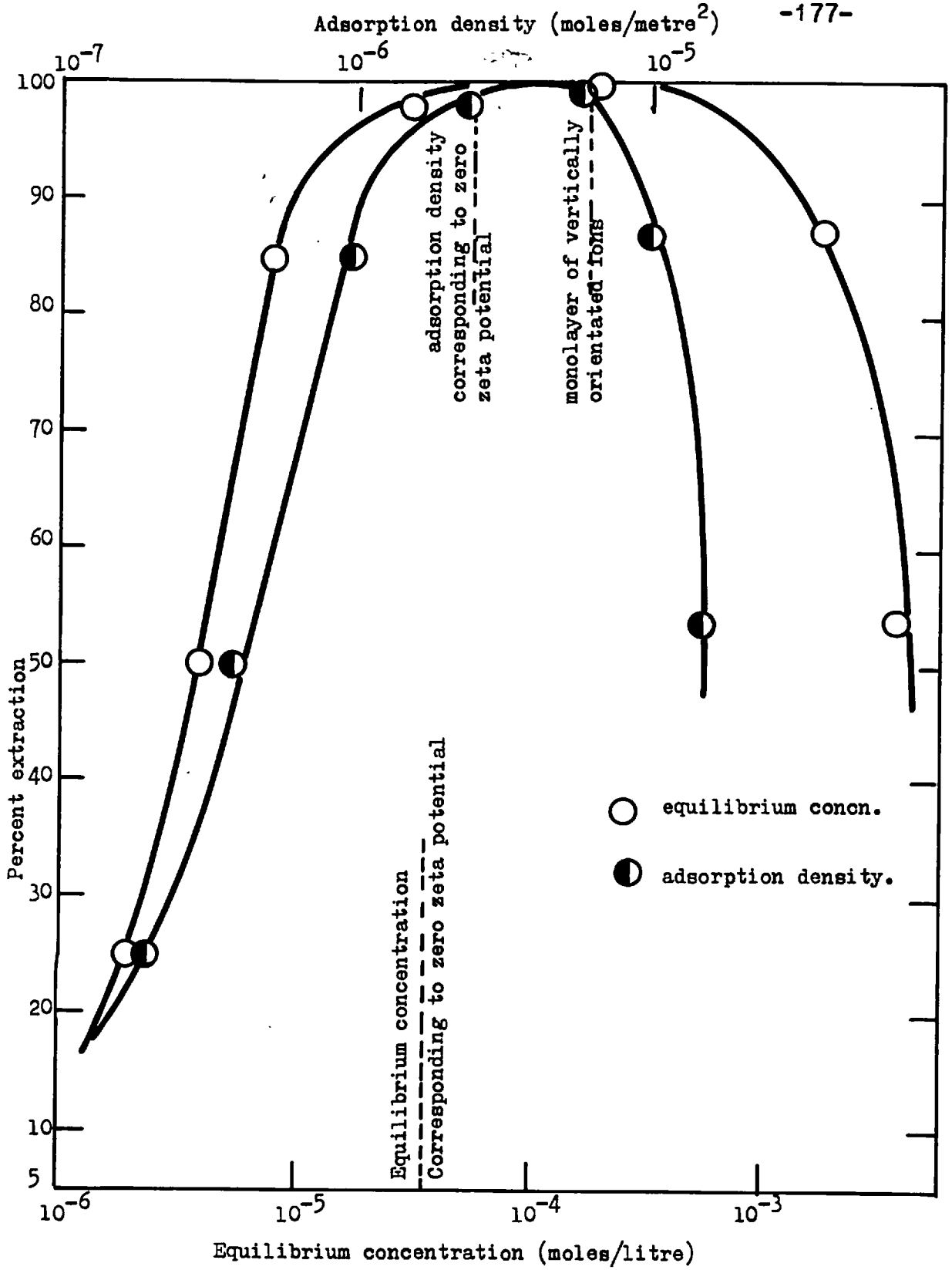

Fig. 44. Percent extraction as a function of equilibrium concn. and adsorption density.

(pH 2.6 $\pm$ 0.1 ionic strength 6 x 10^{-3})

corresponding to a zero zeta potential. At concentrations above 5×10^{-4}M the percent extraction decreased. The curve correlating the percent extraction with the logarithm of the adsorption density shows that the deorease in percent extraction at high adsorption densities and equilibrium concentrations corresponded to adsorption densities greater than that required to form a close packed vertically orientated monolayer.

4.33. The hematite/iso-octane/water system in the presence of dodecylamine

a) The effect of dodecylamine on the hematite zeta potential

It was shown in section 4.32a that the zeta potential of hematite was dependent on the pH and that in the presence of the monovalent anions Cl^-, ClO_4^- and NO_3^- the zero point of charge (z.p.c.) occurred at a pH of 4.75. Figure 45 shows the variation of the hematite zeta potential with pH in the presence of six different concentrations of dodecylamine. All of the amine solutions were prepared in hydrochloric acid. The curve at zero amine concentration represents the HCl - NaOH curve from fig. 34.

At each concentration of amine the curve correlating the zeta potential with the pH, in fig. 45, can be divided into two regions. In the first region the zeta potential was independent of the amine concentration and coincident with that obtained in the absenoe of amine. In the second region the zeta potential was approximately

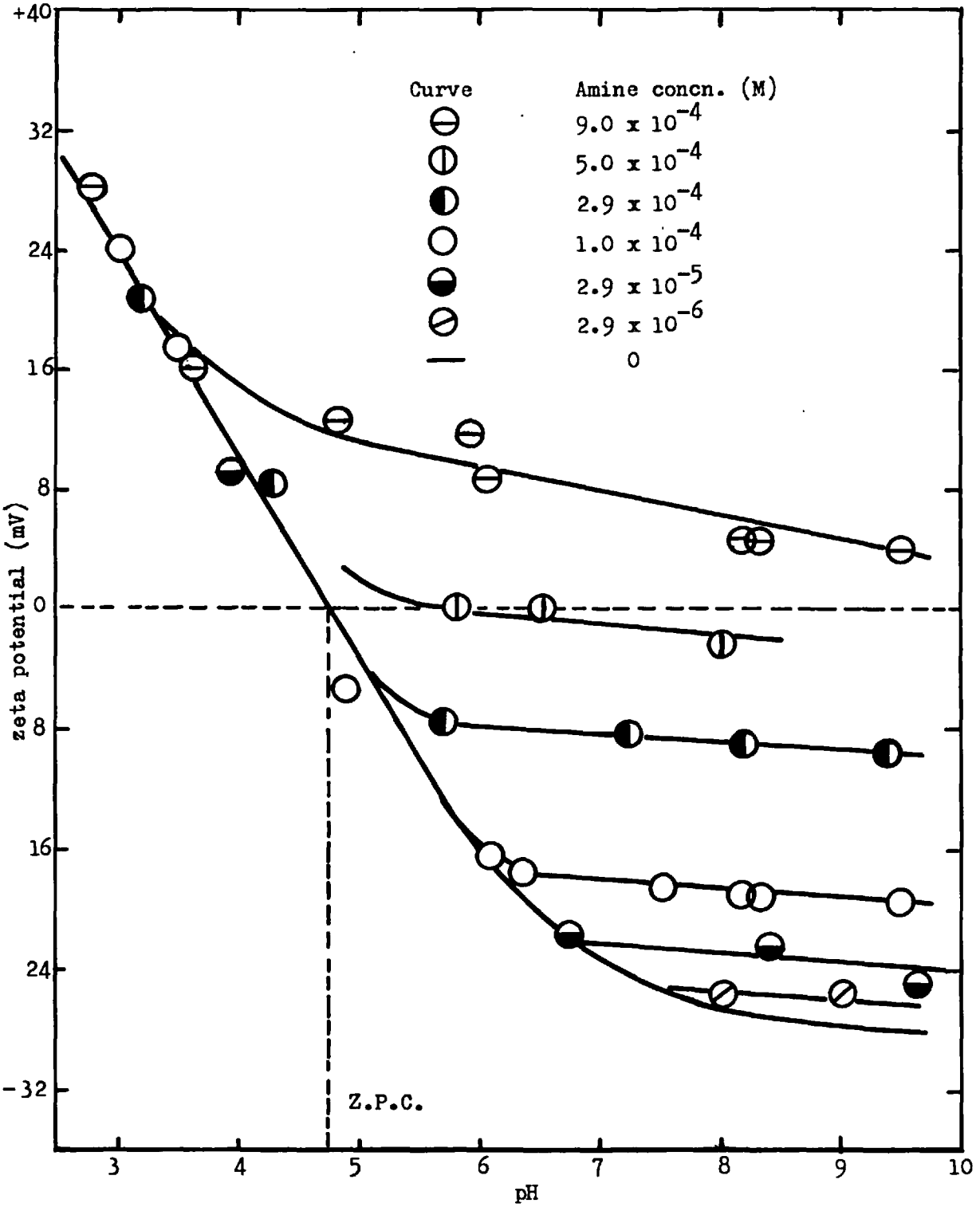

Fig. 45. The zeta potential of hematite in the presence of dodecylamine as a function of pH.

(ionic strength 6 x 10^{-3})

independent of the pH, but however, dependent on the amine concentrations. As the amine concentration was increased both the pH at the transition from one region to the other, and the value of the constant zeta potential decreased until eventually, at high amine concentrations, the transition pH occurred below the z.p.c. and the constant zeta potential changed signs and became positive. The positive zeta potential obtained at the z.p.c., in the presence of high concentrations of amine, indicate that although the surface charge was zero considerable amounts of cationic amine were adsorbed.

In fig. 46 the zeta potential data from fig. 45 has been used to correlate the zeta potential of hematite with the logarithm of the amine concentration, at constant pH values of 4.0, 5.0, 6.5 and 8.0. A characteristic of this set of curves is that each curve can be divided into two regions. A region where the zeta potential was independent of the amine concentration and a region where a small change in the logarithm of the amine concentration produced a large variation in the zeta potential. For example, at pH 6.5 the zeta potential remained constant up to a concentration of 10^{-4}M and then decreased rapidly and reached zero at a concentration of 5×10^{-4}M. The amine concentration corresponding to the transition from one region to the other decreased as the pH was increased. A zero zeta potential at pH values 5.0, 6.5 and 8.0, was obtained at an amine concentration of 5×10^{-4}M. Above this concentration the zeta potential was positive at all pH values.

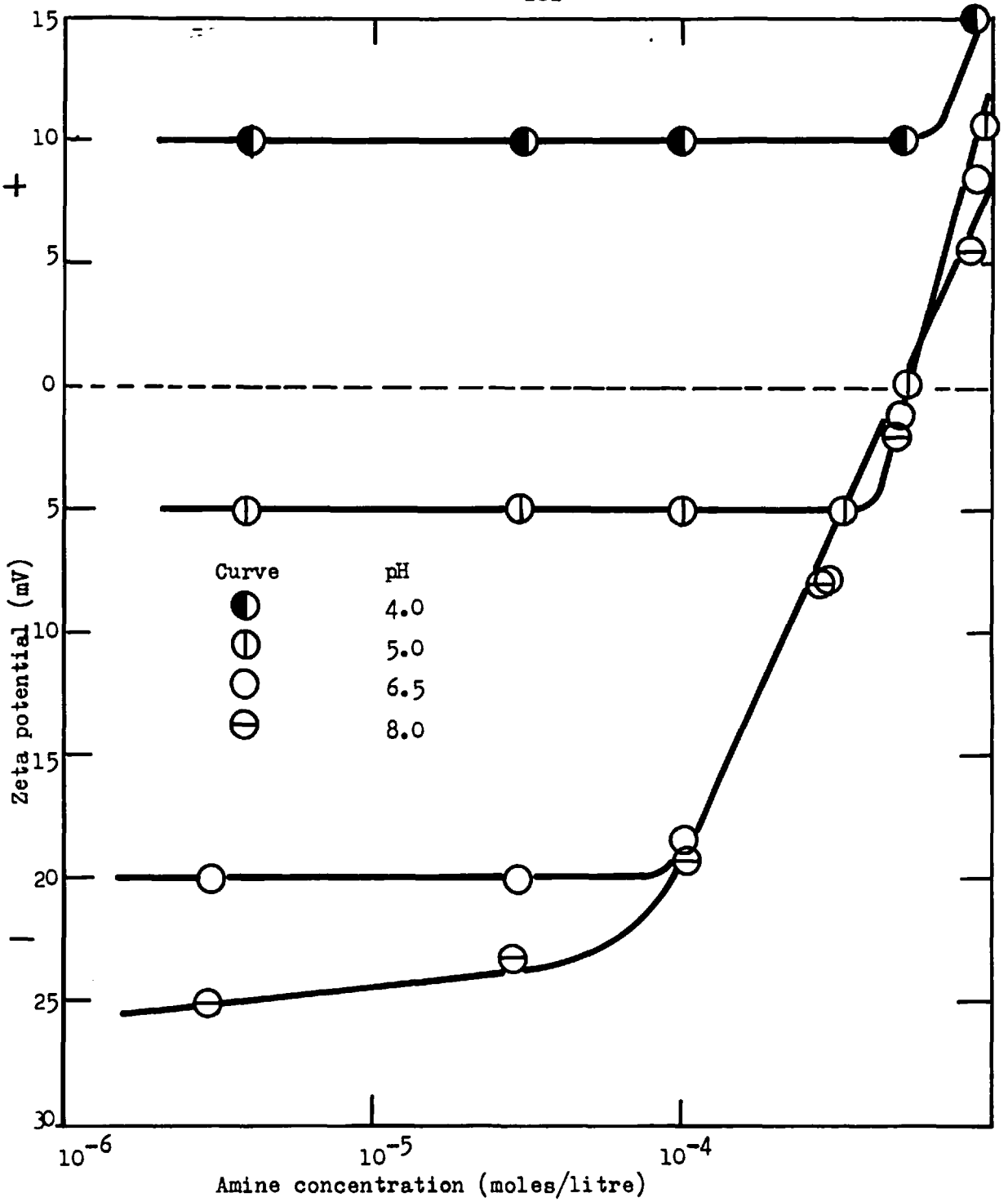

Fig. 46. Variation of the hematite zeta potential with amine concentration of different pH values.
(ionic strength 6×10^{-3})

b) The adsorption of dodecylamine by hematite in the presence of iso-octane

Tests were conducted to determine the adsorption density of dodecylamine at the hematite/water interface in the presence of iso-octane. The logarithms of the adsorption densities obtained at various pH values, in the presence of four different 'total concentrations' of dodecylamine, are presented in fig. 47. At each 'total concentration' of amine the logarithm of the adsorption density increased with an increase in pH to a maximum at neutral pH values and then decreased. A variation in the pH below neutral had only a small effect on the logarithm of the adsorption density. In fact, a tenthousandfold change in the hydrogen ion concentration produced less than a twofold change in the adsorption density. Similar results were obtained by Gaudin and Morrow (132) for the system hematite/dodecylamine solution in the absence of iso-octane.

Plotted also in fig. 47 is the calculated curve correlating the logarithm of the cationic amine concentration in the aqueous phase with the pH, for a total amine concentration of 1.25×10^{-4}M. This curve was obtained using the equilibrium equations derived in section 2.00. It follows from these equations that curves of a similar shape would be obtained at different "total amine concentrations". Comparison of the adsorption density curves with the cationic amine concentration curve shows that the decrease in the logarithm of the adsorption density with increase in pH, in alkaline media, corresponded to a decrease in the logarithm of the aqueous cationic amine concentration. These results are

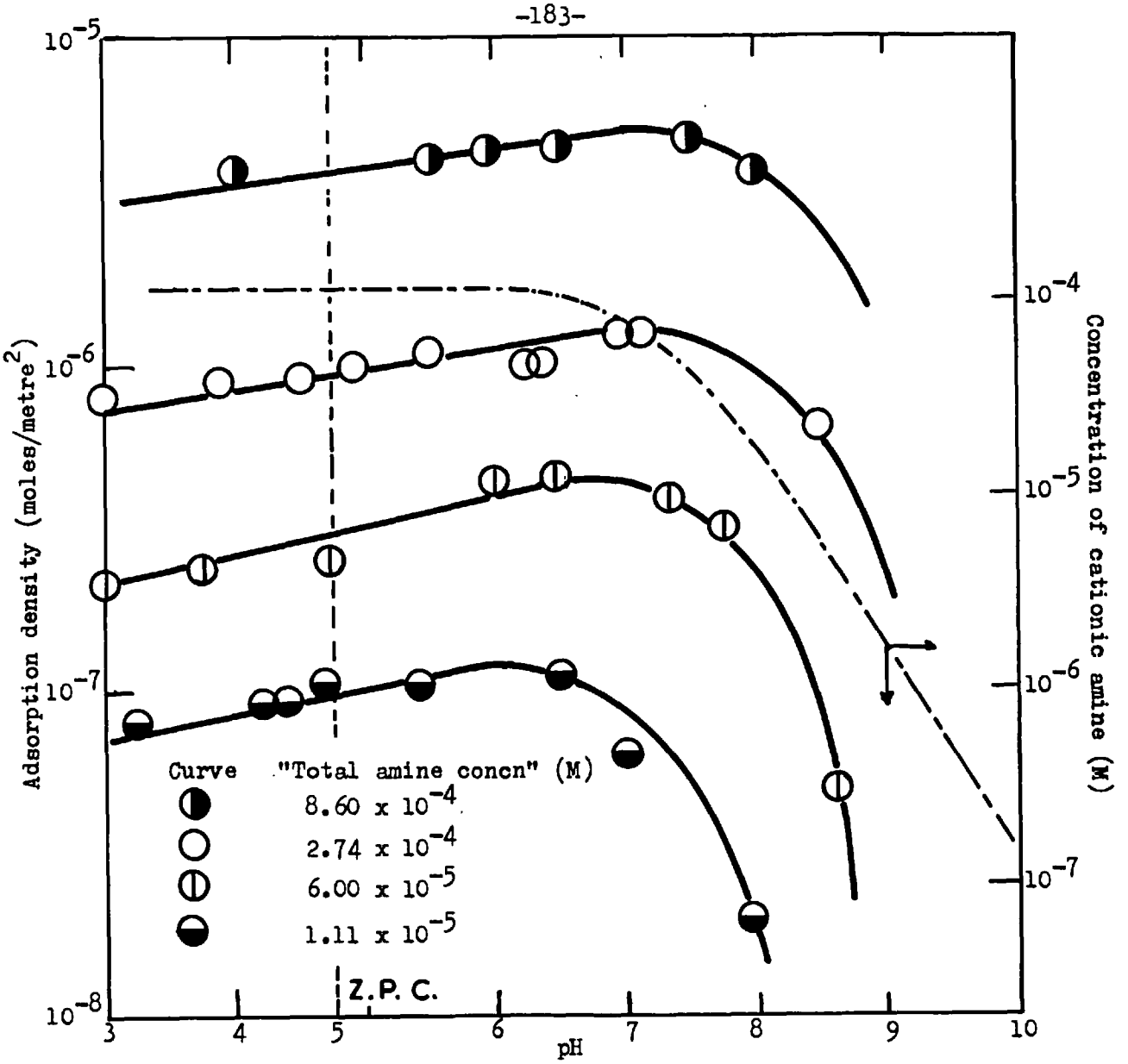

Fig. 47. Adsorption density of dodecylamine on hematite as a function of pH.

(ionic strength 6 x 10^{-3})

similar to those obtained for the iso-octane/water/quartz system in the presence of dodecylamine (fig. 26).

In fig. 48 the logarithm of the adsorption density of dodecylamine on hematite is presented as a function of the logarithm of the equilibrium aqueous amine concentration at two different pH values. The points on these isotherms were obtained either by direct experimental determinations or by a method similar to that used to obtain the points on the amine adsorption isotherm determined for quartz (o.f. section 4.31b). The shape of the isotherms shown in fig. 48 is similar to that determined by Gaudin and Morrow (132) for the hematite/dodecylamine system in the absence of constant ionic strength and iso-octane. The relationship between the logarithms of the adsorption density and the equilibrium aqueous amine concentration, at pH 6.5, was linear with a slope of 0.65 at equilibrium concentrations below 2×10^{-4}M. Above this concentration the isotherm deviated from a straight line and the logarithm of the adsorption density became more dependent on the logarithm of the equilibrium concentration. The adsorption density at the point of deviation from a straight line i.e. 2×10^{-6} moles metre^{-2}, and the slope of the linear part of the adsorption isotherm were in good agreement with the values of 1.5×10^{-6} moles metre^{-2} and 0.6 found by Gaudin and Morrow (132). Generally, however, the equilibrium amine concentrations corresponding to a given adsorption density were slightly lower in this work than those found by these other authors.

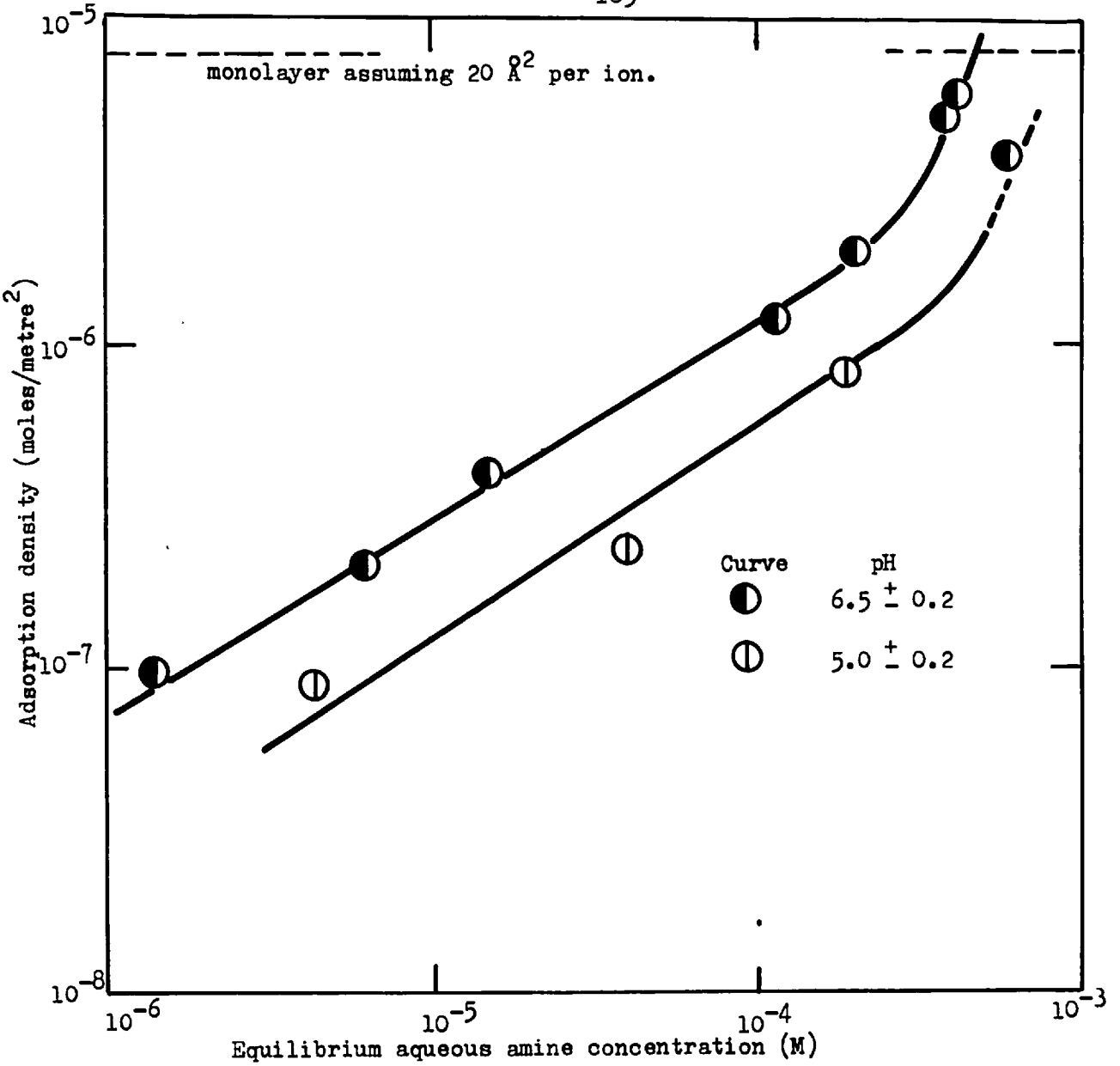

Fig. 48. Adsorption density of amine on hematite as a function of the equilibrium aqueous amine concentration.
(ionic strength 6 x 10^{-3})

Comparison of the adsorption isotherm at pH 6.5 with the curve correlating the zeta potential with the logarithm of the aqueous amine concentration (fig. 46) shows that the amine concentration at the upper limit of the linear part of the adsorption isotherm corresponds approximately to the concentration at which the zeta potential began to show a marked dependence on the logarithm of the amine concentration. Comparison of fig. 48 with fig. 27a shows that the amine adsorption isotherm obtained, at pH 6.5, for the system iso-octane/quartz/water was very similar to that obtained for the hematite/water/iso-octane system under similar conditions.

c) <u>The effect of dodecylamine concentration on the contact angle</u>

The receding contact angles of iso-octane on hematite, at five different 'total concentrations' of amine, are presented in fig. 49 as a function of pH. For a given 'total concentration' of amine the receding contact angle increased from zero, at pH values below 2, to a maximum between pH values 7 and 8 and then decreased to zero at high pH values. An increase in the 'total amine concentration' produced an increase in the magnitude of the contact angles.

Included in fig. 49 is a plot of the difference in zeta potential ($\Delta\zeta$), at various pH values, between that obtained in 9×10^{-4}M amine solution and that obtained in the absence of amine. Comparison of fig. 49 with fig. 47 shows that as the pH was increased the adsorption density, $\Delta\zeta$ and contact angles increased to a maximum at between pH values 7 and 8. A further increase in

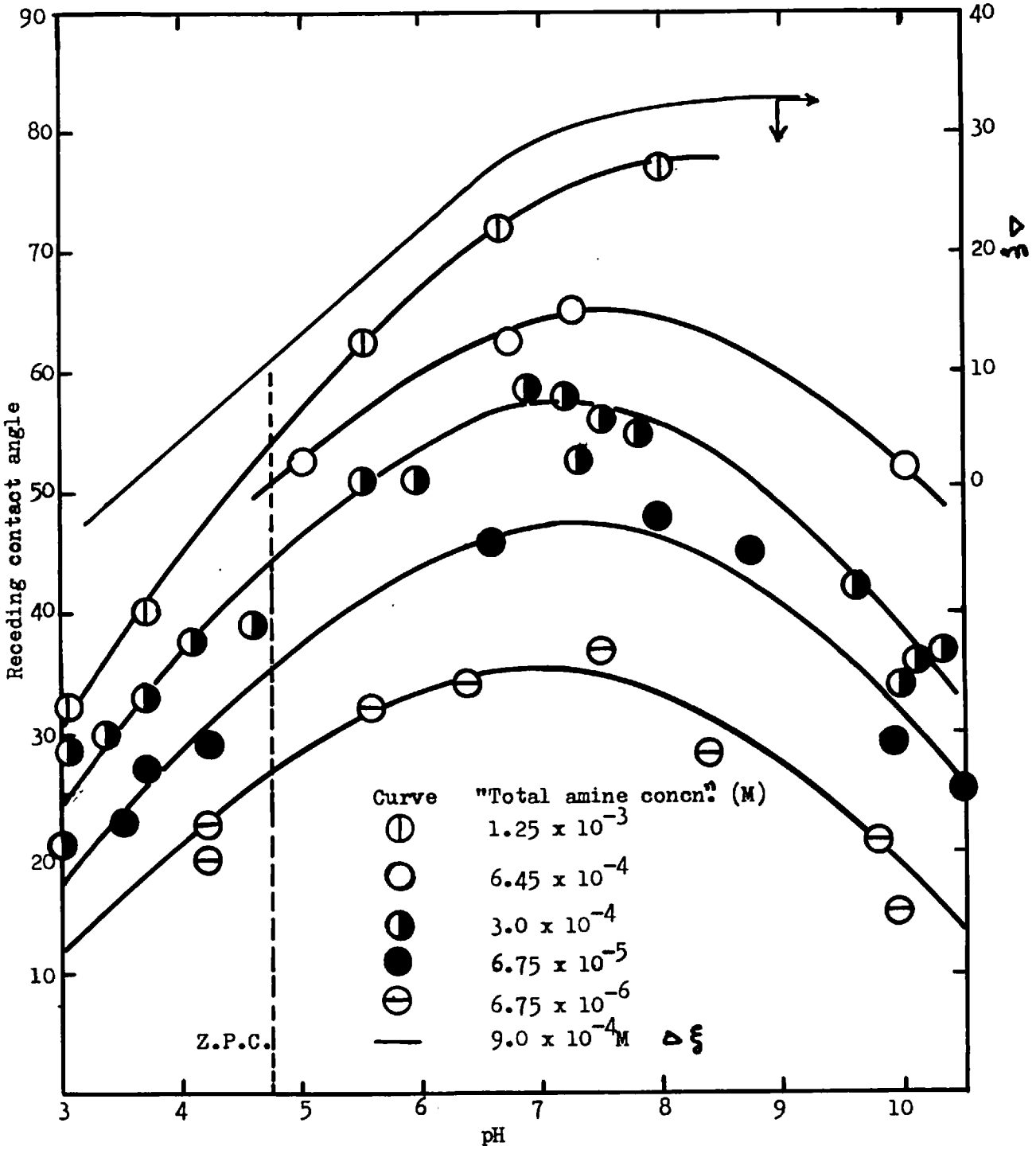

Fig. 49. Receding contact angle on hematite in the presence of dodecylamine as a function of pH.

(ionic strength 6 x 10^{-3})

the pH produced a decrease in the adsorption density, contact angles and cationic amine concentration of the aqueous phase. This comparison also shows that at pH values below the z.p.c. the contact angles gradually decreased to zero whereas the logarithm of the adsorption density only decreased slightly.

In fig. 50 the contact angles from fig. 49 have been replotted to show the correlation between the contact angles and the logarithm of the aqueous amine concentration at five different pH values. A characteristic of this set of curves is that each curve can be divided into two linear regions of slopes 10 and 33 degrees per ten-fold increase in the aqueous amine concentration. The receding contact angle at the point of intersection of the two linear curves was approximately the same at all pH values and equal to 47°. The aqueous amine concentration at this point decreased as the pH increased as shown in Table VIII.

TABLE VIII

pH	Aqueous amine conc. at point of intersection (M)
8.0	2.1×10^{-5}
6.5	1.7×10^{-4}
5.0	5.6×10^{-4}
4.0	4.0×10^{-3}

The curves correlating the contact angles (fig. 50), adsorption density (fig. 48) and zeta potential (fig. 46) with the

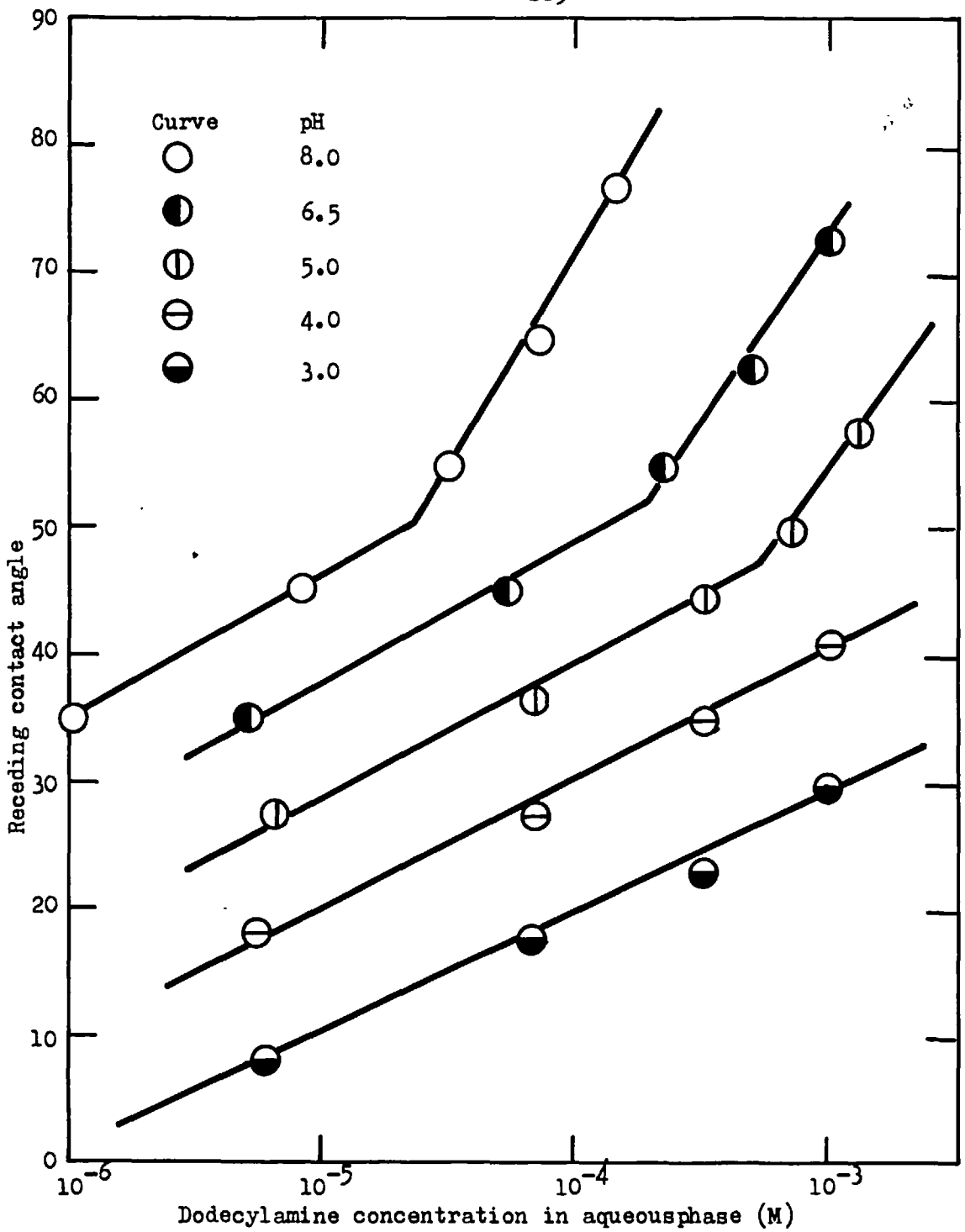

Fig. 50. Variation of the contact angle on hematite with the aqueous amine concentration.
(ionic strength 6×10^{-3})

logarithm of the equilibrium aqueous amine concentration have a similarity in that they can be divided into two regions. The aqueous amine concentrations at the transition from one region to the other for the three different sets of data, at pH 6.5, are approximately the same at 1 to 2 x 10^{-4}M. This correlation will be considered in more detail in section 4.43 (b).

The relationships between the advancing contact angles, and the pH, and the equilibrium aqueous amine concentration were similar to those obtained with the receding contact angles. These curves have not, however, been included because the advancing angles were much smaller than the receding angles and not so reproducible.

d) Extraction results

In fig. 51 the percent extraction, at four different 'total concentrations' of amine, is presented as a function of pH. At each 'total amine concentration' the percent extraction increased from zero, at low pH values, to a maximum, at between pH values 5 and 7, and then decreased to zero at high pH values. Figure 52 presents the percent extraction, contact angle and the logarithms of both the adsorption density and the aqueous cationic amine concentration as a function of pH for a 'total amine concentration' of 3.0 x 10^{-4}M. The percent extraction, adsorption density and contact angle at a given pH and 'total amine concentration' are not directly comparable because the sample surface area and hence the adsorption in the contact angle tests was negligible compared to

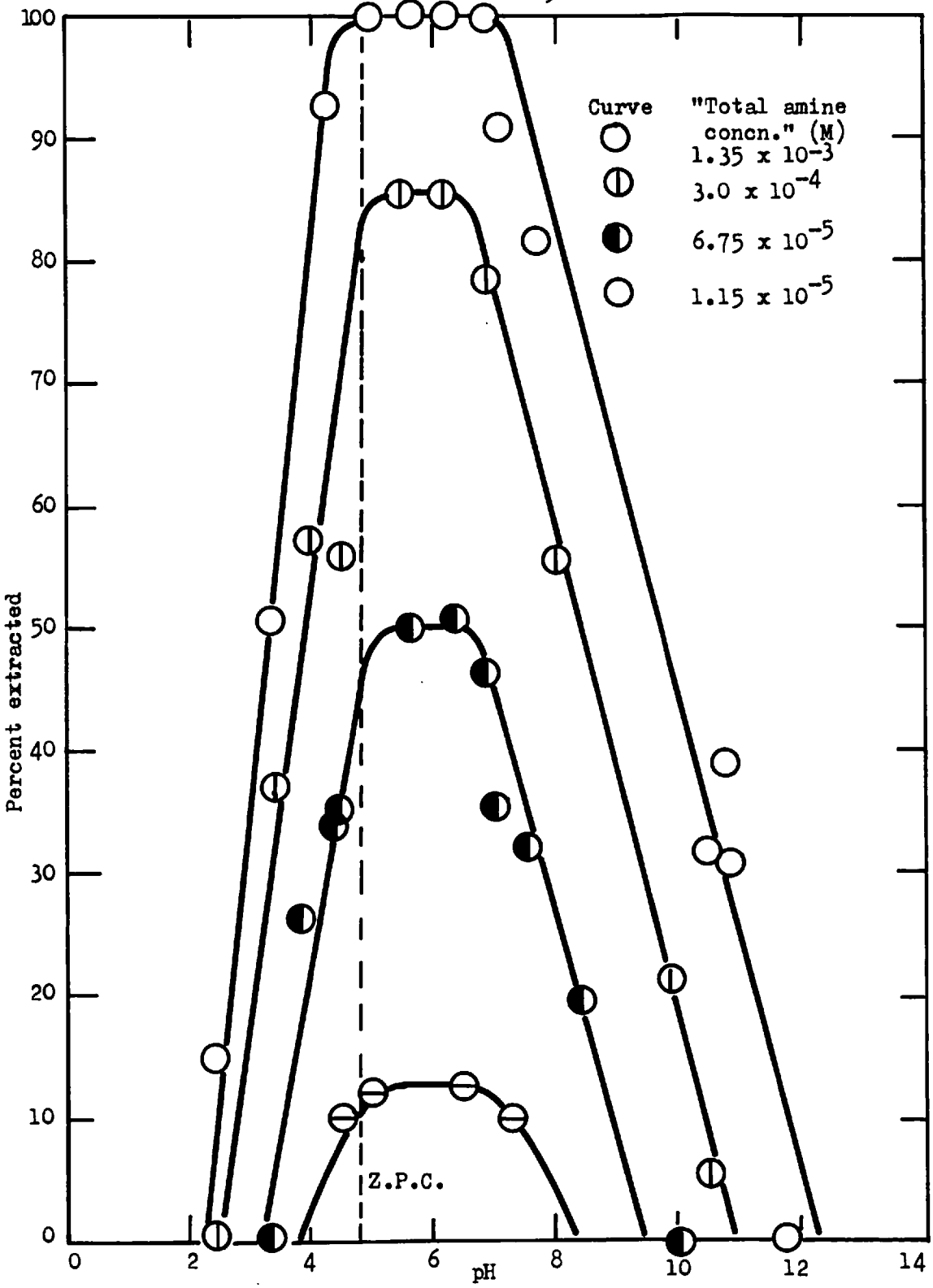

Fig. 51. Extraction of hematite with dodecylamine as a function of pH.

(ionic strength 6×10^{-3})

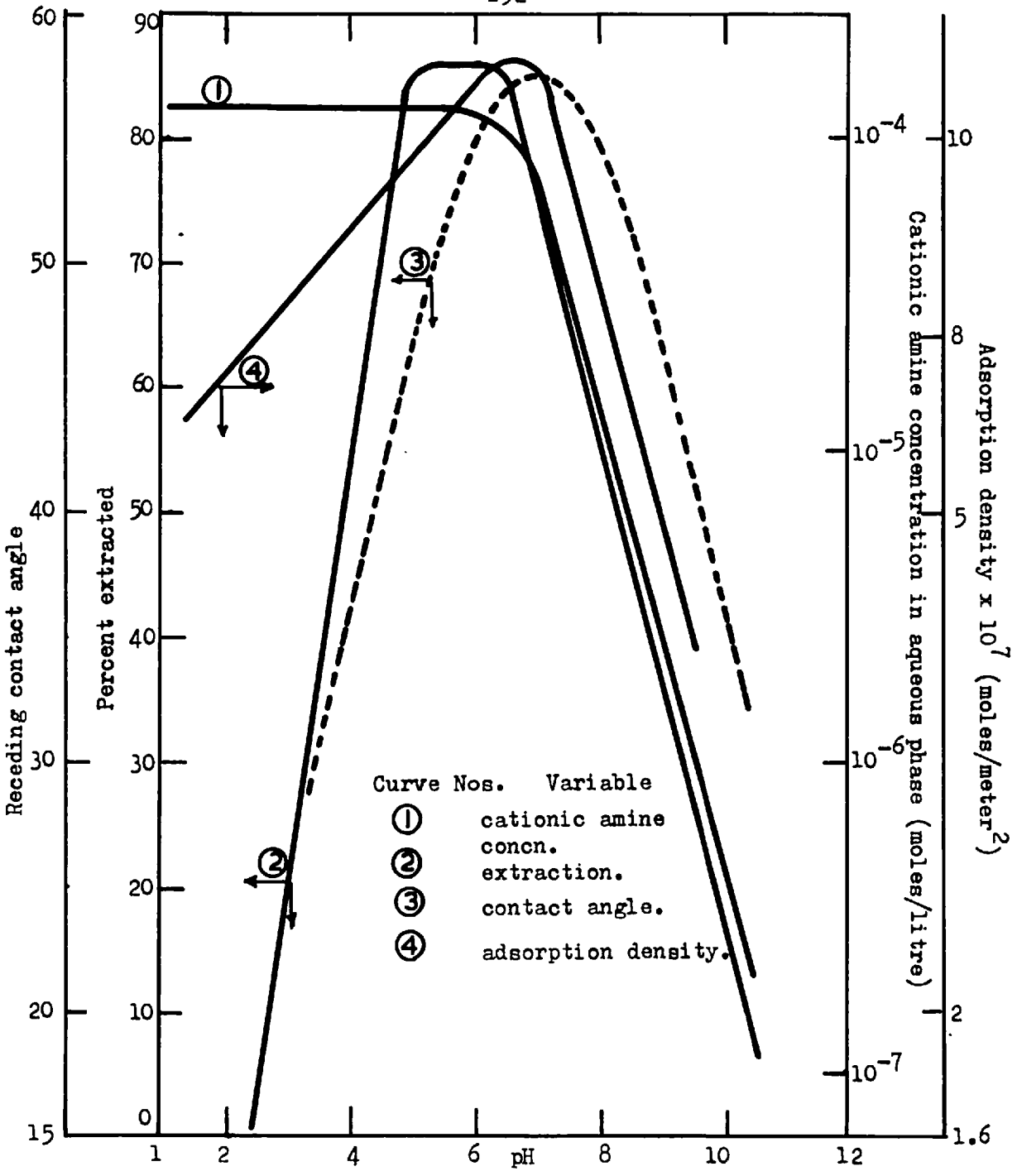

Fig. 52. Percent extraction, adsorption density, contact angle and cationic amine concentration as a function of pH. ("Total amine concn" = 3.0×10^{-4}M; ionic strength 6×10^{-3})

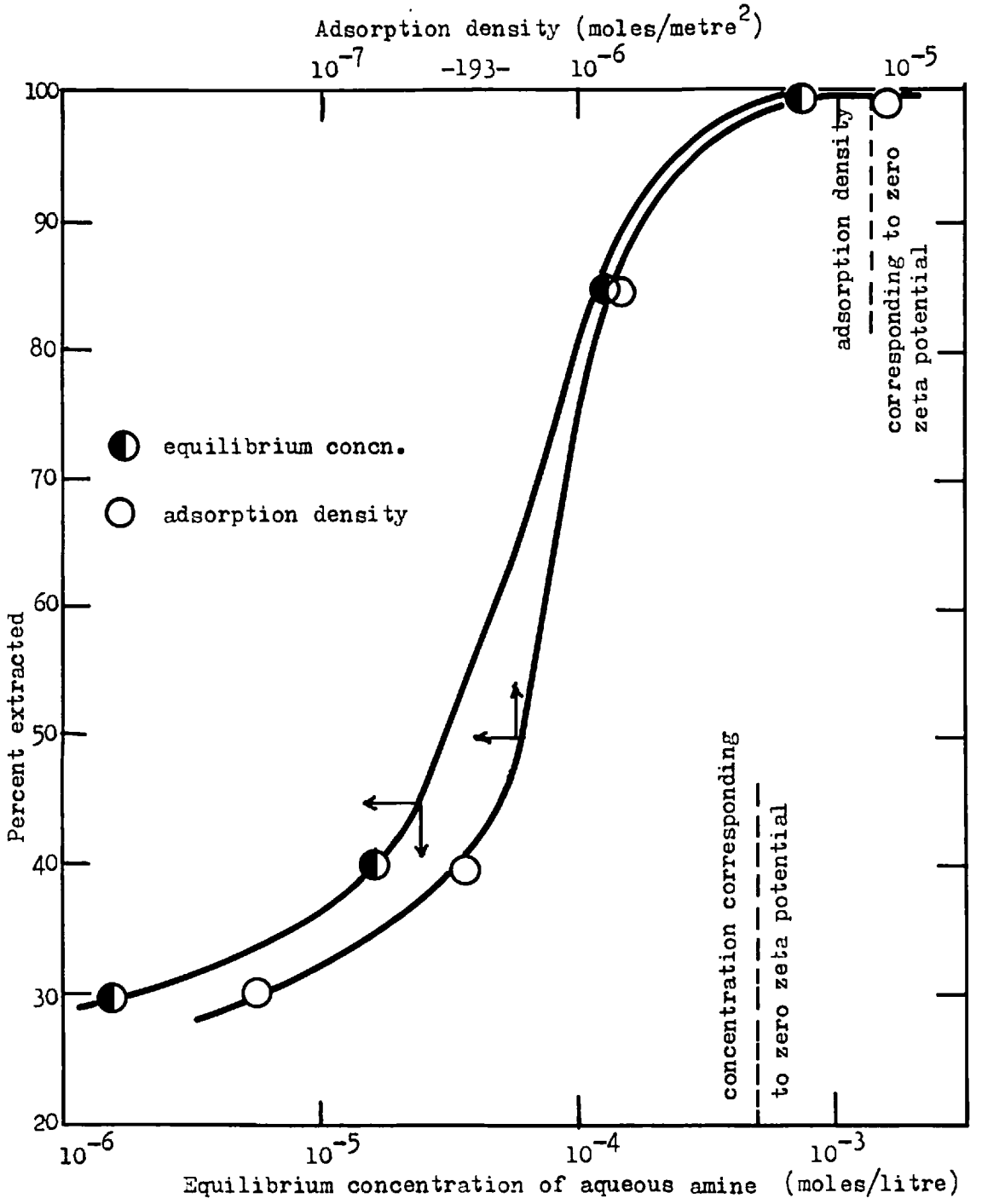

Fig. 53. Percent extraction as functions of adsorption density and equilibrium aqueous amine concentration.

(pH. 6.5 ionic strength 6×10^{-3})

that in the extraction and adsorption tests. Figure 52 does, however, show that as the pH was increased the adsorption density, contact angles and percent extraction increased to a maximum between pH values 5 and 7.5 and then decreased. The decrease in these variables in alkaline media corresponded to a decrease in the cationic amine concentration in the aqueous phase.

In fig. 53 the percent extraction, at pH 6.5, has been presented as a function of the logarithms of both the aqueous amine concentration and the adsorption density. These curves show that 100% extraction was obtained at the equilibrium concentration and adsorption density corresponding to zero zeta potential.

4.34. The hematite/iso-octane/water system in the presence of dodecanoic acid

a) The effect of dodecanoic acid on the zeta potential

The zeta potential of a hematite suspension in 6×10^{-3}M sodium hydroxide was measured as the pH was decreased. The results obtained are shown in fig. 54, curve (2). Curve (1) shows the zeta potentials obtained when the pH of a hematite suspension in 6×10^{-3}M hydrochloric acid was increased. Comparison of these two curves shows that the zeta potentials of the suspension initially in sodium hydroxide were more negative, at pH values below neutral, than the suspension initially in acid. As a result of this, the z.p.c. of the pH decreasing suspension was lower than that of the pH increasing one.

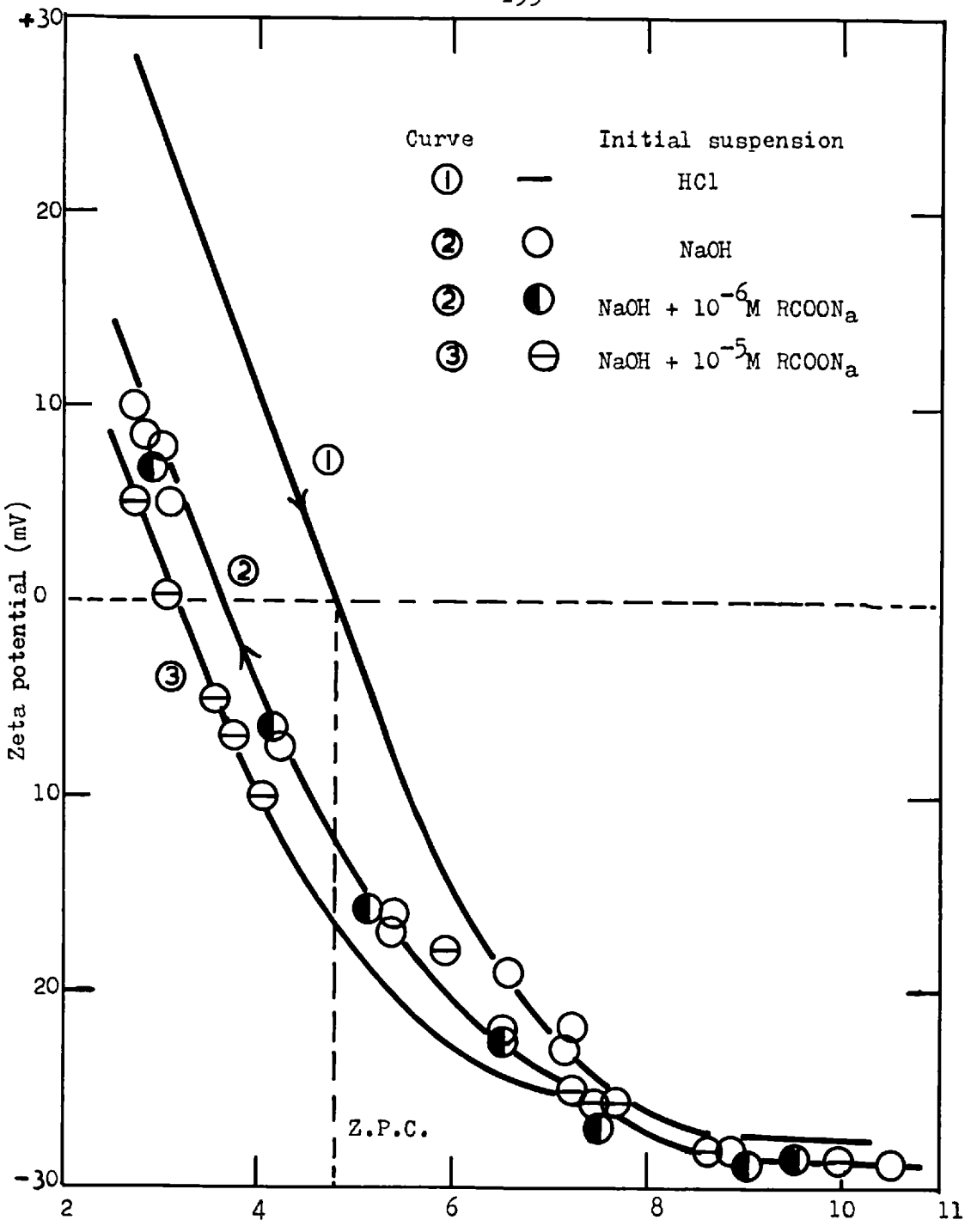

Fig. 54. Zeta potential of hematite as a function of pH in the presence of sodium dodecanoate.
(ionic strength 6×10^{-3})

Curve (3) shows the effect on the zeta potential of decreasing the pH of a suspension of hematite in a solution initially composed of 6×10^{-3}M sodium hydroxide and 10^{-5}M sodium dodecanoate. At pH values above 7 the zeta potential was not affected by the presence of fatty acid molecules and ions. Below pH 7, however, the curve correlating the zeta potential with the pH in the presence of fatty acid species was displaced to slightly more negative zeta potentials than the curve obtained in the absence of fatty acid. The zeta potential was not measured at higher concentrations of fatty acid because of the precipitation of dodecanoic acid.

b) The effect of dodecanoic acid concentration on the contact angle

The receding contact angles of iso-octane on hematite at five different 'total concentrations' of dodecanoic acid are presented in fig. 55, as a function of pH. (The 'total concentration' of dodecanoic acid is that concentration if all the fatty acid species were initially in the aqueous phase). At each 'total concentration' of fatty acid the contact angle was approximately constant at pH values below 6. Above pH 6, the contact angles increased rapidly to a maximum at pH 8. to 8.5 and then decreased.

In fig. 56 the receding contact angles from fig. 55 have been used to show the correlation between the receding angles and the logarithm of the concentration of fatty acid species in the aqueous phase. These concentrations were obtained using the equilibrium equations derived in section 2.00. The curve obtained

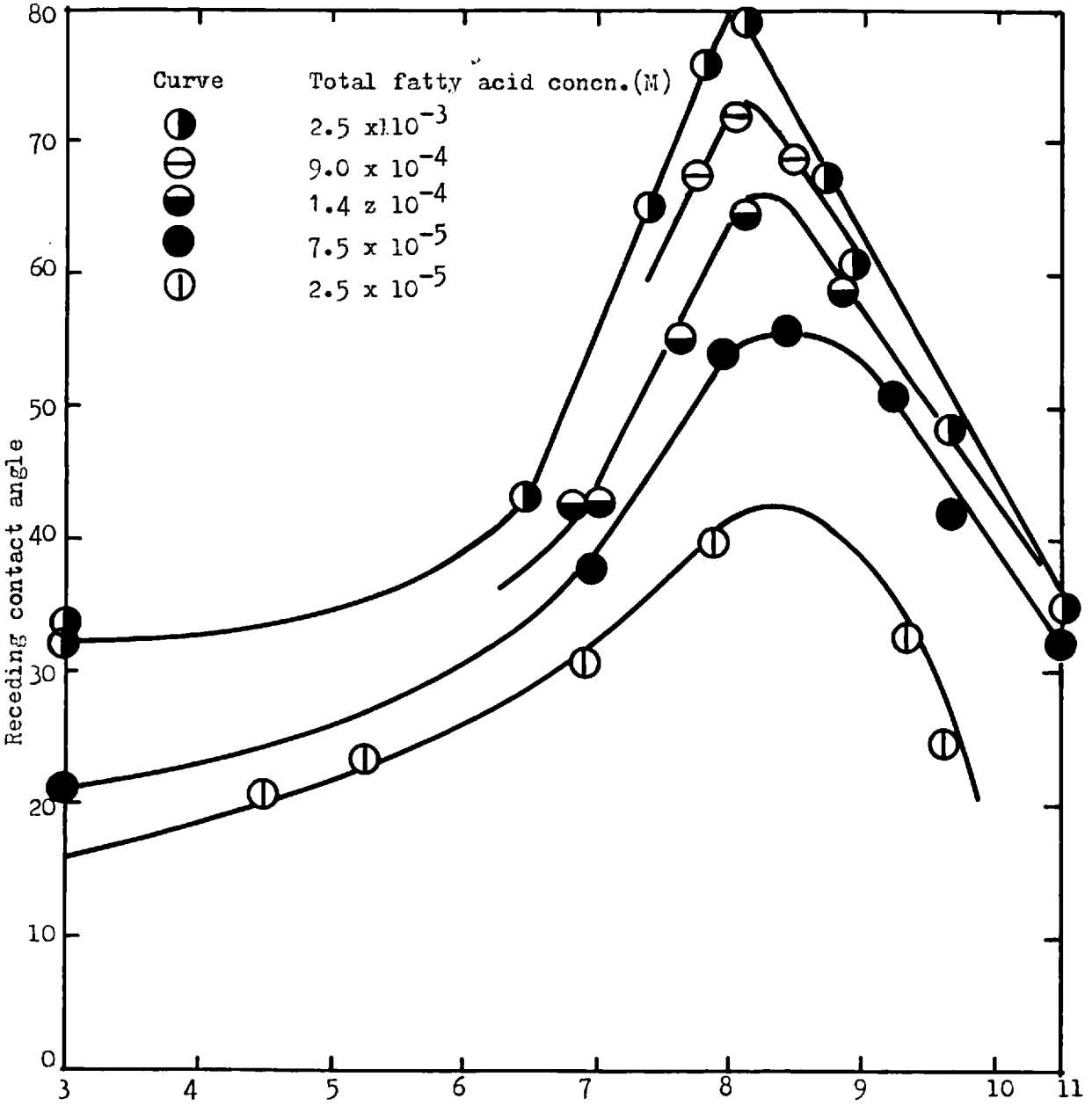

Fig. 55. Receding contact angle on hematite, in the presence of dodecanoic acid, as a function of pH.
(ionic strength 6 x 10^{-3})

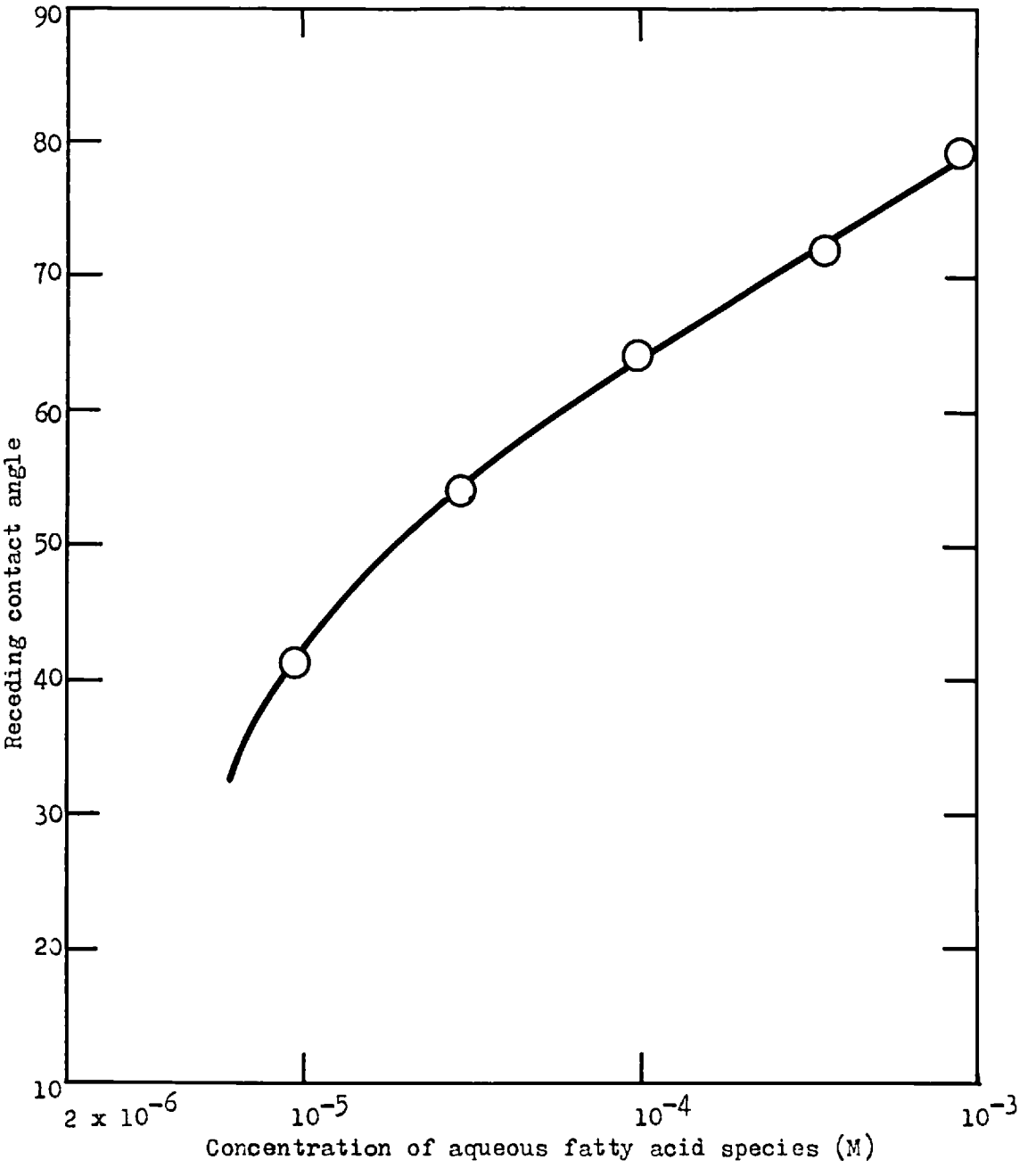

Fig. 56. Contact angle on hematite as a function of the aqueous fatty acid concentration.
(ionic strength 6×10^{-3}; pH 8.0)

shows that as the logarithm of the concentration was increased there was a gradual increase in the contact angle. Between a concentration of 3×10^{-5} and 1×10^{-3}M the curve was almost linear with a slope of about 20 degrees per tenfold increase in the concentration.

Similar to the systems involving sodium dodecyl sulphate and dodecylamine the advancing angles have not been included because they were very much smaller than the receding angles.

d) Extraction results

The extraction results presented in fig. 57 show the correlation between the percent extraction and pH at four different 'total concentrations' of fatty acid. At each 'total concentration' the percent extraction increased from zero at low pH values to a maximum at pH 8.0 and then decreased. An increase in the 'total fatty acid concentration' produced higher percent extractions.

Superimposed on the curves correlating the percent extraction with the pH is a plot of the concentration of the various fatty acid species as a function of pH for a 'total fatty acid concentration' of 2.5×10^{-3}M. These concentrations were also obtained by using the equilibrium equations derived in section 2.00. It follows from these equations that similar curves would be obtained for the different 'total concentrations' of fatty acid. Comparison of the percent extraction curves with the concentration curve shows that maximum extraction occurred at the pH where the fatty acid concen-

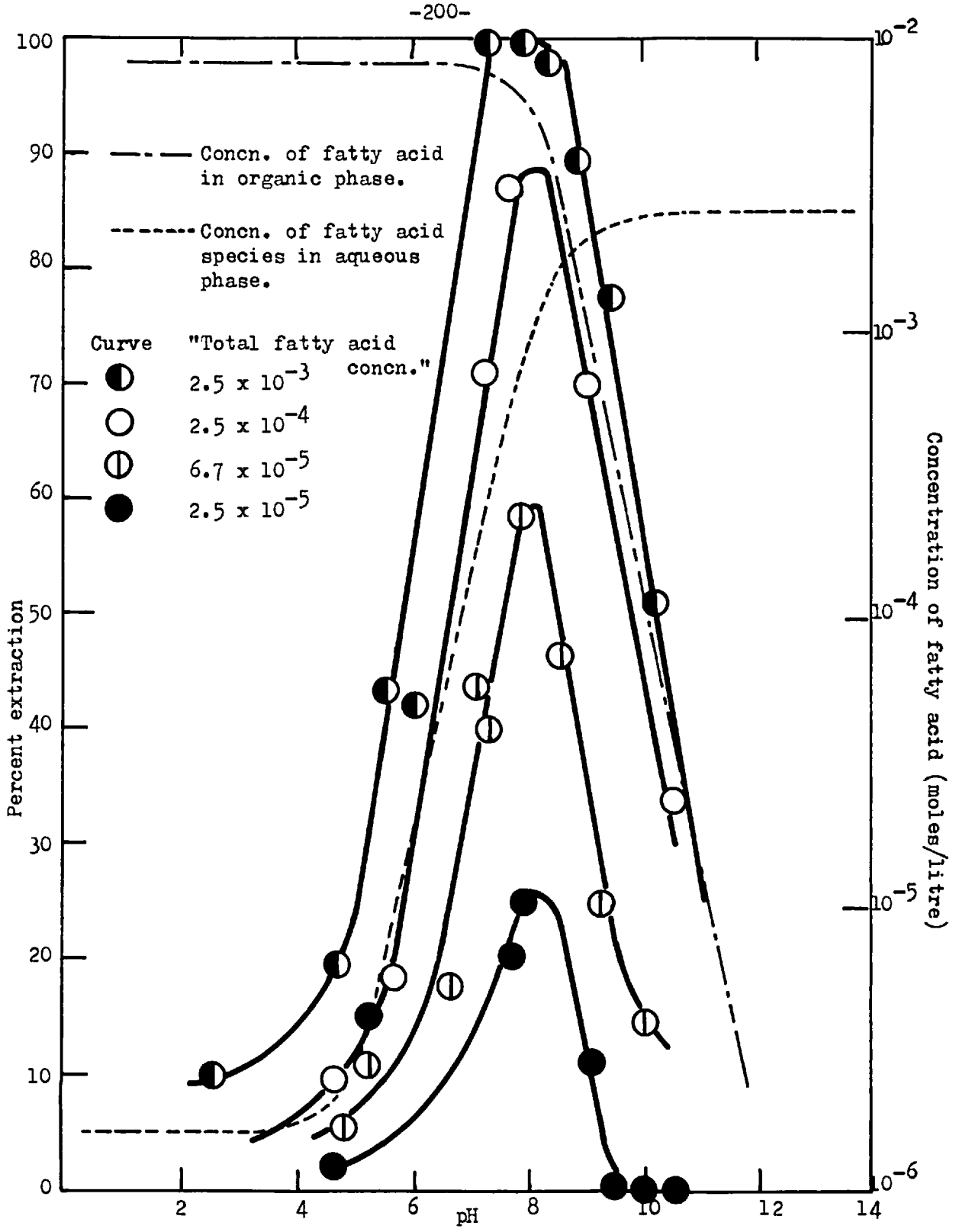

Fig. 57. Percent extraction of hematite with dodecanoic acid, as a function of pH.

tration in the organic phase was slightly higher than that of the carboxylic ion in the aqueous phase.

4.35. Selective extraction tests

Extraction tests were conducted on synthetic mixtures of hematite and quartz, and ilmenite and quartz using collectors of dodecylamine, sodium dodecyl sulphate and dodecanoic acid. The amounts of quartz in the products obtained from the extraction apparatus were determined by treating known weights of the products with hot concentrated HCl and stannous chloride. The insoluble quartz remains were collected in 'ashless' filter papers and the filter papers were fired at 800°C in weighed crucibles.

The results from these tests are shown as a function of pH in figs. 58 to 60 inclusive. No attempt was made to obtain maximum selectivity or extraction by varying the concentration of collector. Figs. 58 and 59 show that it was possible to separate hematite from quartz using sodium dodecyl sulphate and dodecanoic acid as collectors. The hematite extraction curves were similar to those obtained for the pure hematite/water/iso-octane system in the presence of the relevant collectors.

It was found that the grade of the hematite concentrate could be improved by allowing the two phases to stand for several minutes in the separating column. During this period quartz

particles were seen to fall from between the oil drops in the upper layer. This indicated that the quartz impurities in the concentrate were trapped between the oil drops rather than adhered to the oil/water interface.

No attempts were made to selectively extract hematite from mixtures of hematite and quartz using dodecylamine, because reference to figs. 31 and 52 showed that with amine the extraction properties of hematite and quartz were similar. In conventional flotation systems hematite can be separated from quartz by depressing the hematite with starch (158) (159) and floating the quartz with amines. In the system investigated here, however, hematite was not depressed over a wide range of starch concentrations. To ascertain the reasons for this non-depressability would require a study of the adsorption of starch at the oil/water and hematite/water interfaces together with a study of the effect of the order of reagent addition.

Fig. 60 shows the extraction of ilmenite from an ilmenite-quartz mixture, using a collector of sodium dodecyl sulphate. Ilmenite has similar electrokinetic properties (160) to those of hematite and so it is not surprising that figs. 60 and 58 are similar.

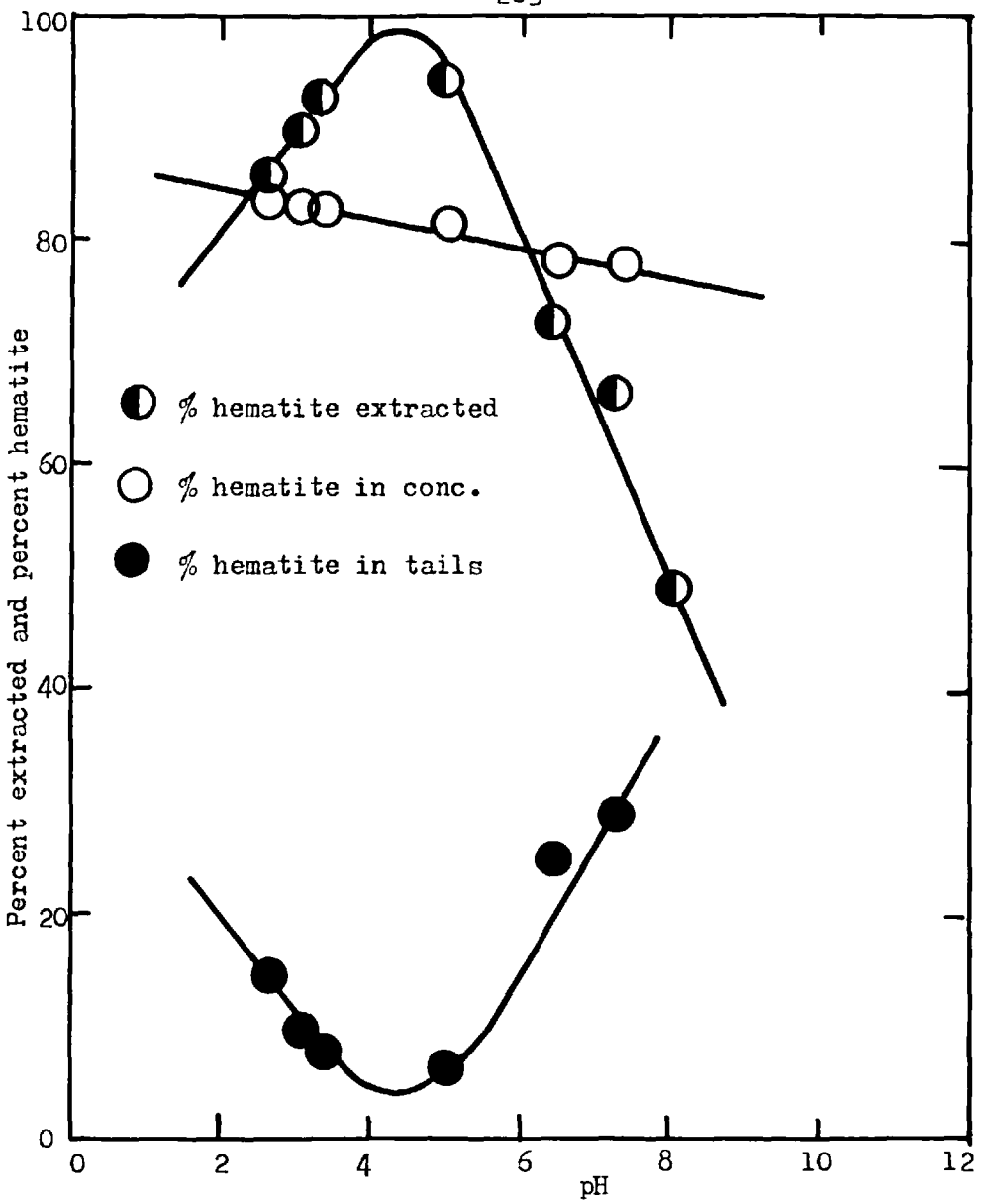

Fig. 58. Selective extraction of hematite using S.D.S. of concn. 2×10^{-4} M. (ionic strength 6×10^{-3})

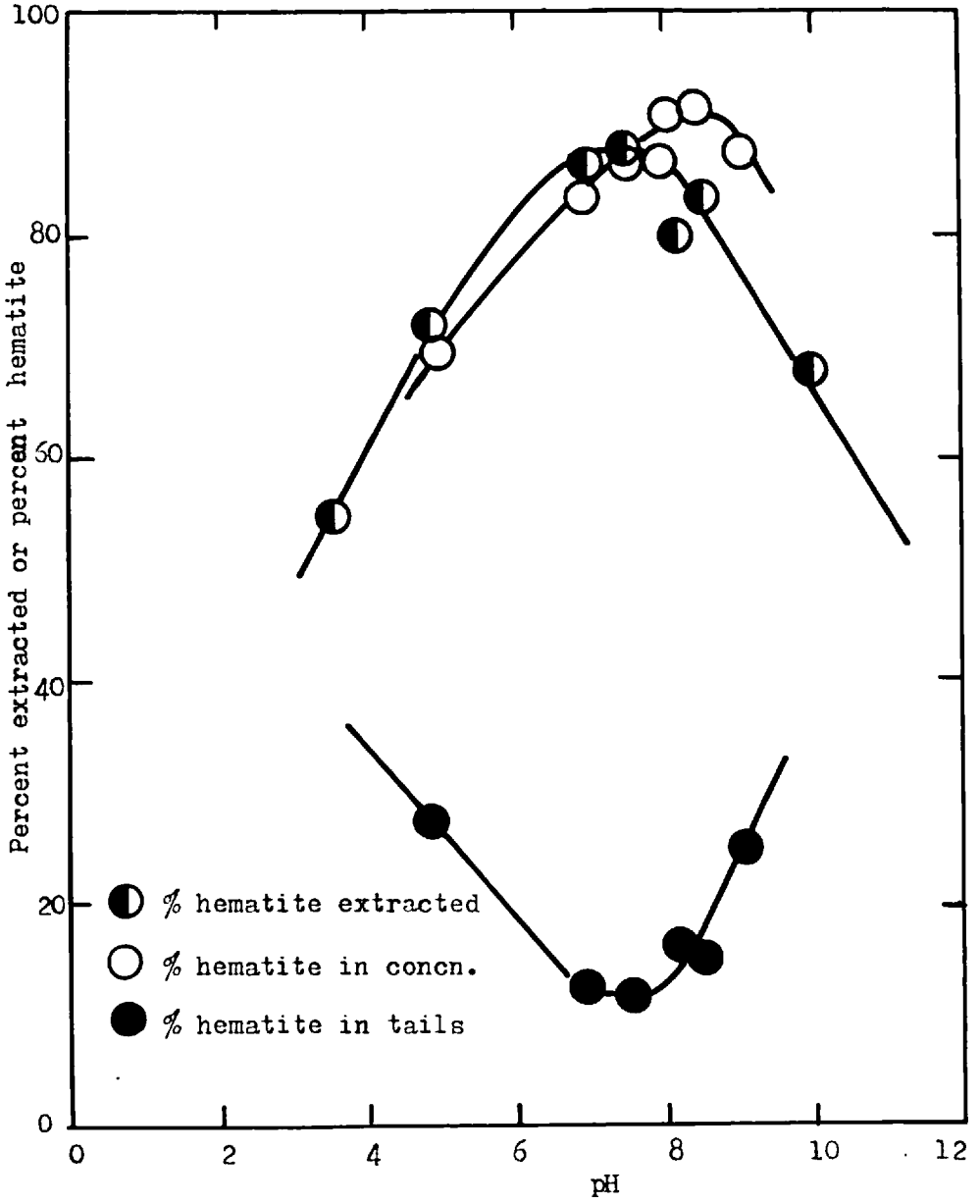

Fig. 59. Selective extraction of hematite using 5×10^{-3} M dodecanoic acid.

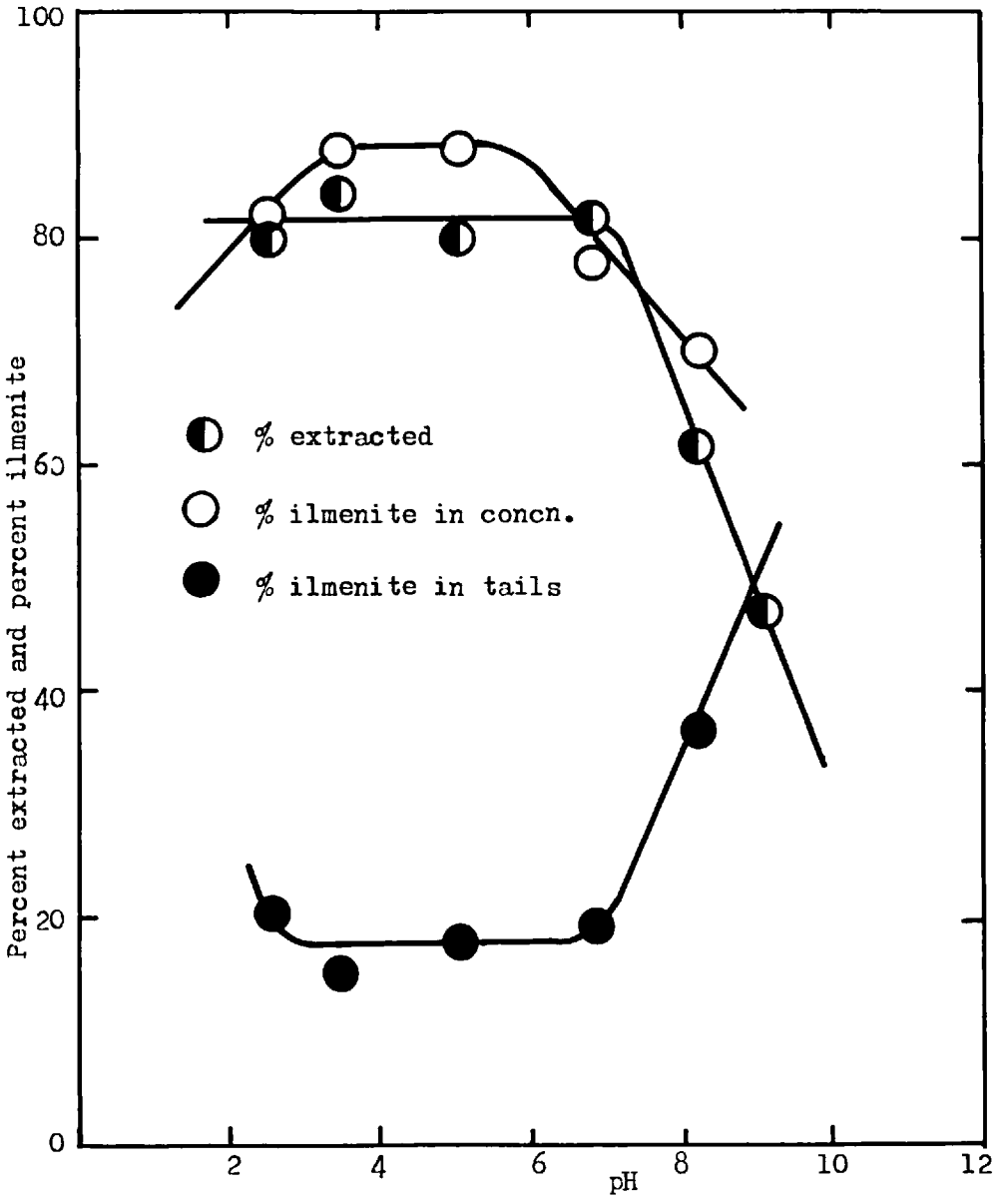

Fig. 60. Selective extraction of ilmenite using 2×10^{-4}M S.D.S.

4.40. Discussion

4.41. The quartz/water/iso-octane system in the presence of dodecylamine

a) The quartz/water interface

When quartz is crushed, a breaking of - Si - O - Si - bonds occurs and as a result Si^+ and SiO^- sites are formed at the fractured surface. In aqueous media H^+ ions react, with the oxygen sites and OH^- ions with the silicon sites, to give a surface silicic acid. The equations for such reactions can be represented as

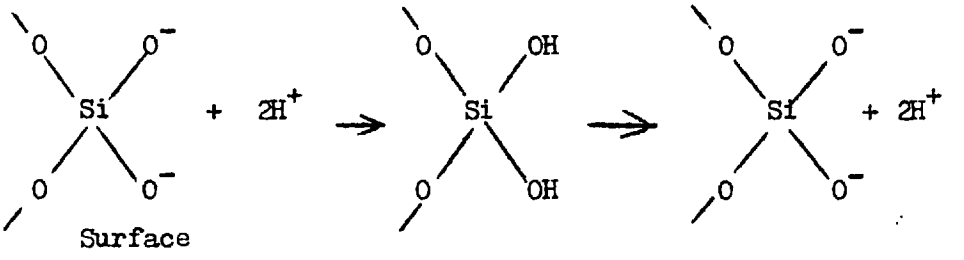

and

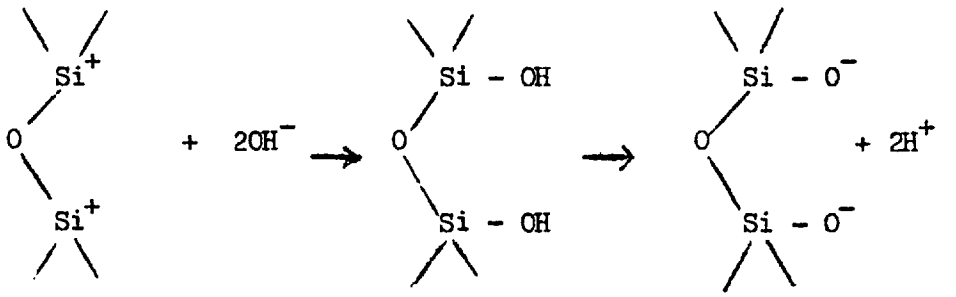

The negatively charged surface of quartz obtained in aqueous solutions can be explained by the dissociation of H^+ ions from the surface silicic acid. The extent of this dissociation is dependent on the pH.

Although several authors (153) (152) (161) have studied the potential determining rôle of H^+ and OH^- ions on the surface of quartz, there is some controversy over the exact location of the zero point of charge (z.p.c.) and whether the quartz can acquire a positive surface. It would appear that the position of the z.p.c. is dependent on the type of pretreatment (153) used to clean the quartz sample. De Bruyn and Li (153) found that by reacting a quartz sample with hydrofluoric acid the z.p.c. was increased to slightly higher pH values. This shift in the z.p.c. was attributed to the removal of the amorphous silica layer coating the quartz particle. Such an explanation is unsatisfactory because fluoride ions affect silicas and quartz by increasing the rate of ageing (162) and also by catalysing the condensation of silicic acid (163). Furthermore Joy and co-workers (164) have indicated that in the presence of fluoride ions divalent SiF_6^{2-} sites might be formed.

The possible reasons for the discrepancy between the published values of the quartz z.p.c. are probably related to the presence of impurities (165) and also to the nature of the amorphous layer of silica that surrounds the quartz particles. Generally the z.p.c. of quartz samples occurs at pH values below 3. The notable exception to this being the determination by Fuerstenau (152), who found a z.p.c. of pH 3.7. The value obtained by extrapolation in this work was consistent with the values determined by other authors (161) (165) (166).

The published data on the zeta potential of quartz, offers no

conclusive evidence for the presence of a cationic quartz surface. The reluctance of a quartz surface to take up a positive charge is thought by O'Connor and Buchanan (166) and also Li and de Bruyn (153) to be related to the strong polarization of the surface OH groups in the field of the small tetravalent silicon cations. In other words the increased covalent nature of the Si - OH bond will be such that it will not be overcome by an approaching proton or protonated water molecule.

According to eq^{n} (13) (section 4.12a) the surface potential ψ_o should vary linearily with the pH. Since the total potential drop across the double layer is equal to the sum of the potential drops in the Stern and diffused layer, the ψ_δ potential (or zeta potential) for a given constant ionic strength should vary linearily with the pH also. It is shown in fig. 23 that such a linear relationship existed at pH values below neutral, but that above neutral the zeta potential became independent of the pH. This constant zeta potential can be attributed to either the formation of a completely ionized quartz surface or to the relocation of the slipping plane at which the zeta potential was measured.

Li and de Bruyn (153) have determined the adsorption of Na^+ ions on quartz and the zeta potential under comparative conditions. From the adsorption results they evaluated ψ_δ by the Gouy-Chapman relationship and compared the values with the determined zeta potentials. At low ionic strengths ($<<10^{-4}$) and below pH 9, they found that the zeta potential was identical with the ψ_δ potential.

However, at higher and much lower ionic strengths than this value, the ψ_δ was consistently larger than the zeta potential. Lyklema and Overbeek (167) have explained this phenomenon by proposing that the slipping plane has a variable thickness as measured from the solid surface, and tends to move further from the surface with increasing ψ_o and ψ_δ. The effect of this is that at high values of ψ_o, the zeta potential becomes independent of ψ_o and the pH, and tends to a constant value that is dependent on the ionic strength.

The value of the constant zeta potential obtained in this work, at high pH values, was consistent with that obtained by Fuerstenau (152) and Li and de Bruyn (153) for an ionic strength of 10^{-2}. It is therefore thought that this zeta potential was a result of the relocation of the slipping plane.

b) The quartz/water interface in the presence of dodecylamine

In order to maintain electroneutrality the sum of the charges in the diffuse layer (σ_d^o) and the Stern layer (σ_s^o) must be equal and opposite to the surface charge (σ). If surface active ions are added to the quartz/water interface, at constant ionic strength and pH, the total surface charge (σ) will not change, but the distribution of charges in the diffuse (σ_d) and Stern (σ_s) layers will do so. The charge balances for systems with and without surface active ions, can be presented as

$$\sigma = \sigma_d^o + \sigma_s^o \qquad (39)$$

$$\text{and} \quad \sigma = \sigma_s + \sigma_d \qquad (40)$$

Subtraction of eq^n (40) from (39) gives

$$\sigma_s - \sigma_s^\circ = \sigma_d^\circ - \sigma_d = \Delta\sigma_d \qquad (41)$$

By the use of the Gouy-Chapman relationship (section 4.12 eq^n (2)) it can be shown that at 25°C

$$\sigma_d^\circ - \sigma_d = 3.53 \times 10^4 \sqrt{C} \left[\text{Sinh.} \frac{\psi_\delta^\circ ve}{2\,kT} - \text{Sinh} \frac{ve\psi_\delta}{2\,kT} \right] \qquad (42)$$

If ψ_δ is small ($\ll$25 mV) Sinh $\frac{ve\psi_\delta}{2\,kT}$ and Sinh $\frac{ve\psi_\delta^\circ}{2\,kT}$ can be expanded to give

$$\Delta\sigma_d = \sigma_d^\circ - \sigma_d = \sigma_s - \sigma_s^\circ = 3.53 \times 10^4 C^{\frac{1}{2}} \frac{ve}{2kT} (\psi_\delta^\circ - \psi_\delta) \qquad (43)$$

Assuming that the zeta potentials are identical or at least similar to the Stern potentials (ψ_δ), then measurement of the zeta potential difference ($\zeta^\circ - \zeta$) = $\Delta\zeta$, as a function of the amine concentration will give an indication of the variation in charge distribution in the diffuse and Stern layer.

In fig. 61, $\Delta\zeta$ is plotted as a function of dodecylamine concentration at different constant pH values. The data was obtained from fig. 24. If it is assumed that the adsorption isotherm represents the adsorption of cationic amine at the quartz/water interface, a comparison of the adsorption isotherm at pH 6.5 (fig. 27a) with the electrokinetic data and the curve of $\Delta\zeta$ (fig. 61)

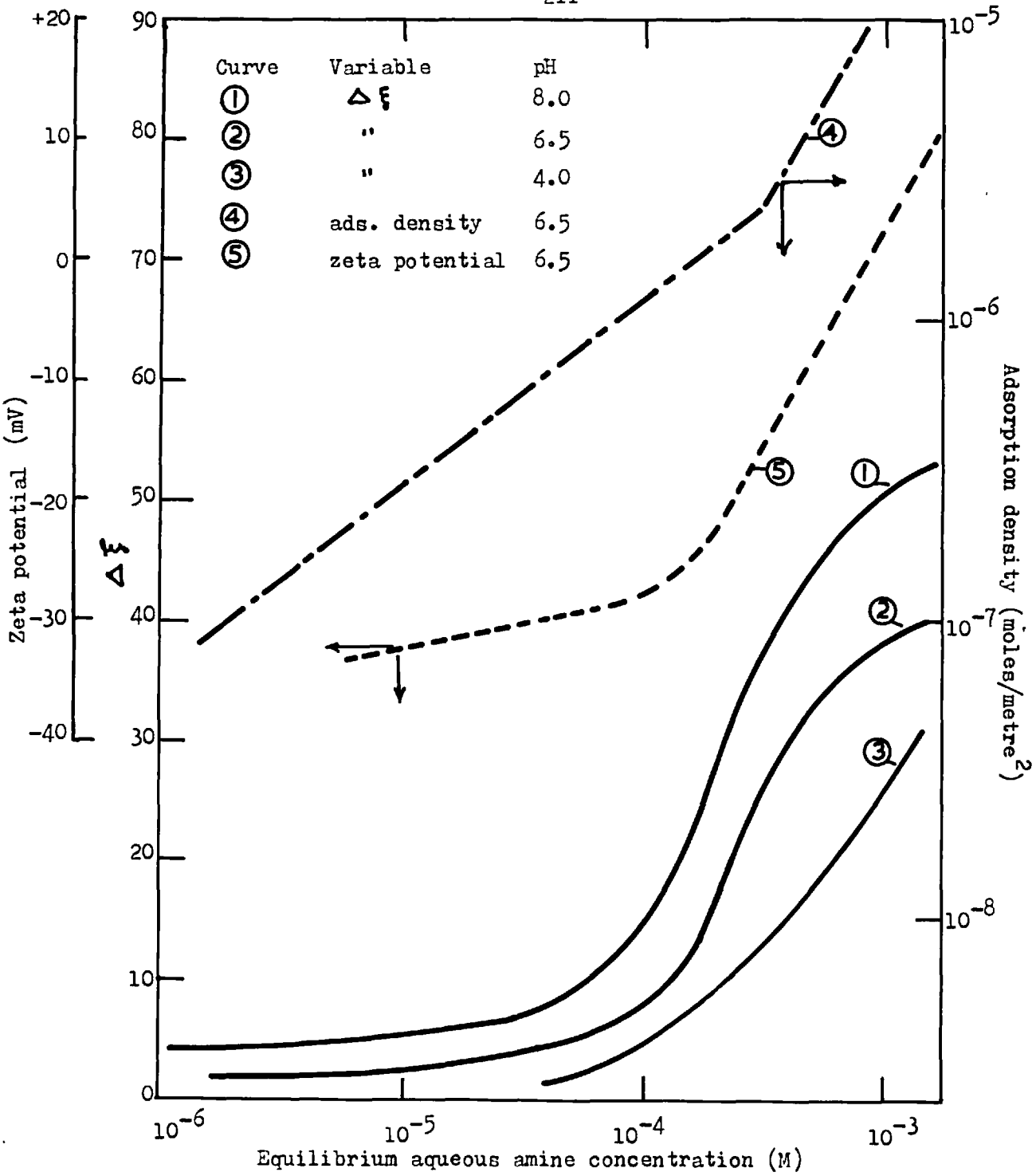

Fig. 61. Comparison of the adsorption density, zeta potential and $\Delta\xi$ as functions of the aqueous amine concentration.

(ionic strength 6×10^{-3})

as a function of the logarithm of the cationic amine concentration, shows that at concentrations below 10^{-4}M, amine was adsorbed without markedly changing the zeta potential or the distribution of charge in the double layer.

The total adsorption density of positively charged counter ions, in moles cm^{-2} (Γ_+), can be evaluated from the Gouy-Chapman relation

$$\Gamma_+ = \frac{\sigma_d}{vF} = 6.1 \times 10^{-11} \sqrt{C} \left[\exp 19.46 \psi_\zeta - 1 \right] \quad (44)$$

The total number of positive ions in the bulk, C_+, was kept constant at 6×10^{-3}M throughout the experiments by the addition of hydrochloric acid and sodium hydroxide. Thus, at pH 6.5 and at concentrations below 10^{-4}M the zeta potential, ψ_ζ and consequently Γ_+ was approximately constant. It is therefore suggested that in this concentration range the cationic amine was adsorbed by an ion exchange mechanism with cationic counter ions in the diffuse layer or with H^+ ions on the surface of the quartz.

If there was no preference of the dodecylamine ions over the other cationic counter ions for the quartz surface, the ion exchange will be governed by the simple law

$$\frac{\Gamma_{RNH_3^+}}{\Gamma_{Na^+}} = \frac{C_{RNH_3^+}}{C_{Na^+}} \quad (45)$$

Equation (45) predicts that the slope of a plot of log. $\Gamma_{RNH_3^+}$ against log. $C_{RNH_3^+}$ should be unity. Jaycock, Ottewill and Tar

(168) found that for the adsorption of dodecyl sulphate ions on stannic oxide, this was in fact the case. The value obtained in this work of 0.7 is only in approximate agreement with this prediction. Somasundaran and Fuerstenau (169) found a similar value for the adsorption of alkyl-sulphonates at the alumina/water interface. The possible reasons for the discrepancy between the theoretical and experimental slope are a) although the ionic strength was kept constant, the N_a^+ ion concentration varied and b) the possibility of some neutral amine being deposited at the solid/water interface after the recession of the oil interface.

An increase in the amine concentration above 10^{-4}M at pH 6.5, produced a greater dependence of the adsorption density, zeta potential and $\Delta \zeta$ on the logarithm of the amine concentration. Reference to eq^n (41) shows that at constant ionic strength and pH an increase in $\Delta\sigma$ must result in a decrease of σ_d and an increase in σ_s. The charge in the Stern layer will only increase markedly when there is a marked increase of ions being specifically adsorbed into the Stern layer. It would therefore appear that the marked change in the zeta potential at concentrations above 10^{-4}M was attributable to the increase in the number of cationic amine ions in the Stern layer. Any mechanism postulated to explain this increase in adsorption density should include a reason for continued adsorption after all the available surface sites have been 'neutralized'.

Gaudin and Fuerstenau (170) consider that once the adsorbed

ions in the Stern layer reach a certain critical concentration, they begin to associate into two dimensional patches of ions, in much the same way as they associate into three dimensional aggregates to form micelles in the bulk solution. The forces responsible for these associations are believed to be van der Waals forces of interaction between the hydrocarbon chains. Hydrocarbon chains will always have a tendency to be expelled from an aqueous phase because the van der Waals attraction of water to water is greater than that of hydrocarbon to water. Because of the proposed structural formation of these adsorbed ions, the associated ions have been termed 'hemimicelles' (170). The critical concentration at which the associations begin is referred to as the critical hemimicelle concentration (C_{HMC}), and it is believed to be coincident with the concentration at which the zeta potential and adsorption density show a marked specific dependence on the logarithm of the collector concentration.

The evidence for association between the adsorbed chains has been supplied by a number of authors (171) (172) (173). Somasundaran and co-workers (174)(175) divided the W term in the equation for the specific adsorption into the stern plane i.e. $n = 2\, rn_i \exp.(-W/kT)$ (see section 4.12a) into an electrical and chemical term, thus

$$W = ve\psi_\delta - N\phi' \qquad (46)$$

where ϕ' was the van der Waals energy of interaction per CH_2 group

between adjacent chains of surface active ions and N the number of carbon atoms in the hydrocarbon chain. The value of ϕ' determined by different techniques (174) (175) was shown to be (1.0 ± 0.1) kT. A value in good agreement with that found from solubility data (49) or from studies of micelle formation as a function of alkyl chain lengths of monofunctional surface active agents (176).

From Gaudin and Fuerstenau's (170) concept of hemimicelles it would appear that the adsorbed ions associate before all the available ionic surface sites have been neutralized. Adsorption above that required to reduce the zeta potential to zero is assumed to be a continuation of the association process with the polar head groups still orientated toward the solid surface (see fig. 61a).

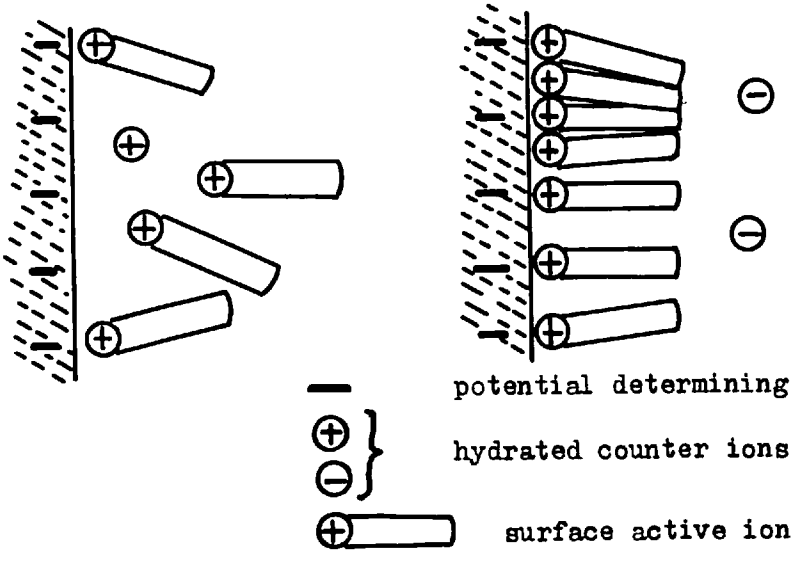

a) Adsorption as single ions at low concentrations

b) Hemimicelle formation at higher concentrations

Fig. 61a.

It is possible, however, that at concentrations of ionic surface active agents above that required to neutralize the surface sites, the ions are adsorbed by hydrocarbon chain interaction with the polar heads pointing into the aqueous phase (177) (178). As a result a more hydrophilic surface will be obtained.

In view of the correlation between the adsorption density and electrokinetic results found in this work and their similarity with those of de Bruyn (154) and Fuerstenau (152) the concentration of aqueous amine, at which both the adsorption density and the electrokinetic data showed a marked dependency on the concentration, is termed the C_{HMC}. The increase in adsorption density above the C_{HMC} is believed to be attributable to neutralization of the surface sites with increasing associations between the hydrocarbon chains.

From a sterical analysis of the arrangement of silicon atoms and oxygen atoms at various crystal planes in quartz, Gaudin and co-workers (179), have calculated that the area per available surface site is 23.4 $\mathring{A}^2$. This value is nearly the same as the cross sectional area of the hydrocarbon chain. Therefore, if the quartz surface is in a fully ionized state, a vertically orientated monolayer of oationic amine is likely to be completed at the equilibrium amine concentration, which reduced the zeta potential to zero. From figs. 27a and 25 this appeared to be the case at pH 6.5.

The adsorption density of amine on quartz decreased (fig. 26) at pH values above 7 in the presence of iso-octane. According to fig. 5 the cationic amine concentration decreased also in this pH

range. The adsorption density results, therefore, clearly show the importance of the cationic amine concentration in the aqueous phase on the adsorption density at the quartz/water interface.

In summary, the electrokinetic and adsorption measurements indicate that the primary mechanism of amine adsorption was one of coulombic attraction of the amine ions for surface sites. Above a certain adsorption density (approx. 1.6×10^{-6} moles metre^{-2}) (154) the adsorption in the Stern layer increased markedly possibly because of the formation of patches of associated ions or hemimicelles.

c) <u>The quartz/water/iso-octane line of contact</u>

The Young's expression for the iso-octane/water/quartz system can be expressed as

$$\gamma_{so} = \gamma_{ow} \cdot \cos\theta + \gamma_{sw} \qquad (47)$$

If the contact angle (θ) is zero, $\gamma_{so} = \gamma_{ow} + \gamma_{sw}$ and the quartz surface will be hydrophilic (c.f. section 4.13b). In the presence of amine the three interfacial tensions γ_{ow}, γ_{sw} and γ_{so} are denoted by γ_{sw}', γ_{ow}' and γ_{sw}' because of the adsorption of amine at the three interfaces. Values of γ_{ow}', under various values of pH and aqueous amine concentration were presented in section 3.00. The results showed that a pH values between 3 and 10 the magnitude of γ_{ow}' was dependent on the adsorption of cationic amine from the aqueous phase and neutral amine from the organic phase. Evidence was also provided that

the adsorbed species formed molecular associations at the interface. Only at low and high pH values was δ_{ow}' dependent on the adsorption of one of the amine species only.

It follows therefore that when an oil drop is brought into contact with a quartz surface, the resulting quartz/oil interface will be of a complex nature. The recession of a water meniscus over the quartz surface will probably leave behind, at the quartz/oil interface, cationic amine ions which were originally adsorbed at the quartz/water interface (180) (181). In addition to the presence of cationic amine ions, there is the possibility that as the pH is increased, neutral amine from the organic phase will be adsorbed at the quartz/oil interface (182). The presence of neutral amine at this interface will complicate the interpretation of the contact angle data.

The two lines correlating the contact angle and the logarithm of the aqueous amine concentration, at pH 6.5 (fig. 30), intersected at a cationic amine concentration of 1.25×10^{-4}M for the receding angles and 3.0×10^{-4}M for the advancing angles. These concentrations are very similar to the C_{HMC} derived from the adsorption and electrokinetic studies (figs. 25 and 27a). It is therefore assumed that the contact angles represent the oleophilicity of the quartz surface when the cationic amine was adsorbed by an ion exchange process followed by increased adsorption in the Stern plane, at pH 6.5, although some neutral amine was present in the organic phase.

If the adsorbed cationic amine ions are predominantly in the

diffuse layer, at concentrations below the C_{HMC}, no fixed orientation of the ions is expected because the ions are distributed at random. Some ions will, however, be orientated with their polar groups pointing toward the surface because of the electrostatic attraction between the head groups and the surface. Above the C_{HMC} the contact angle increased proportionately to the increase in adsorption density. Presumably in this region the adsorbed cations in the Stern layer, in addition to being closer packed, took up a more vertical position with the hydrocarbon chains pointing toward the aqueous phase. Associations and vertical orientation of the adsorbed ions would shield the hydrophilic nature of the quartz surface and the polar head groups. As a result a more hydrophobic surface would be formed.

The studies on the distribution of amine (cf section 2.0) between the iso-octane and water phases showed that as the pH was increased above 7, the neutral amine concentration in the organic phase became far greater than that of the cationic amine in the aqueous phase. The aqueous cation amine concentration was approximately ten times lower at pH 8.0 than at pH 7 and also, twenty five times lower than the neutral amine concentration in the organic phase. Despite this decrease in the cationic amine concentration and the corresponding decrease in the adsorption density, higher contact angles (figs. 28-29) were obtained at pH 8 than at pH 6.5. According to the electrokinetic data (fig. 25), if only cationic amine was adsorbed at the quartz/water interface, the C_{HMC} at pH 8

should occur at a cationic amine concentration of 6.3×10^{-5}M. Reference to the contact angle data (fig. 30) for the natural quartz sample shows that, at pH 8.0 the 'apparent' C_{HMC} occurred at 3×10^{-5}M for the advancing angles and 6.3×10^{-6}M for the receding angles.

It is therefore suggested that at pH values where the neutral amine concentration in the organic phase was large relative to the cationic amine concentration in the aqueous phase, adsorption of both the neutral and the cationic amine controlled the magnitude of the contact angle. That the cationic amine was essential for the wetting of the quartz by the iso-octane, was illustrated by the fact that at high pH values (>8) the contact angles decreased markedly with increase in pH. It would therefore appear that cationic amine plays a primary rôle either at the quartz/iso-octane/water interline of contact or at the quartz/iso-octane interface before the neutral amine is involved. The suggested mechanism of neutral amine adsorption is that of interactions between the hydrocarbon chains of the cationic amine ions and the hydrocarbon chains of the neutral molecules.

The importance of neutral molecules in flotation systems has been demonstrated by other authors. Smith (183) showed that when neutral molecules were added to a system composed of quartz and dodecylamine solution, the contact angles increased markedly. Similarly Fuerstenau and Yamada (173) showed that neutral molecules increased the pH range and concentration range over which a given

collector was effective. Leja and Schulman (171) demonstrated that the contact angle between benzene and polished copper in a solution of ethyl xanthate could be increased by adding long-chain alcohols to the benzene phase. The mechanism of adsorption of the neutral molecules was ascribed by these authors to molecular interactions between the chains of the adsorbed species and the chains of the neutral molecules.

As the pH was increased for each "total concentration" of amine the contact angle hysteresis of the natural quartz increased from about 15^{o} at pH 3 to a constant value of $25-30^{o}$ at pH 8.0. A similar effect although not so pronounced was obtained for the optical quartz sample. The fact that the hysteresis was less for the smoother optical quartz sample does suggest that surface roughness was a contributing factor to the higher hysteresis of the natural quartz sample. However, Gaudin and Decker (182) measured the dynamic advancing and receding angles for the system quartz/dodecane/water in the presence of dodecylamine and found that the hysteresis at pH 10.0 was larger than that at pH 8.0 and 6.0. It is therefore possible that at pH 8.0 the larger hysteresis effect was partially attributable to the low rate of attainment of equilibrium at the advancing and receding interfaces because of the presence of large amounts of neutral amine. In other words the measured contact angles were probably not true equilibrium angles.

The magnitude of the adsorption of neutral amine or cationic amine at the oil/quartz interface is difficult to assess. A number

of authors (127) (184) have shown that, at equilibrium, thermodynamics demands that the adsorption of collector at the solid/air or solid/oil interface should be greater than that at the corresponding solid/water interface. Smolders (184) using the Young's equation with Gibbsian thermodynamics has derived an expression relating the adsorption (Γ') at the three interfaces with the contact angle and air/water interfacial tension. For the system oil/quartz/water this becomes

$$\Gamma'_{so} = \Gamma'_{sw} + \Gamma'_{ow} \cos\theta + \frac{\gamma'_{ow} \sin\theta}{RT} \frac{d\theta}{d\ln C} \qquad (48)$$

where Γ'_{so}, Γ'_{sw} and Γ'_{ow} represent the adsorption at the solid/oil, solid/water and oil/water interfaces respectively. Whether such an expression is valid or not, for the very complex quartz/iso-octane interface in the presence of amine is questionable. Application of eq^{n} (48) to the results obtained in this work, at pH 6.5, gives adsorption densities at the quartz/oil interface corresponding to layers between 8 and 17 amine monolayers thick. Clearly if this is a true representation of the adsorption at the oil/quartz interface then the interpretation of the contact angle data will be far more complex than that indicated in the preceding paragraphs.

d) Work of adhesion and extraction results

An oil/mineral interface cannot be created without the

simultaneous destruction of the oil/water and mineral/water interfaces. Energetically the requirement for the adherence of an oil drop to the quartz surface is that the sum of the surface energy terms after the change must be less than the sum before the change i.e. $\gamma_{os'} < \gamma_{ow'} + \gamma_{sw'}$. The work done per unit area by the system during the adhesion of an oil drop to the mineral surface is given by

$$W = \gamma_{wo'} + \gamma_{sw'} - \gamma_{os'} \qquad (49)$$

Substituting in eq^{n} (49) for $\gamma_{sw'} - \gamma_{os'}$ from the Young's expression (eq^{n}47) gives

$$W = \gamma_{ow'} (1 - \cos\theta) \qquad (50)$$

which relates the work of adhesion (W) of the oil drop to the solid surface with the oil/water interfacial tension and the contact angle. The work of adhesion, as determined from eq^{n} (50), is the theoretical maximum free energy available for the adhesion process. It is not however a measure of how much of the available free energy is utilized (185). Determination of the work of adhesion should give an indication of the conditions necessary for the attachment of mineral particles to oil drops.

The results from the calculation of the work of adhesion as a function of pH, at three different 'total concentrations' of dodecylamine are shown in fig. 62. Comparison of this figure with fig. 61 shows that maximum extraction was obtained at the pH

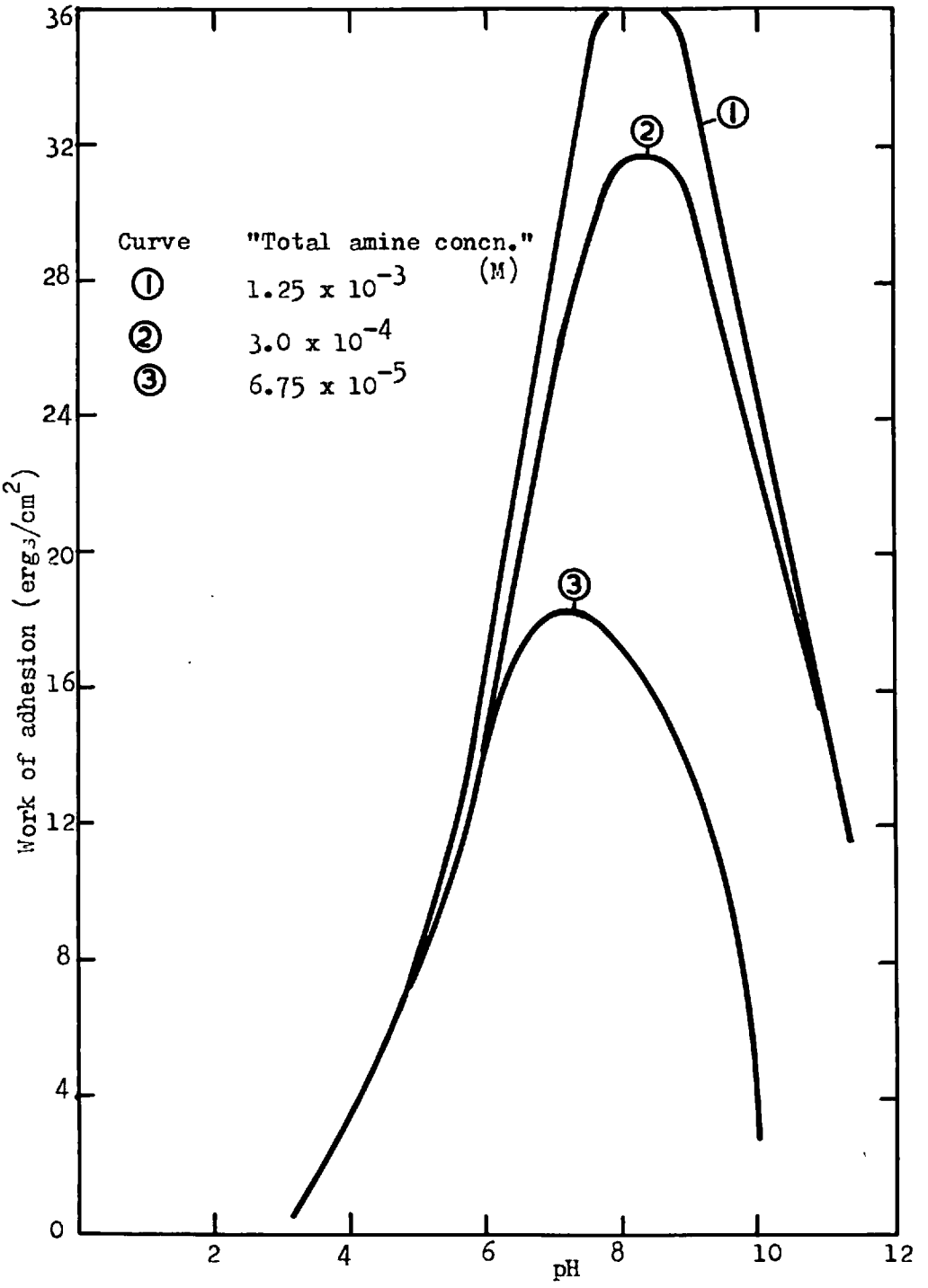

Fig. 62. Work of adhesion of iso-octane to quartz in the presence of dodecylamine. (ionic strength 6×10^{-3})

where the contact angles, work of adhesion and adsorption density were a maximum. The correlation between the four sets of data, in alkaline media was good. As the pH was increased the contact angles, percent extraction, adsorption density, work of adhesion, and the cationic amine content of the aqueous phase decreased.

At acid pH values, however, good extraction was obtained under conditions where the contact angles and work of adhesion were comparatively small. The reason for this is not fully understood. The distribution of particle shape and size and hence adsorption densities might be a contributing cause.

The relationship between the work of adhesion and the logarithm of the equilibrium aqueous amine concentration, at pH 6.5 and 8.0, (fig. 63) was similar to that found for the contact angle data at the same pH values (fig. 30). The work of adhesion showed a marked dependence on the logarithm of the aqueous amine concentration at concentrations above 1.3×10^{-4}M at pH 6.5, and 9×10^{-6}M at pH 8.0. These concentrations were in excellent agreement with the C_{HMC} and 'apparent' C_{HMC} predicted from the contact angle data. Figure 64 shows the work of adhesion as a function of the adsorption density of amine at the water/quartz interface. For a given adsorption density the work of adhesion at pH 8.0 was much higher than that at pH 6.5. This indicates that in the presence of large amounts of neutral amine in the organic phase higher contact angles and works of adhesion were obtained.

Maximum extraction, at pH 6.5, was obtained at an equilibrium

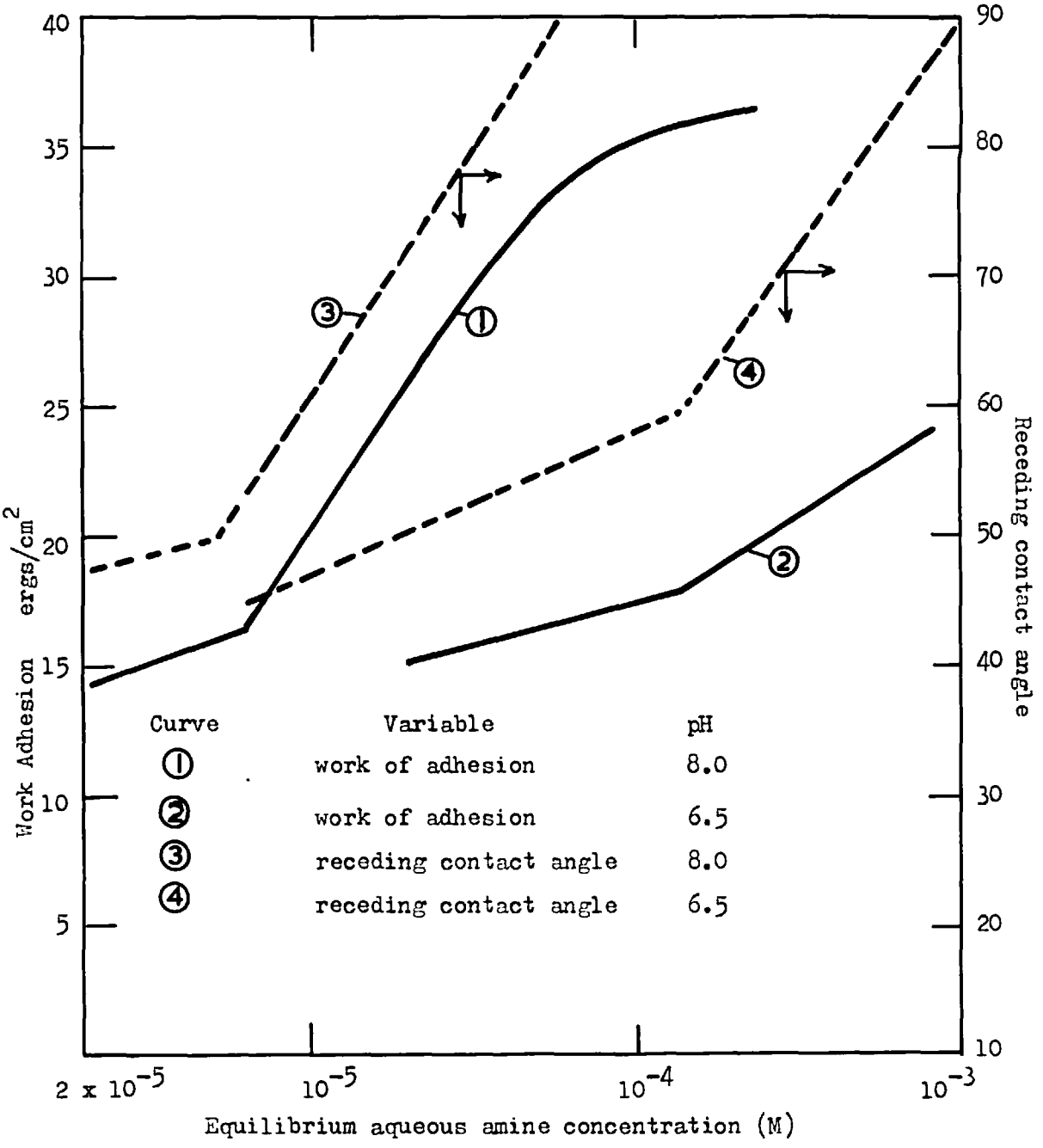

Fig. 63. Work of adhesion of iso-octane to quartz as a function of aqueous amine concentration. (ionic strength 6×10^{-3})

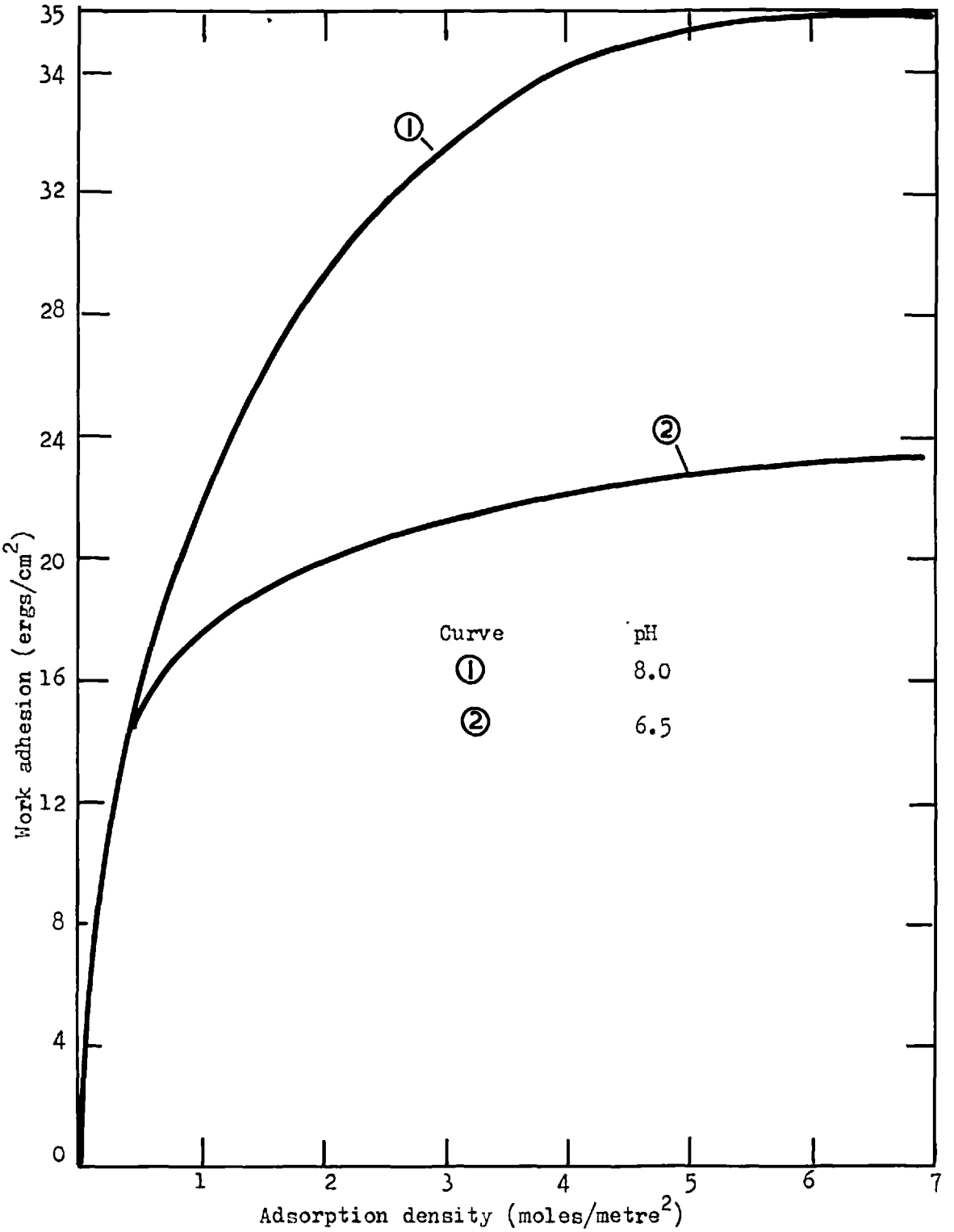

Fig. 64. Work of adhesion of iso-octane to quartz as a function of dodecylamine adsorption density.
(ionic strength 6 x 10^{-3})

aqueous amine concentration corresponding to that required to reduce the zeta potential to zero. This is not surprising because under these conditions the electrostatic repulsive forces between the particles will be minimum. The particles will be able to aggregate and form a close packed layer at the oil/water interface. The minimum receding contact angle required for 100% extraction was approximately 90° at pH 6.5. Under these conditions $\gamma_{so} = \gamma_{sw}$ and the particle would be equally wetted by the aqueous and organic phases. Contact angles greater than 90° would result in more than half of the particle being wetted by the organic phase (von Rheinders case 3 ; cf. Section 1.30).

e) Summary

The results indicate that the mechanism of adsorption of amine at the quartz/water interface is primarily one of coulombic attraction of the cationic amine ions for negative sites on the quartz surface. The amine ions are adsorbed, at low amine concentrations, by an ion exchange process with cationic counter ions in the diffuse layer, and at higher concentrations, into the Stern layer where they associate and become vertically orientated.

The contact angles, at pH 6.5, reflect the two steps involved in the adsorption process. At pH 8, however, the neutral amine in the organic phase influences the contact angles either by adsorption at the solid/oil interface or the solid/water/oil interline of contact. The adsorption density, contact angles and extraction

results when compared to the solution chemistry data shows, however, that the neutral amine, in the organic phase, is not involved unless substantial quantities of cationic amine are present in the aqueous phase.

The correlation between the contact angles, work of adhesion, percent extraction and adsorption density was good throughout the pH range. One hundred percent extraction was obtained when the contact angles were approximately 90° and the zeta potential was zero. This latter condition would correspond to low repulsive forces between the particles and hence tighter packing at the oil/water interface. Under no conditions were the quartz particles completely extracted into the organic phase. This is not surprising in view of the 'second situation' outlined by von Rheinders (41) i.e. the solid will only be dispersed in the organic phase when $\gamma_{sw} > \gamma_{wo} + \gamma_{so}$ (cf. section 1.30). For the system investigated here this situation will only be realized when the contact angle reaches 180°.

4.42. The hematite/iso-octane/water system in the presence of sodium dodecyl sulphate

a) The hematite/water interface

By definition the potential determining ions for pure hematite, in the absence of specifically adsorbed surface active ions, will be the constituents of the ionic lattice (i.e. Fe^{3+} and O^{2-}).

However, many authors working on both synthetic (186) (187) and natural hematites (188) (189) have shown by electrokinetic and potentiometric methods that H^+ and OH^- ions are the potential determining ions. The ferric hydroxy complexes in equilibrium with the hematite surface will have an effect on the surface potential. Solubility data (186), however, shows that this effect is negligible because throughout the pH range the concentration of H^+ and OH^- ions is far greater than that of the ferric complexes.

Although the potential determining rôle of H^+ and OH^- ions has been well established, there appears to be a large discrepancy between the zero points of charge (z.p.c.) of the synthetic and natural hematites. Values of the z.p.c. for synthetic hematites are usually found between pH values 8 and 9 (186), and for the natural hematite between 3 and 9 (188) (189). Joy and Watson (190) have indicated that the z.p.c. of the natural hematite is dependent on the origin, size and previous treatment of the sample. Parks (191) after summarising the work of many authors concluded that the position of the z.p.c. was dependent on the degree of hydration of the surface. Acid z.p.c. values were thought to be attributable to surface or bulk dehydration.

The processes by which a surface can be hydrated can be summarised as follows a) physical adsorption of non-dissociating water molecules, including hydrogen bonding to surface oxygen sites, b) chemisorption of water which dissociates resulting in surface Fe - OH groups and c) reaction resulting in conversion to oxyhydro-

xides or hydroxides. Whereas the precipitated hematite prepared by hydrolysis is hydrated or at least is coated by a layer of hydrous material, the natural hematite only hydrates partially and in most cases gives a z.p.c. approaching that of α- Fe OOH (goethite). The hematite sample used in this work had a zero point of charge of 4.75. This suggests that the surface was somewhat less hydrated than that corresponding to Fe OOH. Parks (191) considers that low z.p.c. values might be attributed to the physical adsorption of water only.

The process by which the hematite surface charge is established may be viewed either as an adsorption of H^+ or OH^- ions, or as a dissociation of surface sites. A schematic representation of the reactions taking place would be

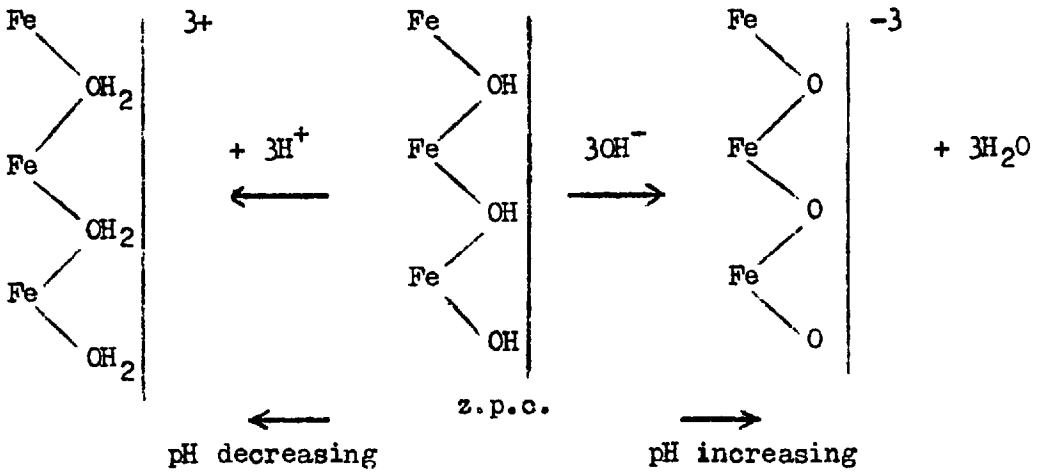

Alternatively the dissociation of the hydroxide surface to yield a positively or a negatively charged surface may be represented by the following reactions

$$Fe\ (OH)_{3\ surface} + H^+ \longrightarrow Fe\ (OH)_2^+\ (surface) + H_2O \qquad (51)$$

$$Fe\ (OH)_{3\ surface} \longrightarrow FeO_2^-\ (surface) + H^+ + H_2O \qquad (52)$$

These reactions suggest that a positive surface is produced by the binding of a proton (H^+) to the hydroxide surface; this is of course equivalent to the removal, by dissociation, of one OH^- group from the surface. A negative surface is produced by the removal of a proton by dissociation (or the addition of an OH^- ion). The z.p.c. will lie at a pH where the number of negative and positive sites are equal, or in other words when the surface is uncharged with respect to the solution.

The hydrated complexes in equilibrium with the hematite surface will be of the form $Fe\ (H_2O)_6^{3+}$, $Fe\ (OH)\ (H_2O)_5^{2+}$, $Fe\ (OH)_2\ (H_2O)^+$, $Fe_2\ (OH)_2^{4+}$ and $Fe\ (OH)_4^-$. The concentration of the first four species will decrease, and the concentration of the anionic complex will increase, with an increase in the pH. Between the pH values 3 and 14, the concentration of all the complexes will, however, be below 10^{-8}M. In the presence of chloride ions the hydroxyl complexes can form ferric chloro-hydroxy complexes of the type $Fe\ Cl\ (H_2O)_5^{2+}$ etc. Since these complexes are known to exist in aqueous solution it is reasonable to assume that they may exist on the hematite surface.

The zeta potentials of hematite in the presence of different anions (fig. 34) indicated that the surface became more negative with Cl^- than with NO_3^- and ClO_4^- ions. The order in which the

ions complex readily with ferric (192) is the same as the order in which they increase the negative zeta potential i.e. $Cl^- > NO_3^- > ClO_4^-$. The mechanism by which the different anions or ferric complexes affect the zeta potential is not understood. Specific adsorption in the Stern layer is unlikely because the different anions did not change the location of the z.p.c.

In the presence of divalent sulphate ions the zeta potential was made more negative than in the presence of the monovalent anions and the apparent zero point of charge was moved to more acid pH values. Similar results were obtained by Mattson and Pugh (193) for a hematite that had sulphate impurities in the crystal lattice. These results are consistent with the postulate of Overbeek (108) for specific adsorption of ions into the Stern layer. Akinson, Posner and Quirk (194) consider that ions such as phosphate are specifically adsorbed by ligand exchange reactions with OH^- or H_2O in the ferric first co-ordination shell. A similar mechanism can be postulated for the adsorption of sulphate ions.

b) <u>The mechanism of adsorption of S.D.S. at the hematite/water interface</u>

The electrokinetic data (fig. 35 and 36) and the adsorption density results (fig. 37) indicate that the primary mechanism of adsorption of sodium dodecyl sulphate at the hematite/water interface was one of coulombic attraction of the anionic collector ions for positive sites on the hematite surface. The dependence of the zeta potential on the logarithm of the collector ion concentration,

at pH 2.5 and low concentrations of S.D.S., was small. This indicates that in this concentration range the dodecyl sulphate ions were adsorbed by an ion exchange with chloride ions in the double layer. The large variation of the zeta potential with change in the logarithm of the concentration, at higher concentrations of S.D.S., is indicative of specific adsorption in the Stern layer.

Further evidence for specific adsorption in the Stern layer can be obtained by plotting the logarithm of $\Delta\zeta$ as a function of the logarithm of the S.D.S. concentration and pH. In section 4.41b it was shown that for zeta potentials below 25 mV

$$\sigma_s - \sigma_s^\circ \propto (\zeta^\circ - \zeta)$$

Since the charge in the Stern layer is directly proportional to the specific adsorption of ions, a plot of the logarithm of $\Delta\zeta$ against the logarithm of the collector concentration and pH, should, if the adsorption is taking place in the Stern layer, give curves similar to the adsorption results. Such plots are shown in figs. 37 and 65. In fig. 37 it was shown that the logarithms of $\Delta\zeta$ and the adsorption density decreased rapidly as the pH increased above the z.p.c. Comparison of fig. 65 with the adsorption isotherm (fig. 39), at pH 2.6, shows that there was a fairly good correlation between the shape of the isotherm and the curve of the logarithm of $\Delta\zeta$ against the logarithm of the equilibrium S.D.S. concentration, at concentrations below 5×10^{-4}M.

Although the primary mechanism of adsorption would appear to

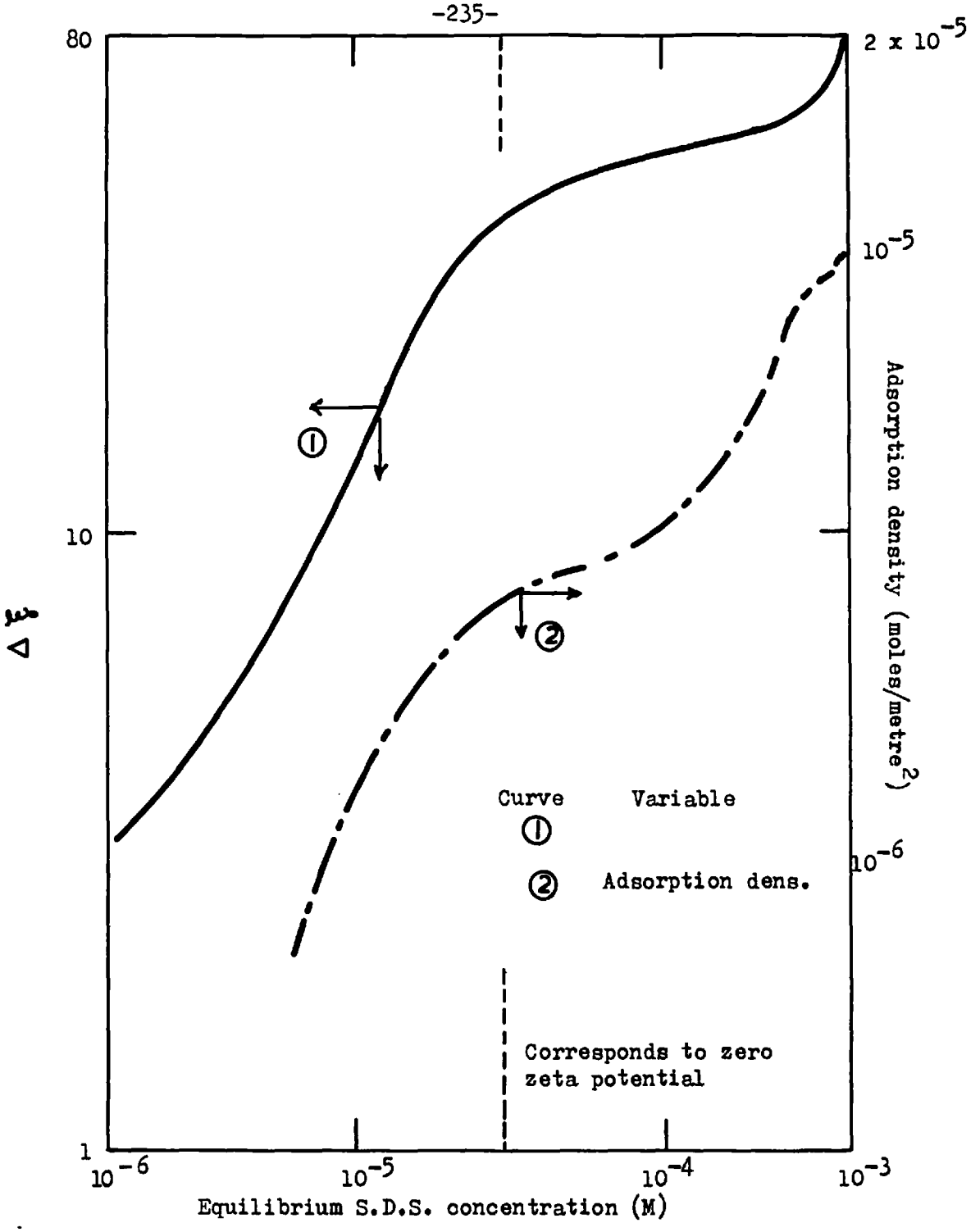

Fig. 65. The logarithm of $\Delta\zeta$ as a function of S.D.S. concentration.

(pH 2.6; ionic strength)

be one of coulombic attraction, an alternative mechanism must be postulated to explain the continued adsorption after neutralization of the surface sites. The two most likely mechanisms are:

a) At a certain critical adsorption density of S.D.S. the hydrocarbon chains began to associate to form hemimicelles. According to the Gaudin-Fuerstenau concept of hemimicellization the adsorbed ions begin to associate at a concentration identical to that at which the zeta potential begins to show a marked dependence on the logarithm of the collector concentration. The hematite zeta potential, in this work, decreased rapidly with increase in the logarithm of the S.D.S. concentration, at pH 2.5, at concentrations above 5×10^{-6}M. Furthermore, assuming that the adsorption density at the C_{HMC} is dependent only on the hydrocarbon chain length, then association of dodecyl sulphate ions should occur at an adsorption density similar to that found for dodecylamine adsorbed at the quartz/water interface i.e. approximately 1×10^{-6} moles metre^{-2}. Such an S.D.S. adsorption density, at the hematite/water interface at pH 2.6, was reached at an equilibrium concentration of 8×10^{-6}M. It is therefore possible that above this concentration associations between the adsorbed dodecyl sulphate hydrocarbon chains occurred. The assumption that the adsorption density at the C_{HMC} will be dependent only on the collector chain length is not unreasonable because in bulk solution the C.M.C. of sodium dodecyl sulphate is only approximately 1.5 times higher than that of dodecylamine (195).

b) The formation of a chemisorbed layer between the dodecyl

sulphate ions and sites, in addition to potential determining sites, on the hematite surface. Dean and Ambrose (196) have shown that when industrial sodium dodecyl sulphate is added to ferric solutions a precipitate results. It is possible that such a precipitated ferric dodecyl sulphate complex will be formed at the hematite/water interface.

c) The orientation of the dodecyl sulphate ions adsorbed at the hematite/water interface

In fig. 66, the contact angle as a function of the logarithm of the adsorption density of S.D.S. at the hematite/water interface is presented. The data was derived from figs. 39 and 41. The curve has been divided into three regions, each region extending over the same contact angle and adsorption density range as that indicated in figs. 39 and 41. In region I the contact angle increased slowly with an increase in the logarithm of the adsorption density. At an adsorption density slightly higher than that required to reduce the hematite zeta potential to zero, the contact angle increased markedly. (region II). Initially in region III, the contact angle increased slower, with an increase in the logarithm of the adsorption density, than in region II, but at an adsorption density roughly corresponding to a close-packed vertically orientated monolayer the contact angle increased markedly and then levelled off to become constant at a value of 125°.

There are three basic modes of orientation of a collector ion adsorbed at the solid/water interface and these are a) the ion is

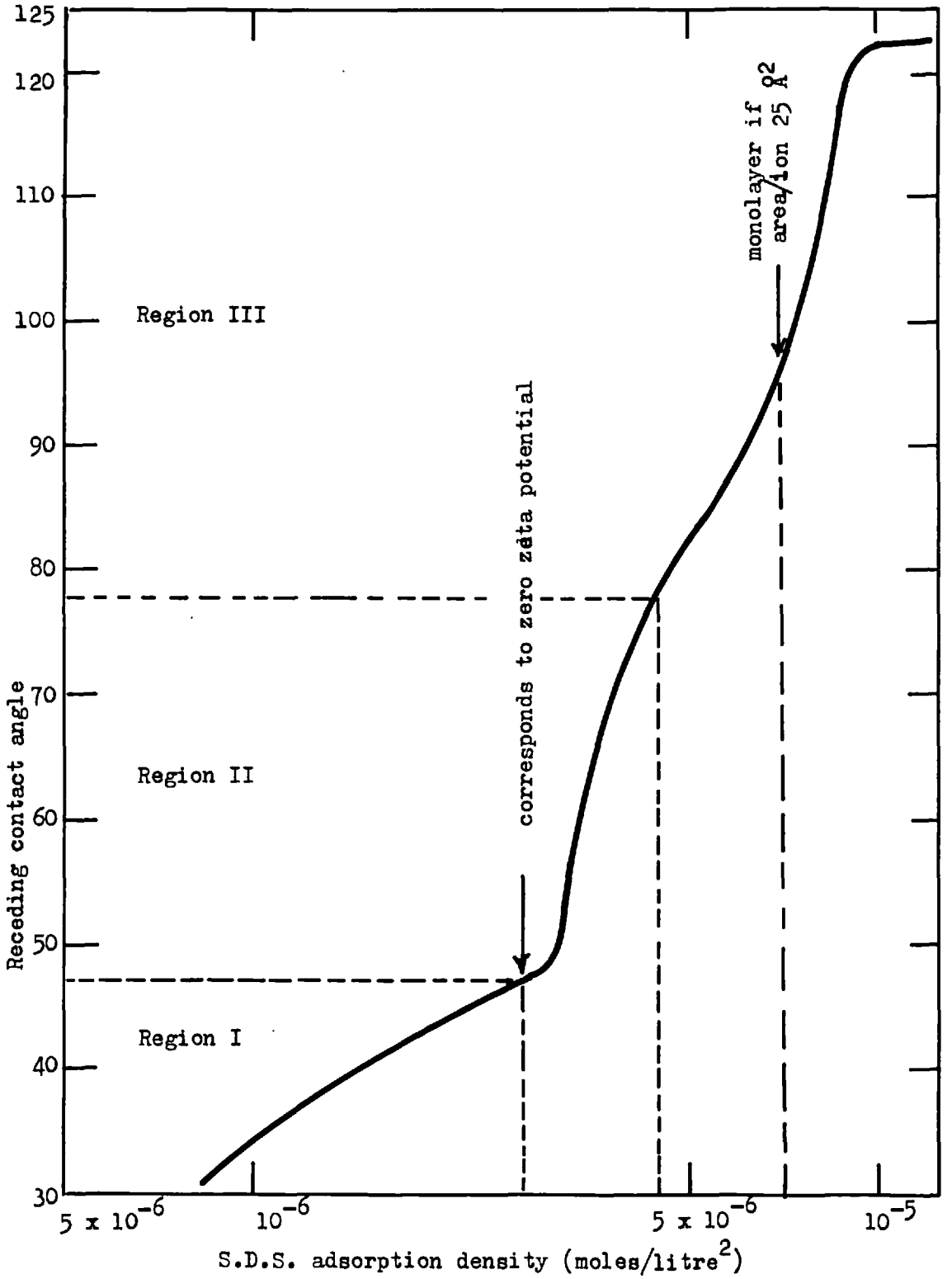

Fig. 66. The contact angle of iso-octane on hematite as a function of S.D.S. adsorption density.

(pH 2.6; ionic strength 6 x 10-3)

adsorbed with the hydrocarbon chain normal to the solid surface and with the polar groups pointing into the aqueous phase; b) the ion is adsorbed with its polar group attached to the solid and with the hydrocarbon chain normal to the surface; and c) the collector ion is adsorbed so that the hydrocarbon chain lies flat on the surface and the polar head is attached to the surface. Intermediate positions are also possible. Figure 66 shows that, in general, an increase in the adsorption density produced an increase in the contact angle. This occurs only when the hematite surface becomes more oleophilic because of the presentation of hydrocarbon groups to the aqueous phase. Orientation of the adsorbed ions with the polar group pointing into the aqueous phase is therefore unlikely. Vertical orientation of the adsorbed ions with the hydrocarbon chains normal to the surface, and pointing into the aqueous phase is likewise unlikely because the van der Waals forces of attraction between the water molecules will be greater than the forces of attraction between the hydrocarbon chain and water molecules. Energetically, therefore, the most favourable position for the hydrocarbon chain would be lying flat on the solid surface where it would be removed, as far as possible, from an aqueous environment. For an ion to take up this position, however, the work involved in displacing the water from the surface would have to be less than that required to insert the hydrocarbon chain into water.

In the case of charged solids there is evidence that water molecules are bound by ion-dipole interactions and hydrogen bonding

to the solid surface. Such bound water is considered to have a well ordered structure (197) (198). If the energy binding the water to the surface is greater than the energy available for the displacement of water by the hydrocarbon chain, then the hydrocarbon chain will be forced to take up an angled orientation. Depending on whether the bound water is strongly or weakly held there are two possible interpretations of the contact angle and adsorption density results obtained in this work.

Interpretation 1

This interpretation of the experimental data is essentially the same as that used by Jaycock and Ottewill (178) and Billet and Ottewill (199) to interpret the adsorption density and contact angle results obtained on silver iodide in the presence of dodecylpyridinium bromide. In region I, it is suggested that the increase in contact angle was a result of the adsorption and angled orientation of the dodecyl sulphate ions. At the adsorption density corresponding to zero zeta potential it is possible that the sites responsible for the bound water were neutralized, so that the hydrocarbon chains displaced the water and took up a horizontal orientation. The adsorption density at this point corresponded to a monolayer if the area per adsorbed ion was 70Å^2. According to a 'Catalin' model, a dodecyl sulphate ion horizontally orientated, occupies approximately 76Å^2. It is therefore suggested that at this point most of the adsorbed ions were in a horizontal position.

The rapid rise in the contact angle in region II would

correspond to, the removal of bound water from the surface and, the presentation of hydrophobic CH_2 groups to the aqueous phase. A very high contact angle would not be expected here because of the presence of exposed hydrophilic sulphate groups in the CH_2 layer. In region III the slight decrease in the rate of increase of contact angle with increase in the logarithm of the adsorption density would correspond to the adsorbed ions taking up a vertical position and in doing so allowing the water to penetrate, to the surface, between the ions. At an adsorption density near to that required to form a close packed vertically orientated monolayer the associations between adjacent hydrocarbon chains would 'squeeze' out the water and the contact angle would increase rapidly to a maximum value characteristic of the system.

Interpretation 2

This interpretation considers the results if the hydrocarbon chains were capable of removing the bound water from the hematite surface. In region I the ions would be adsorbed and orientated parallel to the solid surface. As the adsorption density increased a close packed horizontally orientated monolayer would be formed. The rapid increase in contact angle in region II would now correspond to the hydrocarbon chains associating and building up a vertically orientated layer. Water at the surface would be 'squeezed' out as a result of these associations. The continued increase in the contact angle in region III would be the result of continued associations and the formation of a close packed vertically orientated monolayer.

In comparing the results of contact angle measurements with those of adsorption measurements, which are based on the solid/water interface, there is always the uncertainty of the magnitude of the adsorption density of collector at the solid/air or solid/oil interfaces. Ter-Minassian-Saraga (180) (181) has demonstrated that as the air/water meniscus recedes, collector is deposited at the solid/air interface. It is therefore likely that as the water receded over the surface of hematite some dodecyl sulphate ions were deposited at the oil/hematite interface. If the theory of Smolders (184) is applicable, the adsorption at the oil/solid interface will be far greater than that at the water/solid interface.

In table V it was shown that the adsorption density at the oil/water interface varied from 1×10^{-6} to 3×10^{-6} moles metre^{-2} in the S.D.S. concentration range 1×10^{-5}M to 2×10^{-3}M. According to Smolders (184) if $d\theta / d \operatorname{Ln} C$ (see eq^{n} 48 section 4.41c) is positive, $\Gamma_{so} > \Gamma_{sw} + \Gamma_{ow} \cos\theta$. This will mean that a given adsorption density will be reached at the hematite/oil interface at an equilibrium concentration lower than that required to give the same adsorption density at the hematite/water interface. It is possible that the effect of this will be to displace the curve correlating the contact angle with the logarithm of the S.D.S. concentration to lower equilibrium concentrations than the data acquired on the solid/water interface i.e. the adsorption isotherm. If the contact angle data in fig. 41 has been displaced because of

adsorption at the solid/oil interface, then 'Interpretation 2' is more likely to be valid than 'Interpretation 1'.

d) Work of adhesion and extraction results

The work of adhesion, at two constant concentrations of S.D.S., is presented in fig. 67 as a function of pH. Comparison of these curves with fig. 43 shows that as the pH increased above the z.p.c. the percent extraction, $\Delta \xi$, contact angle, adsorption density and work of adhesion all decreased rapidly. Thus showing that the work of adhesion and percent extraction were directly related to the cationic nature of the hematite surface and the adsorption density of dodecyl sulphate ions at the surface. Figure 68 shows the work of adhesion of the iso-octane drop to the hematite surface as a function of the logarithm of the equilibrium S.D.S. concentration. The shape of this curve is very similar to the contact angle and adsorption density data shown in figs. 41 and 39. The work of adhesion increased markedly at an equilibrium concentration just above that required to reduce the zeta potential to zero. This increase would either correspond, to the displacement of bound water from the hematite surface and the formation of a hydrophobic horizontally orientated monolayer, or to the adsorbed ions associating and becoming orientated in a vertical position, depending on which interpretation of the adsorption density and contact angle data is used.

The work of adhesion as a function of the adsorption density

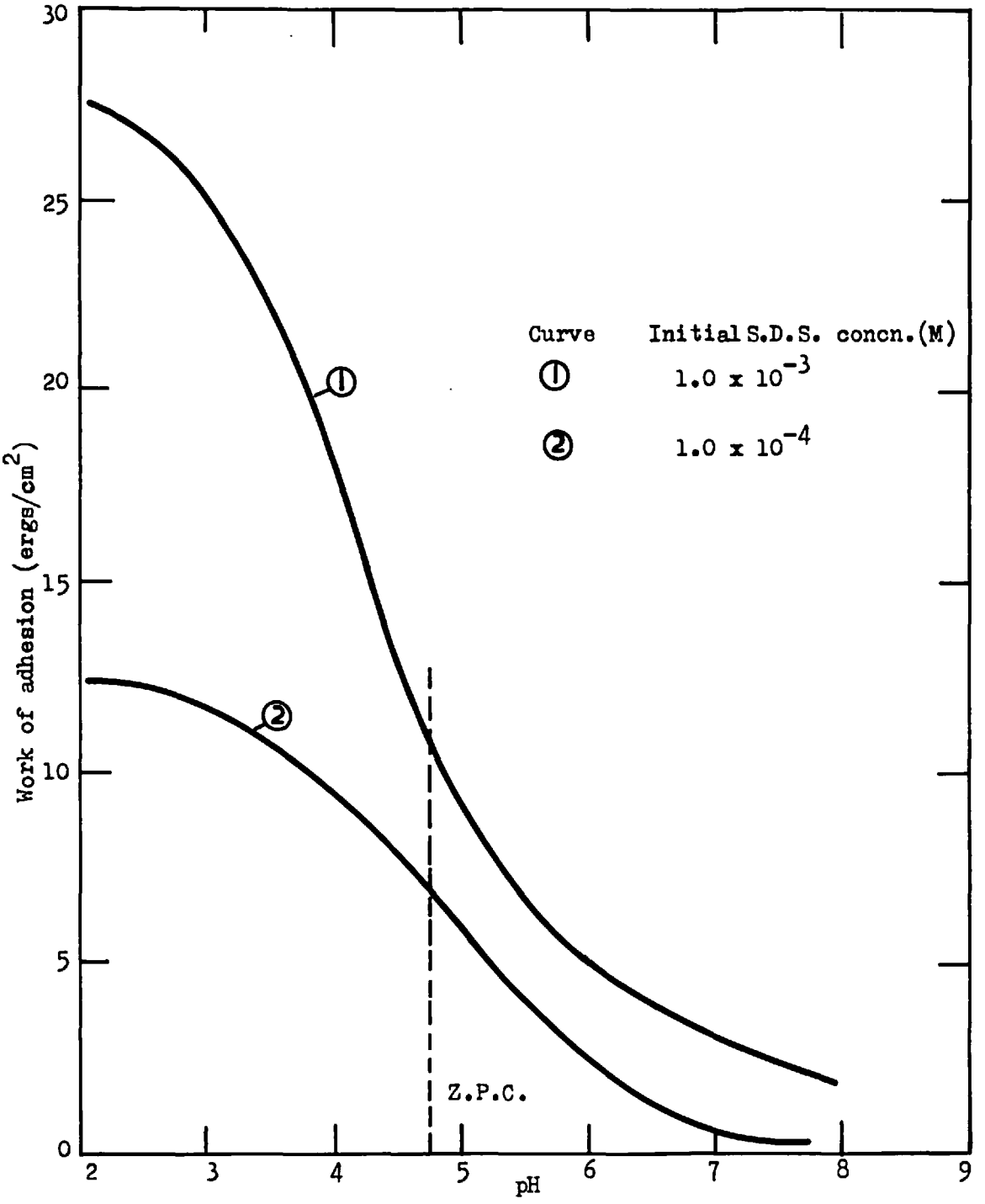

Fig. 67. Work of adhesion of iso-octane to hematite as a function of pH in the presence of S.D.S. (ionic strength 6 x 10^{-3})

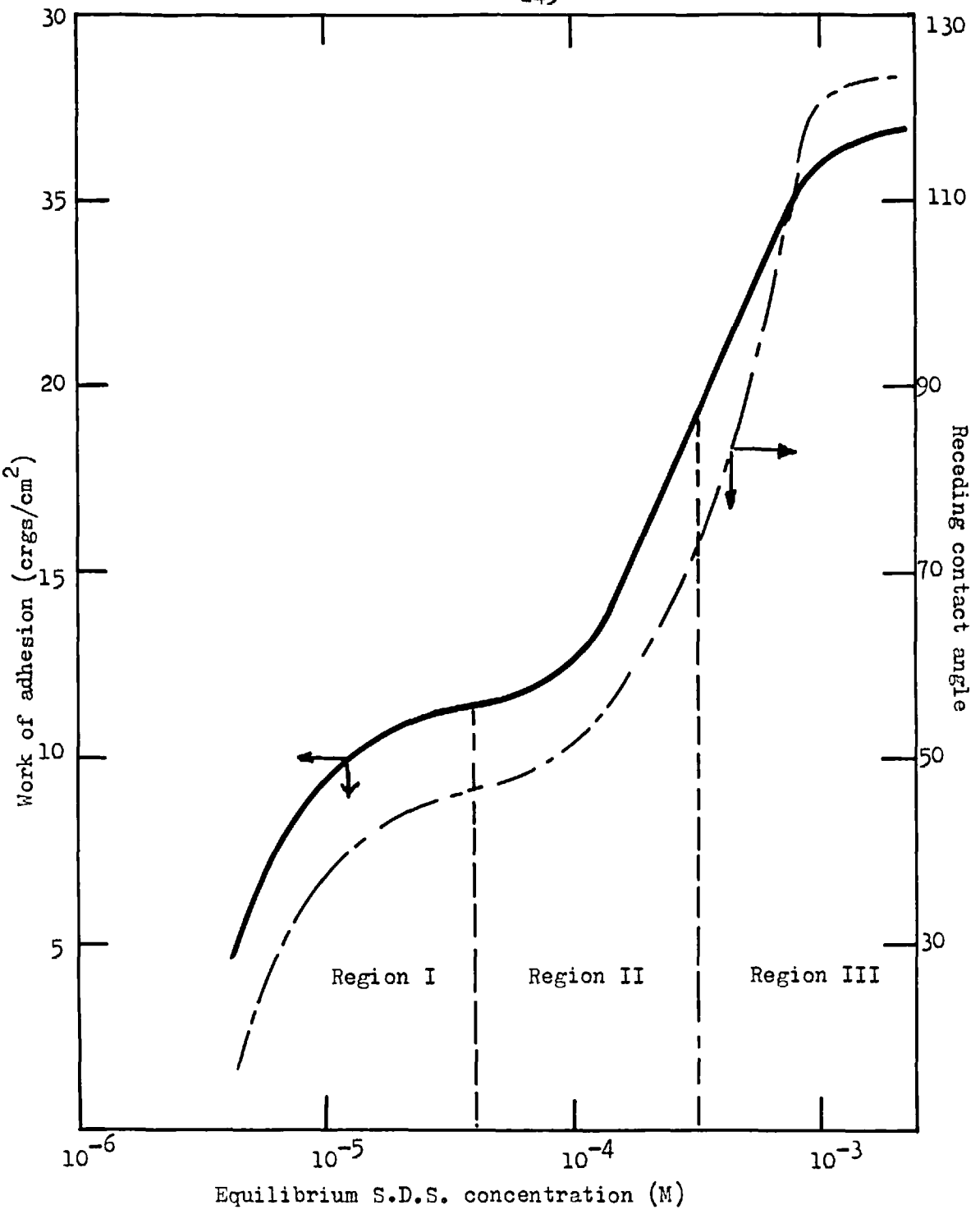

Fig. 68. Work of adhesion of iso-octane to hematite as a function of equilibrium S.D.S. concentration.

(fig. 69) shows that the adsorption of S.D.S. onto the hematite surface was a two step process. In region I it could well be, that a horizontally orientated monolayer was formed and that the constant work of adhesion obtained corresponded to the maximum obtainable from a layer of CH_2 groups interspersed with hydrophilic polar groups. The increase in work of adhesion in regions II and III would then correspond to the shielding of these hydrophilic heads by the chains becoming normal to the surface and associating with each other.

It is very difficult to differentiate between the two possible interpretations of the experimental data. However, the results show that two steps were involved in the adsorption process. First the completion of a horizontally orientated monolayer and then at higher equilibrium concentrations the formation of a close packed vertically orientated monolayer.

The percent extraction as functions of the logarithms of the S.D.S. equilibrium concentration and adsorption density (fig. 44) show that 100% extraction was first obtained when the zeta potential was approximately zero. Under these conditions the repulsive forces between the particles will be nearly zero and the particles will be able to pack tightly at the oil/water interface. The percent extraction decreased at adsorption densities and equilibrium S.D.S. concentrations higher than that required to form a close packed vertically orientated monolayer. At these high adsorption densities the formation of a second, adsorbed layer, at the solid/water inter-

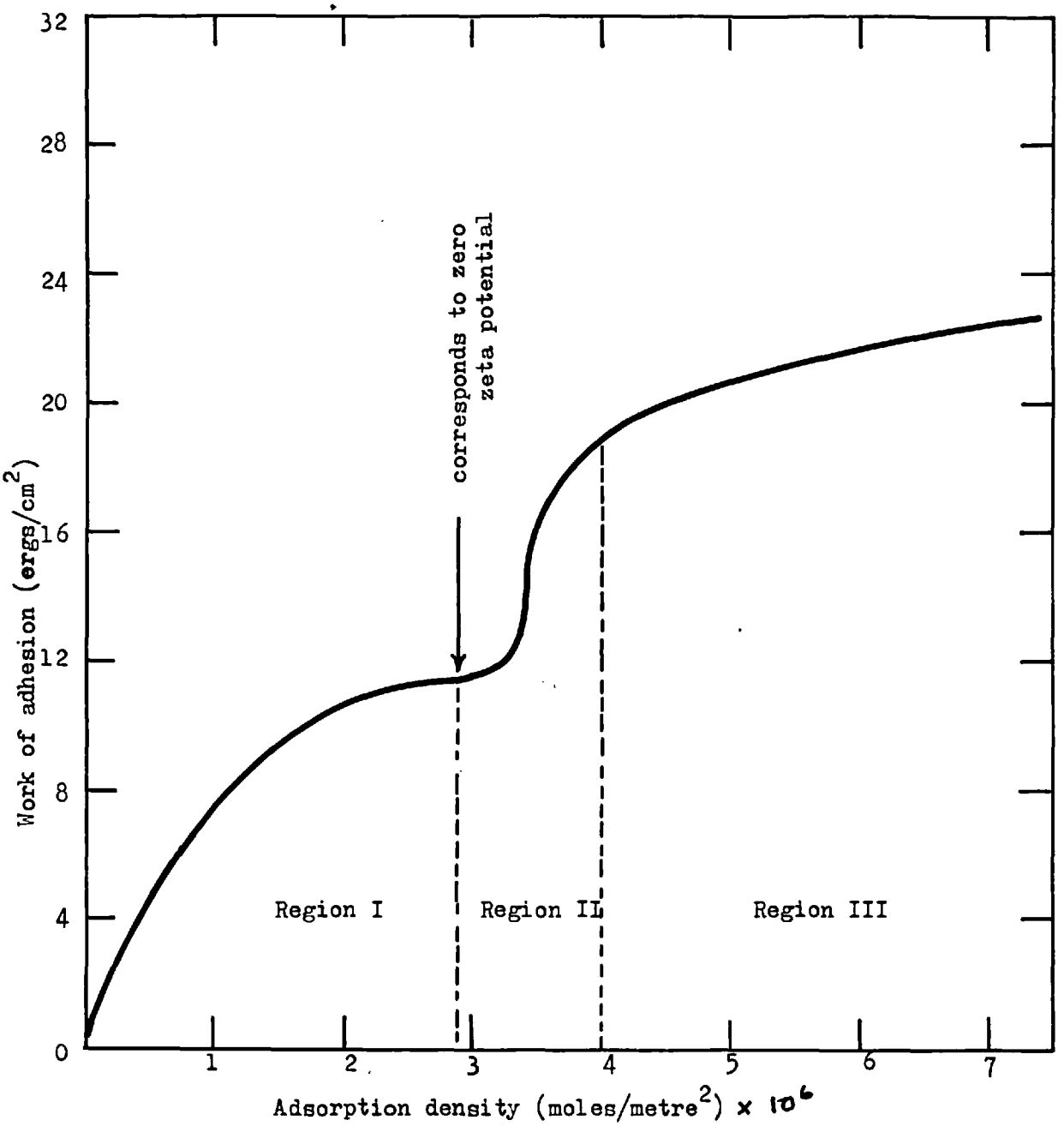

Fig. 69. Work of adhesion of iso-octane to hematite, as a function of S.D.S. adsorption density.

(pH 2.6; ionic strength 6×10^{-3})

face, with the hydrophilic polar groups pointing into the aqueous phase is likely. When an oil drop comes into contact with such a surface instead of the contact angle decreasing, as it would for an air/water/solid system, it increases slightly or remains constant. The reason for this, according to Schulman and Leja (42) (171), is that the second layer is squeezed into the oil, and solubilized by the organic phase. A reversely orientated adsorbed layer, cannot, therefore, be used as an explanation for the decrease in the percent extraction at high equilibrium concentrations and adsorption densities of S.D.S. especially since the contact angle did not decrease in a similar way. A probable explanation is, that at high S.D.S. concentrations the charge on the hematite particles was so large that the repulsive forces between the particles inhibited close packing at the oil/water interface.

The slight decrease in the percent extraction with decrease in pH, at pH values below the hematite z.p.c., was thought to be attributable to the formation of an anionic surface complex (200), between chloride ions and the hematite surface, which inhibited the adsorption of dodecyl sulphate ions. However, in view of the fact that the contact angle and adsorption density remained constant and similar results were obtained with $HClO_4$ (an acid which does not readily complex with ferric) an anionic complex was thought unlikely. A possible reason, for this decrease in percent extraction, is that at low pH values the high charge on the particles, once again, inhibited close packing at the oil/water interface.

The percent extraction obtained as a function of pH (fig. 42) were similar to the recovery against pH curves obtained in the conventional flotation of iron oxides with alkyl sulphates. Iwasaki (189) (161) et al. has shown that with both hematite and magnetite, maximum flotation with S.D.S. was obtained at pH values below the z.p.c. Similar results were obtained on ilmenite by Choi, Kim and Paik (160).

e) Summary

The results show that the mechanism of adsorption of sodium dodecyl sulphate at the hematite/water interface was primarily one of coulombic attraction between the dodecyl sulphate ions and the positive hematite surface. Two steps were involved in the adsorption process. First the formation of a horizontally orientated layer and then at higher equilibrium S.D.S. concentrations the formation of a vertically orientated monolayer with the hydrocarbon chains pointing into the aqueous phase.

The correlation between the adsorption density, contact angle, percent extraction, and work of adhesion was good throughout the pH range. As the pH increased above the z.p.c. (i.e. 4.75) the values of all these variables decreased rapidly. Similar to the iso-octane/water/quartz system in the presence of dodecylamine maximum extraction was obtained when the zeta potential was zero.

4.43. The hematite/water/iso-octane system in the presence of dodecylamine

a) The hematite/water interface

The rôle of H^+ and OH^- ions in determining the sign and magnitude of the hematite zeta potential has been discussed in section 4.42a. The zeta potential results in the presence of dodecylamine (figs. 45 and 46) indicated that the primary mechanism of adsorption of amine by hematite, was one of coulombic attraction of the cationic amine ions for negative sites on the hematite surface. A similar mechanism has been postulated by Joy and Watson (188).

If it is assumed that the measured adsorption density of amine was attributable to that of the cationic amine at the hematite/water interface, the electrokinetic and adsorption density data (figs. 45 to 48) can be interpreted in a similar way to the data obtained for the quartz/water system (section 4.31b). It is suggested that at pH values above the z.p.c. of hematite the cationic amine was first adsorbed into the double layer by an ion exchange process and then at higher concentrations into the Stern layer by forming associations (hemimicelles) between the hydrocarbon chains. The presence of hydrocarbon chain interactions will account for the adsorption of cationic amine at adsorption densities higher than that required to neutralize the negative sites on the hematite surface.

It was shown in section 4.13b that for an ion exchange process in the diffuse layer, the adsorption isotherm (fig. 48), below the C_{HMC}, should have a slope of unity. The value obtained in this work (approximately 0.65) was lower than the predicted value. A discrepancy as large as this, is perhaps not surprising in view of the possibility of the measured adsorption density including some of the adsorption of amine at the solid/oil and oil/water interfaces. As the zeta potential remained constant over this concentration range, it is reasonable to conclude that, the most likely mechanism of adsorption would be one of an ion exchange between the cationic amine ions and the cationic counter ions in the diffuse layer.

The electrokinetic data (fig. 46) indicates that the C_{HMC}, i.e. the concentration of amine at which the zeta potential became dependent on the logarithm of the amine concentration, decreased as the pH was increased. This is consistent with the hemimicellization theory of Gaudin and Fuerstenau (170). At high pH values, and hence surface potentials, the critical adsorption density necessary for the formation of associates between adjacent hydrocarbon chains, will be reached at lower equilibrium concentrations than when Ψ_o is small.

Considerable quantities of amine were adsorbed, at pH values below the z.p.c. of hematite, without changing the zeta potential. A mechanism of ion exchange in the diffuse layer under these conditions is unlikely because the counter ions were anionic. Adsorption of neutral amine from the aqueous or organic phase is, likewise,

unlikely because at these pH values nearly all of the amine was in the cationic form. A possible mechanism, suggested by Joy and Watson (188), is that of an ion exchange between RNH_3^+ ions and H^+ ions at surface sites. Such a mechanism would account for the adsorption of cationic amine without changing the zeta potential.

The adsorption density of amine on hematite, in the presence of iso-octane, decreased at pH values above neutral. According to fig. 5 the cationic amine concentration in the aqueous phase, decreased also in this pH range. The adsorption density results, therefore, clearly show the importance of the cationic amine concentration on the adsorption density at the hematite/water interface.

In summary, the results obtained for the hematite/water/iso-octane system in the presence of dodecylamine were very similar to those obtained for the quartz/iso-octane/water system under the same conditions. The primary mechanism of adsorption of the amine at the hematite/water interface was one of coulombic attraction of the cationic amine ions for the negative hematite surface. The adsorption, was attributed to an ion exchange process at low amine concentrations and at higher concentrations specific adsorption in the Stern layer, possibly to form hemimicelles.

b) Contact angles at the hematite/iso-octane/water line of contact

The contact angles of iso-octane on hematite in the presence of dodecylamine were similar to those obtained for the quartz/water/

iso-octane system. The contact angles (fig. 49), at pH 8.0, were slightly higher than those at pH 6.5 although there had been a reduction in both the cationic amine concentration and the adsorption density (fig. 47). Furthermore comparison of the aqueous amine concentration, at the point of intersection of the two linear parts of the curve correlating the contact angles with the logarithm of the equilibrium aqueous amine concentration, with the C_{HMC} values predicted from the electrokinetic (fig. 46) and adsorption (fig. 48) data, shows that at pH 6.5 and 5.0 there was a good agreement but not at pH 8.0. This comparison is demonstrated in Table IX.

TABLE IX

pH.	C_{HMC} (M)		Conc. at intersection of contact angle curves
	Electrokinetic	Adsorption	
5.0	4.0×10^{-4}	approx. 5×10^{-4}	5.0×10^{-4}
6.5	1.0×10^{-4}	approx. 2×10^{-4}	1.6×10^{-4}
8.0	8.0×10^{-5}		2.0×10^{-5}

The good agreement between the aqueous amine concentration at the point of intersection of the two linear parts of the contact angle curve and the evaluated C_{HMC} values, at pH 6.5 and 5.0 indicates, that the determined contact angles were attributable to the mode of orientation (cf. section 4.42c) of the cationic amine ions at the hematite/water interface. Thus, the slow increase in the contact angle with increase in the logarithm of the aqueous amine concentration, at concentrations below 10^{-4}M and at pH 6.5 (fig. 50), indicates that the ions were orientated in such a way that they did

not markedly increase the oleophilicity of the surface. If these ions were adsorbed into the diffuse layer it is likely that, although there would be some orientation due to the force of attraction between the cationic head group and the anionic surface, there would be a random selection of orientations. A large variation in contact angle would, therefore, not be expected. The rapid increase in contact angle, at concentrations above 10^{-4}M, indicates that when the adsorbed ions associated, a more oleophilic surface was attained. Presumably because of the increased adsorption density and vertical orientation of the adsorbed cationic amine ions.

It appears that at pH 8.0, similar to the quartz system, the contact angles do not reflect the orientation and adsorption of cationic amine at the hematite/water interface. At this pH the neutral amine concentration in the organic phase was much higher than that of the cationic amine in the aqueous phase. It would, therefore, appear that the neutral amine, possibly by being adsorbed at the hematite/oil and oil/water interfaces, influenced the contact angles. The adsorption of neutral amine, and the necessity of the presence of cationic amine before the neutral amine is involved, has been discussed in section 4.41c in conjunction with the quartz/water/iso-octane system. It is thought that a similar discussion would be valid here.

c) <u>The work of adhesion and extraction results</u>

Comparison of the work of adhesion and extraction results

(figs 70 and 52 respectively) shows that 100% extraction was obtained when the work of adhesion was a maximum. The correlation between the contact angles, work of adhesion and percent extraction, was good throughout the pH range. However, at low pH values the percent extraction and work of adhesion decreased to zero, whereas the logarithm of the adsorption density did not decrease markedly. It is suggested that although the cationic amine was adsorbed, the surface attained a hydrophilic character because of the high positive charge on the hematite surface. A surface carrying a large charge will be hydrophilic (201), since an orientated layer of water will form round the particle, in much the same way as cations become heavily solvated in solution.

The decrease in percent extraction, adsorption density and work of adhesion, at pH values above 8.0 indicates the dependence of these variables on the cationic amine concentration in the aqueous phase. A number of authors (202) (183) (203) (204) have shown that in conventional flotation systems, the contact angles and flotation response of quartz and hematite increases at pH values above 6. The reasons for this increase in hydrophobicity have been attributed to the increase in neutral amine concentration with increase in the pH. Some authors (203) have postulated dipolar interactions between the neutral amine molecules and the quartz surface, others (183) (202) (204) interactions between the adsorbed cationic hydrocarbons and the neutral molecules and others (149) (205) (206) an ion exchange or chemical reaction between the neutral amine molecules or cationic

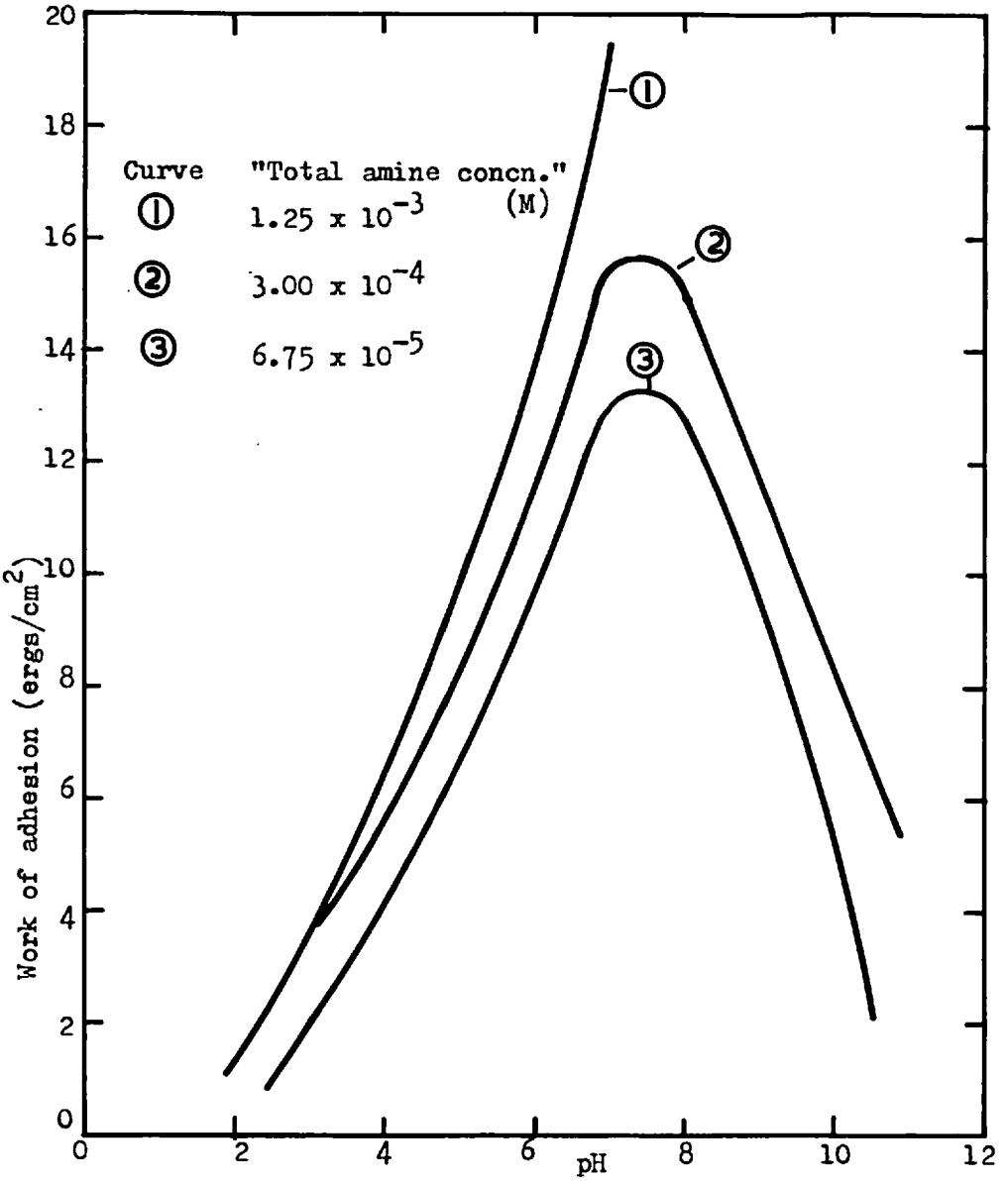

Fig. 70. Work of adhesion of iso-octane to hematite in the presence of dodecylamine.

amine ions and the surface sites. The results obtained in this work show that at high pH values, even though neutral amine was present in both the organic and aqueous phases, a hydrophobic, or at least an oleophilic surface was not obtained unless cationic amine was present in appreciable quantities.

The works of adhesion, determined for the hematite/iso-octane/water system, as functions of the logarithms of the aqueous amine concentrations, at pH 6.5 and 8.0, are shown in fig. 71. These curves are similar to those obtained for the quartz/amine system (fig. 63). The curves at both pH 6.5 and 8.0 were similar to the contact angle data (fig. 50) and can be divided into two linear regions. The aqueous amine concentration at the point of intersection of the linear parts of the work of adhesion curves were in excellent agreement with the point of intersection of the contact angle data. In the presence of large amounts of neutral amine e.g. at pH 8.0 the works of adhesion for a given aqueous amine concentration, were higher than when the neutral amine concentration was lower than the cationic amine concentration in the aqueous phase (e.g. pH 6.5).

Comparison of the works of adhesion for the hematite and quartz samples as functions of the adsorption density of amine at the mineral/water interface, at pH 6.5 (figs. 72 and 64) shows that at relatively high adsorption densities the works of adhesion obtained for the quartz system were about 7 ergs cm^{-2} higher than those obtained for the hematite system. Whether this difference is significant, or not, is doubtful because an increase in the hematite

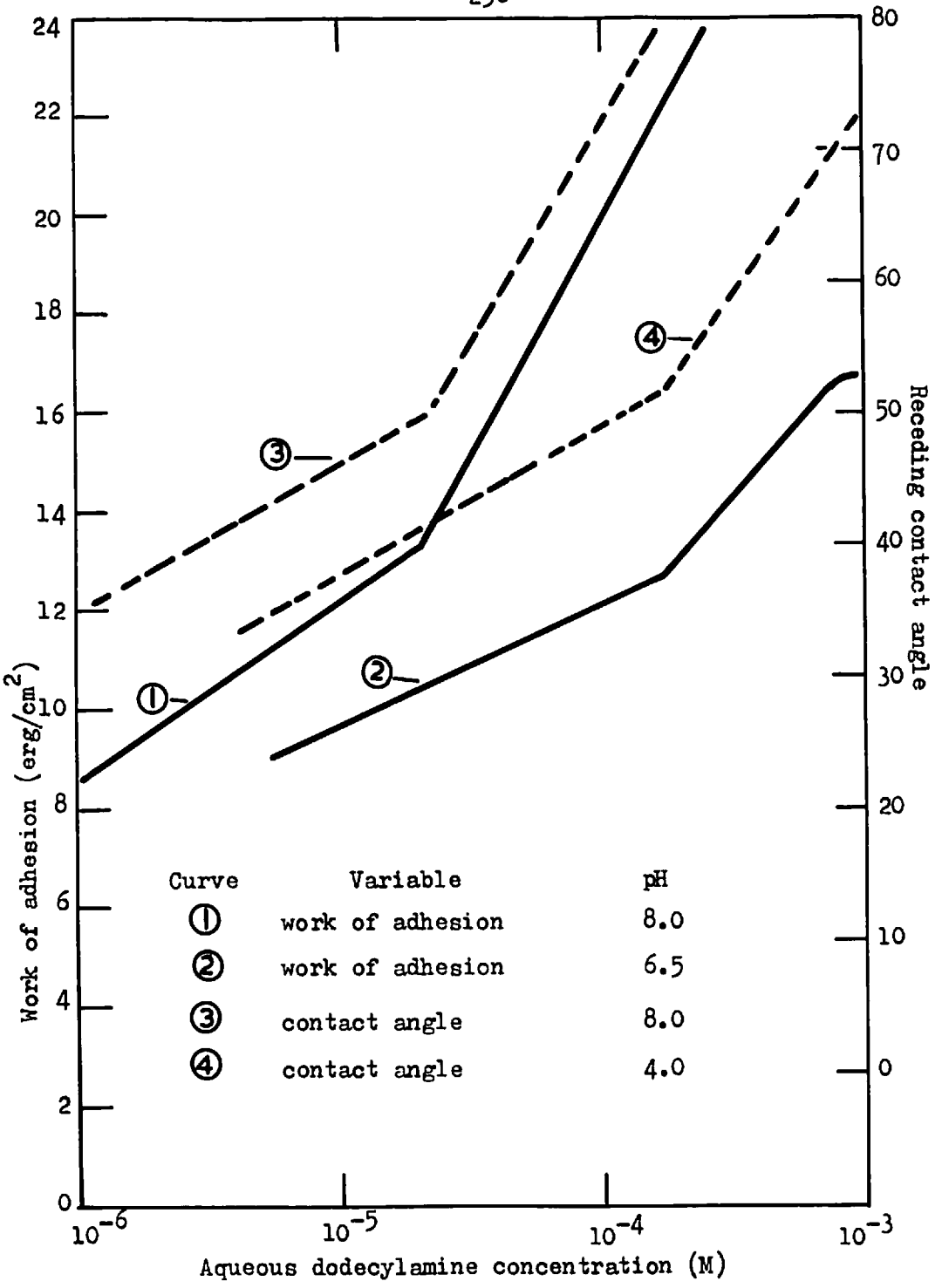

Fig. 71. Work of adhesion of iso-octane to hematite in the presence of dodecylamine.
(ionic strength 6×10^{-3})

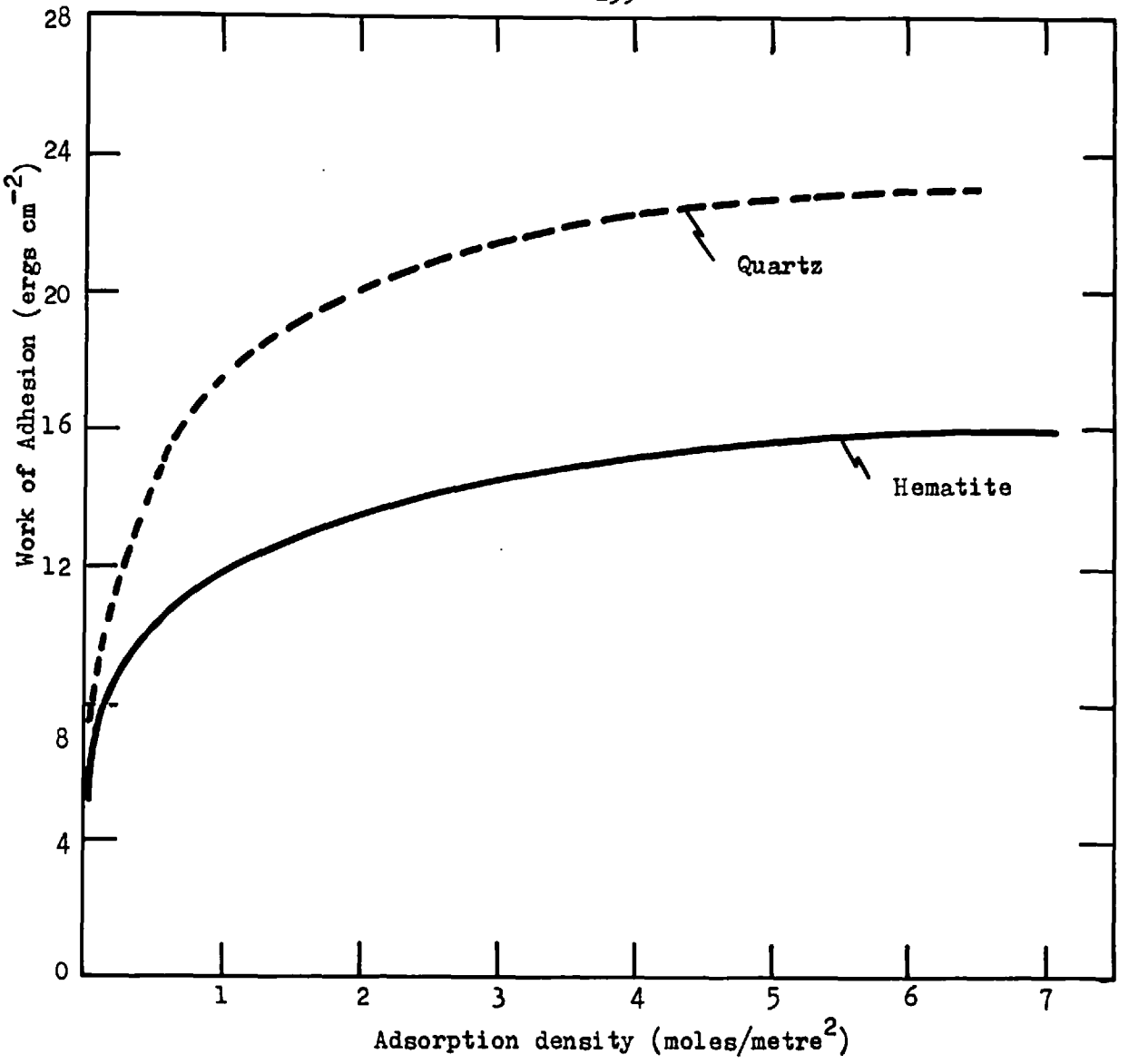

Fig. 72. Work of adhesion of iso-octane to hematite and quartz as a funotion of dodecylamine adsorption density.
(pH 6.5; ionic strength 6×10^{-3})

contact angles of 8^{o} would give works of adhesion similar to those obtained using quartz.

The reason for the large contact angle hysteresis, found when using the hematite sample, is thought to be attributable to the microcrystalline nature of the polished specimen. It is likely that the presence of crystal edges and grain boundaries produced a surface roughness effect which enhanced or impeded the advancing and receding oil/water meniscus as it passed over the hematite surface. Under these conditions the contact angles will not be true equilibrium angles and the Young's expression can be used, only as an indication of the variation of the work of adhesion with change in the pH, adsorption density and collector concentration.

Similar to the quartz/iso-octane/water and hematite/water/iso-octane systems in the presence of dodecylamine and sodium dodecyl sulphate, respectively, one hundred percent extraction was obtained, for the hematite/iso-octane/water system in the presence of dodecylamine, when the zeta potential of the mineral particles was small or zero. In none of these three systems was the mineral completely extracted into the organic phase.

e) Summary

The results obtained for the hematite/iso-octane/water system in the presence of dodecylamine were very similar to those obtained for the quartz/iso-octane/water system under the same conditions. A similar interpretation of the results has been used, for both systems.

Maximum extraction of the hematite occurred when the contact angle was approximately 70° and the zeta potential nearly zero. This latter condition is similar to that required for the maximum extraction of quartz with amine and hematite with sodium dodecyl sulphate.

4.44. The hematite/iso-octane/water system in the presence of dodecanoic acid

The flotation of hematite with fatty acids has been used for a number of years (11) (161) (207) but little conclusive research has been done on the mechanism of collection or adsorption. When studying the interaction of carboxylic collectors with minerals, it must be kept in mind that when dissolved in water soaps, despite their ability to ionize, form a complex system of anions, cations, unionized carboxylic acid as well as molecular and ionic micelles (if the concentration is high enough). In addition to the complexity of the solution chemistry there is the possibility that the fatty acid molecules form dimers alongside the usual monomers.

The extraction results obtained in this work were analogous to those found in conventional flotation systems (11) (161) (207) in that maximum extraction was obtained when the hematite surface was very anionic. Clearly a mechanism of coulombic attraction of the carboxylic ions for the hematite surface is unlikely under these pH conditions. It is known that the fatty acids, especially the unsaturated ones, do increase the negative zeta potentials of some

minerals. Purcell and Sun (208) have shown that with oleic, linoleic and linolenic acid the negative zeta potential of rutile at pH values above the z.p.c. ($\sim$ 6.5) was increased appreciably as the concentration was increased. In the present work however the effect of dodecanoic acid on the hematite zeta potential, was not measured because of the low solubility of the neutral acid and the uncertainty of the nature of the hematite surface.

The apparent dependence of the position of the z.p.c. on whether the pH of a suspension of hematite was initially alkaline or acidic (fig. 54) is difficult to understand. Smolik et al. (209) found that by treating alumino-silicates with dilute acids or by cycling between acidic and basic solutions, the apparent position of the z.p.c. decreased. The reason for this was thought to be attributable to the selective dissolution of alumina from the surface and hence the increase in the fraction of the surface occupied by SiO groups. Such a mechanism of selective dissolution of a species from a hematite surface is unlikely unless there are impurities present. It is possible that in the initially alkaline suspensions a surface ferric hydroxide was formed which retained its anionic properties to lower pH values. In aqueous systems it is known that when the pH of an acid solution of, say, ferric chloride is increased precipitation occurs. If however the pH is decreased the precipitate does not readily disappear even at 1 pH unit below the precipitation pH. The dissolution or ionization of the precipitate is very dependent on time. It is therefore possible that if the initially alkaline

suspension had been aged at a given pH e.g. 5.0 the zeta potential would slowly approach that obtained for the initially acid suspension, at pH 5.0.

Polkin (210) (211) has revealed that sodium oleate is capable of forming polylayer coatings on a hematite surface. The first layer was assumed to be a chemisorbed layer of oleate ions and the subsequent layers of up to 80 layers thick of a mixed composition of ferric oleates, oleic acid and oleate ions. It would appear from these studies that an increase in adsorption above 2 layers does not increase or decrease the hydrophobicity of the mineral surface. In a recent investigation, Peck, Raby and Wadsworth (212) using an infra-red technique showed that in the pH range 8.0 - 9.0 there was a very strong chemisorption of oleic molecules and ions to form a surface ferric oleate. Flotation was directly related to the concentration of chemisorbed oleate. Furthermore, the maxima in the flotation - pH curves coincided with the maxima of the chemisorption - pH curves. At pH values below 8 there was an increase in the physical adsorption of oleic acid but this had a depressive action on the hematite flotability. This is similar to the effect of physically adsorbed oleic acid on the flotability of fluorite (213). According to these authors the chemisorption was related to the position of the z.p.c. of the synthetic hematite samples used.

In view of all the other flotation results obtained with mineral hematite samples it seems probable that the correlation obtained, by Peck, Raby and Wadsworth between the pH of maximum chemisorption and the z.p.c., was coincidental.

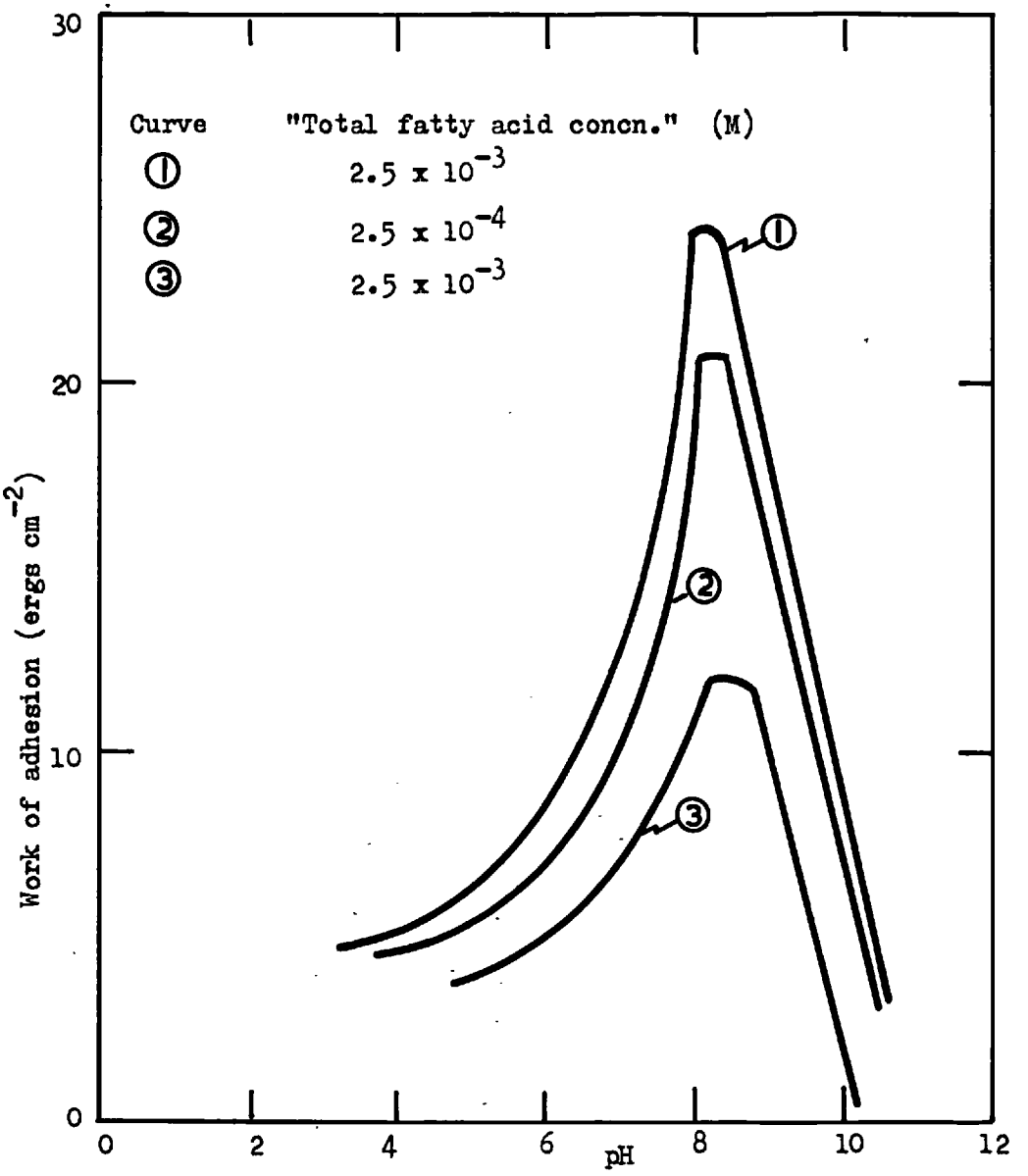

Fig. 73. Work of adhesion of iso-octane to hematite as a function of pH in the presence of dodecanoic acid.
(ionic strength 6×10^{-3})

The nature of the distribution chemistry of dodecanoic acid (fig. 7) makes it impossible to ascertain from the extraction and contact angle results (figs. 55 and 57) whether the neutral acid molecule or the carboxylic ion was responsible for the collection of hematite. It is probable, however, that similar to conventional flotation systems, both the carboxylic ion and molecule were adsorbed onto the hematite surface.

Comparison of the contact angles, extraction and work of adhesion (figs. 55, 57, 73) as a function of pH shows that the correlation between the three sets of data was excellent. Maximum extraction was obtained when the contact angles and work of adhesion were a maximum. The increase in contact angles and extraction with increase in concentration of dodecanoic acid indicates that the adsorbed species must have been orientated with the hydrocarbon chains pointing into the aqueous phase.

Summary

Maximum contact angles, work of adhesion, and percent extraction were obtained at between pH 8 and 9. In this pH range the surface of hematite was highly anionic and the concentration of neutral fatty acid in the organic phase was slightly higher than that of the carboxylic ion in the aqueous phase. No conclusion was reached as to which fatty acid species was responsible for the formation of an oleophilic coating on the hematite particles.

5.00. SUMMARY AND CONCLUSIONS

An investigation was made of the concentration of - 44 μm hematite and quartz at the iso-ootane/water interface using collectors of dodecylamine, sodium dodecyl sulphate and dodecanoic acid. The equilibrium chemistry of the oollectors in an oil/water mixture was established by direct analytical and potentiometric procedures. The drop-volume method was used to determine the interfacial tensions between iso-octane and water under various oonditions of collector concentration and pH. An electrophoresis and extraction apparatus was designed to determine the zeta potential and extraction characteristics of the minerals. The variables studied were collector concentration and pH.

Electrokinetic, contact angle, adsorption density and extraction measurements were made. From the results an attempt was made to elucidate the mechanism of collector adsorption at the mineral/water interface.

From the results of these investigations the following information was obtained.

a) In oil/water mixtures neutral amine and fatty acid molecules are distributed between the organic and aqueous phases. The values of the distribution coefficient (D), i.e. the ratio of the concentration of the neutral molecules in the organic phase to that in the aqueous phase, is 1.0×10^4 for the neutralamine and 5.6×10^3 for the neutral fatty acid. The relationship between the total distri-

bution (K_D), i.e. the ratio of the concentration of all the species in the aqueous phase to all those in the organic phase, and the pH is of the form

$$\log K_D = - pH - (\log K + \log D)$$

for dodecylamine provided that $pH \ll pK$. A similar relationship is valid for dodecanoic acid.

b) A minimum interfacial tension occurs in the curve correlating the interfacial tensions with the pH for dodecylamine and dodecanoic acid. The position of this minimum does not, however, correspond to the minimum predicted from solution chemistry considerations and the use of a Dalton's law of partial pressures analogue. The suggested reasons for the differences between the theoretical and experimental curves are a surface pH effect and molecular interactions between the adsorbed species at the oil/water interface.

A variation in the pH produces only a small change in the interfacial tension when sodium dodecyl sulphate is present in the aqueous phase. The order in which the different collector species are effective in lowering the interfacial tension is $RSO_4^- > RNH_3^+ > RCOO^- > RNH_2 > RCOOH$. The latter two species being in the organic phase.

c) The zero point of charge (z.p.c.) of the quartz and hematite samples occurred at pH values 2.5 and 4.75 respectively.

d) Quartz aged for more than 7 days has a less negative zeta potential than quartz aged for 24 hours. Ageing of a hematite suspension has a negligible effect.

e) The primary mechanism of adsorption of dodecylamine on quartz and hematite and sodium dodecyl sulphate on hematite is one of coulombic attraction of the collector ions for the oppositely charged mineral surface.

f) The adsorption isotherms of dodecylamine on hematite and quartz are similar, to each other and, to those determined by other authors in the absence of iso-octane and constant ionic strength. The adsorption process is divided into two regions, a region where adsorption takes place without changing the zeta potential and a region where the adsorption density and zeta potential vary markedly with a change in the logarithm of the equilibrium aqueous amine concentration. It is suggested that in the first region the cationic amine ions are adsorbed by an ion exchange with cationic counter ions in the diffuse layer, and in the second region by specific adsorption into the Stern layer and the formation of associations (hemimicelles), between the hydrocarbon chains of the adsorbed ions.

g) The adsorption of sodium dodecyl sulphate on hematite is also a two step process. Combination of the contact angle data with the adsorption density results indicates that the first step consists of the formation of a horizontally orientated monolayer and the second step the formation of a vertically orientated monolayer with the hydrocarbon chains orientated toward the aqueous phase.

h) The contact angles for the hematite and quartz/amine systems, at pH 6.5, reflect the two steps involved in the adsorption process. In the concentration range where the cationic amine is believed to

be adsorbed into the diffuse layer the contact angles do not vary markedly with a change in the logarithm of the aqueous amine concentration. The adsorption of amine into the Stern layer, produces a greater contact angle dependence on the logarithm of the aqueous amine concentration.

i) The presence of large amounts of neutral amine in the organic phase produces higher contact angles than when the neutral amine concentration in the organic phase is smaller than the cationic amine concentration in the aqueous phase. This effect is, however, dependent on the presence of cationic amine in the aqueous phase. In alkaline solutions the contact angles, work of adhesion, percent extraction and adsorption density decrease rapidly. The decrease in these variables corresponds to a decrease in the cationic amine concentration.

j) A good correlation is obtained between the adsorption density, contact angles, work of adhesion and percent extraction, as functions of pH, for the systems quartz or hematite/iso-octane/water in the presence of dodecylamine and hematite/iso-octane/water in the presence of sodium dodecyl sulphate. Maximum extraction is obtained when the adsorption density, contact angle and work of adhesion are at a maximum.

k) The minimum requirement for one hundred percent extraction in the three systems outlined in (j) is that the equilibrium collector concentration and adsorption density should be such that the zeta potential is zero or nearly zero. The contact angles at these points

are approximately 70° and 90° for the hematite/amine and quartz/amine system, respectively, and for the hematite/sodium dodecyl sulphate system approximately 45°.

l) Maximum extraction for the hematite/iso-octane/water system in the presence of dodecanoic acid is attained at between pH 8 and 9, where the hematite surface is highly anionic. Maximum contact angles and works of adhesion are also obtained in this region.

m) Hematite and ilmenite can be selectively extracted from mixtures of hematite and quartz, and ilmenite and quartz, using collectors of sodium dodecyl sulphate and dodecanoic acid.

n) Complete wetting of the mineral particles by the oil phase is not achieved under any of the conditions employed in this work. The particles concentrate at the oil/water interface.

REFERENCES

1. SUN, S.C., Trans. A.I.M.E. 153, 476, 1943.
2. INCE, C.R., Trans. A.I.M.E. 87, 261, 1930.
3. DEL GUIDICE, G.R.M., Trans. A.I.M.E. 112, 398, 1934.
4. DORENFELD, A.C., Eng. and Mining J. 154, 87, 1953.
5. TAGGART, A.F., TAYLOR, T.C., and INCE, C.R. Trans. A.I.M.E. 87, 285, 1930.
6. FUERSTENAU, D.W., GAUDIN, A.M., and MIAW, H.L., Trans. A.I.M.E. 211, 792, 1958.
7. IWASAKI, I., COOKE, S.R.B., HARRAWAY, D.H., and CHOI, H.S., Trans. A.I.M.E., 223, 97, 1962.
8. MORRIS, T.M., Trans. A.I.M.E. 193, 794, 1952.
9. GAUDIN, A.M., GROH, J.O., and HENDERSEN, H.B., A.I.M.E., Tech. Publ. 414, 1931.
10. KID, R.L., and WALL, W.A., Trans. I.M.M. 14, 421, 1933
11. KLASSEN, V.I., and MOKROUSOV, V.A., "An introduction to the theory of flotation". (London: Butterworths) 1963.
12. GAUDEN, A.M., SCHUHMANN, R., and SCHLECTEN, A.W., J. Phys. Chem. 46, 902, 1942.
13. TOMLINSON, H.S., and FLEMING, M.G., 6th Intern. Mineral Processing Congr. (Cannes) 1965.
14. SUTHERLAND, K.L., J. Phys. Chem. 52, 394, 1948.
15. PHILIPPOFF, W., Trans. A.I.M.E. 193, 386, 1952.
16. EVANS, L.F., Ind. Eng. Chem. 416, 2420, 1954.

17. DERJAGUIN, B.V., and DUKIN, S.S.,
Trans. I.M.M. 70, 212, 1961.

18. MELOY, T.P., '50th Aniv. Froth Flotation', 247, A.I.M.E.
(New York) 1962.

19. DUKIN, S.S., Russ. J. Phys. Chem. 501, 1960.

20. DERJAGUIN, B.V., DUKIN, S.S., and LISICHENKO, V.A.,
Russ. J. Phys. Chem., 248, 1960.

21. GAUDIN, A.M., and MALOZEMOFF, P., J. Phys. Chem. 37, 597, 1933.

22. GREENE, E.W., and DUKE, J.B., Trans. A.I.M.E. 223, 389, 1962.

23. STEINBRUCH, R., Tech. Data Sheet x - 901.
Minerals and Chemicals Philipp. Corp. 1961.

24. DECO TREFOIL. Bull. Nos. M7-F91, May-June-July 1961.

25. GAUDIN, A.M., MIAW, H.L., and SPEDDEN, H.R.,
Proc. 2nd Intern. Surf. Act. Congr. 3, 202, 1957.

26. GATES, E.H., Trans. A.I.M.E., 208, 1368, 1957.

27. McCARROLL, S.J., Trans. A.I.M.E., 199, 289, 1954.

28. MILLIKEN, F.R., Trans. A.I.M.E., 183, 101, 1949.

29. RUNOLINNA, U., RUINNE, R., and KEIRONEN, S.,
Intern. Miner. Proc. Congr. I.M.M.(London) 447,1960.

30. MELLGREN, O., and LAPIDOT, M.B.E., Trans. I.M.M. (in press).

31. FAHRENWALD, A.W., Mining Congr. J., 72, August 1957.

32. BISSE, A.H., McMORRIS, W.L., Mining Eng. 10, 258, 1958.

33. FARNAND, J.R., MEADUS, F.W., TYMCHUK, P., PUDDINGTON, I.E.,
Can. Met. Quart. 3, 123, 1964.

34. MEADUS, F.W., MUKYTIUK, A., PUDDINGTON, I.E., and MACLEOD, W.D.,
Trans. Can. M.M. 69, 303, 1966.

35. FARNAND, J.R., SMITH, H.M., and PUDDINGTON, I.E., Can. J. Chem. Eng. 39, 94, 1961.

36. Nat. Research. Counc. Canada. British Pat. 934, 796.

37. SUTHERLAND, J.P., Can. J. Chem/Eng. 40, 268, 1962.

38. SMITH, H.M., and PUDDINGTON, I.E., Can. J. Chem. 38, 1911, 1960.

40. YOUNG, T.A., Phil. Trans. Roy. Soc. (London) 95, 65, 1805.

41. VON RHEINDERS, W., Koll. Zeit. 13, 235, 1913.

42. SCHULMAN, J.H., and LEJA, J., Trans. Faraday Soc. 50, 598, 1954.

43. SCARLETT, A.J., MORGAN, W.L., and HILDEBRAND, J.H., J. Phys. Chem. 31, 1566, 1927.

44. TAKAKUWA, T., and TAKAMORI, T., Proc. 6th Intern. Min. Proces. Congr. (Cannes) 1963. (Pergammon 1965).

45. COLEMAN, R.D., SUTHERLAND, J.P., and CAPPER, C.E., J. Appl. Chem. 17, 89, 1967.

46. PETHICA, B.A., Trans. Faraday Soc. 50, 413, 1954.

47. HOER, C.W., McCORKLE, M.R., and RALSTON, A.W., J. Amer. Chem. Soc. 64, 97, 1942.

48. DANILOVA, E.V., 'Concentration of valuable minerals' (papers) Mekhanbor Inst. No. 1. 1952.

49. RALSTON, A.W., 'Fatty acids and their derivatives' John Wiley and Sons, New York, 1948.

50. RALSTON, A.W., and HOER, C.W., J. Org. Chem. 7, 546, 1942.

51. PLANTE, E.C., A.I.M.E. Tech. Publ. 2163, 1947.

52. GIBBS, J.W., 'The collected works of J.W. Gibbs' Longmans, Green and Co., New York, 1, 219, 1931.

53. GUGGENHEIM, E.A., Trans. Faraday Soc. 36, 397, 1940.

54. GADDUM, J.H., Proc. Roy. Soc. (London) B.109, 114, 1931.

55. HARKINS, W.D., and BROWN, F.E., J. Am. Chem. Soc. 41, 499, 1919.

56. ADAM, N.K., 'The Physics and Chemistry of Surfaces', 2nd Edn. Ox. Univ. Press. (1938)

57. KLING, W., and LANGE, H., Proc. 2nd Intern. Surf. Acti. Congr. (London) 1, 295, 1957.

58. HAYDON, D.A., and PHILIPS, J.N., Trans. Faraday Soc. 54, 698, 1958.

59. REHFIELD, S.J., J. Phys. Chem. 71, 738, 1965.

60. COCKBAIN, E.G., and McMULLEN, A.J., Trans. Faraday Soc. 47, 322, 1951.

61. POWNEY, J., and ADDISON, C.C., Trans. Faraday Soc. 33, 1243, 1937.

62. MUSSLEWHITE, P., Ph. D. Thesis (London) 1968.

63. READ, A.D., M. Phil. Thesis (London) 1968.

64. AVEYARD, R., and HAYDON, D.A., Trans. Faraday Soc. 61, 2255, 1965.

65. COCKBAIN, E.G., Trans. Faraday Soc. 50, 874, 1954.

66. COOK, M.A., and TALBOT, E.L., J. Phys. Chem. 56, 412, 1952.

67. DAVIES, J.T., Trans. Faraday Soc. 48, 1052, 1958.

68. ROE, C.P., and BRASS, P.D., J. Am. Chem. Soc. 76, 4703, 1954.

69. SAWYER, W.M., and FOWKES, F.M., J. Phys. Chem. 62, 159, 1958.

70. VAN DEN TEMPEL, M., Rec. Trav. Chim. 72, 415, 1953.

71. VAN VOORST VADER, F. Thesis (Utrecht 1959).

72. VAN VOORST VADER, F., Trans. Faraday Soc. 56, 1067, 1960.

73. SPINK, J.A., J. Coll. Sci. 18, 512, 1963.

74. DANIELLI, F., Proc. Roy. Soc. B, 122, 155, 1937.

75. HARTLEY, S.S., and ROE, J.W., Trans. Far. Soc. 36, 101, 1940.

76. DAVIES, J.T., and RIDEAL, E., "Interfacial Phenomenan". 2nd Ed. Academic Press (London) 1963.

77. HARKINS, W.D. and ZOLLMAN, H., J. Am. Chem. Soc. 48, 69, 1926.

78. HUTCHINSON, E., J. Coll. Sci. 3, 219, 1948.

79. POWNEY, J., and ADDISON, C.C., Trans. Faraday Soc. 34, 356, 1938.

80. PETERS, R.A., Proc. Roy. Soc. 133A, 140, 1931.

81. OSTWALD, W., Kolloid Zeit. 7, 64, 1910.

82. BHATNAGER, S.S., J. Chem. Soc. 117, 542, 1920.

83. PICKERING, S.U., J. Chem. Soc. 91, 2002, 1907.

84. BECHER, P., 'Emulsions' 1st. Edn. Rheinhold Pub. Co. 1957.

85. MANEGOLD, E., 'Emulsionen' Heidelberg, Strassenbau, Chemie and Technik. p. 23, 1957.

86. CLOWES, G.H.A., J. Phys. Chem. 20, 407, 1916.

87. WELLMAN, V.E., and TARTAR, H.V., J. Phys. Chem. 34, 370, 1930.

88. KING, A., Trans. Faraday Soc. 37, 68, 1941.

89. HARKINS, W.D., DAVIES, E.C.H., and CLARK, G.L., J. Am. Chem. Soc. 39, 541, 1917.

90. BANCROFT, W.D., J. Phys. Chem. 17, 501, 1913.

91. CLAYTON, W. 'The Theory of Emulsions and their Technical Treatment'. J. A. Churchill Ltd. 1954.

92. BANCROFT, W.D., and TUCKER, C.W., J. Phys. Chem. 31, 1681, 1927.

93. VERWEY, E.J.W., Trans. Faraday Soc. 36, 192, 1940.

94. VAN DEN TEMPEL, M., Rec. Trav. Chim. 72, 419, 1953.

95. DERJAGUIN, B.V., and LANDAU, L.,
Acta. Phys. Chim. U.S.S.R. 14, 633.

96. VERWEY, E.J.W., and OVERBEEK, J.Th.G. 'Theory of the Stability of Lyophobic Colloids' Elsevier (Amster) 1948.

97. GILBERT, E.D., Proc. 2nd Intern. Congr. Surf. Activ. 1957.

98. SCHULMAN, J. H., and COCKBAIN, E.G.,
Trans. Faraday Soc. 36, 651, 1940.

99. PICKERING, S.U., J. Soc. Chem. Ind. 29, 129, 1910.

100. BRIGGS, T.R., Ind. Eng. Chem. 13, 1008, 1921.

101. CHEESMAN, D.F., and KING, A.,
Trans. Faraday Soc. 34, 594, 1938.

102. KING, A., BENNISTER, H.L., and THOMAS, R.K.,
J. Soc. Chem. Ind. 59, 226, 1940.

103. MUKERGEE, L.N., and SRIVASTAVA, S.N.,
Kolloid Z. 147, 146, 1956.

104. MUKERGEE, L.N., and SRIVASTAVA, S.N.,
Kolloid Z. 170, 32, 1960.

105. SRIVASTAVA, S.N., Kolloid Z. 174, 36, 1961.

106. GREENWALD, H.L., J. Soc. Cos. Chem. 6, 164, 1955.

107. HELMHOLTZ, H., Wied. Ann. 1, 537, 1879.

108. KRUYT, H.R., 'Colloid Science, Vol I'. Elsevier, London, 1952.

109. STERN, O., Z. Elektrochem. 30, 508, 1924.

110. GRAHAME, D.C., Chem. Rev. 41, 441, 1947.

111. HUCKEL, E., Physik Z. 25, 204, 1924.

112. ALEXANDER, A.E., and JOHNSON, P., 'Colloid Science'. Oxford Univ. Press 1950.

113. HENRY, D.C., Proc. Roy. Soc. (London) 133, 106, 1931.

114. ABRAMSON, H.A., MOYER, L.S., and GORIN, M.A., 'Electrophoresis of Proteins and the Chemistry of Cell Surfaces' (Rheinhold) p.50 1942.

115. OVERBEEK, J.Th.G., Thesis (Utrecht) 1941.

116. BOOTH, F., Proc. Roy. Soc. (London) A.203, 514, 1950.

117. WIERSEMA, P.H., LOEB, A.L., OVERBEEK, J.Th.G., J. Coll. Sci. 22, 78, 1966.

118. BOOTH, F., Trans. Faraday Soc. 44, 955, 1948.

119. HENRY, D.C., Trans. Faraday Soc. 44, 1021, 1948.

120. KOMAGATA, S., Researches electrolech lab. Japan., Nos. 348, 8, 1933.

121. EDSER, E., Brit. Assoc. Adv. Sci. H.M. Stationary Office London (1922).

122. SULMAN, H.L., Trans. I.M.M. 29, 44, 1920.

123. BICKERMAN, J.J., J. Phys. and Coll. Chem. 54, 653, 1950.

124. SHUTTLEWORTH, R., and BAILEY, G.L.J., Discuss. Faraday Soc. 3, 16, 1948.

125. WENZEL, R.N., Ind. Eng. Chem. 28, 988, 1936.

126. CASSIE, A.B.D., Discuss. Faraday Soc. 3, 11, 1948.

127. DE BRUYN, P.L., OVERBEEK, J.Th.G., and SCHUHMANN, R., Mining Eng. 6, 519, 1954.

128. GAUDIN, A.M., 'Flotation' 2nd Edn. Mc.Graw-Hill 1957.

129. GAUDIN, A.M., BANGS, L.B., and WITT, A.F.,
Proc. 7th Int. Process. Congr. 1964.

130. GAUDIN, A.M., WITT, A., BISWAS, A.K., and DECKER, T.G.,
Proc. 6th Intern. Min. Process. Congr.
(Cannes) 1963.

131. ZISMAN, W.A., 'Contact Angle, Wettability and Adhesion'
Adv. in Chem., 43, 1, 1964.

132. GAUDIN, A.M., and MORROW, J.G., Mining. En. 6, 1196, 1954.

133. WADSWORTH, M.E., CONRADY, G.C., and COOK, M.A.,
J. Phys. Chem. 55, 1219, 1951.

134. PHILIPPOFF, W., COOKE, S.R.B., and CALDWELL, D.E.,
Mining Eng. 4, 283, 1952.

135. PLAKSIN, I.N., SHAFEYEV, R.S., and ZAITSEVA, S.P.,
Bull. Acad. Sci. S.S.S.R. Tech. Sci. Sect. 3, 1957.

136. BILLET, D.F., and OTTEWILL, R.H.,
S.C.I. Monograph No.25, 253, (London) 1967.

137. TER-MINASSIAN-SARAGA, L., C.R. Séanc. hebd. Acad.
Sci. Paris. 252, 1596, 1961.

138. JAYCOCK, M.J., OTTEWILL, R.H., and RASTOGI, M.C.,
Proc. 3rd Int. Cong. Surf. Acti. (Cologne)
2, 283, 1960.

139. CLAYTON, W., 'The Theory of Emulsions and their Technical
Treatment'. J.A. Churchill Ltd. page 491. 1954.

140. MARSHALL, J.K., J. Sci. Instr. 43, 769, 1966.

141. MOYER, L.S., and ABRAMSON, H.A., J. Gen. Physiol. 19, 72, 1935.

142. PEARCE, A.S., and STREAFIELD, E.L., Analyt. Abs. 6766, 12, 1965.

143. PEARCE, A.S., and STREAFIELD, E.L., German. pat. 1, 190, 229.

144. GREGORY, G.R.E.C., Analyst, 19, 251, 1966.

145. FUERSTENAU, D.W., and GAUDIN, A.M., Trans. A.I.M.E. 202, 66, 1955.

146. GAUDIN, A.M., and CHANG, C.S., Trans. A.I.M.E. 193, 93, 1952.

147. DEMPSTER, P.B., and RITCHIE, P.D., J. Appl. Chem. 3, 182, 1953.

148. GIBB, J.G., et al. J. Appl. Chem. 3, 213, 1953.

149. LINDSTROM, L., Acta. Polytechna. Scandinavica, 75, 1968.

150. ALEXANDER, G.B., HESTON, W.M., and ILER, R.K., J. Phys. Chem. 58, 453, 1954.

151. OKKERSE, C., and J.H. De BOER., Colloque 'Silice' de l'Association belge pour favoriser l'étude des Verres et des Composés siliceux (Bruxelles 1960).

152. FUERSTENAU, D.W., (Thesis) M.I.T. 1953.

153. LI, H.C., and DE BRUYN, P.L., Surf. Sci. 5, 203, 1966.

154. DE BRUYN, P.L., Trans. A.I.M.E. 202, 291, 1955.

155. ROGERS, J., Trans. I.M.M. 66, 439, 1957.

156. GILES, C.H., MAC EWAN, T.H., NAKHWA, S.N., and SMITH, T.D., J. Chem. Soc. 786, 3973, 1960.

157. KLASSEN, V.I., and MOKROUSOV, V.A., 'An introduction to the theory of flotation' (London: Butterworths) page 192, 1963.

158. SCHULTZ, N.R., and COOKE, S.R.B., Ind. Eng. Chem. 45, 2767, 1953.

159. CHANG, C.S., Mining. Eng. 6, 922, 1954.

160. CHOI, H.S., KIM, Y.S., and PAIK, G.H.,
Bull. C.I.M. 60, 217, 1967.

161. IWASAKI, I., COOKE, S.R.B., and CHOI, H.S.,
Trans. A.I.M.E. 223, 113, 1961.

162. GRIOT, O., and KITCHENER, J.A., Tran. Faraday Soc. 61, 1038, 1965.

163. ILER, R.K., 'The Colloid Chemistry of Silica and Silicates'.
Cornell Univ. Press., New York, 1965.

164. JOY, A.S., MANSER, R.M., LLOYD, K., and WATSON, D.,
Trans. I.M.M. 75, C75, 1966.

165. DEJU, R.A., and BHAPPU, R.B., Trans. A.I.M.E. 235, 329, 1966.

166. O'CONNOR, D.J., and BUCHANAN, A.S., Trans. Faraday Soc. 52, 397, 1956.

167. LYKLEMAN, J., and OVERBEEK, J.Th.G., J. Coll. Sci. 16, 501, 1961.

168. JAYCOCK, M.J., OTTEWILL, R.H., and TAR, I.,
Trans. I.M.M. 73, 256, 1964.

169. SOMASUNDARAN, P., and FUERSTENAU, D.W.,
J. Phys. Chem. 70, 90, 1966.

170. GAUDIN, A.M., and FUERSTENAU, D.W., Trans. A.I.M.E. 202, 958, 1955.

171. LEJA, J., and SCHULMAN, J.H., Min. Eng. 6, 221, 1954.

172. LEJA, J., Proc. 2nd Int. Congr. Surf. Act. 3, 273, (London) 1957.

173. FUERSTENAU, D.W., and YAMADA, B.J., Trans. A.I.M.E. 223, 50, 1962.

174. SOMASUNDARAN, P., HEALY, T.W., and FUERSTENAU, D.W.,
J. Phys. Chem. 68, 3562, 1964.

175. FUERSTENAU, D.W., HEALY, T.W., and SOMASUNDARAN, P.,
Trans. A.I.M.E. 229, 321, 1964.

176. STIGER, O., and OVERBEEK, J.Th.G.,
Proc. 2nd Int. Congr. Surf. Acti. I,
3, 311, (London) 1958.

177. JAYCOCK, M.J., OTTEWILL, R.H., and RASTOGI, M.C.,
Proc. 3rd Int. Congr. Surf. Act.
2, 283, (Cologne) 1960.

178. JAYCOCK, M.J., and OTTEWILL, R.H., Trans. I.M.M. 72, 1960.

179. GAUDIN, A.M., SPEDDEN, H.R., and LAXEN, P.A.,
Mining Eng. 4, 693, 1952.

180. TER-MINASSIAN-SARAGA, L., J. Chim. Phys. 57, 10, 1960.

181. TER-MINASSIAN-SARAGA, L., 'Contact Angle, Wettability and
Adhesion'. Adv. in Chem. Series 43, 232, 1964.

182. GAUDIN, A.M., and DECKER, T.G., J. Coll. and Interf. Sci.
24, 151, 1967.

183. SMITH, R.W., Trans. A.I.M.E. 226, 427, 1963.

184. SMOLDERS., Thesis (Utrecht) 1961.

185. LEJA, J., and POLING, G.W.,
Intern. Min. Proc. Congr. I.M.M. (London) 1960.

186. PARKS, G.A., and DE BRUYN, P.L., J. Phys. Chem. 66, 967, 1962.

187. TROLESTRA, S.A., and KRUYT, H.R., Kolloid Z, 101, 182, 1942.

188. JOY, A., and WATSON, D., Trans. I.M.M. 73, 289, 1963-64.

189. IWASAKI, I., COOKE, S.R.B., and CHOI, H.S.,
Trans. A.I.M.E. 217, 237, 1960.

190. JOY, A., and WATSON, D., 6th Intern. Miner. Process. Congr.
(Cannes) 1963. (Pergammon 1965).

191. PARKS, G.A., Chem. Rev. 65, 177, 1965.

192. BAILAR, J.C., 'The Chemistry of Co-ordination Compounds'. Rheinhold. New York 1956.

193. MATTSON, S., and PUGH, A.J., Soil Sci. 38, 229, 1934.

194. ATKINSON, R.J., POSNER, A.M., and QUIRK, J.P., J. Phys. Chem. 71, 551, 1967.

195. HARKINS, W.D., 'The Physical Chemistry of Surface Films' Rheinhold. New York. 1952.

196. DEAN, R.S., and AMBROSE, D.M., Bull. 449. U.S. Bur. of Mines. 1944.

197. FRANK, H.S., and EVANS, M.W., J. Chem. Physics. 13, 507, 1945.

198. DERJAGUIN, B.V., Disc. Faraday Soc., 42, 1966.

199. BILLET, D.F., and OTTEWILL, R.H., S.C.I. Monograph 25, 253, (London) 1967.

200. SHERGOLD, H.L., MELLGREN, O., and PROSSER, A.P.P., Trans. I.M.M. (in press)

201. SPURNY, J., and DOBIAS, R., Proc. 3rd. Int, Congr. Surf. Act., 4, 396, 1960.

202. SMITH, R.W., and LAI, R.M.W., Trans. A.I.M.E. 235, 413, 1966.

203. BUCKENHAM, M.H., and RODGERS, J., Trans. I.M.M. 64, 11, 1954-55.

204. FUERSTENAU, D.W., Trans. A.I.M.E. 208, 1365, 1957.

205. KELLOG, H.H., and VASQUEZ-ROSAS, H., Trans. A.I.M.E. 169, 476, 1946.

206. TAGGART, A.F., and ARBITER, N., Trans. A.I.M.E., 169, 266, 1946.

207. SUTHERLAND, K.L., and WARK, I.W., 'Principles of Flotation' 1955. (Melbourne: Australia I.M.M.)

208. PURCELL, G., and SUN, S.C., Trans. A.I.M.E. 226, 13, 1963.

209. SMOLIK, T.J., HARMAN, and FUERSTENAU, D.W.,
Trans. A.I.M.E. 235, 367, 1965.

210. POLKIN, S.I., Intern. Miner. Proc. Congr. I.M.M. (London).
p.360, 1960.

211. POLKIN, S.I., 'Flotation of Tin and Rare Metal Ores'.
Gosgortekhizdat, Moscow (in Russian) 1960.

212. PECK, A.S., RABY, L.H., and WADSWORTH, M.E.,
Trans. A.I.M.E., 238, 301, 1966.

213. PECK, A.S., and WADSWORTH, M.E.,
'50th Aniv. Froth Flotation' p.188 A.I.M.E. 1962.